

TESIS DOCTORAL



Universidad de Granada

Departamento de Geodinámica

**Estudio integrado tierra-mar en el margen
noroccidental de la Cuenca de Alborán entre los
meridianos 5° 30' W y 3° 30' W**

ENRIC SUADES SALA

Universidad de Granada 2015

Editor: Universidad de Granada. Tesis Doctorales
Autor: Enric Suades Sala
ISBN: 978-84-9125-639-7
URI: <http://hdl.handle.net/10481/43250>

Instituto Andaluz de Ciencias de la Tierra (UGR-CSIC)

Programa de doctorado Ciencias de la Tierra (UGR)



Estudio integrado tierra-mar en el margen noroccidental de la Cuenca de Alborán entre los meridianos 5°30'W y 3°30'W

Intergrated onshore-offshore study in the northwestern margin of the Alboran Basin, between meridians 5°30'W y 3°30'W.

ENRIC SUADES SALA

Fdo. El doctorando

V°B° de los directores

Fdo. Ana Crespo Blanc

Fdo. Menchu Comas Minondo

El doctorando **Enric Suades** Sala y los directores de la tesis **Ana Crespo Blanc** y **Menchu Comas Minondo** Garantizamos, al firmar esta tesis doctoral, que el trabajo ha sido realizado por el doctorando bajo la dirección de los directores de la tesis y hasta donde nuestro conocimiento alcanza, en la realización del trabajo, se han respetado los derechos de otros autores a ser citados, cuando se han utilizado sus resultados o publicaciones.

Granada 12 de Noviembre de 2015

Doctorando

Fdo.: Enric Suades Sala

Director/es de la Tesis

Fdo.: Ana Crespo Blanc

Fdo.: Menchu Comas Minondo

AGRADECIMIENTOS

Ante todo quiero dar las gracias a mi tutora, Ana Crespo. En primer lugar por haberme introducido de forma ejemplar a la ciencia, con humildad y rigurosidad pero sobre todo por haberme dado soporte a lo largo de este largo recorrido, mostrando paciencia y animándome en los malos momentos. También quiero agradecer a mi cotutora Menchu Comas por compartir sus conocimientos en mi área de estudio que tanto han mejorado el resultado final de esta tesis.

Quiero darle las gracias a Liviu Matenco, mi supervisor durante mi estancia en Utrecht. Son muchas las cosas que aprendí de él y su grupo de investigación pero sobretodo me alegro de haber conocido a una persona tan entregada tanto para la ciencia como para sus alumnos.

Sin duda, quiero dedicar unas palabras a **todos** mis compañeros de trabajo. Especialmente a Idaira, Yasmina, Edu, Edu(2) y Ari. Los ratos compartidos, las discusiones, esos pequeños favores desinteresados; todo esto se agradece.

Por ultimo agradecer a mi familia, Rosa, Joan y Albert porque, aunque lejos, sé que siempre han estado a mi lado.

Index

Abstract	13
Resumen	15
1. Introduction	17
2. Geological Setting and Background	
2.1 The Gibraltar Arc orogenic system (western Mediterranean).....	23
2.2 The Western Betics.....	25
2.2.1 Subbetic units.....	25
2.2.2 Flysch Trough Complex.....	27
2.2.3 Alboran Domain.....	28
2.2.4 Neogene sedimentary infill (onshore).....	31
2.3 The Alboran Basin.....	32
2.3.1 Basement structure.....	32
2.3.2 Sedimentary infill and seismostratigraphic units.....	33
2.3.3 Tectonic evolution.....	36
2.4 Objectives of this PhD Thesis.....	38
2.5 Structure of this PhD Thesis volume.....	39
3. Dataset and methodology	
3.1 Onshore study.....	43
3.1.1 Dataset.....	43
3.1.2 Methodology.....	44
3.2 Offshore study.....	44
3.2.1 Dataset.....	45
3.2.2 Methodology.....	47
3.2.3 Sequence stratigraphy.....	51

4. Lower to middle Miocene deposits related to gravitational and extensional processes in the Western Betics (onshore studies)

4.1 Introduction.....	65
4.2 Hydraulic brecciation on top of the Alboran Domain and its relationship with Lower Miocene deposits (Western Betics).....	66
4.3 Gravitational dismantling of the Miocene mountain front of the Gibraltar Arc system deduced from the analysis of an olistostromic complex (western Betics).....	72

5. The Malaga Basin: tectonic systems tracts within the extensional history

5.1 Introduction.....	93
5.2 Tectonic system tracts in asymmetric extensional basins: inferences from the evolution of the Malaga Basin in the westernmost Mediterranean.....	94

6. Tectonic and sedimentary evolution of the northern WAB (offshore studies)

6.1 The basement of the Malaga Basin.....	129
6.2 Sedimentary infill and associated tectonic structures.....	142
6.3 Tectonic evolution of the Malaga Basin.....	156

7. Discussion

7.1 Introduction.....	169
7.2 Offshore-onshore correlations and tectonic evolution.....	169
7.2.1 Main extensional event (Aquitanean-Lower(?) Langhian).....	173
7.2.2 Malaga Basin rift episode (upper(?) Langhian-lower Tortonian).....	185

7.2.3 Tectonic inversion (upper Tortonian to Recent).....	187
7.3 Some regional implications in the context of the Gibraltar Arc System.....	189
8. Conclusions	193
8. Conclusiones	197
9. References	203
10. Annex	221

ABSTRACT

The Gibraltar Arc is a case study of an arcuate Alpine orogen where compression in the external zones went hand by hand with back-arc extension in the hinterland of the arc. Extensional tectonics controlled the formation of several basins in the Alboran Domain and the deposition of Miocene to Recent sediments. Those basins are nowadays partially emerged due to the tectonic inversion that affects the whole Gibraltar Arc from Late Miocene onwards.

In this context, a great number of onshore and offshore studies have been carried out for the last decades. Nevertheless, very little has been done to integrate both types of studies in order to better understand the geodynamic evolution of this area. This PhD. Thesis focuses on onshore-offshore correlations of the Miocene sedimentary infill deposited over the metamorphic complexes of the Alboran Domain and its relationship with the synchronous tectonic structures observed either in the basement or in the sedimentary sequence. The study combines the analysis offshore of a comprehensive dataset of multichannel seismic profiles with onshore field work. The studied area is situated in the northern branch of the Arc. It comprises the western part of the Alboran Domain of the Betic cordillera onshore, and the northern half of the Western Alboran Basin, also known as the Malaga Basin.

The study has permitted to differentiated three main episodes that took place in the studied area.

The first episode took place between Aquitanian to Langhian times and corresponds with the main extensional event that thinned the metamorphic complexes of the Alboran Domain through ductile shear zones and low-angle normal faults. The relationship of the lower Miocene deposits with the low-angle normal fault systems show that a hangingwall transport mainly towards the SW during Aquitanian was probably followed by SSE directed extensional transport. Deposition was scarce from Aquitanian to lower Burdigalian times and became more important from Late Burdigalian onwards with the deposition of the La Joya Olistostromic Complex (LaJOC) onshore and Unit VI offshore. Those deposits show similar age, lithology, nature, and can be correlated by onshore-offshore cross-sections. LaJOC crops out extensively onshore and is characterized by turbiditic and *mélange* units that contain mainly extrabasinal blocks and olistoliths. The internal structure of the biggest olistoliths show that they originate from the gravitational dismantling of the Lower Miocene mountain front. LaJOC and Unit VI post-date some of the low-angle normal faults with transport towards the SSE that affect the Alboran Domain.

The deposition of offshore units V- IV during Langhian to early Tortonian times corresponds with the second episode: the Malaga Basin rifting. The onset of a NW directed low-to-middle angle normal fault system, situated along a structural high (High 976), started to form the asymmetric semigraben of Malaga Basin. Sequence

stratigraphic analysis characterized an early to middle rift climax from late Langhian to early Serravallian with high tectonic subsidence rates, followed by a late rift climax from late Serravallian to early Tortonian, during which the tectonic activity diminished. During this episode, the hangingwall of the High 976 normal fault system, that is the northwestern margin of the Malaga Basin and the nowadays onshore area passively rotated. This facilitated the migration of the overpressured Unit VI shales towards the center of the basin and the formation of the shale diapir province. The NW directed extension that produced the Malaga Basin semigraben was accompanied by local extensional and/or sinistral WNW-ESE to NW-SE directed faults like the Gaucín fault.

The third episode corresponds with the tectonic inversion that took place from late Miocene onwards. In the area, compressional structures are restricted to minor uplift and folding and mostly developed during the late Tortonian, at least offshore, which contrast with what is observed in other areas of the Alboran Domain. These structures were accompanied by the development of sinistral and normal faults.

RESUMEN

El Arco de Gibraltar es un ejemplo de orógeno alpino arqueado donde la compresión en las zonas externas fue coetánea a una extensión de tipo back-arc en las zonas internas. La tectónica extensional controló la formación de varias cuencas en el Dominio de Alborán así como la deposición de sedimentos que van desde el Mioceno hasta la actualidad. Estas cuencas se encuentran en la actualidad parcialmente emergidas debido a la inversión tectónica que afecta el sistema del arco de Gibraltar en su totalidad desde el Mioceno superior hasta hoy en día.

En este contexto, durante las últimas décadas se han llevado a cabo un gran número de estudios tanto en tierra como en mar. A pesar de ello, se ha trabajado muy poco en la integración de ambos estudios para poder así entender mejor la evolución geodinámica de este sistema. Esta tesis doctoral se centra en establecer correlaciones tierra-mar de la cobertera sedimentaria del Mioceno que se encuentra depositada sobre los complejos metamórficos del Dominio de Alborán. A su vez, se intenta establecer la relación de estos sedimentos con las estructuras tectónicas que se observan afectando tanto el basamento como la propia cobertera sedimentaria. Este estudio combina el análisis en mar de perfiles de sísmica multicanal con trabajo de campo en tierra. El área de estudio se sitúa en la rama norte del Arco. Está comprendida por la parte oeste del Dominio de Alborán de la cordillera bética en tierra, y la mitad norte de la cuenca oeste del Mar de Alborán, también conocida como la Cuenca de Málaga.

El estudio ha permitido diferenciar tres episodios principales que tuvieron lugar en el área de estudio.

El primer episodio tuvo lugar durante el Aquitaniense - Langhiense y se corresponde con el evento extensional principal que adelgazó los complejos metamórficos del Dominio de Alborán a través de zonas de cizalla dúctil y fallas normales de bajo ángulo. La relación entre los depósitos del Mioceno inferior con los sistemas extensionales de bajo ángulo muestra una dirección principal de transporte del bloque de muro hacia el SW durante el Aquitaniense. Ésta extensión fue probablemente seguida de un cambio en la dirección de extensión hacia el SSE. Durante este episodio la deposición fue muy restringida desde el Aquitaniense hasta el Burdigaliense temprano, y pasó a ser mucho más importante a partir del Burdigaliense tardío con la deposición del Complejo Olistostrómico de La Joya (LaJOC) en tierra, y de la Unidad VI en mar. Estos depósitos muestran similitudes en términos de edad, litología, naturaleza, y pueden ser correlacionados mediante cortes transversales tierra-mar. LaJOC aflora extensamente en tierra i se caracteriza por la presencia de unidades tanto turbidíticas como de mélangé. Éstas últimas contienen bloques y olistolitos provenientes de fuera de la cuenca. La estructura interna observable en los olistolitos de mayor tamaño muestra que se originaron por el desmantelamiento gravitacional del frente montañoso del Mioceno inferior. Tanto LaJOC como la Unidad VI sellan algunas de las

fallas normales de bajo ángulo con transporte hacia el SSE que afectan al Domino de Alborán.

La deposición en mar de las unidades V-IV entre el Langhiense y el Tortoniense temprano se corresponde con el segundo episodio: el Rift de la Cuenca de Málaga. La semifosa que es la Cuenca de Málaga se empezó a formar en este episodio por la activación de un sistema de fallas normales de bajo-medio ángulo, con transporte hacia el NW, situado en un alto estructural (High 976). Un Análisis de estratigrafía secuencial ha mostrado un primer periodo, el “early to middle rift climax”, con altas tasas de subsidencia tectónica durante el Langhiense – Serravaliense temprano. Fue seguido de un segundo periodo, el “late rift climax”, donde la actividad tectónica disminuyó. Durante este episodio, el margen noroeste de la Cuenca de Málaga y el área emergida hoy en día formaban el bloque de techo del sistema extensional del “High 976”. Este bloque de muro rotó pasivamente facilitando la migración de las arcillas sobrepresurizadas de la unidad VI hacia el centro de la cuenca, formando así la provincia diapírica de barro. La extensión hacia el NW fue acompañada también de fallas con una dirección WNW-ESE a NW-SE y un movimiento normal i/o siniestro, como es el caso de la falla de Gaucín.

El tercer episodio se corresponde con la inversión tectónica que tuvo lugar a partir del Mioceno tardío y sigue hasta la actualidad. En el área de estudio, las estructuras tectónicas compresivas se limitan a pliegues de pequeña envergadura y levantamientos de los altos estructurales que se produjeron mayormente durante el Mioceno tardío. Estas estructuras fueron también acompañadas de fallas normales y/o siniestras. La poca afectación de la inversión tectónica en el área de estudio contrasta con lo que se observa en otros lados del Domino de Alborán.

1 Introduction

The Gibraltar Arc System is the westernmost orogenic system of the Alpine-Mediterranean orogenic belt. It developed during the late Mesozoic to Cenozoic convergence between Africa and Iberia and includes the Betic-Rif mountain belt, the Alboran and Argelian-Balearic basins and the accretionary prism present in the Cadiz Gulf. As such, the Gibraltar Arc acquired his arcuate geometry during the westward movement from Miocene onwards of its hinterland, the Alboran Domain. During this process, thrusting and folding its external part was coetaneous with back-arc extension.

The study area of this PhD. Thesis is situated in part of the internal zones of this system. It is located in the northwestern margin of the Arc and includes: a) onshore, the outcropping Alboran Domain in the area and b) offshore, the northern branch of the westernmost Alboran Basin (*i.e.* the Malaga Basin).

The Gibraltar Arc System has been studied extensively during the last decades and very significant progress has been done concerning its geological understanding. Nevertheless, there is still a lot of controversy regarding its geodynamic evolution. In the studied area, one of the reasons which contribute to this this controversy is the lack of integrated study which includes onshore-offshore detailed correlations. Indeed, onshore, while the tectonic structures of the Alboran Domain metamorphic complexes is well known in terms of geometry and kinematics, most of the Miocene sedimentary cover is missing, which prevents a good time constraint in the age of these structures. Only offshore studies focused on the Malaga Basin and realized through seismic and well analysis will permit to ease this lack of time constrain.

Within this context, this PhD. thesis tries to integrate offshore and onshore data and to break the barrier that traditionally exists between both type of studies. The ultimate objective is to use these complementary data to improve the knowledge on the Miocene tectonic evolution of the Western Betics, a key area in the Gibraltar arc tectonic history.

2 Geological setting and background

2.1) The Gibraltar Arc orogenic system (western Mediterranean)

The Gibraltar Arc system (GAS) is a strongly arcuate orogen which corresponds with the western termination of the Alpine-Mediterranean orogenic belt. It comprises the Betic-Rif cordilleras, the Guadalquivir, and Gharb-Saïss basins. Offshore, The GAS includes the Gulf of Cadiz in its frontal part, and the Alboran Sea in the inner part. This orogenic system is constituted by three crustal domains (Fig. 2.1): 1) the South Iberian and Maghrebian covers detached from their respective continental paleomargin basement situated north and south of the Gibraltar strait; (2) the Flysch Trough Complex; and (3) the Alboran Domain which represents the metamorphic hinterland of the system. Additionally, Miocene to-Recent basins were formed on top of these crustal domains.

The GAS was formed during Miocene times by thrusting of the peripheral mountain belt coetaneous with crustal extension in the inner part (Platt and Vissers 1989; Comas *et al.*, 1999; García-Dueñas *et al.*, 1992; Maldonado *et al.*, 1992; Watts *et al.*, 1993; among others). The whole system was formed within a general setting of roughly north-south convergence between African and Eurasian plates but its tectonic evolution was governed by an important westward displacement of the Alboran Domain (e.g. Andrieux *et al.*, 1971; Platt *et al.*, 2003).

Due to the shortening produced by the westward migration of the Alboran Domain that acted as a backstop, the Flysch Trough complex units were detached from their thinned continental or oceanic lithosphere and deformed by folding and thrusting (Durand-Delga and Fontboté, 1980; Dercourt *et al.*, 1986; Balanyá and García-Dueñas, 1988). Subsequently, due to the outward migration of the compression, the paleomargins covers were also detached from their Variscan basement, and incorporated in the Gibraltar Arc system. These deformed covers are represented by the Subbetic-Prebetic Domain in the northern branch of the arc, and the External Rif Domain in the southern one (Vera, 2001; Crespo-Blanc and Frizon de Lamotte, 2006; Chalouan *et al.*, 2008). The Flysch Trough Complex and the paleomargins derived units form the external fold-and thrust belt of the orogenic system (Fig. 2.1).

The westward movement of the Alboran Domain was accompanied by extension in its inner part through several brittle and ductile extensional systems which lead to the formation of the Alboran Basin (Fig. 2.1; Comas *et al.*, 1992; García-Dueñas *et al.*, 1992). Extension due to the westward movement ceased during lower Tortonian times (García-Dueñas *et al.*, 1992; Comas *et al.*, 1999; Rodríguez Fernández *et al.*, 1999). From this time and onwards, The GAS geodynamic evolution is governed by the current motion of Eurasia and African plates (Comas *et al.*, 1999; Fernández-Ibáñez *et al.*, 2007; Vernant *et al.*, 2010; Pedrera, *et al.*, 2011) which produced the tectonic inversion of the Alboran Basin and the partial emersion of the Alboran Domain (Fig. 2.2).

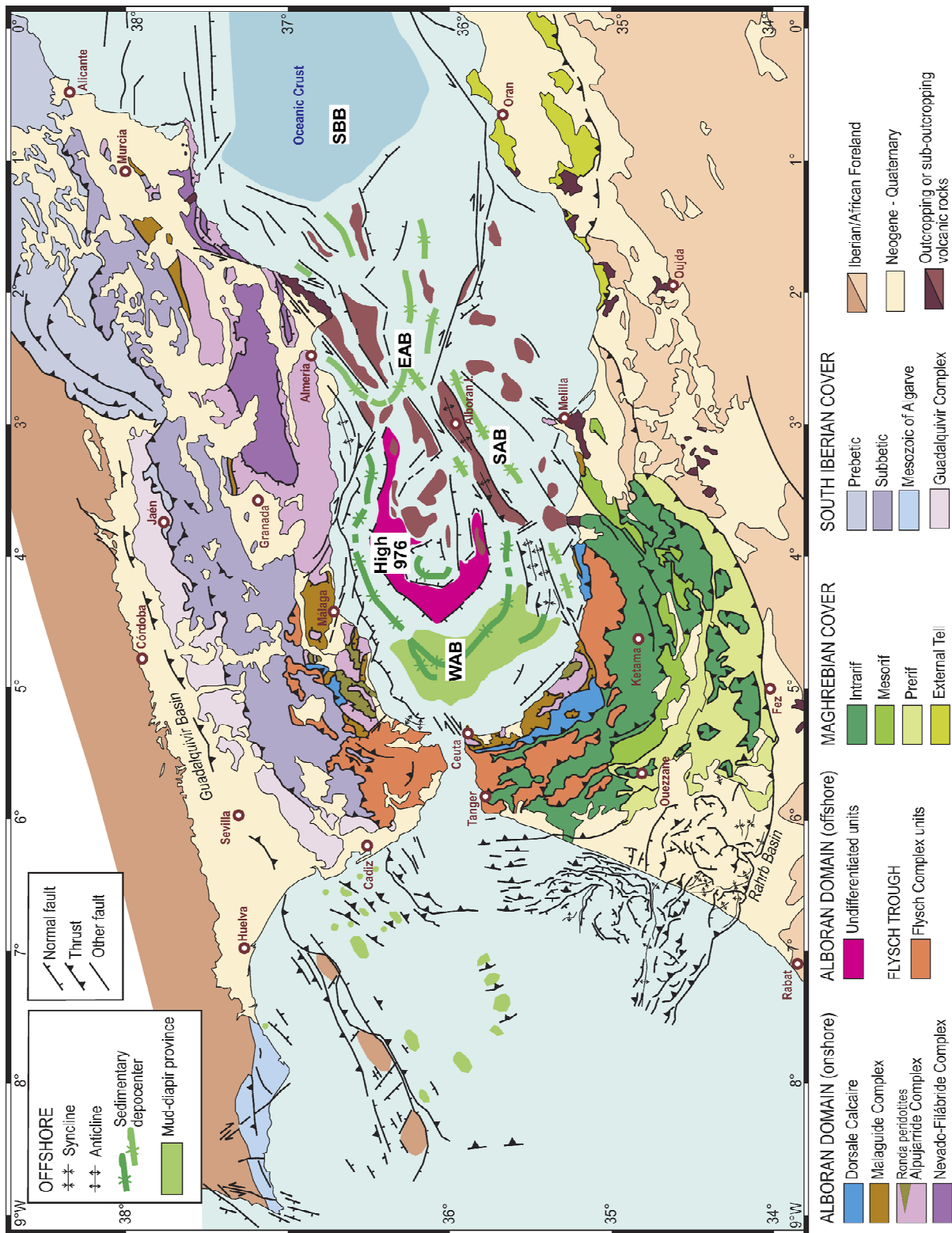


Figure 2.1: Tectonic map of the Gibraltar Arc System (according to Crespo-Blanc and Frizon de Lamotte, 2006). WAB: Western Alboran Basin; EAB: Eastern Alboran Basin; SAB: South Alboran Basin; SBB: South Balearic Basin.

2.2) The Western Betics

The Western Betics corresponds to the northern branch of the so called western Gibraltar Arc which is defined as the hinge zone of the arc (Balanyá *et al.*, 2012). Here, the term Western Betics is limited for the onshore area and extends, approximately, west of 4°W (Figs. 2.1 and 2.2).

The Western Gibraltar Arc has specific structural features in comparison with zones of the Gibraltar arc system that are located east of the 4°W meridian. The most conspicuous one is that the external fold-and-thrust belt mimics the Gibraltar Arc curvature and the transport direction shows a divergent pattern around the arc (Fig. 2.2; Crespo-Blanc and Campos, 2001; Crespo-Blanc and de Lamotte, 2006; Luján *et al.*, 2006; Balanyá *et al.*, 2007; Balanyá *et al.*, 2012). To the north, the continuity of this pattern is cut off by a dextral transpression zone where the structural trend-lines draws a recess and roughly defines the eastern limit of the Western Betics (the Torcal transpression zone in Fig. 2.2; see Balanyá *et al.*, 2012; Barcos *et al.*, 2014). Also, deformation took place between upper Burdigalian to Serravallian times, that is later than the central Betics (Crespo-Blanc and Campos, 2001; Crespo-Blanc and de Lamotte, 2006; Luján *et al.*, 2006; Balanyá *et al.*, 2007). It also stands out that extensional structures accommodating arc-parallel stretching are coetaneous with the folds and thrust that accommodate the arc-perpendicular shortening (Balanyá *et al.*, 2007; 2012). Finally, the presence Flysch Trough Complex is remarkable as this complex is mostly absent east of 40°W in the northern branch of the Arc (Fig. 2.1).

2.2.1) Subbetic units

The Subbetic is a fold-and-thrust belt made of the sedimentary cover of the South Iberian Paleomargin. The rocks involved are non-metamorphosed and range in age from Triassic to Early Miocene (Vera, 2000). The Triassic sequence is characterized by carbonate rock and an upper sequence with typical Keuper facies made of fine-grained sandstones and claystones with evaporites. The Jurassic is a shallow marine sequence dominated by rocks typical of a carbonate platform (marls, limestones, dolomites). In the western Betics, the Jurassic is capped by a regional unconformity followed by the Upper Cretaceous sequence characterized by a pelagic facies of marls and marly limestones. Finally, the Tertiary is only represented locally by an Early Miocene flysch-type sequence of clays alternated with sandstones levels (Martín-Algarra, 1987; Vera, 2000; Crespo-Blanc and Frizon de Lamotte 2006).

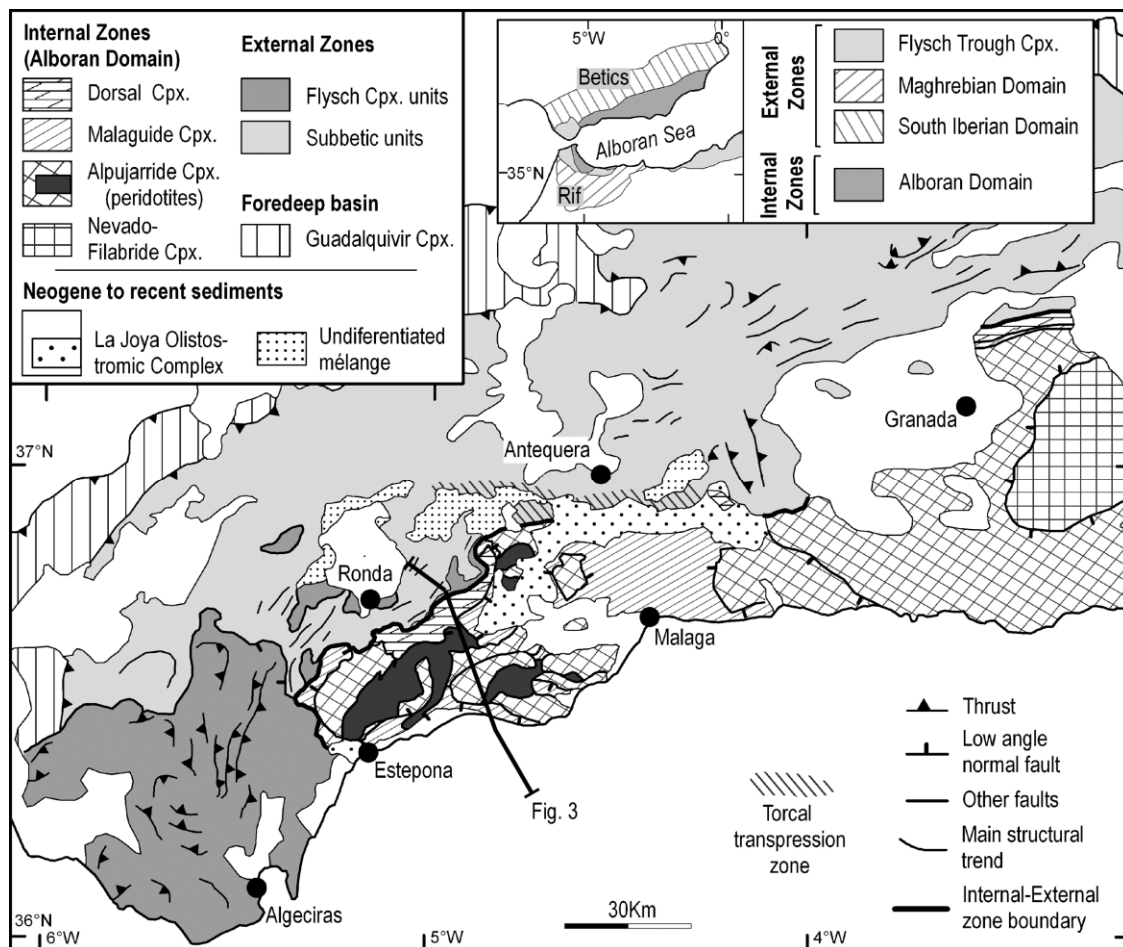


Figure 2.2: Main tectonic domains in the Western Betics. Cpx: Complex. Inset: sketch of the Betic-Rif orogenic system.

The structure of the Subbetic Domain is strongly influenced by the rheology of its sedimentary sequence and, especially, by the Triassic evaporites situated at the bottom. The evaporites provide a ductile level from which the rest of the sedimentary cover is detached. The resulting fold-and-thrust belt is characterized by the presence of out-of-sequence thrust, back-thrusts and box-type folds, especially in the areas where the evaporitic sequence is thick (Fig. 2.3; Crespo-Blanc and Frizon de Lamotte 2006). The folds and thrust show mostly a SW-NE to SSW-NNE direction even though this can vary latter (Fig. 2.2; Crespo-Blanc and Campos 2001; Crespo-Blanc *et al.*, 2012). Additionally, normal faults mainly NW-SE directed, coetaneous with the compressional structural, are also affecting the Subbetic (Balanyá *et al.*, 2007; 2012). Both extensional and compressional structures developed at the same time, producing either arc-perpendicular shortening or arc-parallel extension. Finally, in the Torcal Shear Zone, the structural style of the Subbetic differs from what is observed in the rest of the Western Betics. Here, the major structures are a conjugated set of E-W and NW-SE dextral strike-slip faults, and NE-SW-directed folds and thrusts, upper Miocene to Recent in age. The structural pattern is characteristic of a dextral transpressional regime eventually

2. Geological setting and background

superposed to the lower to middle Miocene structures (Fig. 2.2; Balanyá *et al.*, 2012; Barcos *et al.*, 2014).

The age of the deformation in the Subbetic is diachronous along the Betics. In the western Betics, the youngest rocks considered as pre-tectonic are the Aquitanian to Burdigalian flysch-type sequences. Thus, the formation of the fold-and-thrust belt is considered to have taken place during Burdigalian to Serravallian times (Vera, 2000; Crespo-Blanc and Campos, 2001) even though compression could still be active (Balanyá *et al.*, 2012).

2.2.2) Flysch Trough Complex

In the western Betics the Flysch Trough Complex crops out from the Gibraltar Strait until, approximately, Antequera (Fig. 2.2). This complex consists of Cretaceous to lower Miocene clastic rocks, with dominance of turbiditic facies (Didon, 1969). These deep-water deposits were originally deposited in an accretionary prism over an oceanic or very thin continental crust (Dercourt *et al.*, 1986; Durand-Delga *et al.*, 2000). The Flysch Trough Complex is structured as an imbricated thrust stack and emplaced structurally over the Subbetic units while it is overlain by the Alboran Domain (Fig. 2.3; Balanyá and García-Dueñas, 1988; Crespo-Blanc and Campos, 2001). It is constituted mainly by siliciclastic sediments and also by some carbonates of turbiditic character (Esteras *et al.*, 1995; Stromberg and Bluck, 1998).

The stratigraphic column of the Flysch Trough Complex starts with Cretaceous formations that appear as discontinuous slices beneath the rest of the Paleogene to Miocene sequence (the Facinas unit; Didon, 1969; Martín-Algarra, 1987). The Cenozoic sequence starts with the “Serie de base” formation (Esteras *et al.*, 1995) constituted by reddish-greenish clays that contain intercalations of Paleocene to Oligocene calciturbidites. The Miocene sequence is the thickest one and mostly Aquitanian in age. There are significant differences in the provenance of the detritus present in this turbidite sequence that led to a differentiation of the Flysch Trough Complex in three main units. In the northern branch of the Gibraltar arc these units are called Aljibe, Algeciras, and Bolonia (Didon, 1969). Indeed, the Aquitanian sequence of Aljibe unit contains sandstone levels of quartzite while that of Algeciras unit is made of graywackes. The Bolonia unit shows an alternating of both quartzites and graywackes. Finally, the youngest sediments found in the Flysch Trough Complex belong to the Supranumidian formation (Esteras *et al.*, 1995). This formation is only observed in the Aljibe unit and has been dated as lower Burdigalian. It contains marls, clays and quartzitic-micaceous sandstones.

The general architecture of the Flysch Trough Complex is that of a thin-skinned imbricate thrust system (Luján *et al.*, 2006). The detachment level is localized at the bottom of the “Serie de base” formation and the geometry of the thrust system is

severely influenced by the presence or not of Subbetic Triassic evaporites below the Flysch units. These Triassic evaporites act as a viscous decollement level which is responsible of drastic changes in the direction and vergence of the overlying Flysch Trough Complex thrust system (Luján *et al.*, 2003; Crespo-Blanc *et al.*, 2012). Therefore, even if the main thrusts trend is NNE-SSW oriented with transport towards the WNW important variations of the structural pattern are observed, especially in its southern and western part (Fig. 2.2). Indeed, large oblique structures shaped with crescent-like geometries have been described (Crespo-Blanc *et al.*, 2012). The youngest rocks affected by these structures correspond with the Supranumidian formation, lower Burdigalian in age, and the deformation is considered to have taken place mainly from late Burdigalian to Langhian times (Luján *et al.*, 2006). Additionally, the flysch units have been also affected by extensional faults (e.g. Colmenar fault Luján *et al.*, 2000) and open folds that are associated with arc-parallel extension coetaneous with the main shortening (Balanyá *et al.*, 2012).

Apart from the previous Flysch Trough units, there are other structural units known as the Predorsal units (Durand-Delga, 1972; Olivier, 1984). They are considered as part of the Flysch Trough complex and crop out along the internal-external zone boundary as a thin band (Flysch units next to the Internal-external zone boundary in Fig. 2.2), i.e. between the Alboran Domain on top and the other Flysch Trough Complex units below (Fig. 2.3). These units are characterized by dismembered slices of Jurassic to lower Miocene rocks. From Cretaceous to Neogene, the sequence contains turbiditic-type deposits, similar to the others Flysch Trough Complex units. By contrast the Jurassic rocks are mostly calcareous and show a strong affinity with the Dorsal Complex from the Alboran Domain (Olivier, 1984; Martín-Algarra, 1984; see next epigraph).

2.2.3) Alboran Domain

The Alboran Domain is a Palaeozoic terrane that represents the hinterland of the Gibraltar Arc system. It is subdivided into three main metamorphic complexes, which from bottom to top are: the Nevado-Filabride, the Alpujarride, and the Malaguide Complex (Didon 1969). The first two complexes show a similar metamorphic evolution and contain middle to high grade metamorphic rocks while the Malaguide complex only contains low grade metamorphic rocks in its lowermost parts (Chalouan and Michard, 1990; Balanyá, 1991; Balanyá *et al.*, 1997; Azañón *et al.*, 1998). A fourth non-metamorphic complex, called the Dorsal Complex (Durand-Delga and Foucault, 1967) is also present. It only outcrops discontinuously in the western Betics and the Rif along external-internal zone boundary (IEZB; Fig. 2.2) thrusting the external zones and, at its turn, it is thrust by the Malaguide and Alpujarride complexes (Balanyá and García-Dueñas, 1986; Balanyá, 1991).

2. Geological setting and background

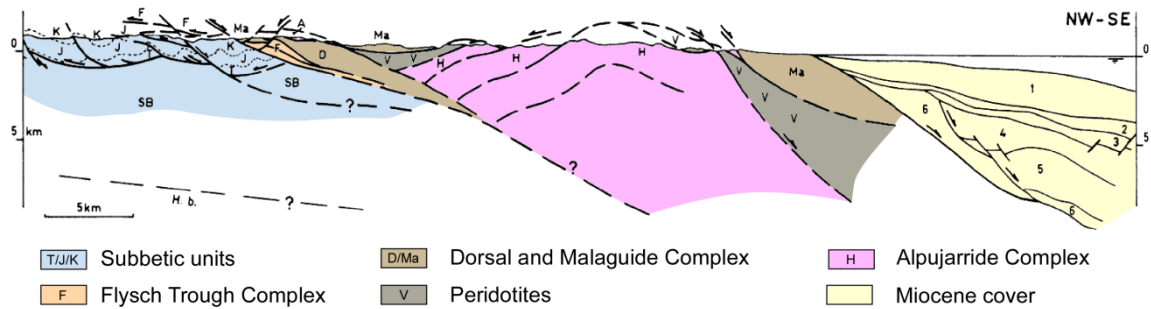


Figure 2.3: Cross-section taken from Crespo-Blanc and Campos (2001) that shows the structural relationship between the Subbetic units, the Flysch Trough units, and the Alboran Domain complexes in the western Betics.

The Nevado-Filabride complex is not represented in the western Betics and only crops out in the central and eastern parts of the northern branch (Fig. 2.1). The Alpujarride Complex is made of a Paleozoic to Permo-Triassic metapelitic-metapsammitic sequence and Triassic carbonate rocks. This complex is made up by units of variable metamorphic grade that are, from bottom to top: Lujar, Escalate Herradura, Salobreña and Adra units (Azañón and Crespo-Blanc, 2000).

In the western Betics, only the three uppermost complexes are present (see Balanyá *et al.*, 1998). Between the two uppermost Alpujarride units it stands out the presence of peridotite slices composed mainly of lherzolite and minor harzburgite layers (Dickey *et al.*, 1979; Sánchez-Gómez *et al.*, 1996; Lenoir *et al.*, 2001). In addition, the lowermost unit (Herradura unit) contains leucogranite bodies (Muñoz, 1991) with an approximate age of 22Ma (Zeck *et al.*, 1989).

The Malaguide Complex, situated on top of all metamorphic complexes, mostly consists of a sequence made of phyllites and carbonates, Paleozoic in age, which show low metamorphic grade. An unconformity is observed on top of the Paleozoic sequence which is overlain mainly by a Triassic non-metamorphic cover that consists of red conglomerates and sandstones. Moreover, scattered outcrops of Jurassic to Eocene carbonates can be observed on top of this complex (Boulin, 1970; Cuevas *et al.*, 2001).

Finally, The Dorsal Complex (Durand-Delga and Foucault, 1967) is mainly composed by Triassic and Jurassic non-metamorphic rocks with a predominance of carbonated series. Occasionally, the sequence contains younger sediments up to lower Miocene in age that show a more siliciclastic sequence (e.g. Brecha de Nava, Aquitanian in age; Martín-Algarra, 1984; Olivier 1984; Balanyá, 1991). The Dorsal Complex is sandwiched between the Malaguide and the Flysch Trough units, thrusting the External zones in the IEZB (Fig. 2.3; Balanyá and García-Dueñas 1988; Crespo-Blanc and Campos, 2001; Balanya *et al.*, 2012).

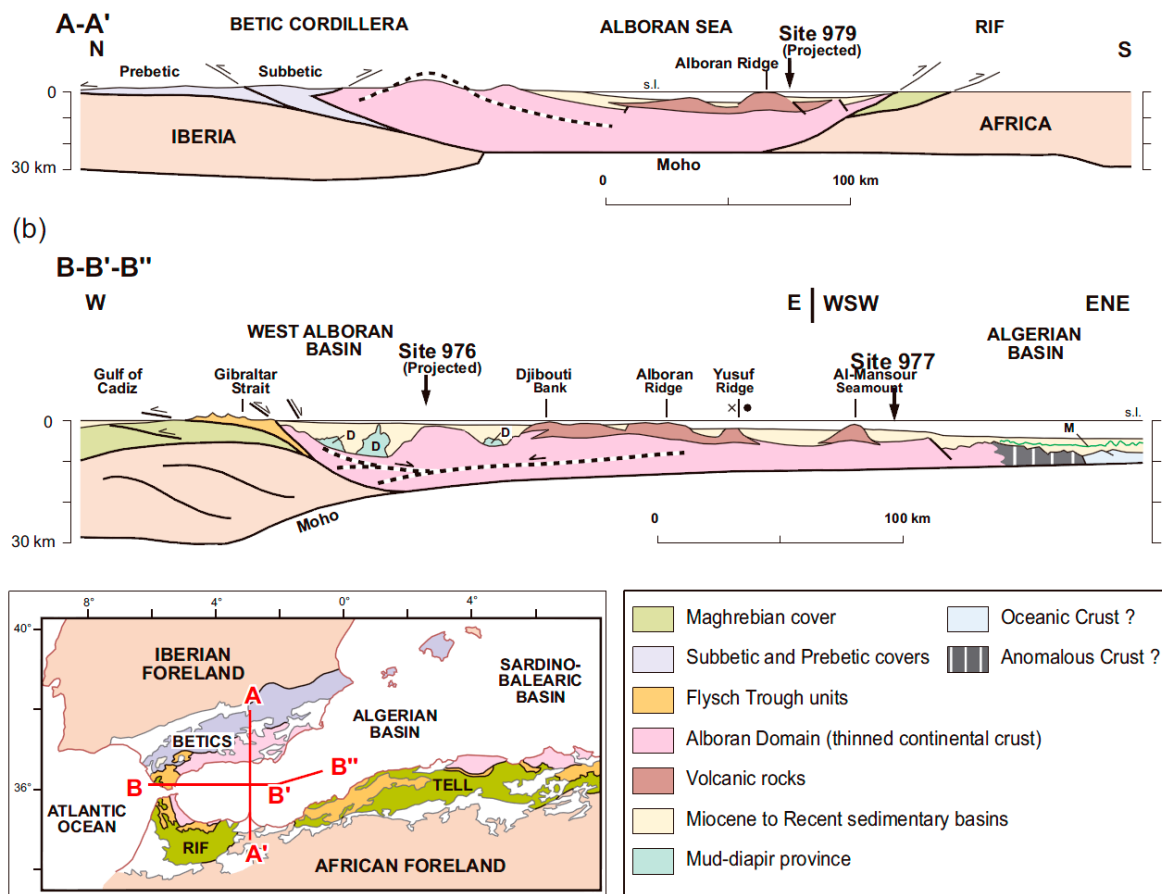


Figure 2.4: Schematic crustal cross-sections of the Alboran Basin. A) North-south section based on a synthesis of structural data from Spain and Morocco and Conrad seismic lines and on a density model obtained by comparing observed and calculated Bouguer anomaly data (Watts *et al.*, 1993). Hatched white lines correspond with intracrustal reflectors interpreted as extensional detachments. B) West-East section based on a synthesis of structural data from the Gibraltar region and MCS profiles in the Alboran Sea, 3D modelling, gravity consideration, surface heat-flow, and elevation data (Torné *et al.*, 2000). Figure taken from Martínez-García (2012). Original cross-section from Comas *et al.* (1999).

The tectonic structure observed nowadays in the Alboran Domain is the result of multiple tectonic events. The lower complexes of the Alboran Domain (Alpujarride and Nevado-Filabride) show a complex ductile metamorphic evolution that evolved from high pressure and low temperature, to low pressure and moderate to locally high temperature (Azañón *et al.*, 1998; Soto and Platt, 1999; Puga *et al.*, 2000). This P-T path suggests that the Alboran Domain underwent crustal thickening followed by ductile extension, then a post-metamorphic nappe stack took place, and finally a third main event occurred (Balanyá, 1991; Azañón, 1994; Balanyá *et al.*, 1997). The third event was related with the back-arc rifting which thinned the post-metamorphic nappe stack of the Alboran Domain (García-Dueñas *et al.*, 1992). This thinning was accommodated by ductile to brittle shear zones and brittle extensional detachments that bound most of the tectonic units of the Alboran Domain complexes in the present day (García-Dueñas *et al.*, 1992; Crespo-Blanc, 1995; Balanyá *et al.*, 1997; Martínez-Martínez & Azañón, 1997).

2. Geological setting and background

Several low angle normal fault systems active during Lower to middle Miocene times (Burdigalian to Serravallian) have been described in the central and western Betics (Fig. 2.1; García-Dueñas *et al.*, 1992; Crespo-Blanc, 1995). In the central Betics these systems are successive and show nearly orthogonal directions of extension. By contrast, in the western Betics such succession of fault systems is not observed and the tectonic transport is broadly centripetal. (Balanyá, 1991; García-Dueñas *et al.*, 1992; Alonso-Chavez and Orozco, 1998; Booth-Rea *et al.*, 2003).

The Alboran Domain complexes are also affected by late Tortonian to Recent structures. The low-angle normal faults presently appear folded (Fig. 2.3) as a consequence of the formation of open folds with NE-SW to E-W direction. High angle normal and strike-slip faults also developed during this period, post-dating previous structures (Sanz de Galdeano and López-Garrido, 1991; García-Dueñas *et al.*, 1992; Sánchez Gómez *et al.*, 1996; Booth-Rea *et al.*, 2003; Insua-Arévalo, *et al.*, 2012).

2.2.4 Neogene sedimentary infill (onshore)

Foredeep basins developed during the main orogenic phase on the external zones of the Gibraltar Arc. One of the most important in the studied area is the Ronda basin (Fig. 2.2). This Basin consists of a basal deposition made of sandstones and conglomerates, followed by a sequence of calcarenites and limestones that range in age between late Tortonian to Messinian times (Serrano, 1979; Rodríguez-Fernández *et al.*, 1999). These deposits are slightly affected by folds that developed during the latest Tortonian to Messinian due to the contractive reorganization of the Gibraltar arc (Crespo-Blanc and Campos, 2001).

In the internal zones, the extensional tectonics contributed to the subsidence of the Alboran Domain which outcrops onshore and to the deposition of Miocene sediments unconformably over the metamorphic complexes (Balanyá and García-Dueñas, 1986; García-Dueñas *et al.*, 1992). In the western Betics the oldest deposits are observed in small, scattered outcrops. These deposits, known as Ciudad-Granada and La Viñuela groups (Martín-Algarra, 1987; Serrano *et al.*, 2007), are characterized by an initial sequence of breccias or conglomerates with clasts that derived from the nearby Alpujarride and/or Maláguide metamorphic rocks (Serrano *et al.*, 2007). Marls and limestones on top of the breccias have been dated as Aquitanian to early Burdigalian in age (González-Donoso *et al.*, 1987; Martín-Algarra, 1987; Aguado *et al.*, 1990; Durand-Delga *et al.*, 1993; Serrano *et al.*, 2007). It can be observed how some of these deposits post-date the low-angle normal faults that affect the Alboran Domain metamorphic complexes (Alonso-Chavez and Rodríguez-Vidal, 1998). Nevertheless, most of the Miocene infill situated over the internal zones corresponds to a *mélange* that rest unconformably over the previous deposits (La Joya olistostromic Complex in Fig. 2.2). The genesis, age and nature of this *mélange* has been controversial and received several

interpretations by various authors (Peyre, 1974; Bourgois, 1978; Olivier, 1984; Martín-Algarra, 1987; Balanyá, 1991). The study of this mélange is an important part of this PhD. Thesis and will be described in detail in chapter 4 (epigraph 4.2).

Finally, near-horizontal conglomerates, sandstones and calcarenites, Tortonian in age, are present outcropping isolated along the onshore Malaga Basin (López-Garrido and Sanz de Galdeano, 1999).

2.3) The Alboran Basin

The Alboran Sea comprises the submerged area between the Gibraltar Strait and 1°W meridian to the east (Fig. 2.1). The Alboran Basin includes not only the Alboran Sea but also onshore areas close to the coast-line where some sedimentary infill of the Alboran Basin can be observed. It is located in the hinterland of the Gibraltar arc.

The basin formed during the Alboran Domain rifting and its tectonic evolution went hand by hand with that observed onshore (Comas *et al.*, 1999; Rodríguez Fernández, *et al.*, 1999). Its tectonic evolution can be summarized in to main events: 1) extensional tectonics which controlled the deposition and shaped the basin during Lower to Middle Miocene times resulting in the compartmentalization of the basin into several sub-basins (Fig. 2.1; see epigraph 2.3.2), 2) tectonic inversion that took place from Late Miocene onwards and responsible for the rough sea floor topography of the Alboran Basin (Comas *et al.*, 1999; Ballesteros *et al.*, 2009; Martínez-García *et al.*, 2010).

2.3.1) Basement structure

The basement of the Alboran Basin is made of the Alboran Domain rocks and volcanic rocks that intruded them.

Regarding the metamorphic rocks, core samples from ODP site 976 in the western part of the Alboran Basin (Fig. 2.5) showed that they are made of high grade schist with marble, migmatites and gneiss. This lithologic sequence of high-grade metamorphic rocks and their pressure-temperature paths are similar to those from the Alpujarride complex and, most likely, from Herradura unit (Sánchez-Gómez, *et al.*, 1996; Soto and Platt, 1999). Even though data from the basement structure is scarce, cores from Site 976 and multichannel seismic profiles analysis reveal that the metamorphic basement has been affected by several normal fault systems (De Larouzière, *et al.*, 1999; Comas and Soto, 1999).

The volcanic rocks have been observed mostly east of the 4°W forming roughly a NE–SW trending band (Fig. 2.1) and result of extinct volcanic edifices (Duggen *et al.*, 2004, 2008). They belong to the tholeiitic and calc-alkaline series and the age of the

2. Geological setting and background

associated volcanism span from middle-upper Miocene to Pleistocene times (Battistini, *et al.*, 1987; Hoernle, *et al.*, 1999; Duggen *et al.*, 2004).

The most relevant basement highs of the Alboran basin are: the Alboran Ridge, and the High 976 (Fig. 2.1). The Alboran Ridge is a narrow SW-NE oriented high which reaches more than 100km long. It registers a complex deformational history during the tectonic inversion (early Pliocene to early Pleistocene) of the basin with three phases of shortening that caused folding and uplift, transpression or transtension depending on the stress field during each moment of time (Martínez-García *et al.*, 2013). The High 976 is also a narrow and elongated High which draws an Arc that mimics the curvature of the whole Gibraltar Arc (Fig. 2.1). High 967 has been considered as a rollover basement structure developed during the extensional episode. It is shaped by normal faults in its external flank that were later affected by tectonic inversion which induced uplift and strike slip tectonics (Comas *et al.*, 1992; Comas and Soto, 1999).

Geophysical and modelling studies indicate that the crustal structure of the Alboran Basin is characterized by an important thinning of the continental crust from the Betics towards the center of the basin. The crustal thicknesses go from ~35km near the orogenic arc to 15-21km in the centre of the Alboran Sea. (Fig. 2.4; Torné & Banda, 1992; Watts *et al.*, 1993; Galindo-Zaldívar *et al.*, 1997; Torné *et al.*, 2000; Fernández-Ibáñez *et al.*, 2007; Soto *et al.*, 2008). Towards the east, a progressive transition of the continental crust of the Alboran Domain to the oceanic crust of the South Balearic Basin with a thickness of ~9km can be observed (Figs. 2.1 and 2.4; Comas *et al.*, 1999; Booth-Rea *et al.*, 2007).

2.3.2) Sedimentary infill and seismostratigraphic units

The sedimentary infill of the Alboran Basin synchronous with the rifting processes comprises a range of deposits from lower Burdigalian to lower Tortonian. From upper Tortonian onwards, deposition took place during tectonic inversion.

The rifting associated with LANF systems resulted in a compartmentalization of the basin. The most important sub-basins are: the West Alboran Basin (WAB), the East Alboran Basin (EAB) and the South Alboran Basin (SAB; Comas *et al.*, 1999; see Fig. 2.1).

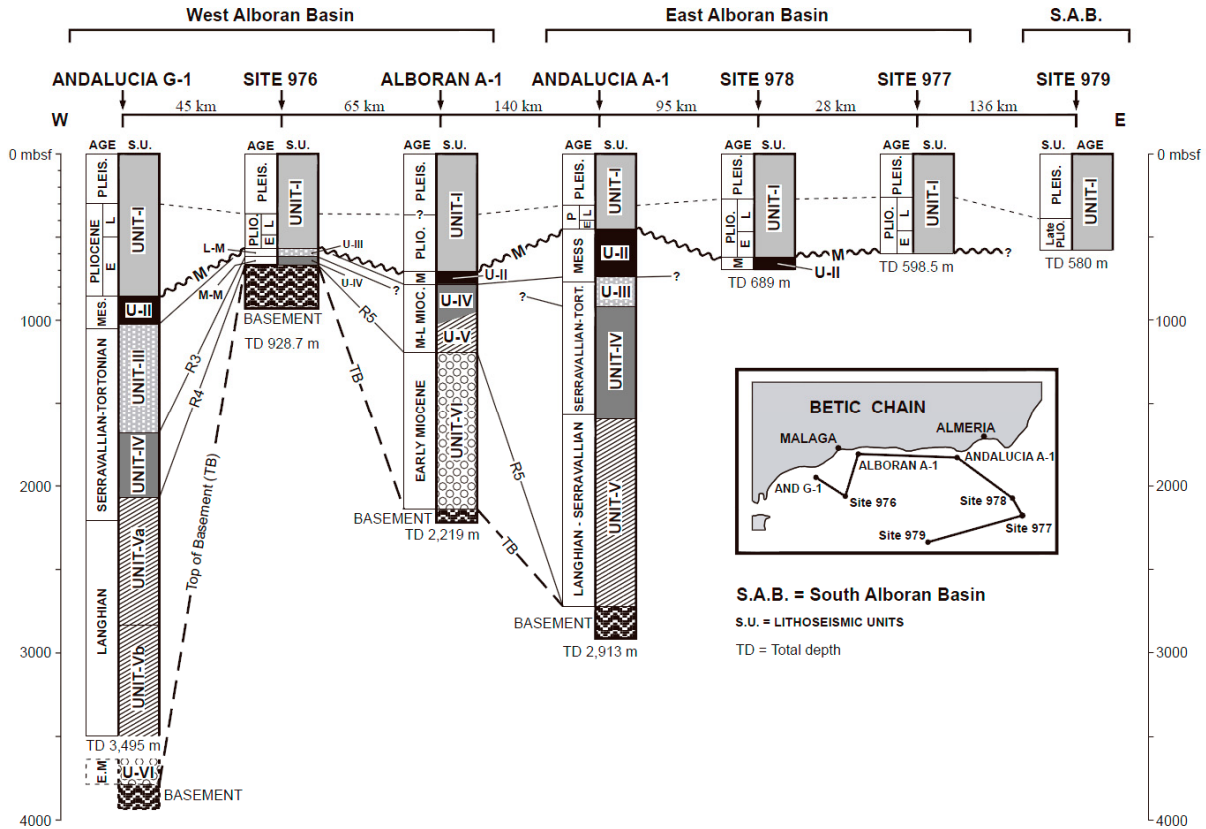


Figure 2.5: Well correlation of the seismostratigraphic units present in the Alboran Basin from Comas *et al.*, (1999). The ages in each well and major unconformities are also shown (R5 to R2 and M). M: Messinian unconformity. Inset: location of wells used in the correlation.

These basins show important differences in terms of sedimentary thicknesses and age of deposits. Thus, the EAB and the SAB are characterized by depocenters from middle-Miocene or post-Tortonian in age while the WAB is the only one that contains deposits from early Miocene (Fig. 2.1). The WAB also presents the maximum thicknesses in the Alboran Basin as the sediments reach more than 8km thick (Soto *et al.*, 1996; Iribarren *et al.*, 2009). This depocentre mimics the curvature of the Gibraltar Arc, in a similar way as the structural High 976. Therefore it shows a general N-S trending and, towards the north, it swings into an E-W direction while, towards the south, a NW-SE direction is observed (Fig. 2.1).

The sedimentary infill of the Alboran Basin has been subdivided into six seismostratigraphic units labeled I to VI from top to bottom (Comas *et al.*, 1992; Jurado and Comas, 1992; Fig. 2.6). These units are bounded by unconformities (R6 to R1) and have been correlated along the available wells (Fig. 2.5), either commercial (Alb-1, And G-1, And-A1) or academic (ODP sites 976, 977, 978 and 979).

The oldest deposits that lie directly over the metamorphic basement are Aquitanian(?) – Burdigalian in age and correspond with Unit VI, the thickest unit in the Alboran Basin. This unit has only been drilled in well Alb-A1 (Fig. 2.5) and its

2. Geological setting and background

lowermost deposits are made of sandstones and breccias that contain fauna indicative of a shallow depositional environment (Jurado and Comas, 1992). Nevertheless, most of Unit VI sequence has been interpreted as olistostromic deposits with an unclear depositional environment. Furthermore, Unit VI contains undercompacted materials revealed by well logs (Jurado and Comas, 1992). Those materials are considered to nourish a large mud diapiric province observed in the center of the WAB (Comas *et al.*, 1992; Chalouan *et al.*, 1997; Talukder *et al.*, 2004; Soto *et al.*, 2010; Comas *et al.*, 2012). Sometimes, the mud diapirs pierce the whole sedimentary sequence and form mud volcanos that have been sampled and confirmed that the mud-diapir matrix is equivalent to unit VI deposits (Sautkin *et al.*, 2003). The top of Unit VI is a strong unconformity (R5) that shows an important erosional character.

Unit V contains mostly red and green clays with some levels of sandstones and conglomerates dated as Langhian to Lower Serravallian in age that are accompanied by scarce volcanogenic deposits. These deposits have been interpreted as deposited in a deep marine environment (Jurado and Comas, 1992; Martínez del Olmo & Comas, 2008). In well And-G1 (Fig. 2.5) the lower half of this unit shows undercompaction, as in unit VI, which led to the subdivision of the unit between subunit Va (upper part) and Vb (lower part). The top of unit V is marked by R4 unconformity which is a high-amplitude reflector associated to rich levels in volcanogenic deposits.

Unit IV contains mainly sandstones and clays with conglomeratic intercalations interpreted as deltaic and turbiditic system. The age of these deposits is Upper Serravallian to Lower Tortonian. Units VI to IV have been considered as the syn-extensional units of the Alboran Basin sedimentary infill and the R3 unconformity, on top of unit IV, as the breakup unconformity (Jurado and Comas, 1992; Comas *et al.*, 1992). R3 is an angular unconformity, although observed as a paraconformity in the deepest parts of the basin.

Unit III is the first post-rift unit. It is upper Tortonian in age and composed by claystones and limestones with sandstones levels deposited in an open marine environment. It is followed by the Messinian sequence that corresponds with Unit II which is made of an alternating carbonates and clays with levels of anhydrite and gypsum. Unit II is a very thin sequence that has been severely affected by a strong erosional unconformity (R2 or M reflector). In consequence, in some parts of the basin, the entire unit is missing. The rest of the sedimentary infill is represented by the Pliocene to Quaternary Unit I which, in the eastern part of the Alboran Basin, represents most of the sedimentary cover (Fig. 2.5).

The sediments deposited in the Alboran Basin are mostly clastic. Studies concerning the clay mineral assemblages indicate that the source area of these deposits is the nearby Betics and Rif mountains, which is mainly represented by the metamorphic complexes of the Alboran Domain (Marsaglia *et al.*, 1999). The total

volume of sediments deposited in the Alboran Basin has been estimated as 89.600 km³ (Iribarren *et al.*, 2009).

2.3.3) Tectonic evolution

The back-arc extension governed the Alboran Basin evolution from Early Miocene until Late Miocene (from ~21Ma to ~9Ma; Fig. 2.6). From Late Miocene onwards rift related extension ceased and the tectonic inversion affected the basin producing mainly shortening and transpression (Fig. 2.6; Maldonado *et al.*, 1992; Watts *et al.*, 1993; Chalouan *et al.*, 1997; Comas *et al.*, 1999; Mauffret *et al.*, 2007).

Based on thermal modelling studies, the crustal thinning of the Alboran Basin basement started around 27Ma (Fig. 2.6) which produced the exhumation of metamorphic rocks from the Alpujarride complex (Platt *et al.*, 1998; Soto and Platt, 1999). The first marine invasion did not take place until Early Miocene times with the deposition of unit VI. During the sedimentation of units VI to IV, basin tectonic subsidence took place (Docherty and Banda, 1992; Watts *et al.*, 1993). Extension is considered to have been accommodated by brittle deformation through the LANF's systems that can be observed onshore in the Betics (Fig. 2.4; Comas *et al.*, 1992; de la Linde *et al.*, 1996; Comas and Soto, 1999; Martínez del Olmo and Comas, 2008).

Backstripping analysis from the available wells point out to various successive phases of tectonic subsidence that took place from early to middle Miocene (Docherty and Banda, 1992; Watts *et al.*, 1993; Rodríguez-Fernández *et al.*, 1999). In the WAB this episode was also characterized by the start of the mud diapirism (~15-16Ma) which also controlled the deposition in the basin until recent times (see profile B of Fig. 2.4; Talukder, *et al.*, 2003; 2004; Soto *et al.*, 2010). The extensional episode was also characterized by the presence of magmatism and volcanism from approximately ~15Ma until ~6Ma (Fig. 2.6; Bellon *et al.*, 1983; Comas *et al.*, 1999; Duggen *et al.*, 2004).

Once the back-arc extension ceased, the Alboran Basin underwent tectonic inversion, governed by the NW-SE convergence between Eurasia and African plates. The shortening was characterized by a deformation dominated by inversion of previous normal faults, folding and uplift of the basement high, associated with strike-slip tectonics (Fig. 2.6; Comas *et al.*, 1992; 1999; Maldonado *et al.*, 1992; Chalouan *et al.*, 1997; Martínez-García *et al.*, 2013). Nevertheless, the amount and the type of tectonic inversion observed are heterogeneously distributed along the basin (Comas *et al.*, 1999). Thus, most of the tectonic inversion is observed towards the east of east, while the inversion observed in the WAB is minor (Suades *et al.*, 2013). Shortening produced the rough sea floor morphology and the partial uplift and emergence of the Alboran Basin while some previous sub-basins were completely isolated and are exposed nowadays onshore (see epigraph 2.2.4; Comas *et al.* 1992; Sanz de Galdeano and Vera, 1992;

2. Geological setting and background

Rodríguez- Fernández *et al.*, 1999; Ballesteros *et al.*, 2009; Martínez-García *et al.*, 2010).

During tectonic inversion the basin architecture was affected by a desiccation event observed throughout the Mediterranean Sea. This event is known as the Messinian salinity crisis and took place approximately between 6.0 and 5.3 Ma. It was caused by the closure of the marine pathways that connected the Atlantic Ocean with the Mediterranean Sea (Clauzon *et al.*, 1996; Krijgsman *et al.*, 1999; García-Castellanos *et al.*, 2009; Estrada *et al.*, 2011; among others). In the Alboran Basin it produced significant erosion of the paleo-seafloor and is observed in the seismic lines as a strong, high amplitude reflector (R2) known as “reflector M”, that affects the entire basin (Fig. 2.6; Jurado and Comas, 1992; Comas *et al.*, 1999).

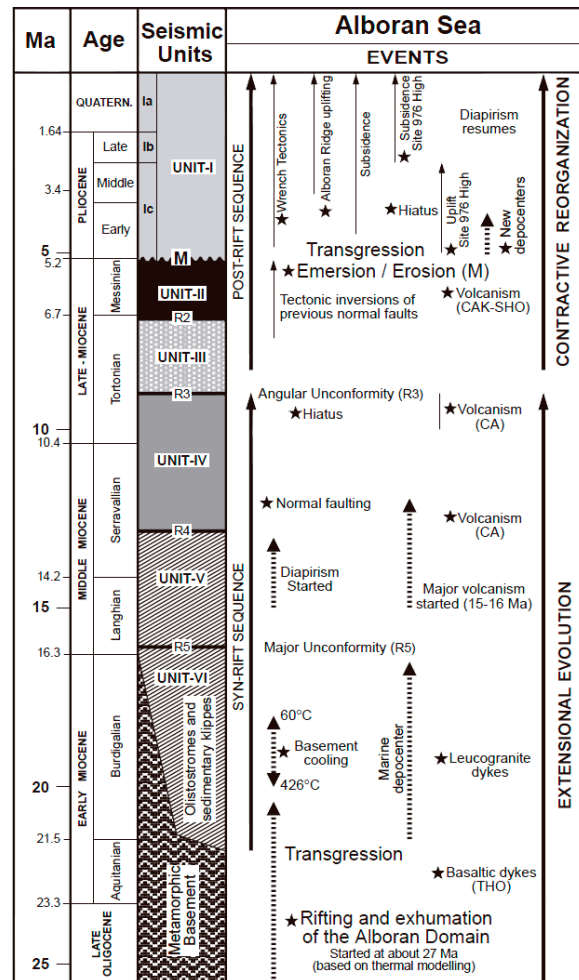


Figure 2.6: Schematic chart from Comas *et al.*, (1999) that shows the seismostratigraphic units and the timing of the main events related with the tectonic evolution of the Alboran Basin.

2.4) Objectives of this PhD Thesis

The aim of this PhD Thesis is to contribute to a better understanding of the tectonic evolution of the Gibraltar Arc orogenic system by studying a selected area situated in the westernmost part of the northern branch of the Arc. This study area is situated in the internal zones of the Arc, between meridians 5°30'W and 3°30' W, along the northwestern margin of the Alboran Basin and my PhD includes both onshore and offshore data. I will focus on the correlations between both types of observations. This integrated study in a key area to decipher the Gibraltar Arc history will permit to better understand the tectonic evolution of the Gibraltar orogenic system during Miocene times.

Within this context, the specific objectives of this PhD Thesis are the following:

Concerning the data collection and their analysis:

- Onshore:
 - a) to characterize the Miocene deposits that lie on the Alboran Domain in the onshore area in order to shed light on their nature and origin;
 - b) to establish the relationships of these sediments with the extensional structures that affected the Alboran Domain during Miocene times.

- Offshore:
 - a) to revise the interpretation of the multichannel seismic lines of various commercial campaigns situated within the Malaga Basin.
 - b) to realize a 3D seismic analysis of this Basin through a careful mapping of the main basin structures and distribution of the Miocene deposits by using updated software (Kingdom Suite).

The onshore data are presented in Chapter 4, meanwhile the offshore ones in Chapter 5 and 6

Concerning the correlation between onshore and offshore data:

- to correlate the Miocene to Recent sedimentary units which outcrop both onshore and offshore and to establish their relationship with the tectonic structures observed in the Alboran Domain.
- to use onshore and offshore complementary data in order to constrain the geometry, kinematics, and age of some major tectonic structures observed in the Alboran Domain.

2. Geological setting and background

- to characterize the extensional mechanisms that led to the formation of the Malaga Basin during Miocene times and to compare it with the tectonic processes that occurred at the same time in its basement and which can be observed onshore.
- to constrain the timing and amount of tectonic inversion that took place in the studied area from late Miocene onwards.

These correlations are essentially presented in Chapter 7.

2.5) Structure of this PhD Thesis volume

Concerning the structure of this PhD Thesis volume, it includes published papers and submitted manuscripts, which agree with the regulations of the “Comisión de Doctorado” of the University of Granada. These papers or manuscripts are enclosed without any modification, neither of the text nor of the figures, in Chapters 4 and 5. A short introduction at the beginning of these chapters presents them.

3 Dataset and methodology

3.1) Onshore study

3.1.1) Dataset

A significant amount of data was already available and served as a starting point for the onshore study. The first one is the MAGNA's series, the 1:50.000 geological maps provided by the Spanish geological service (IGME, *Instituto Geológico y Minero de España*). Table 3.1 shows the full list of IGME maps used in this Ph.D. Thesis. Additionally, Peyre (1974), Bourgois (1978), and Martín-Algarra (1984) realized their Ph.D. Thesis in the studied area (or parts of it) and also made a valuable cartography. It must be stressed that, since all those maps were made by different authors (including the IGME maps), the interpretations and nomenclature of the units and/or lithological sequences differ from one map to the other. Moreover, most of these maps were done during the 70s and 80s and, during the last two decades, a significant advance on the geological knowledge of this area happened (see chapter 2). Accordingly, these maps have been revised.

In addition to the geological maps, a digital terrain model (DTM) of the Andalucía province (southern Spain) has been used. The model was made from aerial photographs carried out during years 2001 and 2002 in black and white. The DTM is at a scale of 1:20.000 and its grid has a resolution of 10x10 meters.

Reference	Name of the map	Authors	Year of the cartography
1023	Antequera	Martín-Serrano García	1982
1024	Archidona	Pineda Velasco	1983
1025	Loja	Lupiani Moreno & Soria Mingorance	1985
1037	Teba	Cruz San Julián	1980
1038	Ardales	Cano Medina	1982
1039	Colmenar	Barba Martín, <i>et al.</i>	1977
1040	Zafarraya	Elorza, <i>et al.</i>	1978
1051	Ronda	Del Olmo Sanz <i>et al.</i>	1981
1052	Alora	Chamón Cobos, <i>et al.</i>	1976
1053/1067	Málaga/Torremolinos	Estévez González & Chamón Cobos	1978
1054	Velez-Málaga	Elorza & García Dueñas	1980
1065	Marbella	Piles Mateo, <i>et al.</i>	1978
1066	Coín	Piles Mateo, <i>et al.</i>	1977
1072	Estepona	Chamón Cobos, <i>et al.</i>	1977

Table 3.1: List of IGME maps used in this Ph.D. Thesis.

Finally, the data is complemented with colored orthophotographs made from aerial photographs realized in 1998 and 1999. These orthophotographs have a resolution of 1 meter and a cartographic scale of 1:10.000.

3.1.1) Methodology

The methodology applied for the onshore study was based on standard field work. Since the geological cartography was already done by previous authors, the focus of the field work in this Ph.D. Thesis has been the reinterpretation on the nature of the contacts between the distinct lithological units. In particular, the orthophotographs and the DTM have been very helpful to identify and catalogue the olistoliths described in chapter 4.

3.2) Offshore study

3.2.1) Dataset

The offshore data used in this volume consist of commercial and academic multichannel seismic reflection profiles and well data.

Cruise/ lines	Year	Company	Grid and cross- lines directions	Grid Spacing	N° of lines	Total Km.
Ray	1972	AMPEX corporation	No grid	--	3	180
	1974	EXXON	NNW-SSE	2-4km	44	1935
75	1975	SHELL	WNW-ESE	4km	20	640
AS	1977	Western geophysical Company of America	N-S	≈14km	11	455
ALB	1981	ENIEPSA	NNW-SSE	4km	57	1475
AM	1984	Elf Aquitaine	NNW-SSE	1-4km	11	170
Talb	2000	academic	No grid	--	4	165
Cab	2003	ConocoPhillips	NNW-SSE	≈3-7km	19	565
Total						5585

Table 3.2: List of seismic surveys realized in the Malaga Basin and the amount of seismic lines used in this Ph.D. Thesis.

Multichannel seismic reflection profiles

The multichannel seismic data consist of 2D profiles, most of them obtained during hydrocarbon exploration by oil companies for but also by academic cruises. Table 3.2 shows the used seismic surveys, the length of seismic profiles, together with their corresponding characteristics. The total length of the available seismic profiles is about 5585km. The localization of the seismic profiles for each survey is shown in figure 3.01 which also shows that most of the seismic profiles are distributed along a grid. The distance between seismic lines varies significantly depending on the seismic survey. Nevertheless, the superposition of all the surveys permits to ensure a 4km separation between lines for the whole area. Moreover, in a great part of the study area, the grid cell is less than 2km. The density of the grid permits to characterize in 3D the main geometry of the basin and its major structures but is not good enough to characterize relatively small structures (less than 2km long).

It must be stressed that most of the seismic profiles correspond to hydrocarbon seismic surveys from the decades of 70' and 80' (table 3.2). Regarding the processing, it must be stressed that the profiles from the two major surveys in the basin, the EAS and ALB lines (table 3.2) have not been deconvoluted (pre-stack). Moreover, the EAS lines also lack of time migration. The imaging of the old profiles is obviously not as good as the modern ones. This is noticeable when comparing the old lines (e.g. EAS, ALB) with the recent ones as, for example, those carried out by Conocco Philips in 2003 (Cab lines in table 3.2), situated in the mud diapir province (see figure 6.11 from chapter 6). Therefore, it must be taken in to account that several geological structures that the modern profiles show very well (e.g. the top basement surface or the mud diapirs contour) are not always observed in the old seismic lines. In addition, most of the old profile resolution in deep is mostly lost beyond the 4-5 seconds (twtt) threshold, meanwhile the resolution of the Conocco ones reach 5-6 seconds (twtt).

Well data

Four wells have been made in the Malaga Basin (Fig. 3.01). Two of these wells, And-G1 and Alb-A1, are localized within the Malaga Basin *sensu stricto*. Both are commercial wells and were carried out by Elf (1983) and Chevron (1986), respectively. The other two wells, the DSDP Site 121 and the ODP Site 976, are situated over the structural high "976 High" which limits the basin towards the southeast. The site 976 was part of an ODP project in 1995 (Leg 161; see Zahn *et al.*, 1999) while the DSDP site 121 well was drilled in 1970. Since both wells are situated in the same area and their sedimentary register is similar, in this Ph.D. Thesis only the most modern has been used (site 976).

The wells Alb-A1, And-G1 and Site 976 have well-logging records for the entire Miocene sequence (Gamma ray, sonic, neutron porosity, etc.). This is not the case for the post-Miocene infill where only Alb-A1 and Site 976 have log records (e.g. see gamma-ray logs in Fig. 6.10 in chapter 6). In Alb-A1 and And-G1 wells, the stratigraphic dating was done using microfauna and no more dating was made after the well report. The original well reports have been used (Bailey *et al.*, 1986). In Site 976 a detailed biostratigraphical study using nannoplankton was made in cores (de Kaenel *et al.*, 1999).

Several scientific studies analyzed and interpreted the well data. Correlations between the wells and the multichannel seismic profiles have been done, either from the geophysical properties (Jurado and Comas, 1992), or from an interpretation of depositional sequences and sedimentary environments (Diaz Merino, *et al.*, 2003). In addition, several subsidence analyses were done by using backstripping techniques (Docherty y Banda 1992; Watts *et al.*, 1993; Rodríguez-Fernández *et al.*, 1999).

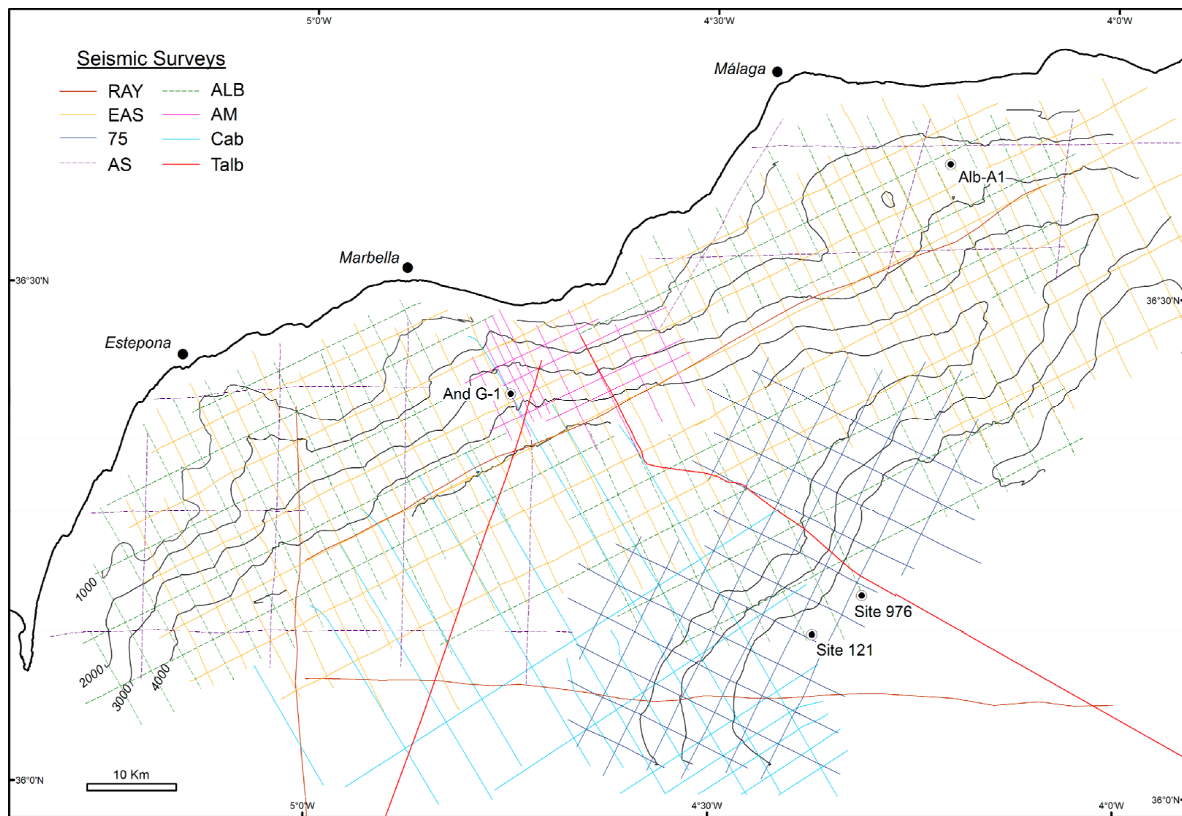


Figure 3.01: Seismic lines used for the study of the Malaga Basin and colored according to their seismic survey. The location of wells is also included as an isopach map of the top basement surface (Chapter 6). Contour lines every 1000msec (twtt).

3.2.2) Methodology

Multichannel seismic reflection and profile digitalization

The study of the Malaga basin has been done mostly through the analysis of the 2D grid multichannel seismic profiles by using the specialized software in seismic analysis “Kingdom suite v.8.7”.

Since the original format of most of the available seismic profiles were in analogue records, it was necessary to digitalize and transform the analogue profiles in to the standard SEG-Y format before they could be implemented in a Kingdom suite project. The digitalization process has been done using the “Lynx” software and can be summarized in five steps:

- 1) *Scanning of the profiles.* In order to be readable by the Lynx software, the images have been scanned at black and white with a resolution of 400ppi. This resolution has to be high enough to ensure a good imaging of each wiggle-trace.
- 2) *Definition of the profile parameters.* These are the parameters that Lynx needs for an adequate digitalization. The most important are the number and spacing between traces, the time window (twtt), and the graphic horizontal scale. It is also necessary to manually adjust the grid of traces/time in order to ensure that each trace will be adequately positioned and that the vertical time scale of the digitalized profile will fit the scanned image.
- 3) *Wiggle-trace conversion.* The Lynx software reconstructs the traces from the black and white pixels of the scanned images by using an algorithm (VAI or Variable Area Integration). As a result, the software obtains the relative values of amplitudes for the peaks of each trace. The precision of this process not only depends of the previous parameters but also of the quality of the imaging from the original profile.
- 4) *Edition.* The resulted digitalized profile can be edited and improved using editing tools as amplitude corrections, flawed traces, removal of seismic noise, etc.
- 5) *Georeference the profiles.* In the digitized seismic profile, already in SEG-Y format, the geographical position of the shotpoints has to be added. This last step is done in the Kingdom suite software.

The resulted seismic profiles can present important differences in the quality of the imaging from one line to another (see Fig. 3.02) which notoriously influences the precision of Lynx during the trace conversion. On the other hand, in some occasions the digital edition of the amplitude’s color scale permits to improve the seismic

interpretation which respects the original one (as it can be the case of the first profile in figure 3.02).

Several factors must be taken in to account when working with digitalized seismic profiles, in particular:

- a) The amplitude values of the digitalized profiles are not real and only represent relative values which respect to all the traces of a single seismic profile.
- b) The minor errors that arise during the digitalization process have to be taken into account in order to be able to disregard them during the seismic interpretation. A good example can be seen in the profile ALB-013 of figure 3.02 where the horizontal line that marks the 2 seconds threshold has not been completely eliminated and must be treated as an artifact during the interpretation.

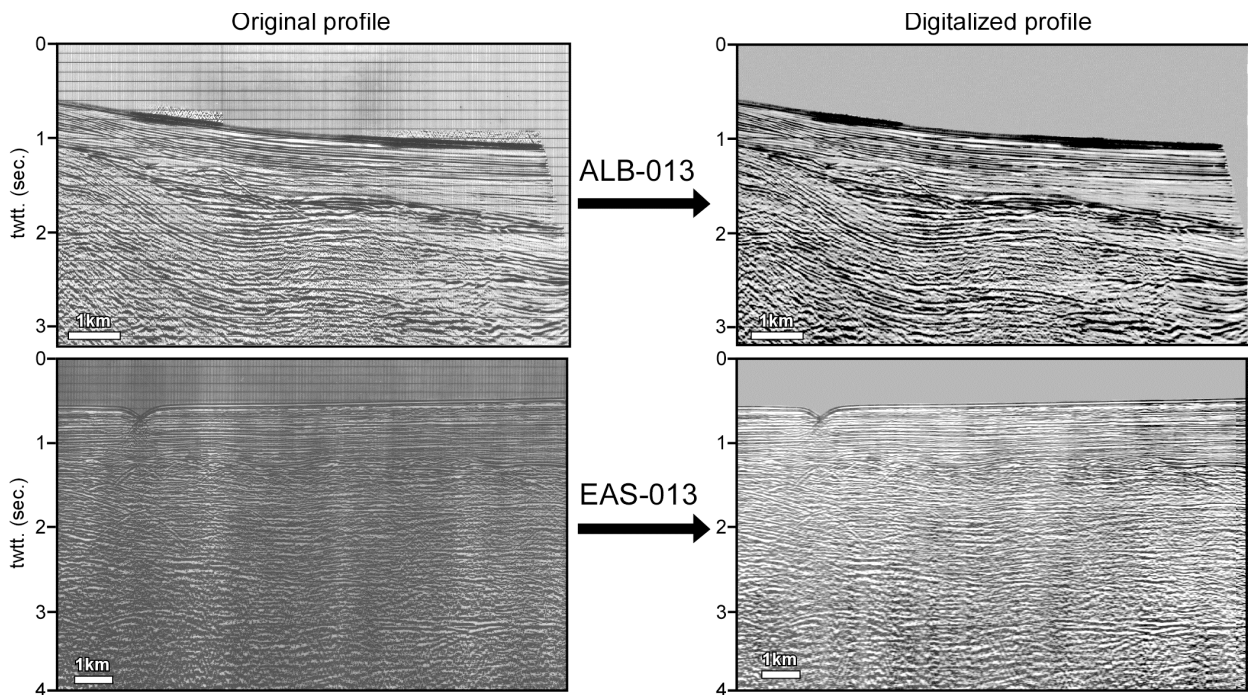


Figure 3.02: Two examples of original and digitized seismic profiles (ALB-013 and EAS-013). Note how the original profile severely constraints the imaging of the digitized one. Some of the features in the original profiles, as the horizontal time lines or the background color, are not completely deleted after the digitalization.

Well logs and seismic tie

Alb-A1, And-G1 and Site 976 wells in the Malaga Basin have been used to calibrate the depth registered in the well with the time scale of the seismic profiles, in order to correlate the depth of the main seismic formation boundaries with the seismic unconformities.

The top of the formations have been taken from well reports and from the previous work of Jurado and Comas (1992). Then, the calibration between depth and twtt has been done by the construction of time-depth (T-D) charts through the kingdom suite software. For this purpose we used the input of both the sonic (DT) and density (RHOB) logs from wells (see annex).

Seismic interpretation and 3D analysis

The major unconformities of the Malaga Basin, which can be correlated at a basin scale, have been interpreted for all the seismic profiles. For this purpose we use the unconformities R1 to R6 proposed by Jurado and Comas (1992) which have been also used previously in many studies (Rodríguez-Fernández *et al.*, 1999; Talukder *et al.*, 2004; Booth-Rea *et al.*, 2007; Marín-Lechado *et al.*, 2007; Soto *et al.*, 2010; Martínez-García *et al.*, 2013; among others). These unconformities comprise the metamorphic basement (R6) up to the Messinian unconformity (R1 or M reflector) and separate six seismic units (figure 3.03).

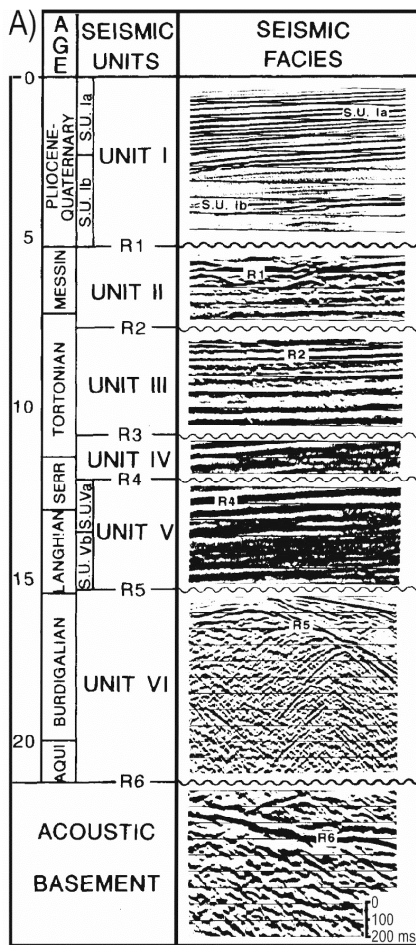


Figure 3.03: Seismic units, and their associated seismic facies that form sedimentary cover of the Malaga Basin (taken from Jurado and Comas, 1992).

The correlation of the unconformities has been done using the Software Kingdom suite which allowed the construction of 3D grids for the unconformities with the same resolution as the spacing of the seismic line grid (2km average). The 3D grids permitted to obtain contour maps of the mentioned unconformities which are a key factor to characterize the evolution of the basin geometry.

In order to characterize the distribution of the sedimentary infill along and across the basin, we also performed a total of four isopachs that correspond to the thickness of several seismic units delimited by the unconformities. For each one of the maps a constant P-wave velocity has been defined:

- 1) Unit VI: 2295m/s
- 2) Unit V: 2930m/s
- 3) Unit IV: 2775m/s
- 4) Unit III+II: 2865m/s

The calculation of these mean velocities was made from the T-D charts. First, the velocity for each log interval is calculated (which varies from 0,5m to

approximately 25m; column E of Annex). Then, these velocities are averaged weighted accordingly to their interval length. When a unit is present in more than one well, a second weighted average is made accordingly to the unit thickness in each well. For the units III+II map the velocities has been calculated separately and, afterwards, averaged by considering the thickness of each unit in well And-G1. The interpolation method used to create all the 3D surfaces has been that of the Gradient projection carried out by the Kingdom suite software.

Finally, the faults identified and correlated in several profiles have been mapped. The method used to trace those faults has been to localize the projection, for each profile, of the point in which the younger major unconformity is cut by the fault (Fig. 3.04A). If the fault plane had been eroded, which is the case for faults that cut the basement (see chapter 6), the tip-line used coincides with the inflexion point in which the erosional surface starts (Fig. 3.04B).

For the faults that affected the basement and the intracrustal reflectors interpreted as faults (see chapter 6), a rough estimation of their real dip has been done using a simplified time-depth conversion. In the case of faults which bound the basement and the sedimentary cover, a 2,5km/s velocity has been used, which corresponds with the average velocity of the sedimentary infill. For the intracrustal faults, the velocity used was that of the metamorphic basement. That is, from the Alboran Domain upper crust. Indeed, it is considered as representative of the metamorphic basement in the Malaga Basin and its seismic velocity has been estimated as 5.7km/s by Calvert et al. (2000). Finally, some seismic profiles were also roughly converted to deep by assuming the average 2,5km/s velocity of the sedimentary cover (e.g. Fig. 7.06).

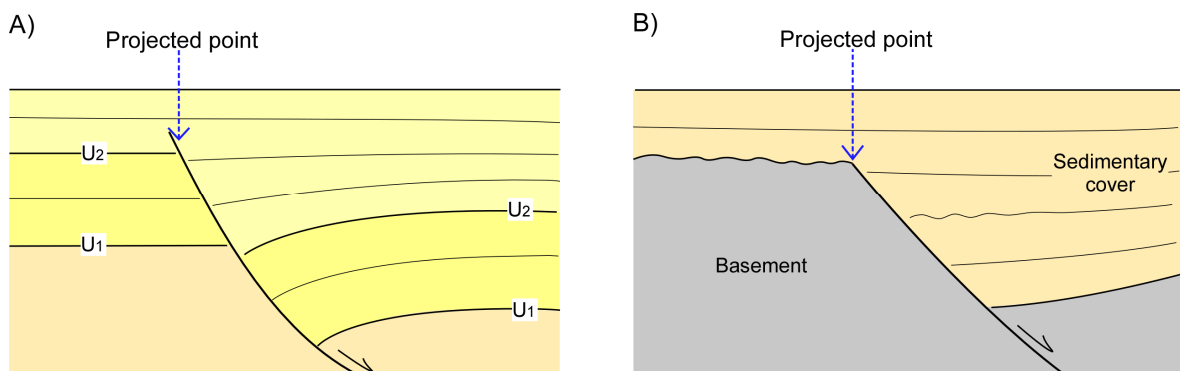


Figure 3.04: Scheme of the two methods used for fault projection: A) Faults that cut the sedimentary cover, and B) faults that correspond with the top of the basement.

3.2.3) Sequence stratigraphy

Sequence stratigraphy is a methodology that provides a framework for the elements of any depositional setting and permits to tie the changes in stratal stacking patterns with the responses of variations in accommodation and sediment supply through time (Catuneanu *et al.*, 2011). It started to develop during the 70's and, more specifically, after the publication of the AAPG special issue "Seismic stratigraphy: applications to hydrocarbon exploration" (Payton, 1977) where researchers from the oil company Exxon settle down the basics of the modern sequence stratigraphy. The use of this methodology is very extensive in basin analysis as it allows studying the relationship between the sedimentary rates and the creation of accommodation space (Schlager *et al.*, 1993). This relationship is controlled by external factors which are normally associated to eustatic fluctuations, climatic changes, tectonics, as well as changes in the sedimentary input into the basin. These factors control substantially the sedimentary architecture of the basin which in turn is described using the terminology of sequential stratigraphy: facies, system tracts, unconformities and depositional sequences (*sensu* Veil *et al.*, 1977).

Generally, the sequence stratigraphy methodology has been applied for the study of passive continental margins where the variations on the accommodation space produced by tectonics can be considered as negligible. This assumption permits to consider the eustatic changes as the main factor that controls the accommodation space in the basin which leads to the definition of system tracts in terms of eustatic cyclicity. In this context, many papers in terms of sequence stratigraphy were carried out after the pioneer works of the 70' (e.g. Galloway, 1989; Posamentier *et al.*, 1993; Schlager, 1993; Miall, 1995; Catuneanu, 2006; Catuneanu *et al.*, 2011). Nevertheless, the approach and terminology used varies slightly depending on the authors which may lead to confusion. In order to avoid it, the main concepts and terminology used in this Ph.D Thesis (Chapter 5) are presented in this chapter. Most of the terminology used is in accordance with that proposed in the reviews of Catuneanu *et al.* (2009; 2011).

Terminology and basic concepts

Seismic facies: It is a sedimentary unit with specific seismic characteristics (amplitude, frequency, continuity, reflectors configuration, among others; see the seismic facies example in Fig. 3.03). It can be considered an equivalent a lithofacies, although it should be necessary to have a litostratigraphical control (mostly achieved with wells) for a reliable correlation between seismic facies and lithofacies.

Accommodation space: This concept refers to the available space in a basin that can be filled with sediments. The variations in the accommodation space are due to **relative sea level changes** (Posamentier *et al.*, 1988). As the eustatic variations is not the only factor that produces relative sea level changes, another term is used in the literature. This is the **base level**, considered as the dynamic surface which balances erosion and deposition (Catuneanu *et al.*, 2009; see Fig. 3.05). This terminology has a more widespread meaning and is therefore more representative when used in basins developed in active tectonic settings (rift related, piggy-back, foreland, etc.). For the study of the Malaga Basin the terminology of base level changes is preferred. Therefore, I refer to base level rise when the accommodation space increases, and base level drop when there is a loss in the amount of accommodation space.

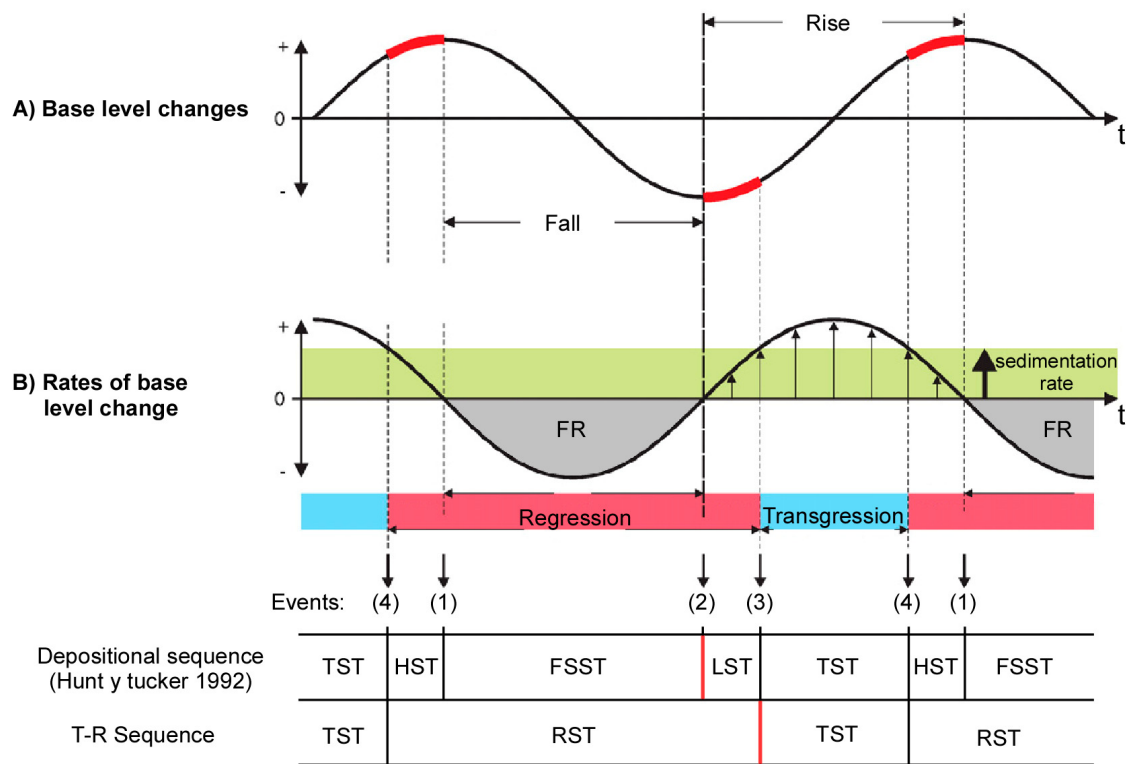
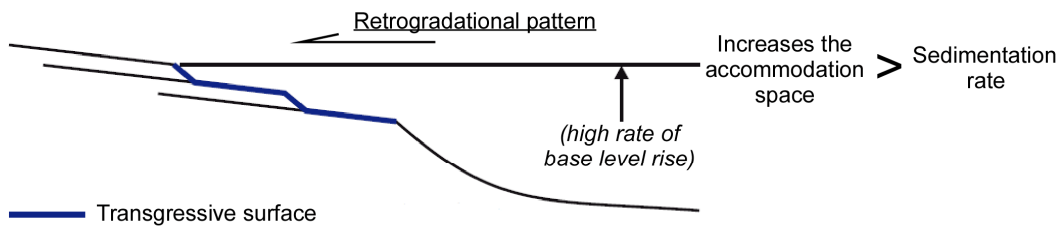


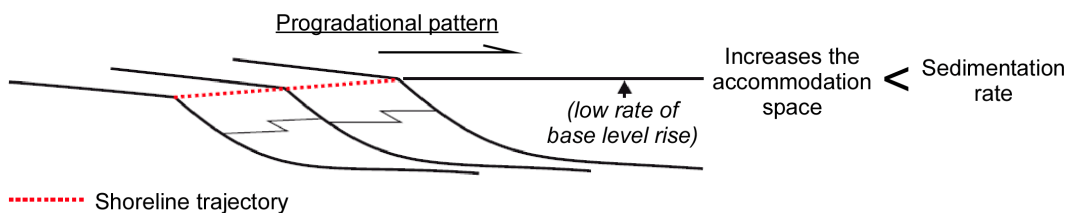
Figure 3.05: Graphs showing the concepts of transgression, normal regression, and forced regression, as defined by the interplay of base-level changes and sedimentation at the shoreline. a) The sinusoidal curve shows the magnitude of base-level changes through time. The portions on this curve highlighted in red indicate early and late stages of base-level rise ('lowstand' and 'highstand' normal regressions respectively), when the rates of base-level rise are outpaced by sedimentation rates. b) The sinusoidal curve shows the rates of base-level changes. Note that the rates of base-level change are zero at the end of base-level rise and base-level fall stages. The rates of base-level change are the highest at the inflection points on the top curve. Transgressions occur when the rates of base-level rise outpace the sedimentation rates. For simplicity, the sedimentation rates are kept constant during the cycle of base-level shifts and the base-level curve is shown as a symmetrical. Events: 1) onset of force regression, 2) end of forced regression, 3) start of transgression, 4) end of transgression. FR: forced regression; TST Transgressive system tract; HST: Highstand system tract; LST: Lowstand system tract; FSST: Falling stage system tract; RST: Regressive system tract. Modified from Catuneanu *et al.* (2009).

Stacking patterns: These patterns are related to the geometric relationships between strata (or seismic reflectors when working with seismic profiles), observed both within the seismic facies and along the different ones. These relationships define characteristic patterns that can be related to variations in the rates of base level changes. There are three main types of stacking patterns (Fig. 3.06). The **progradational** pattern is defined by a progressive migration of the deposits basinwards. In a vertical profile, the pattern is usually characterized to have shallower facies as going up into the vertical section. By contrast, **the retrogradational** pattern shows a migration of the deposits and the shoreline towards the basin margins. It also shows deeper facies as progressing into the vertical section. Finally, the **aggradational** pattern is an intermediate situation and is produced in conditions of equilibrium in which neither migration of the deposits, nor of the shoreline, is observed.

A) **Transgression**



B) **Regression**



C) **Forced regression**

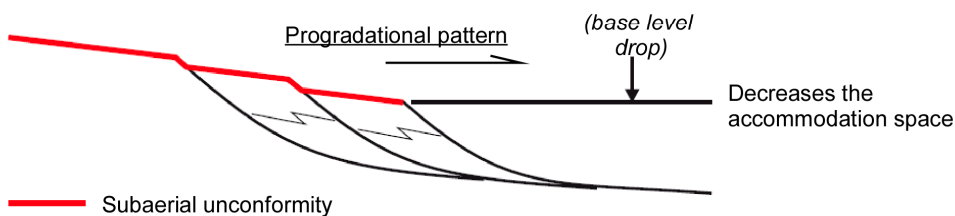


Figure 3.06: Scheme indicating the stacking patterns formed during a period of specific conditions between base level changes and sedimentation rates. The red and blue lines (suberial unconformity and transgressive surface respectively) correspond to the surfaces formed at the end of each period. Modified from Catuneanu et al. (2011).

The formation of a determined stacking pattern is controlled by the correlation between the creation of accommodation space and the sedimentation rate at the moment of its deposition (Fig. 3.06). We use the term **transgression** when the creation of accommodation space is greater than the sedimentary rates (i.e. the space filled by the sediment supply; Fig. 3.06A). By contraposition, the term **regression** is used when the sedimentary rates is greater than the creation of accommodation space (Fig. 3.06B). Note that, in both cases, there is an increase on the available space in the basin (the accommodation spaces increases; Fig. 3.06A and 3.06B) but, during a regression, this increase cannot keep pace with the infill produced by the sediment supply (see regression stage in Fig. 3.05B). This leads to the definition the **forced regression**, which occurs when there is a net decrease of the accommodation space due to a base level drop (Fig. 3.06C; see also the gray colored area in Fig. 3.05B).

Sequence stratigraphic surfaces: Correspond to the surfaces that mark changes in the strata stacking pattern (Embry 2009; Catuneanu *et al.*, 2011) and may define the limits of the system tracts and sequences. Some of these surfaces are used in the sequence stratigraphic analysis of this Ph.D Thesis:

- a) A **subaerial unconformity** (*sensu* Sloss *et al.*, 1949) formed during a drop on the base level and produced by erosion under subaerial conditions. Accordingly, this unconformity is associated with episodes of forced regression (Fig. 3.06C). It is a diachronic surface since it progresses basinwards as the base level gradually drops and new strata are exposed to subaerial conditions.
- b) A **maximum flooding surface** (Frazier, 1974) marks the change from a retrogradational into a progradational stacking pattern. It corresponds to the end of a transgressive episode (event 4 in fig. 3.05B).
- c) A **maximum regressive surface** (Helland-Hansen & Martinsen, 1996) marks the change from a progradational into a retrogradational stacking pattern. It corresponds to the start of a transgressive episode (event 3 in Fig. 3.05B) associated to high positive rates of base level change (see Fig. 3.05B).

Strata terminations: They permit to characterize the sedimentary architecture of seismic reflectors (Mitchum *et al.*, 1977). Strata terminations are used to describe how the geometry of the strata terminates against a specific surface. They are valuable to identify stacking patterns. Several types of terminations are illustrated in figure 3.07:

- a) Onlap: strata deposited originally horizontally that progressively terminates against an originally inclined surface. This relationship is related to a progressive filling of a margin.

- b) Downlap: stratum which was originally deposited with a certain dip and terminates downdip against a surface with lower dip or horizontal. It is indicative of progradation.
- c) Toplap: Upwards termination of the strata against a surface. It is indicative of a non-deposition period.
- d) Erosional truncation: Termination of the strata against an erosive unconformity. It indicates a period of non-deposition and associated erosion.
- e) Offlap: this type of termination is characterized by a conformably succession of strata in which the younger strata terminate upwards against the previously deposited ones. It indicates a progressive retreat of the deposits in a basin-wards direction. Offlap terminations are indicative of an episode of forced regression related to a base level drop (see Fig. 3.06).

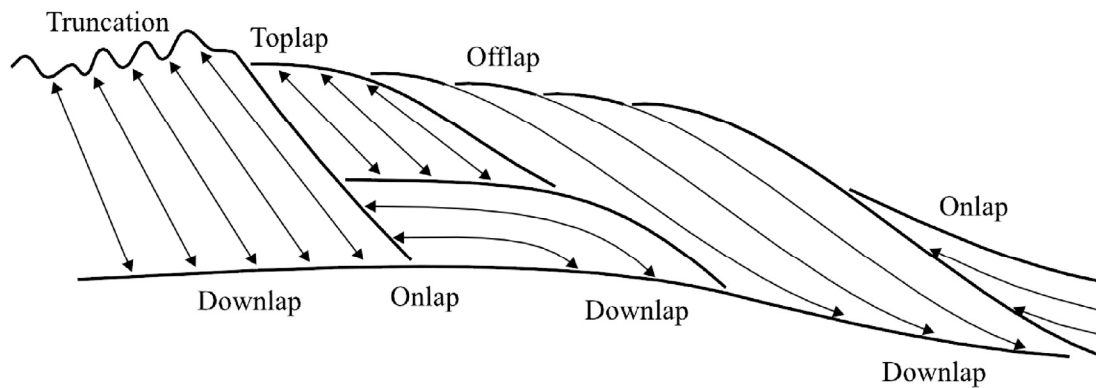


Figure 3.07: Scheme illustrating the geometry of different kind of strata terminations. Modified from Emery and Myers (1996).

Sequence: Broadly, a sequence can be defined as a succession of strata deposited during a full cycle of change in accommodation and/or sedimentary rates (catuneanu *et al.*, 2009). The reason for the use of such a generic definition is that it permits to incorporate all the different types of sequences that have been defined by several authors (e.g. Galloway, 1989; Posamentier *et al.*, 1988; Johnson & Murphy, 1984). The differences between the several types of sequences used in sequence stratigraphy arise on their internal subdivisions and the type of surface that defines their limits. Thus, the **depositional sequence** of Hunt & Tucker (1992), which is probably the most extended in the literature, has its **sequence boundary** defined by a sub-aerial unconformity (Sloss *et al.*, 1949) which is associated with the end of a base level drop (event 2 in Fig. 3.05). The forced regression that occurs during a base level drop (fig. 3.05) implies that this unconformity is an erosional unconformity in the more proximal parts of the basin (those which remain under subaerial conditions), while it becomes an angular unconformity or a paraconformity towards the more distal parts (Fig. 3.06C). Note that, given the cyclicity of sequences, their upper and lower limits (sequence

boundary) are defined by the same kind of unconformity and they bound a full cycle of base level changes (Fig. 3.05).

This feature may present serious limitations when trying to define a sequence. This occurs because, in certain cases, it can be very difficult to identify the sequence boundaries. An example of a sedimentary setting in which a sub-aerial unconformity may not be observed is in tectonically active extensional basins. The continued tectonic subsidence causes a continuous base level rise (increasing the accommodation space) that outpaces any base level drop produced by eustatic changes. Since the subaerial unconformity is the expression of a base level drop, this unconformity will not form in such types of basins (or they would be weak and difficult to identify).

In cases where sub-aerial unconformities are not formed or difficult to observe, the depositional sequence of Hunt & Tucker (1992) is difficult to differentiate and it is preferable to use another type sequences defined by different sequences boundaries. This is the case of the **T-R sequence** (Johnson & Murphy, 1984; Embry & Johnson, 1992; Embry, 1993) as its sequence boundary is defined by the surface that corresponds with the end of a regression stage and the start of a transgression (event 3 in Fig. 3.05).

This surface is known as transgressive surface (TS; Posamentier & vail, 1988) and marks the change from a prograding stacking pattern into a retrograding one. The transgressive surface is not associated with a subaerial unconformity, even though it usually becomes erosional into the more proximal parts of the basin. Therefore, the identification of a T-R sequence does not require a period of base level drop and the formation of the associated subaerial unconformity. On the other hand, the proper identification of T-R sequences requires that periods of transgression occur in the basin, which implies lower sedimentation rates than the formation of accommodation space (Fig. 3.05). Accordingly, the use of T-R sequences is limited in basins with high sedimentation rates and low subsidence where only progradational episodes are expected. Given the extensional nature of the Malaga Basin, the use of T-R sequences is appropriate and they can be easily observed in the multichannel seismic profiles.

Finally, it must be stressed that sequences are not dependent of timescale as they correspond to cyclic events that can be caused by different types of factors (tectonics, eustatic, climatic, etc.) which have different **order of cyclicity**. We refer to high-order sequences to indicate high frequency cycles and low-order sequences to indicate low frequency cycles. Thus, a low-order sequence may contain several high-order sequences that represent shorter cycles.

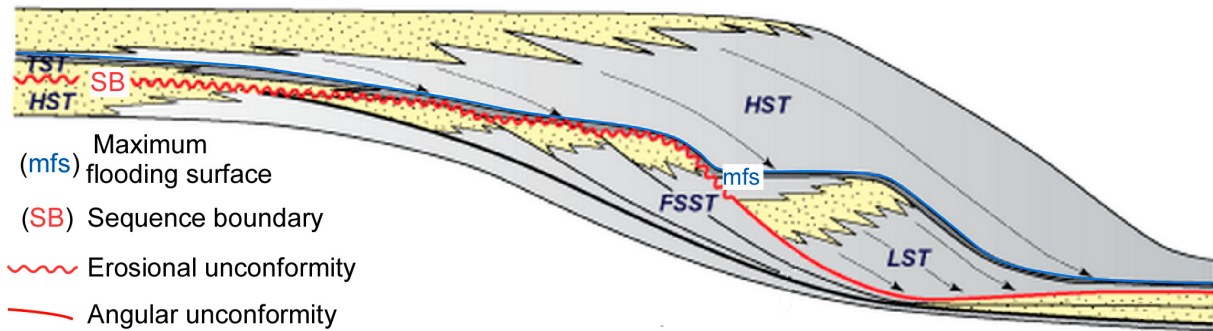


Figure 3.08: Illustration of Hunt and Tucker (1992) depositional sequence for a delta front. Modified from Haugton (2008). TST Transgressive system tract; HST: Highstand system tract; LST: Lowstand system tract; FSST: Falling stage system tract.

System tracts: A system tract is “a linkage of contemporaneous depositional systems, forming the subdivision of a sequence” (Brown & Fisher, 1977). It consists of a relatively conformable succession of genetically related strata which is bounded by sequence stratigraphic surfaces. The system tracts are interpreted according to the strata stacking pattern, their position within a sequence, and the types of surfaces that bound their upper and lower limits. System tracts are the units that divide a sequence and are also independent of timescale.

There are several nomenclatures depending on the sequence used but the depositional sequence of Hunt & Tucker (1992) is subdivided in four system tracts (HST, LST, TST, FSST) while The T-R sequences are only formed by two system tracts (TST and RST).

Lowstand (LST): It corresponds to the sedimentation of prograding deposits over a sub-aerial unconformity (the sequence boundary). This system tract takes place after a sea level drop, when the base level rise does not outpace the sedimentation rates (event 2, Fig. 3.05).

Transgressive (TST): It is characterized by a retrograding pattern due to high rates of base level rise (fig. 3.05). Its base is delimited by a maximum regressive surface and its top corresponds with the maximum flooding surface (Fig. 3.08).

Highstand (HST): It corresponds with the late stage of a base level rise when the rate of base level rise diminishes and it is outpaced by the sedimentation rate (event 4 in Fig. 3.05). The HST is characterized by a progradational to aggradational deposits and limited at its bottom by the maximum flooding surface.

Falling stage (FSST): This system tract includes the sedimentation that take place during the base level drop. The formation of a subaerial unconformity synchronic with deposition is diagnostic of FSST. The strata are characterized by progradation and offlap terminations due to the base level drop (figs. 3.07 and 3.08). This system tract is not always observed as it can be completely eroded during the falling of the base level, or cannot be formed if the base level fall is minor or do not occur.

Regressive (RST): The regressive system tract does not form part of the depositional sequence of Hunt & Tucker (1992); instead it belongs to the T-R sequence. It includes all the sediments deposited during a regressive stage situated between episodes of transgression. The RST groups the other three system tracts associated with progradation during regressive stages (HST, LST and FFST). Therefore, the RST is characterized by a prograding pattern limited at the bottom by a maximum flooding surface and by a maximum regression surface at its top. It is noteworthy to mention that this system tract can be truncated by erosional surfaces if base level drops take place during its deposition.

Sequence stratigraphy in extensional basins

The sequence stratigraphy is a methodology mostly developed in passive margins where the eustatic variations is the main factor controlling the variations in the accommodation space. In this setting it has been widely applied and shown as a useful method to better understand the basin evolution and its sedimentary architecture. On the other hand, there have been few studies that apply the principles of sequence stratigraphy into extensional basins (e.g. Prosser, 1993; Nottvedt *et al.*, 1995; Ravnas & Steel, 1998; Martins-Neto & Catuneanu, 2010).

The studies done in this type of basins conclude that the tectonic activity is the main factor controlling the creation of accommodation space and, in some extent, the sedimentary architecture (see Prosser 1993; Martins-Neto & Catuneanu 2010). This statement does not imply that other factors (climate, eustatics, sedimentary income, etc.) are not constraining the deposited sequence, but their influence is more likely to be less important when compared with tectonics. In addition, sequences related to these factors are associated to cycles of higher frequency than the ones produced by tectonic pulses during the opening of an extensional basin.

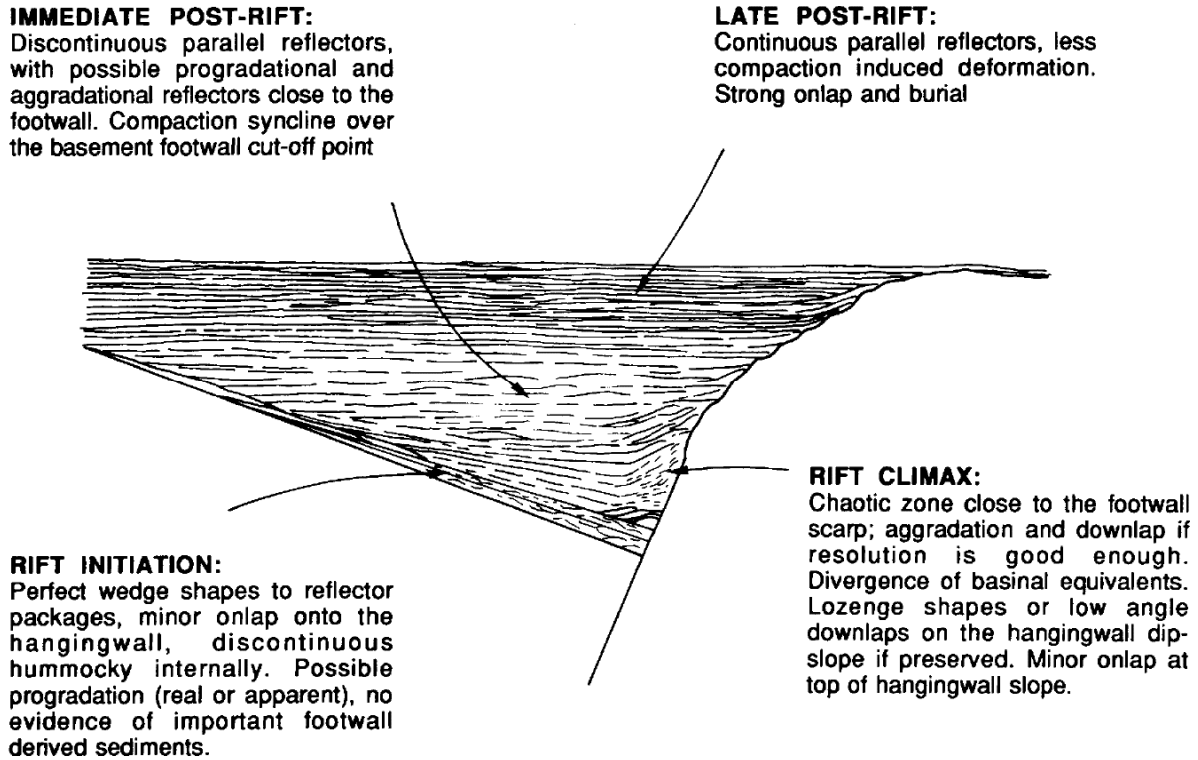


Figure 3.09: Idealized line drawing of a seismic section from a half-graben (taken from Prosser, 1993). The seismic characteristics of the tectonic system tracts are shown and summarized in the annotations.

The sequence stratigraphic study presented in this volume pays special attention to the work of Prosser (1993). She applies the basics of the sequence stratigraphy in half-grabens delimited by normal faults developed in the context of a continental rift (Northern Sea and Barents Sea). The author proposes an archetypal “rift sequence” which would be characteristic of the sedimentary infill on this type of basins.

The rift-sequence ranges from the first sediments deposited at the beginning of the extension until its colmatation during the post-rift. It is subdivided into four stages called “tectonic system tracts” that receive the name of rift initiation, rift climax, immediate post-rift, and late post-rift system tract (Fig. 3.09). The **rift initiation** records the continental sediments deposited during the first extensional pulses that take place in the basin. During the **rift climax** (subdivided in early, middle and late rift climax) the basin is considered to be submerged and is related with the episode when the tectonic activity of the fault that controls the half-graben reaches its peak. In turn, the **immediate post-rift** takes place during the early stages of the post-rift, when the thermal subsidence is still strong and there is a homogenization of the rift topography. Finally, the **late post-rift** corresponds with the sedimentation typical of a passive margin infill and extends upon the basin colmatation. Each one of these system tracts has a specific seismic sedimentary architecture which is related to the tectonic activity and, more specifically, to the movement of the fault that bounds the half-graben.

It is necessary to introduce the main assumptions of the model of Prosser (1993) as well as the principles used to correlate the sedimentary architecture with the tectonic activity. The same principles have been used in the Malaga Basin case-study.

The model applies for a half-graben bounded by a main normal fault which delimitates a hanging-wall and a footwall. In this scenario, the creation of accommodation space is controlled mostly by the sinking of the hanging-wall produced by the fault slip. Accordingly, the sedimentation takes place in the hanging-wall while the footwall is affected in a lesser or greater extend by erosion.

The sedimentary supply is differentiated between axial and longitudinal deposits with respect the axis of the basin (see sketch of Fig. 3.10). The axial deposits would come from the erosion of the footwall or the emerged part of the hanging-wall. These deposits considered as proximal deposits that produce the sedimentation of lobular-type bodies. In turn, the longitudinal deposits would have a more distant source area resulting in the sedimentation of distal deposits characterized by laminar-type bodies (Fig. 3.10).

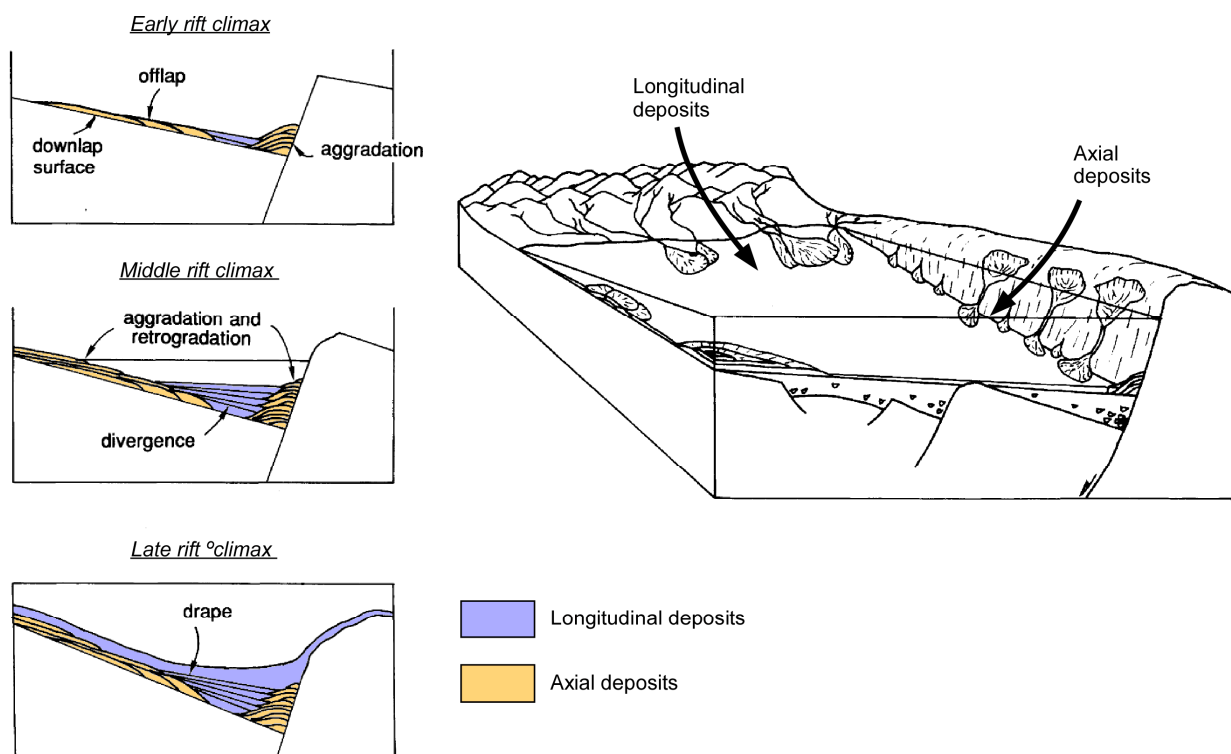


Figure 3.10: Figures taken from Prosser (1993). To the right: a cartoon that shows the relationship between tectonics and sedimentation. On the left side, cartoons showing the stacking patterns that are characteristic of each rift climax stage (Early, Middle and Late). Note that the model assumes a half-graben controlled by a major fault which leads to erosion of the footwall and sedimentation over the hanging-wall.

The stacking patterns of the strata are controlled mainly by the interplay between the sedimentary rates and the creation of accommodation space, in turn produced by the

fault slip. The axial deposits are more sensitive to these variations and they show progradation during episodes of low tectonic activity and retrogradation when the tectonic activity is higher. Concerning the longitudinal deposits the episodes of higher tectonic activity are characterized by the presence of divergent patterns towards the footwall (see rift climax scheme of Fig. 3.10).

Thus, the model differentiates three stages during the main rifting period or rift climax (Fig. 3.10). During the early rift climax, the tectonic subsidence is slow and the prograding to aggrading patterns of axial deposits prevail. As tectonic subsidence increases, the stacking patterns change to retrogradation which is the main characteristic of the middle rift climax. Finally, during the late rift climax, a progressive decrease of the tectonic subsidence results, once again, in the predominance of prograding patterns which are also observed during the post-rift stage. In addition, the model takes in consideration that the tectonic activity is the main factor for the topographic differences between the two fault blocks (hanging-wall and footwall) and that this topography contrast strongly affects the amount of axial deposits sedimented. Therefore, it considers that the disappearance of axial deposits is indicative of the end of fault activity in the graben (see Fig. 3.09 and the late rift climax scheme in Fig. 3.10).

The approach of Prosser (1993) has been revised by Martins-Neto & Catuneanu (2009). The authors have simplified the analysis of a rift sequence by proposing that the sequence consist of alternating Transgressive and Highstand system tracts (TST and HST respectively). The TST are associated with retrograding patterns that take place during pulses of tectonic subsidence and are followed by episodes of relatively tectonic quiescence that correspond with the HST and are associated with prograding patterns.

Therefore, this method permits to characterize the several tectonic pulses that may take place during the extensional history of a basin. By contrast, the model of Prosser (1993) only contemplates one cycle of a progressive increase on the tectonic activity during the rift climax which progressively diminishes during the latter stages.

The sequence stratigraphic analysis applied in the Malaga Basin case-study use a combination of the methods of Prosser (1993), Martins-Neto & Catuneanu (2009) and the T-R sequences (Johnson & Murphy, 1984; Embry & Johannessen, 1992). Despite of that, they have been significantly modified in order to address the peculiarities of the Malaga Basin. The analysis has been done through the interpretation of the available seismic profiles and it will be fully presented in Chapter 5. The main steps of this analysis are the following:

- 1) Selection of the profiles.
- 2) Characterization of the seismic facies
- 3) Characterization of the facies association or system tracts.
- 4) Characterization of the rift system tracts.

**4 Lower to middle Miocene
deposits related to gravitational
and extensional processes in the
Western Betics (onshore studies)**

4.1) Introduction

This chapter is dedicated to the onshore study of selected outcrops of lower to middle Miocene deposits that overly the Western Alboran Domain realized during this PhD Thesis. Their study permits to characterize their relationship with the structures observed in the basement and sheds light to the onshore-offshore correlation in terms of deposits (see chapter 2). The studied outcrops are situated between 4°W to 5°W meridians. To the south, they end along the coast line and towards the north, up to Antequera and El Torcal area (see the location in figure 1 from epigraph 4.3; see also chapter 2). The next two epigraphs (4.2 and 4.3) show the results of these onshore studies. They correspond to published papers without any modification, although the references are included with those of this PhD Thesis volume (Chapter 9). The epigraph titles correspond with the title of each paper.

The first one (epigraph 4.2), by Suades and Crespo-Blanc (2010), has been published in *Geogaceta*. It is a short study that describes characteristic breccia bodies that can be found interbedded with the carboniferous phyllites and carbonates of Malaguide Complex (Alboran Domain). They are situated near of the boundary between the basement and the Miocene deposits and are interpreted as produced by hydraulic fracturing. These bodies are considered to nourish lower Burdigalian deposits that lie over the Alboran Domain.

The second part (epigraph 4.3), by Suades and Crespo-Blanc (2013), has been published in *Geologica Acta*. It mainly focuses on the study of the nature and origin of a Miocene *mélange* that lies over the Alboran Domain widely represented in the studied area. The relationship of this *mélange* with the metamorphic Alboran Domain basement and the related extensional tectonics is addressed. The study constrains the age of this *mélange* through the relative timing of tectonic events that took place in this area of the Gibraltar arc. Key arguments for this relative timing are based on lithological and structural analyses of kilometer-scale olistoliths embedded in the *mélange*. Indeed the age of the structures within the olistoliths (before they were eroded and resedimented) are well constrained.

One thing that must be clarified is the nomenclature used for the *mélange* complex since there have been several authors that studied this *mélange* in the past and resulted in a high variety of names given to these deposits. In Suades and Crespo-Blanc (2013), we gave a new name for the *mélange*: La Joya Olistostromic Complex (LaJOC). This is also the name used in chapters 5 to 7 when I refer to this olistostromic complex. By contrast, the publication that corresponds with epigraph 4.1 was done previously to this redefinition. Therefore, in this specific epigraph the old terminology of “Alozaina Complex” was used (Balanyá, 1991), since the overall concept behind the name was mostly in agreement with our interpretation of the *mélange*.

4.2) Hydraulic brecciation on top of the Alboran Domain and its relationship with Lower Miocene deposits (Western Betics)

Abstract

Al oeste de las Cordilleras Béticas, se describen unos cuerpos de brechas dentro del Complejo Maláguide, muy similares a las brechas del Mioceno inferior del grupo Viñuela. La distribución, geometría interna y características petrográficas de dichos cuerpos muestran que pueden haberse formado durante procesos cataclásticos acompañados por fracturación hidráulica. Se sugiere que estos cuerpos de brechas tectónicas nutren las brechas sedimentarias del grupo Viñuela.

Introduction

The internal zone of the Betics, the Alboran Domain, is formed by a postmetamorphic nappe-stack, strongly thinned during the Miocene back-arc rifting which produce the development of the Alboran Basin in the Gibraltar Arc hinterland (García-Dueñas et al., 1992, Comas et al., 1992) (Fig. 1A). As a consequence, low-angle normal faults affected the Alboran Domain units and marine transgressive sediments deposited. Good example of the relationship between the metamorphic basement and the oldest sediments deposited during rifting can be observed in an area situated north of Malaga (Fig. 1B). There, the brittle boundaries between the Malaguide and the Alpujarride Complexes, the uppermost Complexes of the Alboran Domain, are sealed by the Viñuela group (Martín-Algarra, 1987), which in turn is situated below the wildflysch-type rocks of the so-called Alosaina Complex as defined by Balanyá and García-Dueñas (1986). While La Viñuela group is well known (Serrano et al., 2006), the origin, nature, and tectonic significance of the Alosaina Complex is still a matter-of-debate.

The aim of this paper is to shed light on the nature of the boundary between the Alboran Domain, the Viñuela group and the Alosaina Complex along the easternmost outcrops of this latter (Fig. 1A). We reveal the presence of breccia bodies formed by cataclastic and hydraulic fracturing in the upper part of the Malaguide Complex. Their geometry and their relationship with the Viñuela group and the Alosaina Complex suggest that the tectonic breccias could have nourished the Viñuela deposits. By contrast, the described faults are sealed by the Alosaina Complex.

Geological context

In the study area, the Alboran Domain is mainly represented by the Malaguide Complex (Fig. 1B). Only a small outcrop of Alpujarride rocks is present, composed of garnet and andalucite schists. It is situated structurally below the Malaguide Complex, which in turn is characterized by Silurian black phyllites, together with Devonian and Carboniferous phyllites interbedded with carbonatic levels. The boundaries between these formations are frequently low-angle normal faults which affect not only the Alpujarride-Malaguide contact but also the whole Malaguide (Alonso-Chaves et al., 1993). On top of the Malaguide sequence, unmetamorphosed red conglomerates and sandstones of Permo-Triassic age deposited unconformably over the low grade metamorphic rocks.

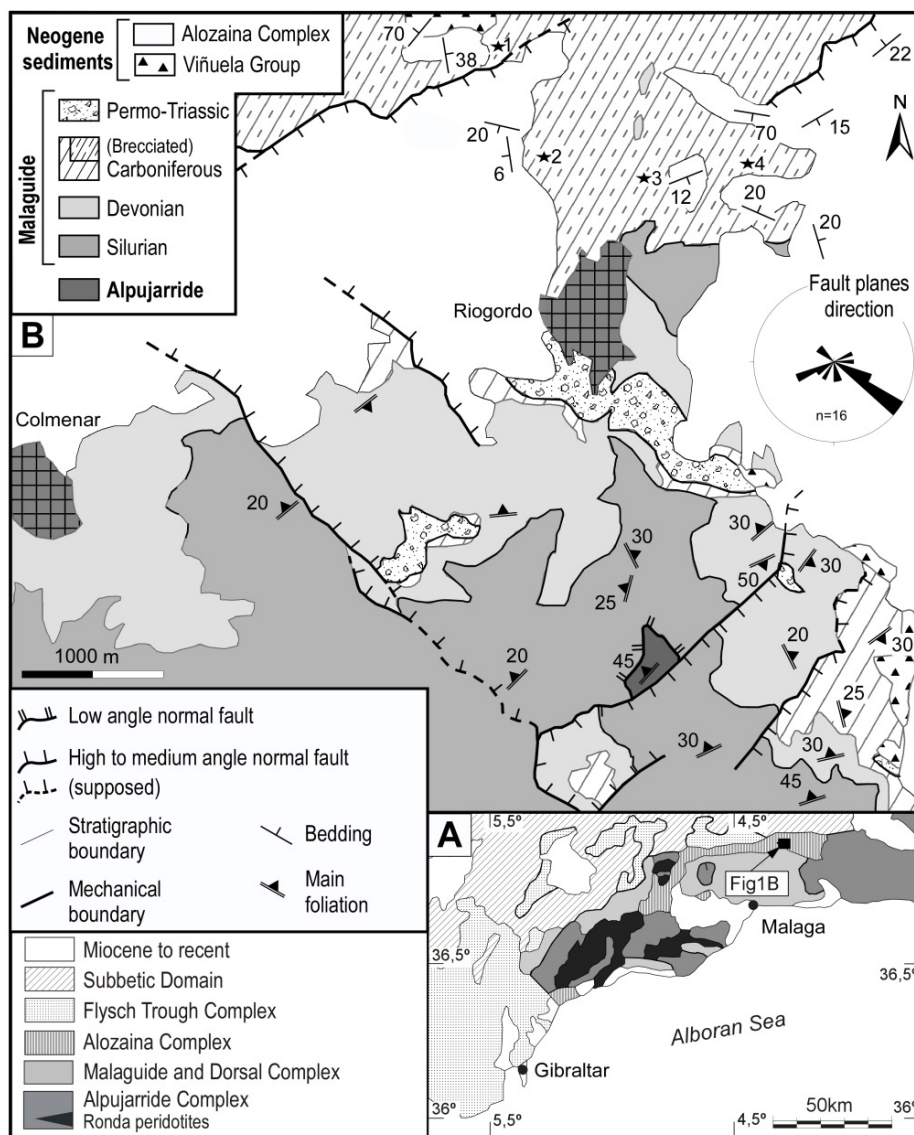


Figure 1: Main complexes in western Betics. B) Geological map of the studied area, modified from Barba Martín et al. (1979). Stars show the location of the photographs of figures 2 and 3.

In the study area, two Miocene sedimentary formations are transgressive over the Malaguide rocks (Fig. 1B). The most characteristic member of the lower one is a polymictic breccia made of heterometric clasts of Malaguide and Alpujarride origin. It corresponds to the Viñuela group dated as lower Burdigalian (Serrano et al., 2006) and records the initial stages of the rifting of the Alboran Domain. The upper one is an olistostromic complex made up of boulders of internal and external domain rocks in a matrix of marls and sandy sediments, the Aozaina Complex of Balanyá and García-Dueñas (1986) (Neonumidian of Bourgois, 1978, or Numidoide of Martín-Algarra, 1987). These authors attributed the age of this complex to Middle Burdigalian.

Detailed mapping reveals the presence of two sets of medium to high angle normal faults that affected the unconformity between the Malaguide and Neogene rocks. They are NE-SW and NW-SE directed (see rose diagram in Fig. 1B).

Breccia bodies within the Malaguide: characteristic features

North of Riogordo village, the Carboniferous phyllites interbedded with carbonatic levels from the upper part of the Malaguide complex are highly brecciated. The process of fracturation is so developed that, when the outcrops are poor, they seem to be an avalanche deposit similar to the lower member of the Viñuela group. Nevertheless, a careful examination, in particular along road trenches (stars of Fig. 1B), shows that these breccias are in fact discontinuous bodies hosted within the Carboniferous rocks (Fig. 2A). Accordingly, in map of Figure 1B they are differentiated as «Brecciated Carboniferous».

These breccia bodies have variable size, with length ranging from some tens of meters to less than a meter, and width from a few centimeters to a meter. They are frequently parallel to the Malaguide phyllite foliation, mainly subhorizontal north of Riogordo, with a sill geometry (Fig. 2A), or following low-angle normal fault planes. They can also show a branched or anastomosing geometry, and sometimes crosscut the foliation (dyke geometry). When present, high angle faults cut the breccia bodies (Fig. 2A).

At hand-sample scale, the breccias are clasts dominated (40-70%), although the matrix is always present. The dun-yellowish color of this latter, which contrasts with the greenish tones of the phyllites, is the most distinctive feature of the breccia. The clasts are mainly angular (Fig. 2B) but can also be sub-rounded (Fig. 2C, 3A and 3D) and scarcely well-rounded (Fig. 3B). The breccias are highly heterometric and mono to polymictic (Figs. 2 and 3). Indeed, the clasts range from a few millimeters to some decimetres, and their composition is similar to that of the host rock (phyllite, carbonate rocks, monomineralic quartz or greywackes, e.g. Fig. 2B).

The clasts are frequently fractured, with separation and differential rotation between fragments (Figs. 2C and 3A), as evidenced by the foliation marked by the micas inside the clasts. It is frequent to observe how the elongated clasts follow a dominant direction, which in turn is subparallel to the hostwall (Fig. 2C). Finally, a size sorting of the clasts can be observed. It is subperpendicular to the hostwall and shows a higher concentration of the finer portion near of the host wall margins (Fig. 3C).

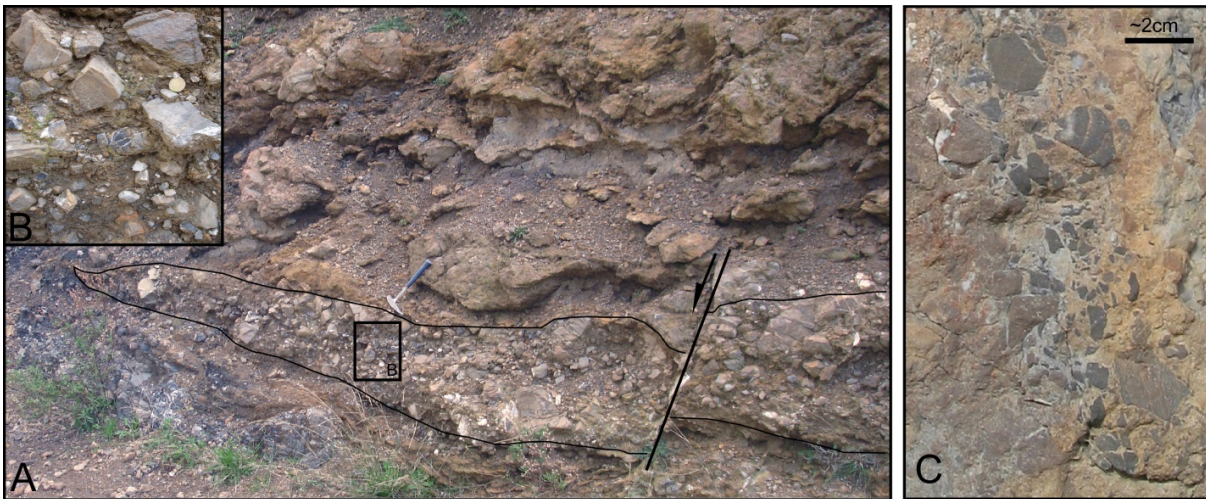


Figure 2: A) Representative breccia body within the Malaguide Complex with a sill geometry. It is cut by a high-angle normal fault. Note the lack of lateral continuity. Location: Star 3 of Fig. 1B. B) Detail of the polymict breccia with heterometric clast population. C) Small subvertical breccia body with angular and sub-rounded clasts. Location: Star 1 of figure 1B.

At thin-section scale, the matrix is made of fine-grained quartz, micas and carbonate minerals, together with a finer portion whose composition has been determined by X-ray diffraction (dolomite, ankerite, calcite, quartz and phyllosilicates), that suggests a mixed nature between a carbonatic cement and very fine rock fragments. Scarcely, the mica grains of the matrix can draw a cataclastic foliation.

Cement is always present and in some cases can be the only component in the matrix. The cement composition is mainly calcite, although small rhombohedral dolomite crystals of replacement have been observed (Figs. 3D and 3E).

Various generations of veins filled by calcite are present. Narrow rims surrounding the clasts (Fig. 3B) and veins filling intraclasts cracks are characteristic geometries of those identified as the oldest ones. Veins filled by calcite of higher crystal size represent late generations (Fig. 3A).

Discussion and conclusions

The breccias described in the previous paragraph can have originated either during sedimentary or tectonic processes. At the moment, we discard a sedimentary origin. Indeed, the clast transport should have been small, as a) the wall rocks and the clasts show the same composition and b) the breccias are highly heterometric.

Moreover, the sill geometry of the breccia bodies, within the Malaguide Complex host rocks would have implied a transport of the sediments from up to down, through neptunian dykes, which have not been observed. Finally, no fossils have been found (although this argument does not exclude a sedimentary genesis).

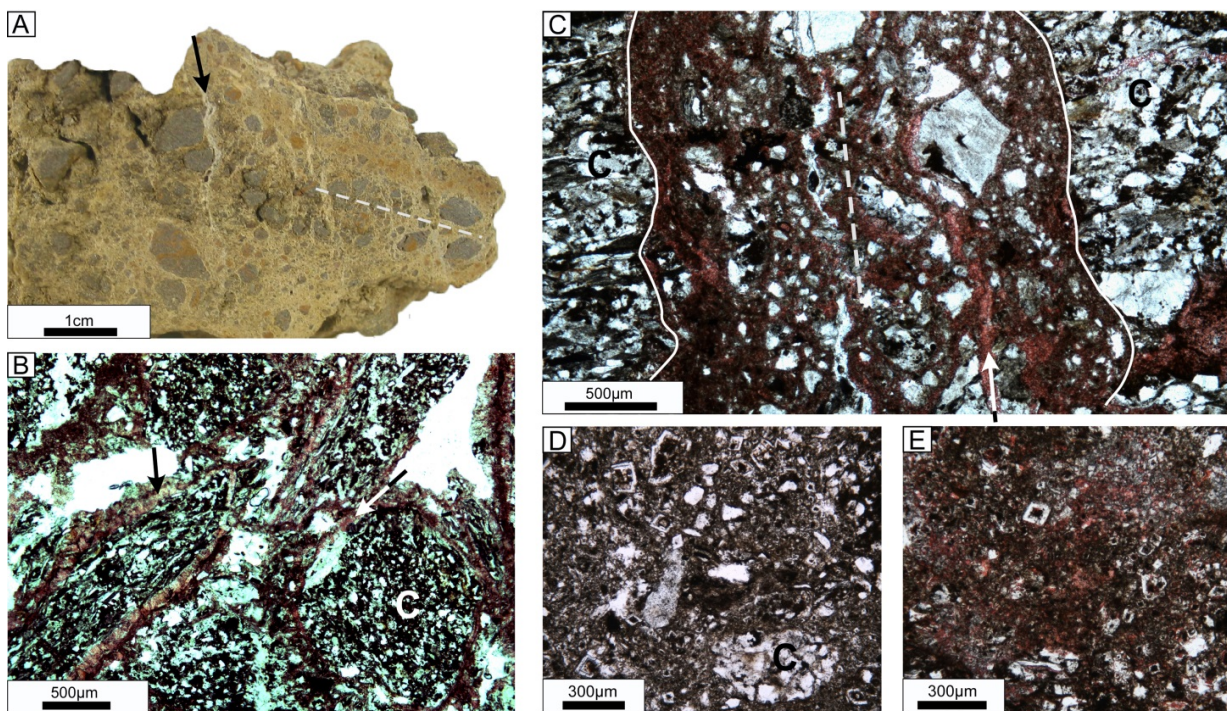


Figure 3: A) Hand-sample with grain size sorting. The band of centimetre-scale sub-rounded clasts bounded by microscopic-scale matrix marks a flow direction (dashed line). Note the veins, which cut the band of clasts (arrow). B) Clasts surrounded by calcite veins forming narrow rims (arrows). Note the well-rounded clast (C) (tinted thin-section). C) Grain size sorting at thin-section scale with smaller clasts in the neighbouring of the host rock walls (continuous lines) and indicating the flow direction (dashed line). The arrow shows a vein alineated with the flow (tinted thin-section). D and E) Cement with rhombohedral crystals of replacement dolomite (E: tinted thin-section). Location of hand-sample: Star 4 of Fig. 1B. Location of thin sections: Star 2 of Fig. 1B.

We suggest that the breccias have a tectonic origin, and generated during processes of cataclastic breakage accompanied by hydraulic fracturing. Indeed, they are not simple cataclastic rocks limited to continuous fault planes (Twiss and Moores, 1992), but are distributed as sill-like bodies included within the upper part of the Malaguide Complex (fig. 2A), although the breccias bodies sometimes also mimic the surfaces of low-angle normal faults. Moreover, at smaller scale, cataclastic foliation in the studied breccias is only very scarce and the presence at same time of large rounded

and highly angular clasts (Fig. 3B) is incoherent with cataclastic fault breccias (Storti et al., 2007). Accordingly, the roundness of the clasts should be due to a remobilization of the fragments, and it is proposed that this remobilization would have occurred during fluid circulation associated with a mechanism of hydraulic fracturing (e.g. Hulen and Nielson, 1988). This process would also explain the size sorting of the clasts perpendicular to the host wall (Fig. 3C; Chown and Gobeil, 1990), the fabric without cataclastic foliation and the fact that the matrix is sometimes composed only by cement (Katz et al., 2006). In the other hand, dolomite of replacement is also indicative of fluid circulation.

If the breccias were formed as a consequence of both processes, hydraulic and cataclastic fracturing, it is not possible yet to determine their relative chronology. Nevertheless, a possible scenario would be that the faults and fractures in the Malaguide rocks acted as pathways for the fluid circulation and subsequent hydraulic fracturing. This interpretation would explain the existence of different breccia fabrics, in terms of clast shape, presence of cataclastic foliation and composition of the matrix, from one sample to another.

The similarity of the breccias forming bodies in the Malaguide Complex with those of the avalanche deposits of the lowest member of Viñuela group and the fact that the tectonic breccias of Riogordo area are situated immediately below the Viñuela sedimentary deposits (Fig. 1B), suggest that the tectonic breccias could have nourished the sedimentary ones. If so, the tectonic processes that produced the breccia bodies would have been previous to the lower Burdigalian. It is also possible that tectonic and sedimentary processes acted coeval. In this case, brecciation of the uppermost levels of the Malaguide Complex would have occurred at very shallow conditions, but in which the presence of highly pressurized fluids required for hydraulic fracturing would be difficult to explain. Finally, in the studied area, Alosaina Complex attributed to Middle Burdigalian seals the relationships between both types of rocks and is affected by normal faulting (medium to high angle faults, Fig. 1B).

Breccias formed with fluid-assisted process have been described by Comas and Soto (1999) in the Alboran Basin. They are very similar to the rocks described in the present paper, and they show the same replacement dolomite habitus observed in Riogordo area, although they developed in the upper Alpujarride Complex. These authors suggest that breccias and fault-gouge zones were an important pathway for fluids that produced dolomitization after the brittle deformation.

4.3) Gravitational dismantling of the Miocene mountain front of the Gibraltar Arc system deduced from the analysis of an olistostromic complex (western Betics)

Abstract

A *mélange* complex seals the internal-external zone boundary of the western part of the Gibraltar Arc orogenic belt and constitutes a key element to establish milestones of the Betic-Rif tectonic evolution. The blocks and olistoliths embedded in this *mélange* provide constraints on the geological history of the main tectonic units involved in the Miocene mountain front. We mapped and analysed the blocks and olistoliths included in this *mélange* in order to understand its age and genesis, which have long been a matter of debate. The relationships of this *mélange* La Joya Olistostromic Complex (LaJOC) with the basement units together with the high variability of the block lithologies suggest a sedimentary origin for this *mélange*. Two large-scale olistoliths retain their original structure prior to their emplacement in the LaJOC Basin. The sedimentological and structural analysis allowed us to correlate these olistoliths with the folded and thrust sequence belonging to the Miocene Betic-Rif accretionary prism (Flysch Trough units), and to constrain the age of deposition of the La Joya Olistostromic Complex. The age of the matrix of the *mélange* deposits is poorly known because of the lack of in-place fauna. Indeed, the formation of the inherited fold-and-thrust structure of these olistoliths is well-known in the western Betics. Accordingly, the LaJOC should have been deposited during middle Miocene times and the blocks and olistoliths included within the *mélange* would derive from the gravitational dismantling of the Gibraltar Arc mountain front. The data presented help us to understand the formation of reliefs and basins in the western part of the Gibraltar Arc orogenic system.

Introduction

Mélange complexes are widespread in the Alpine Mediterranean orogenic belt and can be found in very different geological settings (e.g. Jeanbourquin, 1994 for the Alps; Nemcok and Nemcok, 1994 for the Carpatians; Lucente and Pini, 2008 for the Apennines; Okay et al., 2010 for the Anatolian range; Cavazza and Barone, 2011 for the Calabrian Arc; Alonso et al., 2006 for the Iberian Variscan Massif). Because of its structureless and chaotic appearance, the origin of these *mélanges* is not easy to determine and the processes from which they derive, sedimentary or tectonic, are often subject of discussion (Camerlenghi and Pini, 2009; Festa et al., 2010).

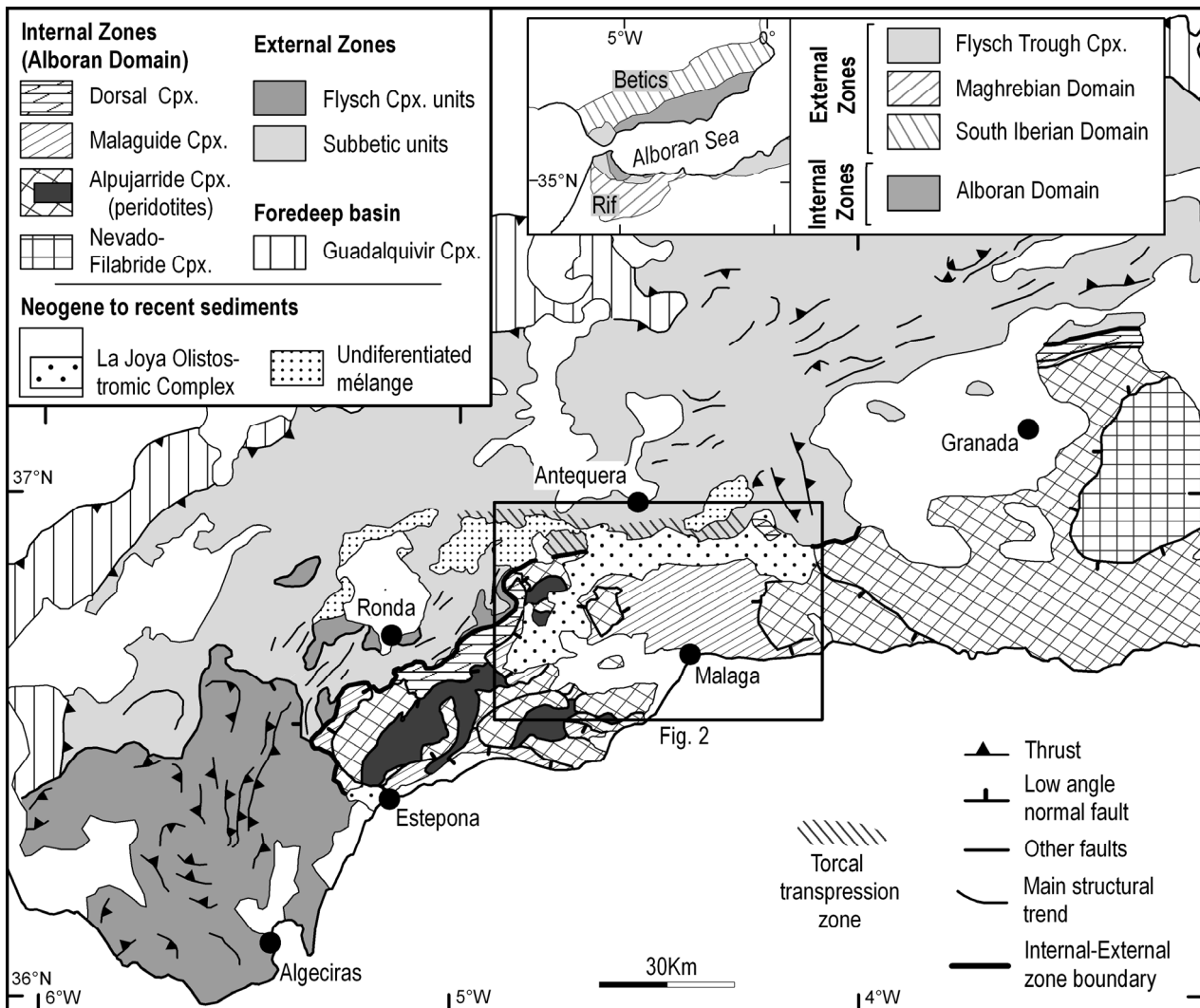


Figure 1: Main tectonic domains of the western and central Betics. Cpx: Complex. Inset: sketch of the Betic-Rif orogenic system.

This type of complexes crops out in the Gibraltar Arc orogenic system, the westernmost link of the Alpine Mediterranean orogenic belt; and is a well-known case of back-arc extensional collapse simultaneous with compression in the external part of the arc (Fig. 1; e.g. García-Dueñas et al., 1992). In particular, north of the Gibraltar Strait, mélanges have been described in the Betic external zones, either included in the paleomargin derived fold-and-thrust belt units (Subbetic units of Fig. 1; Comas et al., 1978; López Olmedo et al., 1988) or in the foreland basin deposits (Guadalquivir Complex of Fig. 1; Vera et al., 2004; and Gulf of Cadiz Complex; Medialdea et al., 2004). In both cases, these mélanges show an olistostromic character.

Another mélangé complex is situated in the boundary between the internal (Alborán Domain) and external zones along the transition between the central and western Betics (essentially between meridians 4° and 5°W, Fig. 1). Its position made well worth its study in order to decipher and correlate the tectonic pulses in this boundary, and its origin was a matter of debate during the 70's and 80's (Peyre, 1974;

Bourgois, 1978; Olivier, 1984; Balanyá and García-Dueñas, 1986; Martín-Algarra, 1987). These studies were based on limited outcrops. In this paper, we provide a comprehensive analysis of this *mélange* complex and we shed light on its nature, origin and emplacement. We characterized the type of boundary with the underlying units, and studied the stratigraphy and structures of the embedded blocks. In particular, we focused on the analysis of large-scale blocks as the tectonic structures preserved within these blocks permitted to determine their source area and to establish time relationships with the main tectonic events that took place during the Gibraltar Arc mountain front evolution at Miocene times.

Geological setting

The Gibraltar Arc orogenic system

The Gibraltar Arc orogenic system bounds the Mediterranean to the west. The main units involved are the following (Fig. 1):

1) The Alborán Domain, in the hinterland, is formed by the metamorphic internal zones. It is subdivided into several complexes, which from bottom to top are: the Nevado-Filábride (not present in the western Betics), the Alpujárride, the Maláguide and the Dorsal complexes (Fig. 1). The Alpujárride Complex is composed of a Paleozoic metapelitic-metapsammitic sequence and Triassic carbonate rocks. The Alpujárride Complex is made up by units of variable metamorphic grade (Adra, Salobreña and Herradura units in the study area, Azañón and Crespo-Blanc, 2000; Fig.2). Peridotite slices can be found in between the uppermost units (Sánchez-Gómez et al., 1996). The Maláguide Complex consists of a Paleozoic sequence of low metamorphic grade made up of phyllites and carbonates, in turn overlain by a non-metamorphic cover of mainly Triassic red conglomerates and sandstones accompanied by scarce Jurassic to Eocene carbonates (e.g. Cuevas et al., 2001). The Dorsal Complex (Durand-Delga and Foucault, 1967) is mainly composed by Triassic to Neogene sedimentary non-metamorphic rocks with a predominance of carbonated series. It is an imbricate thrust sequence that crops out discontinuously along the internal-external zone boundary, tectonically sandwiched by the other units of the Alborán Domain on top and the external zones at the bottom (Balanyá, 1991).

2) The Flysch Trough Complex consists of Cretaceous to lower Miocene clastic rocks imbricated in thrust stacks and emplaced over the South Iberian and Maghreb paleomargin-derived units (Fig. 1; Didon, 1969; Luján et al., 2006). The Oligocene to Miocene sediments of the Flysch Trough Complex were deposited in the accretionary prism which underlined the western Mediterranean subduction zone (Faccenna et al., 2004). Based on the presence of sandstones or greywackes in the Aquitanian sediments (Aljibe or Algeciras formations respectively), three main units have been described in

this complex (Aljibe, Algeciras and Bolonia units; Didon, 1969). The Predorsal units crop out along the internal-external zone boundary and are included in the Flysch Trough Complex. Predorsal units are characterized by dismembered slices of Jurassic to lower Miocene rocks (Fig. 2; Durand-Delga, 1972; Olivier, 1984). The calcareous Jurassic rocks show a strong affinity with the Dorsal Complex whereas the Cretaceous to Neogene sequence is similar to the aforementioned Flysch Trough Complex units. The Predorsal units are structurally sandwiched between the Alborán Domain on top and the other Flysch Trough Complex units below.

3) The Subbetic units represent the detached cover of the South Iberian paleomargin. They are composed by sedimentary rocks of ages generally ranging from Triassic to Cretaceous, although the sedimentary record extends up to the Neogene (Vera, 2000). The detached cover of the Maghrebian paleomargin is represented by the External Rif.

The Gibraltar Arc orogenic system formed mainly during Miocene times because of the westward migration of the Alborán Domain that acted as a backstop. The movement of the Alborán Domain with respect to the external zones produced the detachment of the cover rocks from the Flysch Trough Complex and the South Iberian and Maghrebian paleomargins. These rocks detached from their basement currently form the fold-and-thrust belt of the Gibraltar Arc external wedge (Balanyá and García-Dueñas, 1988). The study area corresponds to the westernmost part of the Gibraltar Arc (west of 4°30'W, Fig. 1). There, the Flysch Trough Complex and the Subbetic units form the external fold-and-thrust belt whose structural trend mimics the Gibraltar Arc curvature (Fig. 1). The formation of this fold-and-thrust belt took place during Burdigalian and/or Serravalian times (Crespo-Blanc and Campos, 2001; Crespo-Blanc and de Lamotte, 2006; Luján et al., 2006; Balanyá et al., 2007). In the central part of Figure 1, the continuity of the structural trend is cut off by a dextral transpression zone which mainly affected the Subbetic units (Barcos et al., 2011, inclined hatching in Fig. 1; Torcal transpression zone of Balanyá et al., 2012). The transpressional regime and associated uplift were active, at least, between the late Miocene and the Quaternary and probably their activity began in middle Miocene times.

While compression was taking place along an orogenic front migrating towards the external zones, rifting was active in the back-arc of the Gibraltar Arc and various systems of low-angle normal faults affected the Alborán Domain (Fig. 1; García-Dueñas et al., 1992; Comas et al., 1999). In the study area (Fig. 2), these structures mainly present a top-to-the-SW transport direction north and east of the city of Málaga (Alonso-Chaves and Orozco, 1998; Booth-Rea et al., 2003), whereas west of the city a centripetal tectonic transport towards the arc is observed (from SSE to SE directed; Balanyá, 1991; García-Dueñas et al., 1992). The interval age during which these fault systems were active is considered to be early Burdigalian-Serravallian (op. cit.).

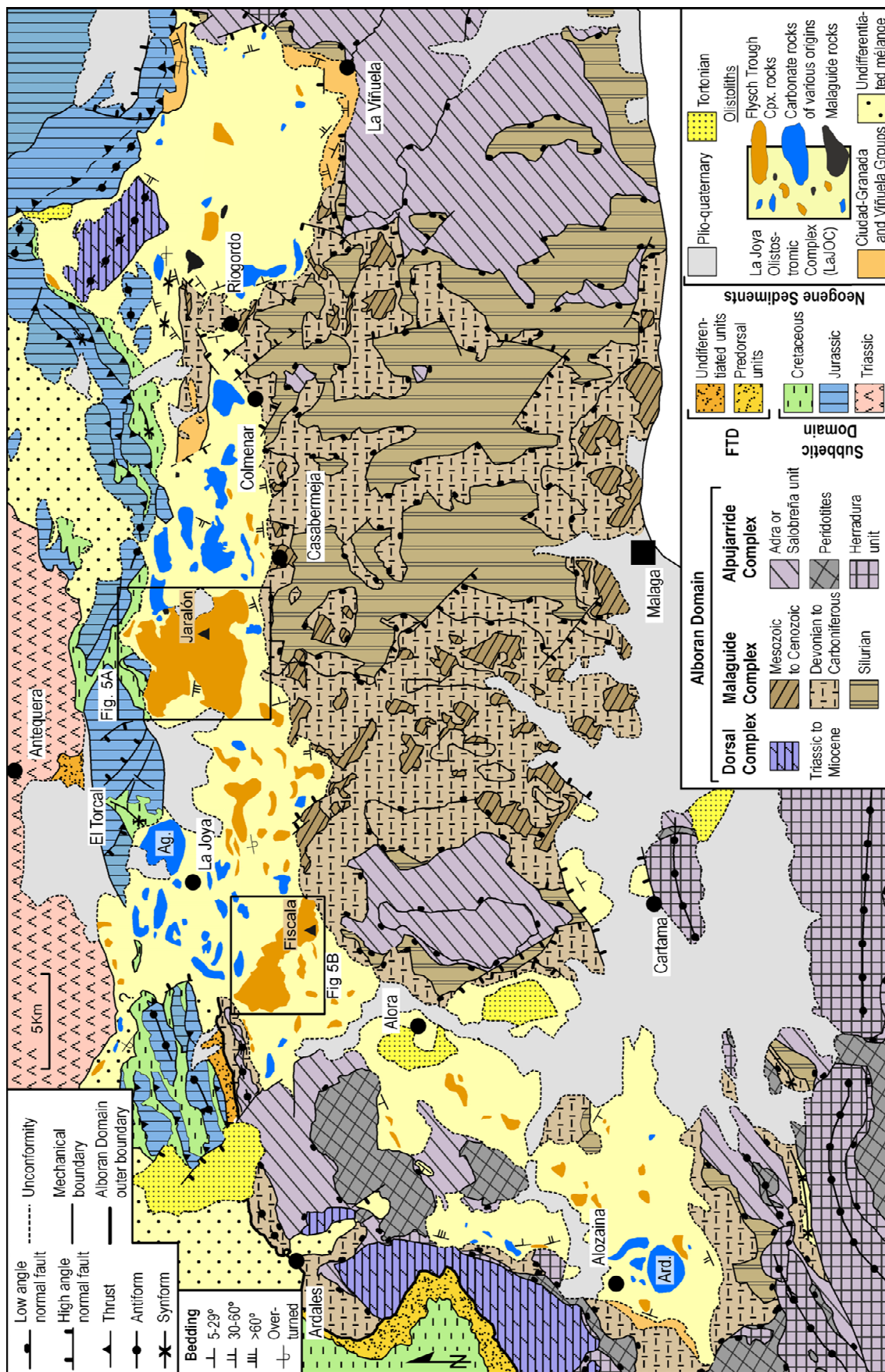


Figure 2: Structural sketch of the La Joya Olistostromic Complex (location in Fig. 1). Modified from Balanyá et al. (2012), Martín-Algarra et al. (2004), Booth-Rea et al. (2003), Cano Medina and Ruiz Reig (1982), Barba Martín et al. (1979), Chamón Cobos et al. (1976). FTD: Flysch Trough Domain units; Ard: Cerro de Ardite olistolith; Ag: Cerro del Águila olistolith.

After these main orogenic episodes of folding and thrusting coeval with the extension, the western Gibraltar Arc area was affected by a contractive episode from Tortonian to Recent (García-Dueñas et al., 1992; Comas et al., 1999; Rodríguez Fernández et al., 1999). This triggered the formation of open folds and high-angle fault systems.

Miocene deposits in the study area

Domain contributed to its subsidence and to the deposition of Miocene sediments unconformably over the metamorphic complexes (Comas et al., 1992; García-Dueñas et al., 1992). Whereas offshore the sedimentary record is fairly continuous during Miocene times (Jurado and Comas, 1992), only scattered outcrops of the same time interval are present onshore.

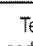
	Defined Units	Age of deposition	Method	Genetic interpretation
Peyre (1974)	Tectono-sedimentary Complex	Lower Burdigalian	<i>Fauna</i>	Tectono-sedimentary Complex
	Flysch de Colmenar	Aquitanian		sedimentary unit
Bourgois (1978)	Neonumidien  Argiles à blocs	Burdigalian	<i>Fauna/super-position criteria</i>	Tectono-sedimentary Complex
Olivier (1984)	Predorsal	Lower Burdigalian	<i>Fauna</i>	Backthrust (dismantled)
Martín-Algarra (1987)	Arcillas Variegadas	Lower Burdigalian	<i>Fauna</i>	Tectonic unit
	Numidoide			resedimented Sedimentary unit
Balanyá (1991)	Alozaina Complex	Upper Burdigalian	<i>super-position criteria</i>	Sedimentary Complex
This-work	La Joya Olistostromic Complex	Langhian to Serravallian	<i>Olistoliths correlation</i>	Olistostromic sedimentary Complex

Figure 3: Schematic chart that summarises the main points of previous works on the La Joya Olistostromic Complex, as well as this work.

In the western Betics, the Ciudad-Granada and La Viñuela groups represent the first sedimentary record (see review in Serrano et al., 2007) and testify the initial stages of the Alborán Domain rifting (García-Dueñas et al., 1992). Both groups outcrop in the studied area (Fig. 2) and are characterized by initial deposits of breccia or conglomerate with clasts that derived from the nearby Alpujarride and/or Maláguide metamorphic rocks (Serrano et al., 2007). The marls that overlie the breccias were dated as Aquitanian to early

Burdigalian (González-Donoso et al., 1983; Martín-Algarra, 1987; Aguado et al., 1990; Durand-Delga et al., 1993; Serrano et al., 2007). The Ciudad-Granada and La Viñuela groups onlap the Alborán Domain and seal some of the extensional fault systems related with the rifting episode, as observed in the eastern part of Figure 2 (10km SSE of Riogordo; Alonso-Chaves and Orozco, 1998). It must be stressed that, locally, hydraulic brecciation associated with some low-angle normal faults could have favoured the supply of the breccias from La Viñuela Group (Suades and Crespo-Blanc, 2010). Analogous sediments, supplied in turn by clasts from the Subbetic Domain (Santana formation of Mathis (1974) in Barba Martín et al., 1979), occur north of La Viñuela

village (Fig. 2). They are presently verticalized, even overturned and thrust by the Jurassic limestones of the Subbetic Domain.

A *mélange* complex overlies the Ciudad-Granada and La Viñuela groups as well as the Alborán Domain metamorphic rocks and the Subbetic units. It is characterized by turbiditic sediments alternating with chaotic deposits. The latter are a mixture of blocks of diverse sizes, ages and lithologies embedded in an argillaceous matrix. The block-in-matrix appearance is characteristic of both tectonic and sedimentary *mélanges* (tectosomes and olistostromes, respectively; Cowan, 1985; Camerlenghi and Pini, 2009; Festa et al., 2010). This complex crops out along two main sectors (Fig. 2): a northern one that follows an E-W depression along the internal-external zone boundary, and a western one, NNE-SSW-directed and located over the Alborán Domain units. A very narrow outcrop is also present 10km SSE of Alozaina, pinched between the Alborán Domain units (García-Dueñas et al., 1992).

Finally, small outcrops of this formation occur near the locality of Estepona (Fig. 1; Balanyá, 1991). This *mélange* complex is the subject of this study and will be described in detail in the next section. Finally, a few outcrops of near-horizontal conglomerates, sandstones and calcarenites dated as Tortonian are present in the studied area (Fig. 2; see López-Garrido and Sanz de Galdeano, 1999 and references therein).

Previous work on the *mélange*

The *mélange* complex that we describe in this paper received several names in the past, because of its enigmatic origin, undetermined age, chaotic appearance and poor outcrops. Previous works were mainly based on small, limited areas being the most important ones listed in Figure 3. The lack of in-place fauna within the *mélange* complex made an accurate dating difficult. However, the paleontological studies of Peyre (1974), Bourgois (1978), Feinberg and Olivier (1983), González-Donoso et al. (1987) and Martín-Algarra (1987) indicated that it cannot be older than early Burdigalian (as indicated by resedimented planktonic foraminifera), which is nonetheless consistent with the fact that the *mélange* lies over the La Viñuela Group (Balanyá, 1991).

The origin and emplacement processes of the *mélange* complex have also been a matter of debate. Peyre (1974), who focused his studies on the northern outcrops, defined two main units in the *mélange* according to the degree of disturbance of the matrix: the Colmenar Flysch, transgressive over the Alborán Domain, and the so-called Tectonosedimentary Complex, in turn thrust over the Colmenar Flysch. He also considered the large-scale blocks of the *mélange* either as tectonic windows or klippen. Bourgois (1978) held again the term of Tectonosedimentary Complex and defined two units, the “Neonumidian” and “Argiles à blocs”. He defined them west of the Ronda Basin (Fig. 1), and included in both units any flysch type unit with a supposed chaotic

structure of sedimentary klippe embedded in a clay matrix. He exported this model to the western sector of the *mélange* and considered the sector as part of the “Tectosedimentary Complex”, which would have been emplaced tectonically over the Alborán Domain.

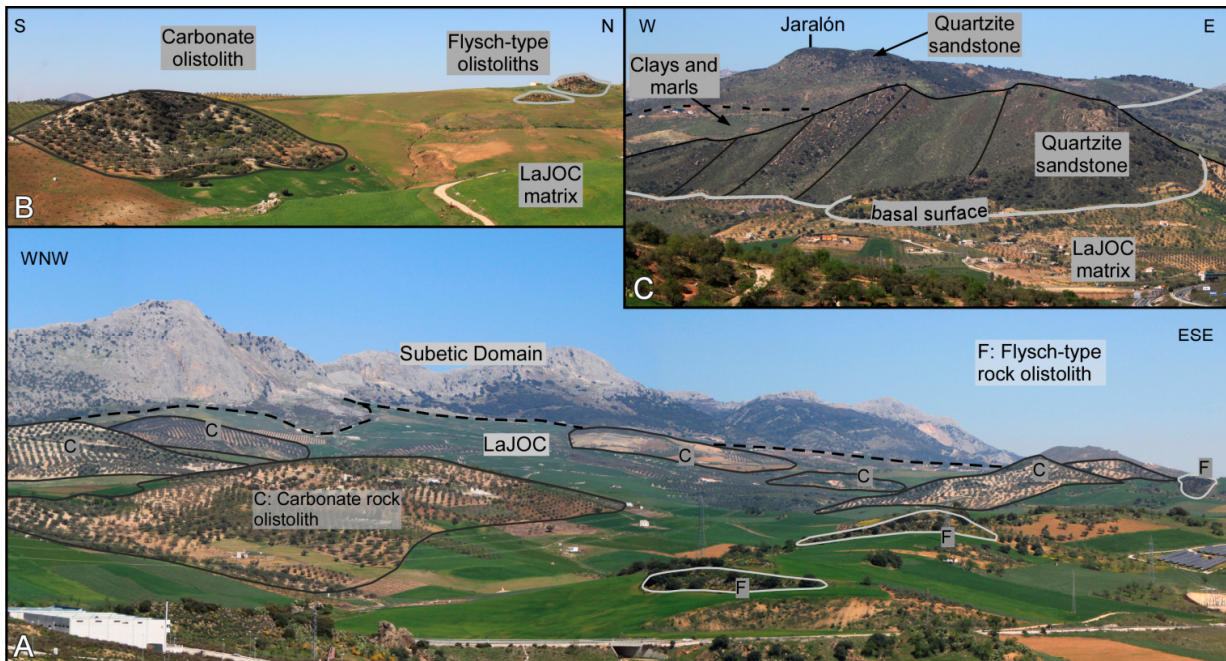


Figure 4: Field photographs of the La Joya Olistostromic Complex (LaJOC). A) General view of the LaJOC northern sector taken from Casabermeja, facing ENE. C: Carbonate rock olistolith, F: Flysch type rock olistolith. B) View of two olistoliths with a positive relief “floating” on the matrix (5km NW of Colmenar). C) View of the Jaralón olistolith. Note beds of quartzite sandstone cut abruptly by the basal surface.

By contrast, Olivier (1984) considered this *mélange* complex as Predorsal units, which would represent part of the dismembered Flysch Trough units, also overthrust on the Alborán Domain. This author interpreted the blocks as tectonic slices which would have lost their internal continuity. Martín-Algarra (1987) considered both processes, tectonic and gravitational, to explain the origin of the *mélange* cropping out in the western part of the northern sector. In his opinion, the “Arcillas Variegadas s.s.” would correspond to Flysch Trough units tectonically emplaced over the Alborán Domain, later dismantled and resedimented; whereas he considered the so-called “Numidoide” as autochthonous and deposited during active tectonics. In this scenario, large-scale blocks can either have an intrabasinal origin, or be individual tectonic units.

Finally, Balanyá and García-Dueñas (1986) and Balanyá (1991) used the term of Aozaina Complex to define the *mélange* deposits cropping out in the southwesternmost sector as well as in the isolated outcrop of Estepona (Fig. 1). For these authors the *mélange* derived from the gravitational dismantling of mainly Dorsal and Predorsal units over the Alborán Domain.

The works of the aforementioned authors deserve several considerations. First of all, it must be stressed that even if this complex contains turbiditic deposits, the use that

most of the cited authors made of the term “Flysch” contributed to generate confusion. Indeed, the term is not appropriate as this *mélange* complex is not a unit of the Flysch Trough Complex, in the sense that it did not belong to its paleogeographic domain (accretionary prism associated with the western Mediterranean subduction zone during Miocene times). Moreover, petrographical similarities with some of the sequences of the Flysch Trough Complex units were observed in blocks or olistoliths embedded in this complex. On the other hand, some authors (Peyre, 1974; Martín-Algarra, 1984) considered the large-scale blocks as individual tectonic units, encouraging the characterization of a great number of tectonic units (e.g. Barba Martín et al., 1979).

In this work, we consider the *mélange* as a single and differentiable complex, although we recognize that it could be made up of several subunits.

We offer for the first time an overall view of it, from the village of Alosaina in the west, to the village of La Viñuela in the east (Fig. 2). We agree with the overall concept of gravitational dismantling of Balanyá and García-Dueñas (1986). However, we think that the term Alosaina Complex has to be abandoned, because it has already been used for the Alosaina Formation, a local formation of the Ciudad-Granada Group, cropping out near the village of Alosaina (Bourgeois et al., 1972) and stratigraphically situated below the *mélange*. Accordingly, we propose the term of La Joya Olistostromic Complex (LaJOC) to refer to this *mélange* complex. La Joya is a small village located at the intersection of the two sectors of this complex, and the term “olistostromic” will be justified in the next section.

Main features of the La Joya Olistostromic Complex

At outcrop scale, we have not found any evidence characterizing the contact between the LaJOC and the underlying units (Alborán Domain, Flysch Trough Complex and Subbetic Domain) as a mechanical contact, but in spite of its poor exposure, we could see that is a sedimentary unconformity. This does not agree with the thrust interpretation that can be found in the national geological maps of Spain (Chamón Cobos et al., 1976; Barba Martín et al., 1979; Cano Medina and Ruiz Reig, 1982). At map scale, it can be observed how the low-angle normal faults bound the Alpujarride and Maláguide complexes and are always sealed by the LaJOC (Fig. 2). The few available measurements in the stratified levels of the LaJOC show that it strikes generally parallel to the contact with the Alborán Domain, and dips gently to moderately towards the centre of both the northern and western sectors of the LaJOC (Fig. 2). This would indicate two main, very smooth, E-W and NNE-SSW trending folds, respectively. On the other hand, the contact between the LaJOC and the Subbetic Domain is generally masked by scree deposits issued from the erosion of the Subbetic carbonate rocks. When observed, this contact is either a high-angle fault or a stratigraphic unconformity (Figs. 2; 4A). Finally, late high-angle normal faults, trending

mainly NW-SE, affect the LaJOC-Alborán Domain unconformity near the villages of Riogordo and Alora (Fig. 2). They belong to the same late fault system that affects the Alborán Domain.



Figure 5: Outcrop views of the La Joya Olistostromic Complex. A) Well-layered turbiditic beds with conchoidal fracture. B) Mélangé matrix with scaly fabric. C) Isolated block in the mélangé matrix. D) Block shaped in a closed fold. E) Lenticular flysch type olistolith within the matrix.

The LaJOC is characterized by chaotic units (mélanges with blocks floating in a matrix) intercalated with well layered stratified levels. In the field, the matrix of the mélangé units and the stratified levels usually correspond to the low-relief cultivated areas and show characteristic colours that range from brown-tobacco to ochre (Figs. 4A,

B). By contrast, the large blocks that belong to the *mélange* units are easily differentiable and appear mainly on top of hills (Fig. 4B). Because of the poor outcrops, it was not possible to differentiate between the stratified levels and the exposure of *mélange* units in the map of Figure 2, although they can be distinguished at outcrop scale (in ravines or along road trenches).

The stratified levels are mainly constituted by turbiditic clays and marls (Fig. 5A) interbedded with scarce, thin and rhythmic levels of fine-grained sandstones. The marls are usually rich in silica and present a conchoidal fracture. Scarce folds are observed, though their origin is still unclear (sedimentary slumps or tectonic folds). Nevertheless, N and NE of the village of Riogordo, near the boundary with the Subbetic Domain, the whole sequence is folded, verticalized and/or even overturned. Accordingly, some of the observed folds may be tectonic in origin.

Regarding the chaotic units, the matrix that supports the blocks is also comprised of marls and clays but in this case with a disrupted aspect. The latter are characterized by anastomosed smoothly undulated surfaces, forming pseudobedding (scaly fabric according to Vannucchi et al., 2003), generally subhorizontal or dipping slightly (Figs. 5B, C, D).

Blocks and olistoliths are all those bodies that are embedded or floating within the chaotic matrix, being the olistoliths all those blocks of more than 4m in length (see Dunbar and Rogdger, 1957). In general, the blocks are isolated. They are isometric with sharp borders and are supported by the matrix (Fig. 5C). Sometimes, blocks are elongated, lens-shaped, and may be folded (Fig. 5D).

The contact of the olistoliths with the matrix is not observable everywhere but, in most cases it is sub-horizontal and the olistoliths seem to “float” on the matrix (Fig. 4B, C). For this reason, Peyre (1974), Barba Martín et al. (1979) and Olivier (1984), among others interpreted some of them as tectonic klippen. Other olistoliths are embedded in the matrix, forming large-scale lens structures (Fig. 5E). Usually, they preserve their internal structure, but they can be also disrupted or fractured. The LaJOC contains a large number of olistoliths and many of them are big enough to be mapped (Fig. 2). Their distribution is not homogeneous: they are very abundant in the northern sector, and scarcer in the western one.

The blocks and olistoliths have been classified according to their lithology. Three main groups are present (Fig. 2):

i) A first group includes all those blocks and olistoliths composed mainly by unmetamorphosed carbonate rocks. They can proceed from the Subbetic Domain, the Predorsal, the Dorsal, or even from the Maláguide cover. Some of them have been dated and their ages mainly range from Jurassic to Paleocene, although some can be as young as Miocene (Peyre, 1974; Bourgois, 1978). The biggest olistoliths of this group are those from the “Cerro del Aguila” hills (Peyre, 1974), situated SW of El Torcal (Ag. in Fig. 2). Martín-Algarra (1987) and Alcalá-García et al. (2002) correlated them either to

the Predorsal units or the Subbetic Domain. Another large olistolith crops out in the “Cerro de Ardite” hill, situated 2km south of Alozaina (Ard. in Fig. 2). It shows an overturned Jurassic to Eocene sequence and has strong similarities with the Predorsal units (Bourgois, 1978; Olivier, 1984).

ii) The second group is poorly represented and is comprised of Silurian to Devonian shales and Permian to Triassic red clays and conglomerates from the Maláguide Complex.

iii) The blocks and olistoliths of the third group are made of rocks that can be directly correlated with the Flysch Trough Complex rocks (Figs. 2; 5E; 6). The most common rocks are mature quartzite sandstones with a high degree of roundness and grain sorting. The grain size varies from one block to another, ranging from fine to very coarse. Another type of rock is a less mature and finer grained greywacke with abundant mica. These two types of sandstones can be correlated with the Aquitanian formations present in the three main units of the Flysch Trough Complex: while the quartzite sandstones are analogous to the sandy levels of the Aljibe Formation (which belongs to the Aljibe unit), the greywackes can be correlated with the Algeciras Formation (Algeciras unit; Fig. 6A; Didon, 1969). Finally, an intercalation of both types of sandstones can be observed in an olistolith (Fig. 6B), similar to the Bolonia unit (Didon, 1969). Moreover, there are other unconsolidated sediments which do not form isolated blocks and can only be distinguished in the large-scale olistoliths, alternating with the sandstones (Fig. 6). They are characterized by marls, clays and carbonates that Peyre (1974) dated as Eocene to Oligocene in the olistolith situated 3 km WNW of Casabermeja (Fig. 2). This succession of sandstones and unconsolidated sediments shows strong similarities with what is known in the Flysch Trough Complex as the “Serie de Base”, a Palaeocene to Oligocene calciturbiditic sequence (Esteras et al., 1995 in Luján et al., 2006).

Large-scale Olistoliths

The two largest olistoliths from the LaJOC are located on top of the hills of Jaralón (5km NW of Casabermeja village) and Fiscala (8km NNE of Alora) (Figs. 2; 6A, B). The Jaralón olistolith is 25km² in area and 450m in height (with respect to its base), and Fiscala olistolith is 13km² in area and 250m in height. Both olistoliths can be correlated with the sedimentary sequences of the Flysch Trough Complex. Peyre, 1974; Cano Medina and Ruiz Reig, 1982; Olivier, 1984 and Martín-Algarra, 1987 considered the olistoliths as tectonic units either nappe or klippe.

A map and a cross-section of the Jaralón hill olistolith is shown in Figures 6A and D. It shows an imbricated thrust sequence composed by Aljibe and Algeciras type rocks, i.e. quartzite sandstones alternating with marls and clays (“Serie de base” sequence) and greywackes, respectively. It trends approximately E-W and the thrust

sequence dips generally gently towards the N or the S (see cross-section in Fig. 6D). In the southern part of the olistolith, the whole imbrication depicts an arcuate geometry and the trend turns from E-W and NW-SE to N-S. The basal surface contact between the structured olistolith and the matrix runs almost horizontal. Accordingly, the olistolith seems to be “floating” on the matrix and its bedding is cut by the basal contact (see Fig. 4C and the cross-section in Fig. 6D), that does not show kinematic indicators.

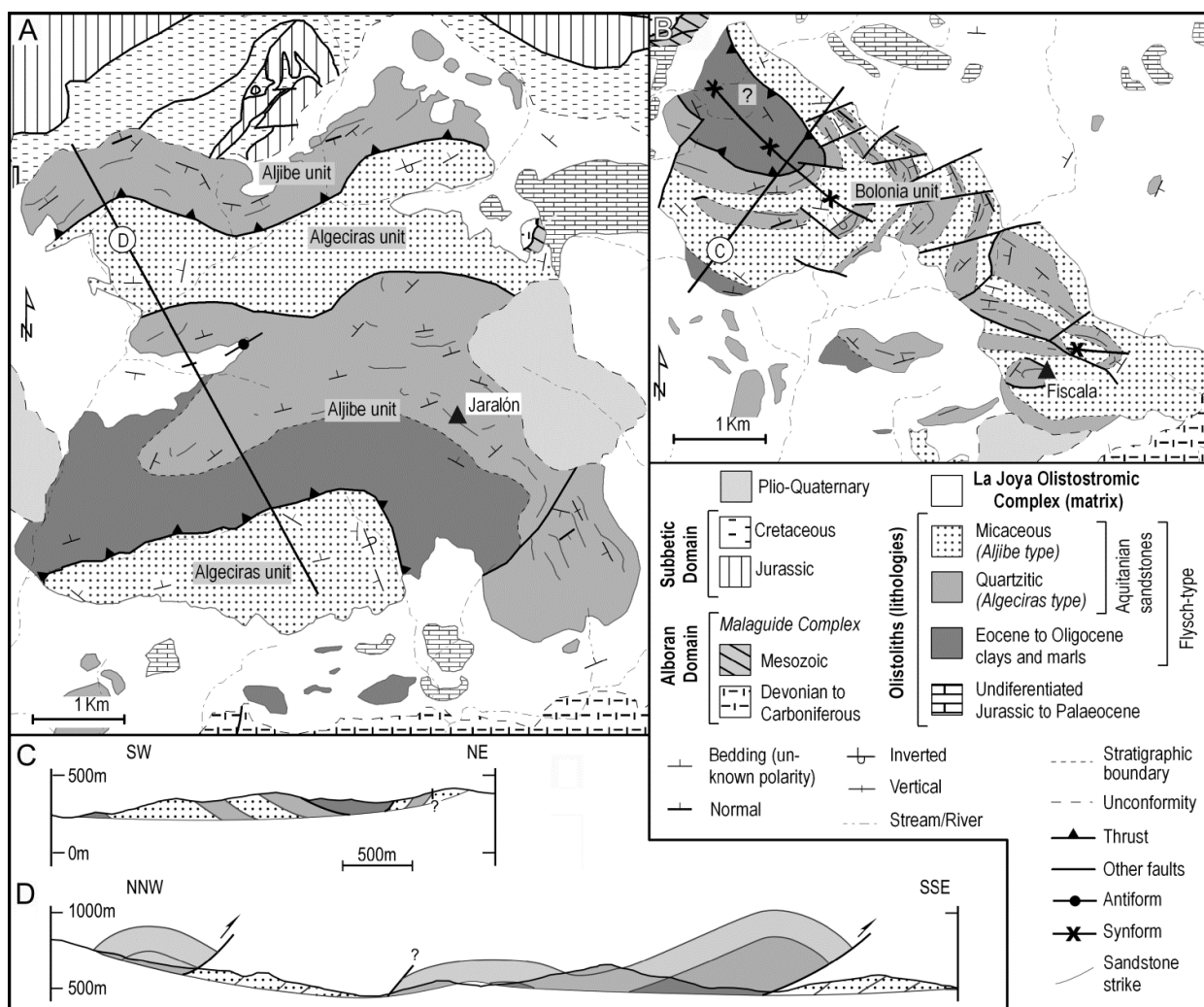


Figure 6: A) and B) Geological maps of Jaralón and Fiscala olistoliths, respectively (see location in Figure 2). Olistolith lithologies are listed in the legend and their correspondence with the Flysch Trough Domain units is indicated on the map. C and D) Cross-sections of Fiscala and Jaralón olistoliths, respectively.

The olistolith that crops out in the Fiscala hill shows decametric to hectometric alternation, characteristic of the Bolonia unit, of Aljibe type quartzite sandstones and fine grained Algeciras type greywackes (Fig. 6B). The Fiscala olistolith forms a NW-SE trending synform plunging towards the NW. The strata that draw this synform are in a normal position. On top of this Aquitanian sequence, an Eocene to Oligocene marly-argillaceous sequence is observed, equivalent to the “Serie de base” sequence. It points to the presence of a thrust of unknown kinematics which separates the Bolonia unit at the bottom and the “Serie de base” sequence on top. As in the Jaralón olistolith, the base

of the Fiscala olistolith shows a flat geometry cutting all the previous thrust imbrications (Fig. 6D). Late high-angle, ENE-SSW faults, cut the olistolith and the matrix.

Discussion

Nature and genesis of the La Joya Olistostromic Complex

The LaJOC is mainly characterized by the presence of very heterogeneous blocks in terms of litology and size. These blocks are dispersed in a matrix where a stratigraphic succession cannot be established. As a matter of fact, only partial sections have been measured (Peryre, 1974; Martín-Algarra, 1987). According to Camerlenghi and Pini (2009) and Festa et al. (2010) among others, the LaJOC description broadly coincides with the current concept of *mélange*, in a descriptive sense. For these authors, the origin of a *mélange* can be associated either with tectonic processes (fault-related), sedimentary processes (due to gravitational falling or sliding into a basin), or diapirism. In our study area, this latter process can be ruled out as it would require the existence of overpressured shales or evaporites in the metamorphic Alborán Domain basement. In addition, if the *mélange* was the result of diapirism a prevalence of basement metamorphic blocks would be expected. These rocks would be eroded during the ascension of the diapir, which is not the case. To distinguish between tectonic and sedimentary origins, outcrop-scale detailed textural analyses are needed (see Camerlenghi and Pini, 2009). Unfortunately, the poor quality of the outcrops excludes the possibility to make this type of analysis. Nevertheless, the following criteria led us to favour a sedimentary origin.

First, the contact between the LaJOC and its basement can be interpreted as a sedimentary unconformity, and the LaJOC indistinctly overlies the internal (Alborán Domain) and the external (Subbetic and Flysch Trough fold-and-thrust belt) zones. Indeed, LaJOC seals the low-angle normal faults related to the Alborán Domain rifting (Fig. 2). Concerning the blocks and olistoliths of the LaJOC, they range in age from Permo-Triassic to Aquitanian, all older than the matrix (at least early Burdigalian). This and the fact that they show a wide range of lithologies, including Flysch Trough rocks which are not present in its surroundings, point to an exotic sedimentary origin for the blocks and olistoliths. Moreover, in tectonic *mélanges*, blocks frequently show an elongated, boudin-like geometry and their preferential orientation results in pseudo-bedding (Cowan and Pini, 2001; Bettelli and Vannucchi, 2003). This is not generally observed in our case study.

If the *mélange* were tectonic in origin, we would expect an alignment with a major tectonic structure. This is true for the northern sector, where the LaJOC outcrops

along the boundary between the internal and external zones and could be related with the fault zone between both. Nevertheless, along the western sector, the LaJOC crops out entirely over the Alborán Domain, where the major tectonic structures (essentially low-angle normal faults) do not affect it. The scaly fabric observed in the matrix of the *mélange* units (Figs. 5B, C, D) is typical of tectonic *mélanges*, but this kind of fabric can also occur in sedimentary *mélanges*. It can be produced, at the base of large olistostromes (see Camerlenghi and Pini, 2009), either by compaction (by burial and/or dewatering) or late tectonics (Flores, 1959; Vannuchi et al., 2003; Lucente and Pini, 2008).

Emplacement of the large-scale olistoliths

The folds and thrusts imbricate structures described in the Jaralón and Fiscala olistoliths are similar to those observed in the Flysch Trough Complex units (Luján et al., 2006; Crespo-Blanc et al., 2010). Peyre (1974), Olivier (1984) and Martín-Algarra (1987), considered these olistoliths as tectonic units. According to them, the olistoliths would have been emplaced through a backthrust from the Flysch Trough Complex over the *mélange*, which, in turn, would have thrust the Alborán Domain. Nevertheless, in the northern branch of the Gibraltar Arc, the Flysch Trough Complex units are always situated structurally below the Alborán Domain (Crespo-Blanc and Campos, 2001; Luján et al., 2006). Even if this is the case for the emplacement of these olistoliths, this tectonic process cannot explain the presence of blocks and small olistoliths of the same lithology dispersed in the matrix. Moreover, the lack of mechanical contacts along the base of the large-scale olistoliths and the fact that their lower boundary does not correspond to a basal thrust, as it cuts all the thrusts located in the interiors, are not coherent with the backthrust hypothesis (although they could be out-of sequence thrusts). Accordingly, we consider that the Fiscala and Jaralón hills are formed by olistoliths that were already structured when they were gravitationally emplaced within the LaJOC.

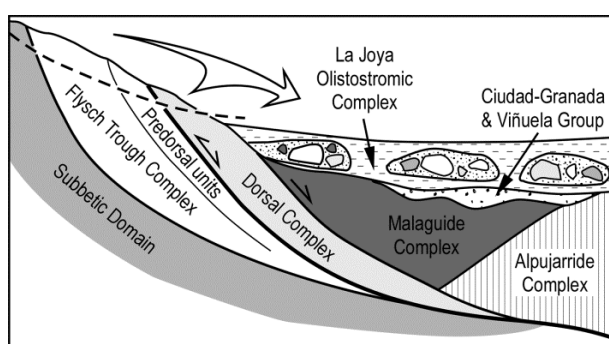


Figure 7: Sketch illustrating the geometry of the main tectonic complexes, the relative position of the LaJOC Basin and the mode of emplacement of the olistoliths.

Figure 7 schematically illustrates the LaJOC deposition and the emplacement of the olistoliths. We propose that the LaJOC was supplied by the erosion and gravitational dismantling of the tectonic units involved in the mountain front, that was growing coetaneously with the development of the

external zone fold-and-thrust belt. By that time, the Alborán Domain was already affected by back-arc rifting and subsidence. Accordingly, it should have been at lower topographic level than the mountain front, which would have favoured the gravitational transport of the olistoliths initially located in a more external position over the Alborán Domain. As for the Jaralón and Fiscala olistoliths, they derive from the deformed Flysch Trough Complex, structurally located between the Subbetic and the Alborán domains (Balanyá and García-Dueñas, 1988; Crespo-Blanc and Campos, 2001). In the case of the Ardite olistolith, it derives from an overturned Predorsal unit.

Age of the La Joya Olistostromic Complex and relationships with the evolution of the Gibraltar Arc

The structural analysis of the large-scale olistoliths suggests a middle Miocene age for the LaJOC (Fig. 8). Indeed, the uppermost deposits of the Flysch Trough Complex fold-and-thrust belt have been dated as lower Burdigalian for the Aljibe unit (Esteras et al., 1995 in Luján et al., 2006) and upper Burdigalian for the Algeciras unit (De Capoa et al., 2007). Consequently: i) the main shortening and thrusting of these units should have taken place from late Burdigalian onwards (Luján et al., 2006; Crespo-Blanc et al., 2012), and ii) the presence of two already deformed Flysch Trough Complex olistoliths implies that sedimentation in the LaJOC probably began around the boundary between early and middle Miocene. Its deposition could have extended up to Serravallian times, since LaJOC is sealed by Tortonian calcarenites and conglomerates.

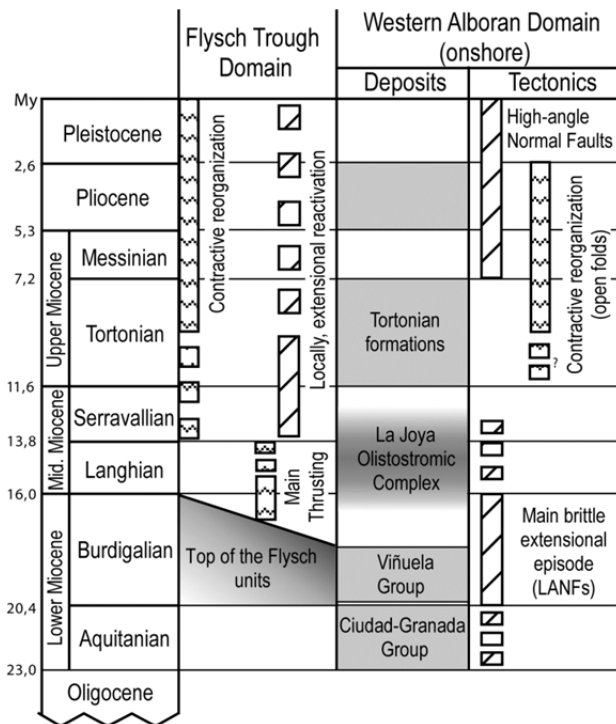


Figure 8: Chronologic chart of the tectonic evolution of the Flysch Trough Domain and western Alborán Domain during Miocene times. Ages of tectonic processes and sedimentary deposits constrain the deposition of the La Joya Olistostromic Complex.

Geological mapping of LaJOC showed that the low-angle normal faults that affected the Alborán Domain, associated with the Miocene extension, are sealed by the LaJOC (Fig. 2). In addition, Suades and Crespo-Blanc (2010) showed that hydraulic brecciation related to some of these low-angle normal faults supplied Malaguide detritus to the breccia deposits of La Viñuela Group (Aquitanian to early Burdigalian in age), situated stratigraphically below the LaJOC. Consequently, the activity of the low-angle normal fault systems that affected the Maláguide and

Alpujarride complexes in this part of the western Betics ceased prior to the emplacement of the LaJOC (Fig. 8). As rifting proceeded, both the basement and LaJOC should have been passively transported on top of the W to SW-ward Serravallian low-angle normal fault system, the basal detachment of which is represented by the Nevado-Filábride/Alpujarride boundary, 80km E of the study area (Fig. 1; see also García-Dueñas et al., 1992; Martínez-Martínez and Azañón, 1997; Alonso-Chaves and Orozco, 1998).

North of the LaJOC northern sector, a dextral transpression zone affecting the southern outcrop of the Subbetic Domain was active at least from late Miocene to Recent (Torcal transpression zone in Fig. 1; Barcos et al., 2011 and Balanyá et al., 2012). The associated uplift and development of relatively high topography with respect to the LaJOC Basin probably promoted gravitational dismantling processes. As a matter of fact, a higher concentration of the mapped olistoliths can be observed south of El Torcal area, in the northern sector of LaJOC (Fig. 2). The deformation associated with the southern boundary of the transpressive zone could also be responsible for the overturning of both the LaJOC NNE of Riogordo village, and the Viñuela Group 8km north of La Viñuela village (Fig. 2).

The few available measurements of bedding show that the LaJOC is folded (scarce, very open folds). The E-W trending syncline of the northern sector of the LaJOC is subparallel to the very open folds drawn by the Alborán Domain units near the village of Cartama and in the southwestern part of the LaJOC (see also Chamón Cobos et al., 1976; Sánchez Gómez et al., 1996). The NNE-SSW direction of the syncline of the western LaJOC sector corresponds to that of the folds developed between the late Tortonian and the late Messinian in the Ronda Basin, 30km WNW of the study area (Fig. 1; see references in Crespo-Blanc and Campos, 2001). Both groups of folds can be related to the latest Miocene to recent contractive reorganization defined onshore, in the western (Crespo-Blanc and Campos, 2001; Booth-Rea et al., 2003; Balanyá et al., 2012) and central Betics (Azañón and Crespo-Blanc, 2000; Martínez-Martínez et al., 2002; Marín-Lechado et al., 2007), as well as offshore (Comas et al., 1999).

Open questions

We focused on the study of the LaJOC in the area mapped in Figure 2, but previous works pointed out that mélanges similar to that described in this paper are also present in the western Gibraltar Arc. West of the study area, on the Ronda Basin (Fig. 1), Bourgois (1978) and Cruz-Sanjulián and Ruiz Reig (1980) described argillaceous sediments with a chaotic appearance and embedded blocks and olistoliths similar to the LaJOC. These authors called them “argiles à blocs” and the existence of blocks of flysch type rocks led them to attribute these sediments to the Flysch Trough Complex.

Nevertheless, the *mélanges* described by these authors are lower Burdigalian or younger, that is younger than the Flysch Trough Complex. Moreover, the aforementioned *mélanges* do not display a coherent structure of thrust stacking, which is characteristic of the Flysch Trough Complex units (e.g. Luján et al., 2006; Crespo-Blanc et al., 2010). Another *mélange* crops out east of Antequera (Figs. 1; 2) and includes essentially carbonate blocks (although some quartzite sandstones of the Aljibe unit are also present; Pineda Velasco and Ruiz Reig, 1983). All these *mélanges* could represent the external counterpart of the LaJOC, in the sense that they could represent the gravitational dismantling of the mountain front in basins situated over the external zones. Finally, in the southern branch of the Gibraltar Strait, a transgressive formation of marls and pelites dated as Burdigalian lies over the internal zones of the Rif (El Kadiri et al., 2001; Serrano et al., 2007; Hlila et al., 2008). Over this unit, Chalouan et al. (1995) and Hlila et al. (2008) describe a large-scale, 7km-long block made of Aljibe type quartzite sandstones, structured in a thrust stack and cut along its base. The similarities between the large-scale olistoliths described in the present paper and this Aljibe type body lead us to consider that it could represent an olistolith included within a sedimentary unit similar to the LaJOC.

All these *mélanges* require additional work in terms of time-space correlations. They are key sequences to understand the relationships between topographic evolution, erosion and basins in the western part of the Gibraltar Arc orogenic system.

Conclusions

1) The La Joya Olistostromic Complex (LaJOC) crops out in the western Betics. It is characterized by turbiditic deposits alternating with *mélange* units that contain blocks and olistoliths of several origins. It is interpreted as a sedimentary complex, lying unconformably over the internal-external zone boundary.

2) In terms of lithology, the blocks and olistoliths included in the LaJOC can be classified into three main groups: Jurassic to Paleocene carbonate rocks from the Subbetic, Flysch Trough Complex or Alborán Domain, Paleozoic shales and Permian-Triassic red clays of the Alborán Domain, and clastic rocks of the Flysch Trough Complex. They are mainly extrabasinal in origin. No tectonic contact has been observed at the bottom of the olistoliths.

3) The deposition of the LaJOC is interpreted as due to the gravitational dismantling of the units situated in the neighbouring of the Miocene mountain front of the western Gibraltar Arc. The blocks and olistoliths which make up the LaJOC were transported mainly towards the hinterland.

4) Two kilometre-scale olistoliths have been described. They preserve the internal structure prior to their emplacement and show an imbricate thrust stack, similar to some units of the Flysch Trough Complex.

5) The sedimentation of the LaJOC should be post-late Burdigalian and pre-Tortonian in age, and it seems to have a wider area than that described in the study area.

5 The Malaga Basin: tectonic systems tracks within the extensional history

5.1) Introduction

The present chapter presents part of the results obtained from the offshore study of the Malaga Basin realized in this PhD Thesis. It focuses on the relationships between tectonics and sedimentation by using the sequence-stratigraphic methodology. This methodology has been widely used in passive margins but in tectonic active basins, such as the Malaga Basin, few studies applied this method.

Therefore, the present chapter has two main objectives: 1) to better understand the tectonic evolution of the Malaga Basin by establishing tectono-sedimentary relationships by using the sequence-stratigraphic methodology, and 2) to use the Malaga Basin as case study of asymmetric extensional basin to check the viability of this methodology in order to propose key characteristics of this type of basin. This will help the analyzing and understanding of similar basins worldwide.

The results have been presented in a scientific journal (*Basin Research*) with the title “Tectonic system tracts in asymmetric extensional basins: inferences from the evolution of the Malaga Basin in the westernmost Mediterranean”. The manuscript, at the time this Ph.D Thesis lecture is under revision and this chapter corresponds with the sent manuscript version, although the references are included with those of this PhD Thesis volume (Chapter 9).

This sequence stratigraphic study is the result of a collaboration between the university of Granada and the tectonic group from the University of Utrecht (Netherlands) and, specifically, with Dr. Liviu Matenco. The authors are, in order, Enric Suades, Liviu Matenco, Menchu Comas and Ana Crespo-Blanc.

5.2) Tectonic system tracts in asymmetric extensional basins: inferences from the evolution of the Malaga Basin in the westernmost Mediterranean

Abstract

Stretching-driven subsidence exerts a primary control on sedimentation in extensional basins. Deposition is usually described by a sequence stratigraphic terminology that includes the kinematics of normal faults within the overall balance between accommodation space and sediment supply. While available for generic rift systems, the architecture of sedimentary sequences in asymmetric extensional basins controlled by major detachments is little known. In this paper, we analyse deposits affected by large-scale footwall exhumation and spatial/temporal migration of normal faulting. Our case study, the Malaga Basin located in the Alboran Domain of the western Mediterranean, shows diachronous extensional detachments associated with normal fault systems that converge into the crustal basement. Moreover, this basin is characterized by the high rates of extension associated with the back-arc of a retreating subduction. The seismo-stratigraphic study applied to this basin permits to develop a new methodological approach, in which the increased seismic resolution associated with the high rates of sedimentation allowed the definition of two orders of cyclicity inside the basin. The low-order sequences formed in response to continental rifting, while the high-order cyclicity formed during moments of activation of normal faults and associated footwall uplift or regional glacio-eustatic events. The overall geometry of such basins may look apparently symmetric due to the migration of detachments and normal faulting, locally with different tectonic transport directions. Nevertheless, the internal architecture of tectonic system tracts and sequences demonstrates the real asymmetry of the basin. These novel results are interesting for understanding the tectonic-driven sedimentation in asymmetric extensional back-arc basins located elsewhere.

Introduction

The depositional infill of sedimentary basins is often described by using various sequence stratigraphic methodologies in continental and marine depositional environments (Vail et al., 1977; Posamentier et al., 1988; Schlager, 1993; Christie-Blick & Driscoll, 1995; Nystuen, 1995; Catuneanu et al., 2009 and references therein). Although less known, sequence stratigraphic methodologies that use specific definitions of system tracts are readily available also in tectonic active basins (e.g., van Wagoner et

al., 1990; Ravnås & Steel, 1998; Hinsken et al., 2007; Răbăgia et al., 2011; Pereira & Alves, 2012). In these basins, the balance between accommodation space and sediment supply is controlled by fault-driven vertical movements and/or associated thermal sag effects (Beaumont 1981; Ziegler & Cloetingh, 2004; Martinsen et al., 2010; Matenco & Andriessen, 2013). In sequence stratigraphic studies based on observations in outcrops or seismic lines, continental rift basins were commonly described either by using transgressive-regressive patterns linked with the activation of normal faults, or by using a specific tectonic system tracts terminology at the scale of the entire (sub-)basin (e.g., Prosser, 1993; Nottvedt et al., 1995; Martins-Neto & Catuneanu, 2010). Significantly different than symmetric continental rifts, much less is known on the sequence stratigraphic architecture of extensional basins formed in the hanging-wall of low-angle detachments. Such extensional basins are highly asymmetric in terms of tectonic-induced vertical movements, the footwall exhumation being almost one order of magnitude higher than the hanging-wall subsidence (Wernicke, 1985; Wernicke & Axen, 1988; Lister & Davis, 1989). This exhumation creates a source area that is dynamic and changes in space and time coeval with the migration of normal faulting. This migration often leads to footwall exhumation and erosion of an area that previously recorded hanging-wall subsidence, or the opposite, hanging-wall subsidence over a previously eroded footwall (Tari et al., 1992; Martín-Barajas et al., 2001; Aragón-Arreola et al., 2007; Matenco & Radivojević, 2012). The resulting geometry is often the one of two gently dipping flanks in an overall symmetric basin that is made up by internal asymmetric syn-kinematic wedges. In sequence stratigraphic terms, the migration may be detected by a transgressive-regressive cyclicity of higher order than the entire rift sequence, which is able to quantify detailed structural patterns and timing of deformation.

Similarly, very few datasets exist on the sequence stratigraphic architecture of rapidly evolving extensional basins driven by slab rollback and these are generally limited to parts of the syn- and post-kinematic depositional sequences (e.g., Juhász et al., 2007; ter Borgh et al., 2014). In such settings, the differences in sedimentation across the basin are accentuated and can be better studied due to the high strain rate. Such rapid asymmetric extension is observed in the Mediterranean area during the Tertiary evolution of the Gibraltar, Calabrian or Carpathians systems (Doglioni et al., 1998; Faccenna et al., 2004; Horváth et al., 2006). This is where rapidly evolving rollback subduction systems have created a significant number of arcuate orogenic geometries associated with the formation of extensional basins in their hinterland, flooded by either continental or oceanic lithosphere (e.g., Pannonian and Aegean basins, Black Sea or Western Mediterranean). These basins are extensional back-arcs in terms of geodynamic evolution (Royden, 1993; Jolivet & Faccenna 2000; Faccenna et al., 2004; Horváth et al., 2006; Doglioni et al., 2007; Brun & Faccenna, 2008) although

their relative position behind a magmatic or island-arc is not always very clear (Uyeda and Kanamori, 1979; Dewey, 1980; Mathisen and Vondra, 1983).

One such area in which the sequence stratigraphy of rapidly evolving asymmetric extensional basins can be studied is the Malaga Basin, which is located in the NW part of the Alboran Basin, in the western Mediterranean Sea (Figs. 1 and 2). This basin formed during Miocene times in response to a back-arc extension that produced a series of (half-) grabens bounded by major detachments (García-Dueñas et al., 1992; Comas et al., 1992). We apply the principles of seismo-stratigraphic interpretation to a network of 2D seismic lines and correlation wells in the Malaga Basin in order to study the kinematic geometries and to define a novel sequence stratigraphic model for asymmetric extensional systems. This model can be, potentially, applied to other extensional (back-arc) basins that share a similar tectonic history.

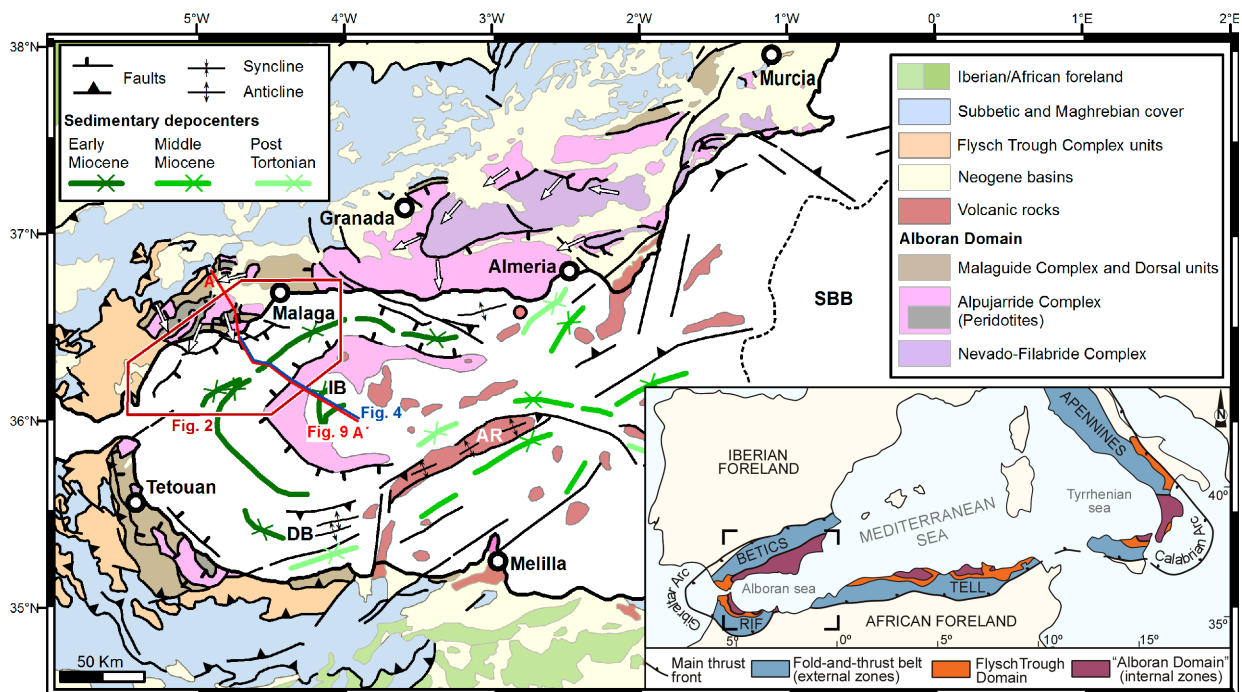


Figure 1: Tectonic map of the Gibraltar Arc System (modified from Comas et al., 1999). White arrows: transport direction along extensional detachments; Polygon: location of the Malaga Basin. SBB: South Balearic Basin; IB: Internal Basin; AR: Alboran Ridge; DB: Djibouti Bank Inset: Tectonic domains in the Western Mediterranean.

An overview of the Malaga Basin in the context of the western Mediterranean

The basement of the Malaga Basin, the Alboran Domain, corresponds with the hinterland of the Western Mediterranean subduction zone, surrounded by the Betics, Rif and Tell Mountains (Fig. 1). There is a general consensus that this zone acquired its highly arcuated geometry during the W to SW rapid roll-back of a lithosphere

subducting beneath an Alboran upper plate during the overall NE-SW convergence between Europe and Africa (Platt & Vissers, 1989; Lonergan & White, 1997; Faccenna et al., 2004; Spakman & Wortel, 2004; Vergés & Fernández, 2012; Mancilla et al., 2013). Alternative scenarios of an E-ward subduction of the Atlantic oceanic lithosphere beneath the Gibraltar arc have been also proposed (e.g., Gutscher, 2012). The Alboran Domain outcrops onshore and was drilled offshore in the Alboran Sea (Fig. 1; Comas et al., 1999). It is made up by a thinned continental crust containing dominantly Palaeozoic to Triassic metamorphic rocks, overlain by a significant number of Neogene basins.

The Gibraltar Arc formed during Neogene times in response to the collision between the Alboran Domain and the Mesozoic to Tertiary cover of the South Iberian and Maghrebian paleo-margins (Fig. 1; Michard & Martinotti 2002; Crespo-Blanc & Frizon de Lamotte, 2006; Balanyá et al., 2007). During this convergence, Lower Miocene syn-kinematic trench turbidites were deposited and deformed between the African/Iberian foreland and the Alboran Domain, composing what is commonly known as the Flysch Trough Complex (Luján et al., 2006).

Partly coeval with the contraction recorded by the orogenic foreland, extension and significant crustal thinning initiated in the Alboran Domain likely during the late Oligocene and continued during Miocene times (Platt et al., 1998). Geophysical and modelling studies indicate variable crustal thicknesses, from ~35km near the orogenic arc, to 15-21km in the centre of the Alboran Sea, while the E-ward located South Balearic Basin is characterized by a 9km thick oceanic crust (Fig. 1; Torné & Banda, 1992; Galindo-Zaldívar et al., 1997; Comas et al., 1999; Torné et al., 2000; Booth-Rea et al., 2007; Soto et al., 2008). The thinning was largely accommodated by normal faults and extensional detachments of various ages and kinematics that presently bound the main tectonic complexes of the Alboran Domain (i.e. the Nevado-Filabride, Alpujarride and Malaguide, Fig. 1). These fault systems are syn-kinematic or sealed by the Miocene deposition (Fig. 1; García-Dueñas et al., 1992; Crespo-Blanc, 1995; Martínez-Martínez & Azañón, 1997). Extension and crustal thinning was associated with rapid exhumation of Alboran Domain rocks previously buried at mantle depths (Platt & Vissers, 1989; Balanyá et al., 1997; Soto & Platt, 1999; Azañón & Crespo-Blanc, 2000). The Miocene deposition started locally with an Upper Aquitanian to Lower Burdigalian marine sequence that is well studied onshore (e.g. Bourgois et al., 1972; Jurado & Comas, 1992; Martín-Algarra, 1987; Martín-Martín et al., 1996; Serrano et al., 2007). Offshore in the Alboran Sea, the onset of the main extensional sedimentation started during early Miocene in the west and middle Miocene - late Tortonian in the east (Fig. 1; Comas et al., 1999). This deposition was locally interrupted by a large number of local or regional unconformities (Rodríguez-Fernández et al., 1999).

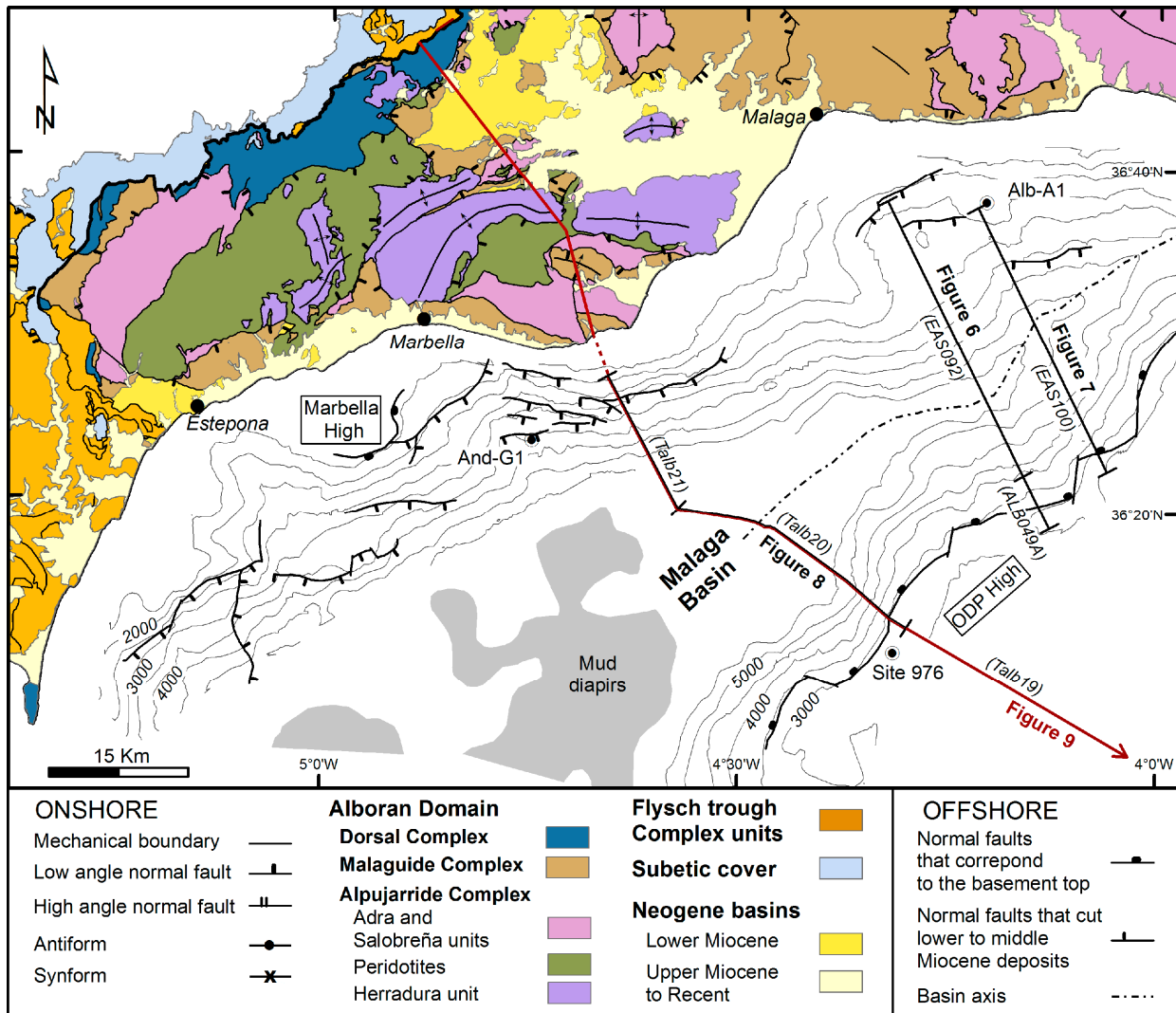


Figure 2: Onshore tectonic map simplified from Crespo-Blanc et al. (2012) and offshore structural map with basement contours, numbered in milliseconds two-way travel time. Circled dots: wells locations. Faults traced are structures active during early - middle Miocene times (from Suades et al., 2013). The full location of Fig. 4 and 9 is displayed in Fig. 1.

The activity of the normal faults in the Alboran Domain ceased at around 9Ma and the subsequent evolution was controlled mainly by the ongoing NE-SW directed convergence between the Eurasian and African plates (Mazzoli & Helman, 1994; Comas et al., 1999; Fernández-Ibáñez et al., 2007; Mauffret et al., 2007; Pedrera et al., 2011). This convergence inverted pre-existing normal faults, created transpressional and transtensional fault zones and produced open folds with kilometeric-scale wavelengths (Fig. 1; Comas et al., 1999; Crespo-Blanc & Campos, 2001; Martínez-Martínez et al., 2002; Booth-Rea et al., 2004; Muñoz et al., 2008; Martínez-García et al., 2013). Furthermore, the inversion exhumed the sedimentary basins that are exposed onshore (Braga et al., 2003; Do Couto et al., 2014). At present, the eastern part of the Alboran Sea displays a rough seafloor morphology controlled by major fault zones (Woodside & Maldonado, 1992; Ballesteros et al., 2008; Martínez-García et al., 2011). By contrast,

the western part of the Alboran Sea, including the Malaga Basin, has a fairly uniform bathymetry.

In the NW part of the Alboran Sea, the Malaga Basin extends in a south-western direction from the 4°W meridian up to the Gibraltar Strait (Campillo et al., 1992; Figs. 1 and 2). Across its strike, the basin is presently bounded by the Spanish shelf to the NNW and the High 976 to the SE. It shows gentle dipping flanks towards a depocenter that represents the northern branch of the Western Alboran Basin (Fig. 2; de la Linde et al., 1996; Comas et al., 1999; Suades et al., 2012). The half-graben geometry can be depicted by the steeper southern flank dipping towards a basin axis that plunges SW-wards, where more than 7km of sediments have been interpreted (Soto et al., 1996). In this deep part, the sediments are affected by large-scale mud diapirs that started to develop during the middle Miocene, piercing the overlying sedimentary sequence and distorting the original extensional geometry (Fig. 2; Talukder et al., 2003; Soto et al., 2010).

Deposition in the Malaga Basin is controlled by low-angle normal faults dipping towards the centre of the half-graben (Comas et al., 1992). Their kinematics appear to be similar with the along strike-equivalents exposed onshore as brittle low-angle normal faults (García-Dueñas et al., 1992; Martínez del Olmo & Comas, 2008; Suades et al., 2012). A number of early - middle Miocene normal and transfer faults affect both flanks of the basin, which display erosional features along structural culminations, such as the High 976 or Marbella High (Fig. 2; de la Linde et al., 1996; Suades et al., 2012). The SE flank of the basin (i.e. near High 976) is affected by a fault system with large offset. By contrast, the NW flank is affected by antithetic faults with small offsets and variable strikes, in particular from ~4° 30' meridian westwards (Fig. 2, Suades et al., 2013). Existing studies infer that the subsequent contraction, which started during the late Miocene, has inverted some of these structures and produced minor folds in the sedimentary basin fill (Comas & Soto, 1999).

Seismic interpretation studies correlated with the few available wells (And-G1, Alb-A1 and Site 976, Fig. 2) inferred that the sedimentary infill of the Malaga Basin is composed of six Miocene to Holocene seismo-stratigraphic units bounded by unconformities (Fig. 3; Jurado & Comas, 1992). The age and depositional environment of these units is constrained by microfauna and sedimentary facies observed in wells (Martínez del Olmo & Comas, 2008). In the lower part of the basin, the Aquitanian(?) - Burdigalian unit VI lies directly over the metamorphic basement. The chaotic reflectors that characterize this unit in seismic lines have been interpreted as olistostromic deposits (Jurado & Comas, 1992), which correlates with the chaotic sedimentation of clays with exotic blocks reported in well Alb-A1. Laterally in the onshore, this unit may correlate with olistostromic deposits with a block-in-matrix fabric (Bourgeois, 1978; Suades & Crespo-Blanc, 2013) that have an age not older than Burdigalian (Feinberg & Olivier, 1983; González-Donoso et al., 1987), possibly even younger (Suades & Crespo-Blanc,

2013). Although its genesis is still controversial (see Bourgeois, 1978; Martín-Algarra et al.,

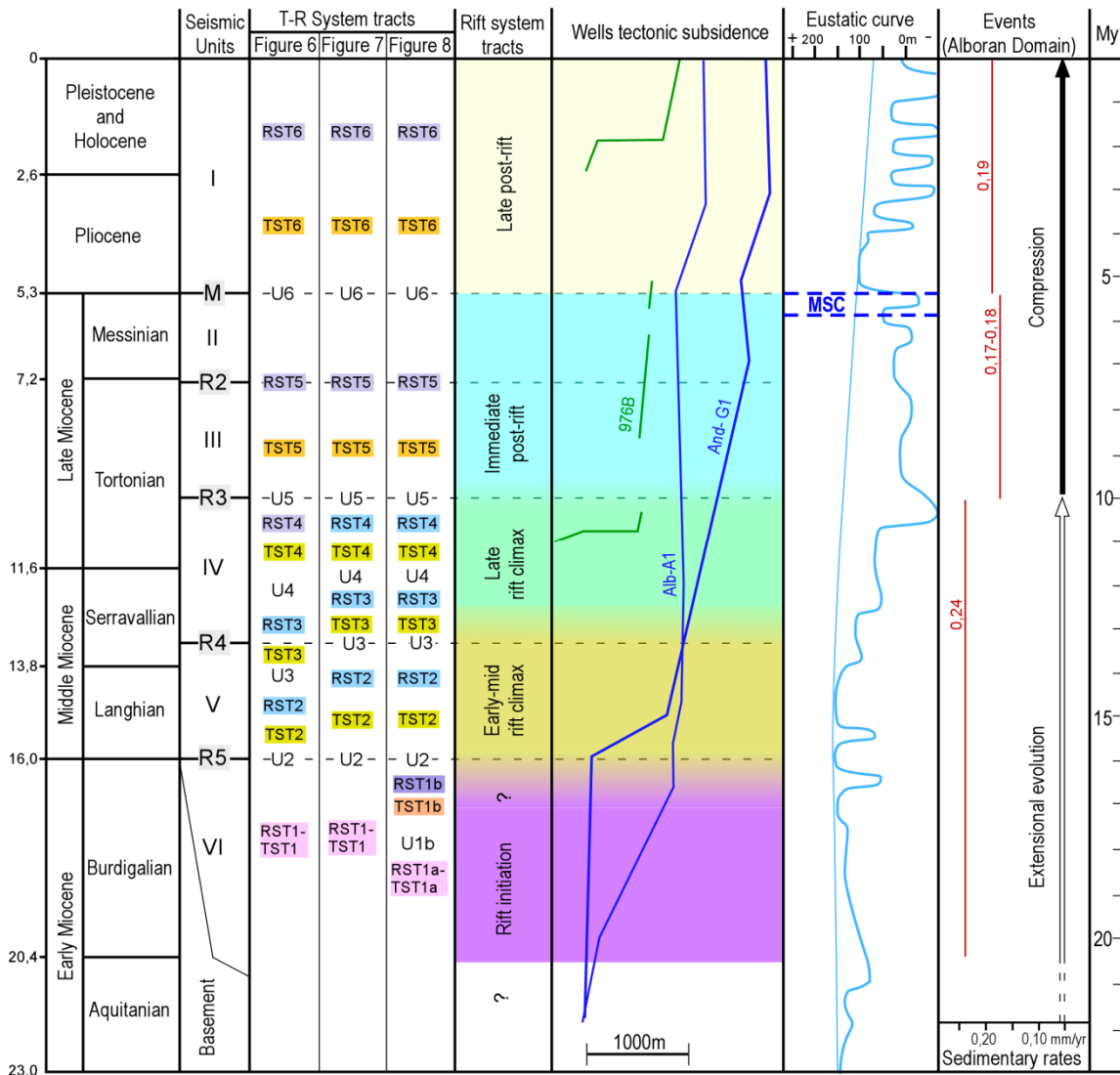


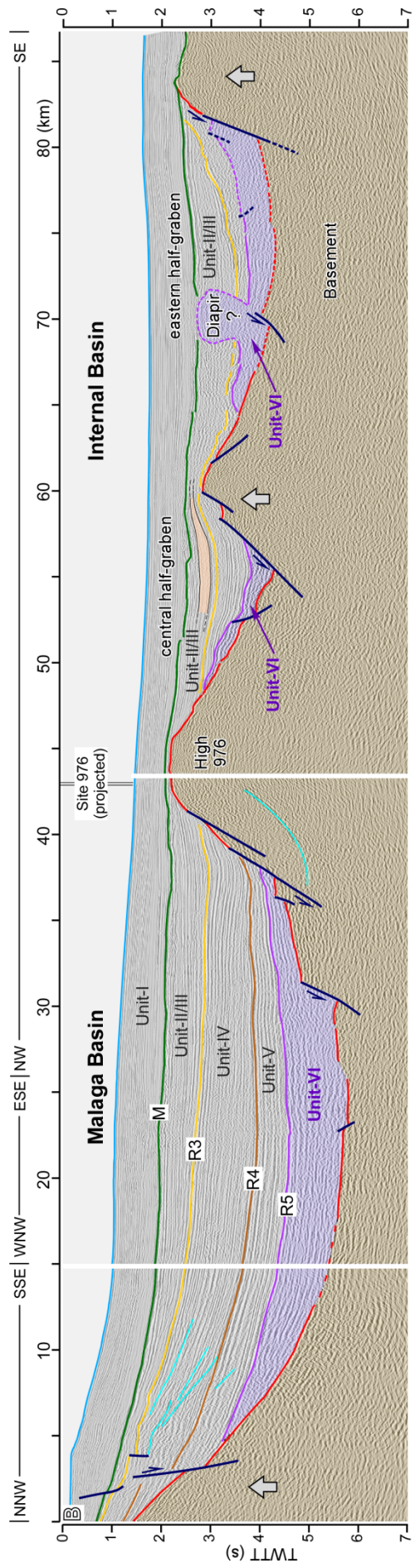
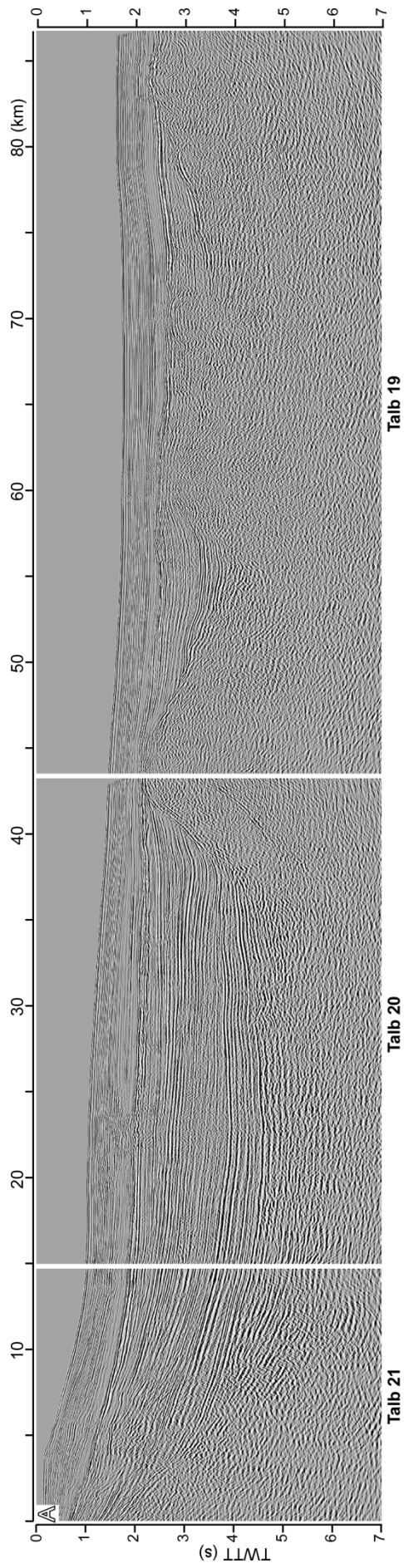
Figure 3: Relationship between the seismic units and unconformities from Comas and Jurado (1992), the system tracts of this study, the well tectonic subsidence curves (from Watts et al., 1993) and Rodríguez-Fernández et al., 1999), the eustatic curve of Haq et al. (1987); thin and thick blue lines are third and second order absolute sea level variations), the sedimentary rates (Iribarren et al., 2009) and the tectonic events in the Alboran Domain. MSC: Messinian Salinity Crisis (5.97-5.33, Krijgsman et al., 1999).

2009; Suades & Crespo-Blanc, 2013), we favor the extensional nature of unit VI because, onshore, olistostromic deposits post-date the low-angle normal fault system that bounds the metamorphic basement (Alonso-Chaves & Rodríguez-Vidal, 1998; Suades & Crespo-Blanc, 2013). Unit VI has nourished and was affected partly by mud diapirism (Comas et al., 1992; Talukder et al., 2003; Soto et al., 2010; Comas et al., 2012). This is in agreement with biostratigraphic dating that indicates a similar age of the mud-diapir matrix and unit VI (Sautkin et al., 2003). The general depositional environment of this unit is still unclear. The onset of sedimentation in well Alb-A1

indicates likely shallow marine sandstones, while onshore marls of Burdigalian age indicate mainly a bathyal environment (Serrano et al., 2007). The top of unit VI is a major erosional unconformity (R5) that is overlain by the Langhian - Lower Serravallian unit V (Fig. 3). Unit V has been observed only in the deepest parts of the basin, where it drapes the paleo-relief of the R5 unconformity, and contains clays with scarce conglomeratic levels, interpreted as deep marine deposits (Martínez del Olmo & Comas, 2008). Unit V is separated from the overlying Upper Serravallian – Lower Tortonian unit IV by another unconformity often observed as a high-amplitude reflector (R4). The latter unit contains sandstones and clays with conglomeratic intercalations, interpreted as a deltaic to turbiditic system (Martínez del Olmo & Comas, 2008), considered as being deposited during the final part of the extension. The Upper Tortonian unit III is considered as post-tectonic in respect to extension (Comas et al., 1992; Martínez del Olmo & Comas, 2008). In its lower part, this unit is bounded by a regional unconformity (R3) that has an angular character over the basin margins and changes to a paraconformity in its centre. This unit is composed of open marine (50-200m depth) claystones and limestones with sandstones levels (Martínez del Olmo & Comas, 2008). The Messinian unit II is composed of shallow marine alternation of carbonates and clays with anhydrite and gypsum levels. Unit II is affected by erosion and is locally absent, its top being marked in seismic lines by a high amplitude, low frequency reflector (M). This unconformity formed in response to the erosion that took place during or after the Messinian Salinity Crisis (MSC; Jurado & Comas, 1992; Clauzon et al., 1996; Krijgsman et al., 1999). In the upper part of the basin fill, the Pliocene - Quaternary unit I was deposited unconformably above the MSC unconformity.

Structural data: a seismic transect over the NW part of the Alboran Sea

The regional distribution of seismic units, unconformities and the first order relationship with deformation can be understood through the interpretation of a regional seismic profile that crosses the entire NW part of the Alboran Sea (Fig. 4). The profile crosses the central part of the Malaga Basin and extends further to the SE in the Internal Basin, where two more sedimentary depocenters are observed (Figs. 1 and 4). These are fault-bounded half-grabens (the central and eastern half-grabens, Fig. 4) separated by structural highs. Among them, the High 976 appears to indicate the largest amount of exhumation by the erosional surface observed in seismic lines (km 45 in Fig. 4). This erosion is less clear over the other two structural highs (Km 60 and south-easternmost corner in Fig. 4), although the geometry of the basement at the SE termination is more difficult to interpret.



The Malaga Basin is bounded to the SE by a major fault system next to High 976 (Fig. 2) and to the NW by a smaller offset antithetic fault (Fig. 4, NW of High 976 and near the NW termination of the profile, respectively). The latter belongs to the system of faults with small offsets located SE of Marbella (Fig. 2). Although faults dipping in opposite directions are observed in the central half-graben, syn-kinematic wedges indicate that the main controlling faults are dipping towards the NW (km 55-60, Fig. 4) and are associated with hanging-wall tilting in the half-graben. The sedimentary infill of the eastern half-graben has been distorted by, most likely, a mud-diapir structure (Km 70, Fig. 4) as its geometry is similar with the mud-diapirs affecting the SW part of the Malaga Basin, outside the studied area (Fig. 2, see also Soto et al., 2010). However, the alternative explanation of a volcanic structure cannot be disregarded, given the common occurrence of such late Miocene structures in the neighbouring regions (e.g., Duggen et al., 2004). The geometry of the eastern half-graben is similar to the central one and indicates exhumation of the basement high at the SE termination of the profile (km 80-85, Fig. 4) by the means of NW dipping faults truncating the basement. Given the vertical exaggeration of the seismic transect, the real inclination of these controlling normal faults is in the order of 20-30 degrees.

The distribution of the unconformities across the NW part of the Alboran Sea suggests that the infill of the Malaga Basin is much thicker prior to the formation of the R3 unconformity when compared with the other half-grabens (Fig. 4). The basal unit VI can be interpreted in all (half-)grabens crossed by the profile. It forms a large diapir in the eastern one, which was active in pre-Pliocene times as suggested by sediments overlying the Messinian Salinity Crisis unconformity (M in Fig. 4). The seismic resolution of the thin sequence bounded at the base by the unit VI and at the top by the unconformity R3 does not allow a separation between units V and IV in the central and eastern half-grabens.

Figure 4: Un-interpreted (a) and interpreted (b) seismic transect over the entire NW part of the Alboran Sea (location in Fig. 1 and Talb19, Talb20 and Talb21 in Fig. 2). The seismic interpretation displays the major sedimentary units, unconformities and faults. Because the seismic grid is only available in the Malaga basin, the interpretation along the Internal Basin is less constrained. Note that R4 unconformity is present only in the Malaga Basin. Grey arrows indicate uplifted areas during tectonic inversion and one associated syn-kinematic wedge is highlighted in ochre (Km 53-60). A couple of seismic artefacts (multiples) are present in the seismic line and are highlighted in light blue.

Flanking the high that separates the eastern and central half grabens, a syn-kinematic wedge can be observed (Fig. 4; Km 53-60) overlying R3 and beneath the M unconformity. This post-extensional wedge is coherent with a relative uplift of the structural high due to tectonic inversion. Furthermore, the inclined geometry of reflectors at the NW margin of the Malaga Basin suggests uplift of the neighbouring onshore (NW termination of the profile in Fig. 4). This tilting is post-Messinian as it affects the sediments of Unit I. All these features infer a rather reduced amount of tectonic inversion post-dating late Tortonian times, which is in contrast with areas situated in the southern part of the Alboran Basin where the inversion is associated with large-scale deformation and basement uplift (Martínez-García et al., 2011).

Seismic sequence stratigraphic data: tectonic system tracts in the Malaga Basin

Sequence stratigraphy is a methodology well developed in studying passive continental margins, where the main changes in accommodation space are primarily caused by eustatic sea-level fluctuations (e.g. Vail et al., 1977; Posamentier & Allen, 1993; Schlager, 1993; Catuneanu et al., 2006; Catuneanu et al., 2011). Although much less known when applied to tectonically active basins (e.g., van Wagoner et al., 1990), the evolution of system tracts and sequences can be directly related to tectonically driven vertical movements and is part of what is often referred as tectonic sequence stratigraphy. In these basins, the coeval deposition of system tracts and sequences are related to episodes of fault activation. Therefore, they are independent of the timescales of cyclicity order defined by classical sequence stratigraphy (see discussion in Miall & Miall, 2001).

There are no readily available tectonic sequence stratigraphic models for half-grabens bounded by low-angle detachments. But such models are available for other types of extensional basins, where the relationship between sedimentation and the tectonic subsidence of hanging-walls has been described (e.g., van Wagoner et al., 1990; Prosser, 1993; Nottvedt et al., 1995; Ravnås & Steel, 1998; Martins-Neto & Catuneanu, 2010). In a similar fashion with other studies defining concepts of tectonic system tracts (e.g., Hinsken et al., 2007; Răbăgia et al., 2011; Pereira & Alves, 2012), we have defined a novel sequence stratigraphic model for asymmetric extensional basins by modifying one of these readily available seismic stratigraphic methodologies. The choice of the existing starting model (Prosser, 1993) is obviously subjective, but was driven by a similar methodology (seismic interpretation), and a closest meaning of tectonic system tracts. In this model, the system tracts reflect stages of evolution during rifting from its onset to the final demise of fault offsets and post-tectonic cover. Similar to the original definition, the rift initiation system tract records the first extensional pulses in the basin and is followed by a rift climax system tract, which reflects the

moments of maximum fault activity and subsidence rates. Based on their seismic character, two higher order system tracts were differentiated during the rift climax: an early to middle rift climax, and a late rift climax system tracts. The end of faulting marks the start of an immediate post-rift system tract, when the continued thermal sag subsidence resulted in the burial of inherited rift topography. The last stage corresponds to the late post-rift system tract, when compaction and gradual slowing of thermal sag subsidence drives a final stage of regressive basin fill. However, when compared with the original definition, these system tracts have a different seismic expression and meaning. They reflect the specific evolution of asymmetric extensional (back-arc) basins and the interplay between the relative uplift of the footwall and subsidence in the hanging-wall. Each system tract is associated with a characteristic seismic expression (group of seismic facies units) that reflects the depositional environment.

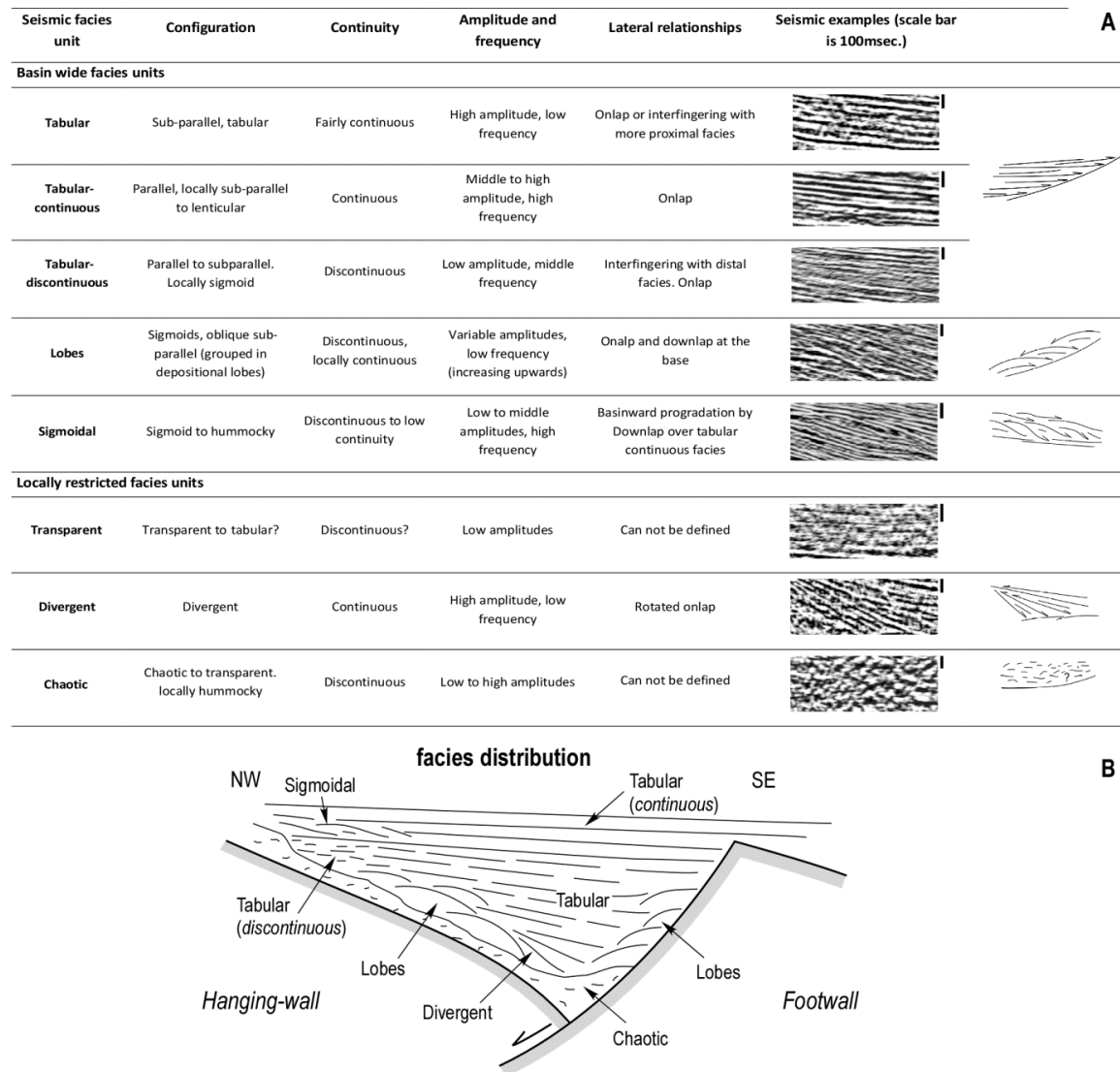


Figure 5: a) Characterization of seismic facies units used on the seismic sequence stratigraphic interpretation. b) Cartoon showing the relationship between seismic facies units in an extensional half-graben that was used by the present study.

In addition to the overall rift sequence stratigraphy, the increased time resolution in seismic lines, driven by the large syn-kinematic sedimentation rate in the Malaga Basin, provides the critical advantage of being able to detect a higher order sequence stratigraphic cyclicity. This higher-order cyclicity can be related to individual episodes of normal faults activation and was analysed by defining transgressive – regressive sequences (e.g., Johnson & Murphy, 1984; Embry & Johannessen, 1992; Catuneanu, 2002; Catuneanu et al., 2009).

The methodological approach included first the definition of the main seismic facies units based on their amplitude, frequency, continuity, lateral terminations, spatial distribution of the reflectors and relationship with the normal faulting (Fig. 5a). The seismic facies units were subsequently grouped in progradational, retrogradational or aggradational geometries. These are controlled by the balance between the sediment supply and the variability in creating the accommodation space by the rate of slip along the controlling normal faults (Catuneanu et al., 2009). Converting these geometrical patterns into high order stratigraphic sequences relies on the specific structural evolution of asymmetrical extensional systems that creates continuous footwall exhumation and a gradual migration of faulting in time and space. As long as erosion is detected over the footwall, the onlap of seismic facies units is coastal and, therefore, a direct interpretation of these geometrical patterns in stratigraphic sequences is possible. Footwall erosion, combined with the correlative maximum regression surface defined by the geometry of the seismic facies units, is an expression of the composite surface that bounds a Transgressive – Regressive (TR) sequence (Embry & Johannessen, 1992; Catuneanu, 2002). The syn-kinematic deposition against gradually migrating normal faults provides the control over the coeval nature of erosion and sedimentation, whenever available. The variations in paleobathymetries observed in the drilled sediments over the basin flanks (Martínez del Olmo & Comas, 2008) are furthermore used to correlate the definition of TR sequences. The later has an increased resolution in the uppermost part of the basin (i.e. towards the NE; see Fig. 2) and is more important for our interpretation, because the coastal control provided by the eroding footwall is gradually lost due to its burial. Given the geometry of the normal faulting (Fig. 5b), the maximum flooding surface of a TR sequence is less controlled in our interpretation in older sediments located in the centre of the basin, where direct observation is scarce. In these situations, the maximum flooding surface has been simply approximated as the boundary between progradational and retrogradational geometries. Although this is an important approximation in theory, its error bars do not affect significantly the practical interpretation at the given seismic resolution.

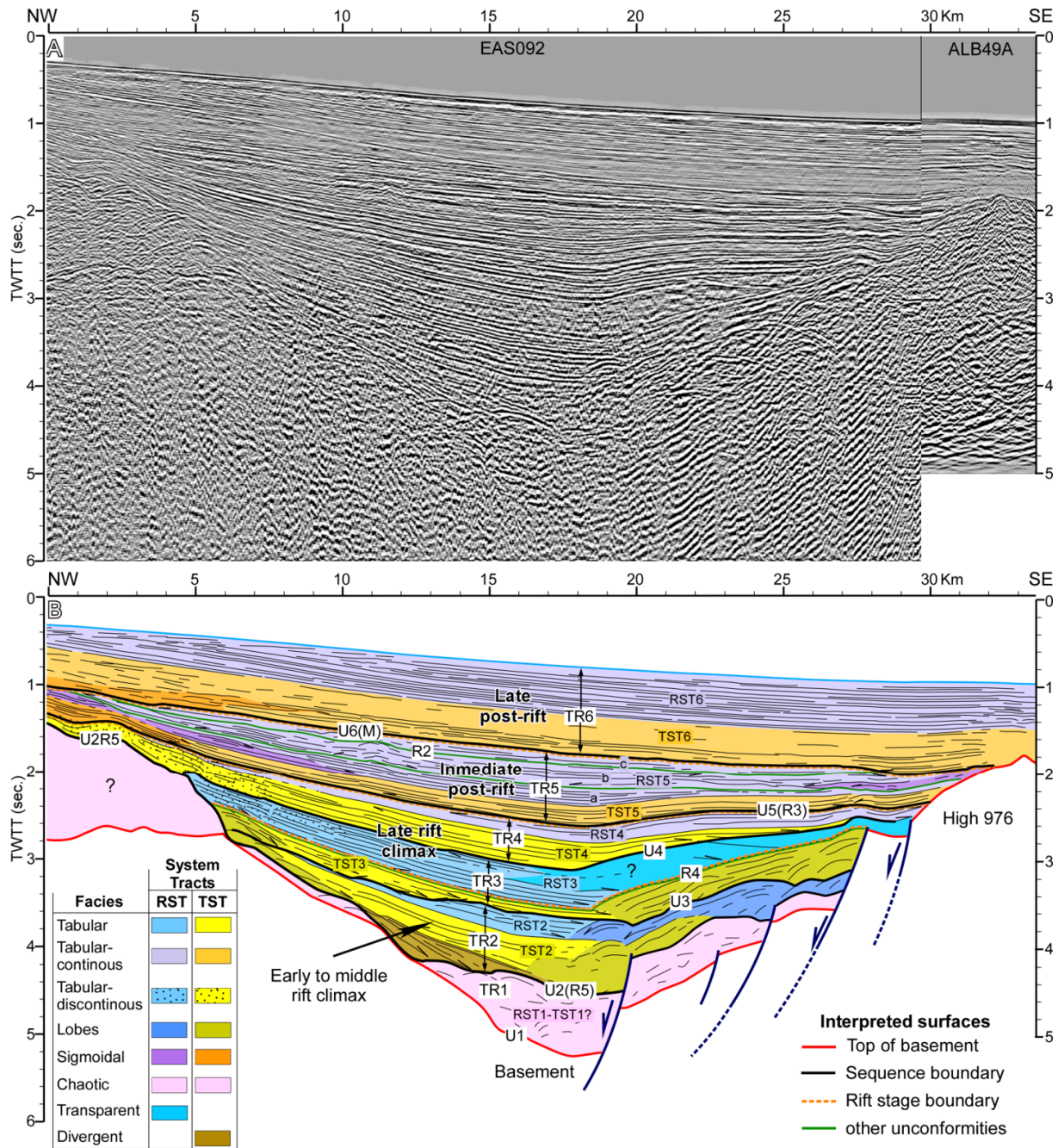


Figure 6: Un-interpreted (a) and sequence stratigraphic interpretation (b) of a seismic profile in the NE part of the Malaga Basin (lines EAS092 and ALB49A, location in Fig. 2) displaying an overall half-graben structure and the relationship between faulting and sedimentation. The seismic sequence stratigraphic interpretation separates seismic facies units, system tracts and sequences. Two levels of cyclicity are interpreted, high-order transgressive-regressive system tracts and their sequence boundaries are subsequently grouped in lower-order tectonic system tracts (i.e. rift initiation, early to middle rift climax, late rift climax, immediate post-rift and late post-rift). For the definition of the system tracts see the text. These sequence boundaries (U1-6) locally correlate with previously defined major unconformities of the Alboran Domain (R5-R1 and M, see Comas et al., 1999). The facies displayed in the legend are defined in Fig. 4. Rift stage boundaries are the limits of between the low order tectonic system tracts. Other unconformities are local system boundaries with unclear significance, possibly the boundaries of even higher order cycles. TST: transgressive system tract; RST: regressive system tract; TR: Transgressive-regressive sequence; M: Messinian Salinity Crisis unconformity.

This overall methodology was applied to a large network of 2D multichannel seismic lines acquired for petroleum exploration. The seismic sequence stratigraphic interpretation is illustrated in this study with three representative seismic profiles, located in the central and NE part of the Malaga Basin, outside the influence of the mud-diapirism (Figs. 2, 6, 7 and 8). The profile in Fig. 8 is a higher resolution seismic stratigraphic interpretation of the NNW part of Fig. 4. These profiles have also the advantage of relative reduced structural deformation in the centre of the basin, which is otherwise minor. This allows a good correlation of the key reflectors across the basin, which facilitates the sequence stratigraphic analysis. Although the analysed seismic lines show in the lower part a reduced number of typical artefacts (such as diffractions), a careful interpretation allows a relatively straightforward differentiation. Our seismic interpretation demonstrates that the main controlling faults of the Malaga Basin are located on its SE margin, near High 976 (Figs. 2 and 4), which corresponds with the footwall actively exhuming during extension (Fig. 5b). The NW margin is also affected by normal faults, in particular in the SW deeper parts of the basin. However, these faults have reduced offsets and influence in the sedimentary evolution. Although not apparent in our interpretation, faults in the High 976 may have also a strike-slip component of movement (Comas and Soto, 1999), but this component is likely minor to produce any relevant effects in the spatial geometry of tectonic system tracts. The previously interpreted regional unconformities (R1 to R5 and M) may correspond with the six unconformities interpreted by the present sequence stratigraphic study in the Malaga Basin (U1 to U6), but the latter carry an additional genetic significance (Fig. 3).

Seismic facies units

We have differentiated eight main seismic (sub-) facies units in the Malaga Basin. The characteristics of these seismic facies units are summarized in Fig. 5a, while their common spatial arrangement is illustrated in Fig. 5b. Some of these facies units are broadly distributed over the entire basin, while others are restricted to specific stages of basin evolution, to the activity of specific faults or other deformation features. Some of these seismic facies units reflect sedimentation at the basin margins with a close range transport (such as the lobe facies unit deposited against erosional unconformities), being eroded from the footwall crests or the tilting hanging-wall across the strike into the basin. Other seismic facies units reflect likely sediments transported along the basin strike from a more distal source area (e.g., tabular facies units, Fig. 5b, see also Prosser, 1993).

The most common seismic facies unit in the Malaga Basin is the tabular facies unit (Fig. 5) that is observed on most of the rift related sequences in a basin-ward position and onlaps older surfaces or is inter-fingered with more proximal seismic facies

units. It onlaps directly over the basin margins, in particular when more proximal units (i.e. lobes) are absent. Based on the continuity of the reflectors, this facies can be locally sub-divided into a tabular continuous sub-facies unit, common in the upper part of the stratigraphic succession, and a tabular discontinuous sub-facies unit, that is common near the basin margins (Fig. 5). The lobes facies unit (Fig. 5) is generally observed near the basin margins where its presence is associated to erosional unconformities and short-range sediment transport over the basin slope. Its mode of deposition across the basin is clear and can be easily interpreted as the marginal equivalent of the tabular facies unit. The lobes are always in close spatial contact, either prograding toward the centre of the basin, retrograding towards its margins or aggrading. In the lower part of the basin fill, this facies shows rapid progradation or retrogradation, while these patterns become more attenuated in its upper part. The sigmoidal facies unit (Fig. 5) is observed in the profiles located in the NE margin of the basin above the R3 unconformity (Figs. 6 and 7). The transparent facies unit (Fig. 5) is observed in the profiles located in the NE (Figs. 6 and 7), above the R4 reflector near the SE margin of the profiles. The divergent facies unit (Fig. 5) is seldom observed in the lower part of the stratigraphic succession in the vicinity of the SE margin. The chaotic facies unit (Fig. 5) is typical for the olistostromic unit situated at the base of the stratigraphic sequence (Unit VI, Figs. 3 and 4). When this unit is located at higher depths, this facies becomes less chaotic and passes to a hummocky configuration in its upper parts.

High-order transgressive - regressive (TR) seismic system tracts

The combination of the previously defined seismic facies units during the seismic interpretation has resulted in the identification of six high-order retrograding/prograding geometries that can be correlated across the basin. The five lower combinations are always in lateral contact with the gradual eroding footwall or hanging-wall (Figs. 6 and 7). Normal faulting demonstrates that the sedimentation and erosion are coeval at the scale of one sequence and, therefore, the internal lateral terminations are in fact coastal onlaps. Therefore the unconformity that separates these retrograding-prograding geometries is the composite surface that bounds a transgressive-regressive (TR) sequence. The uppermost retrograding-prograding units can also be interpreted as a TR sequence, as its base is an obvious sequence boundary (the Messinian Salinity Crisis unconformity, e.g., Fig. 6).

The six unconformities (U1 to U6, Figs. 6, 7, and 8) that define sequences boundaries separating the six TR sequences are generally marked by erosion near the basin margins that changes laterally to simple angular or para-conformities near the basin centre. The exceptions are the unconformity U2, which has a widespread erosional paleorelief in the NE part of the basin, and the unconformity U6, which records the large-scale erosion of the Messinian Salinity Crisis event.

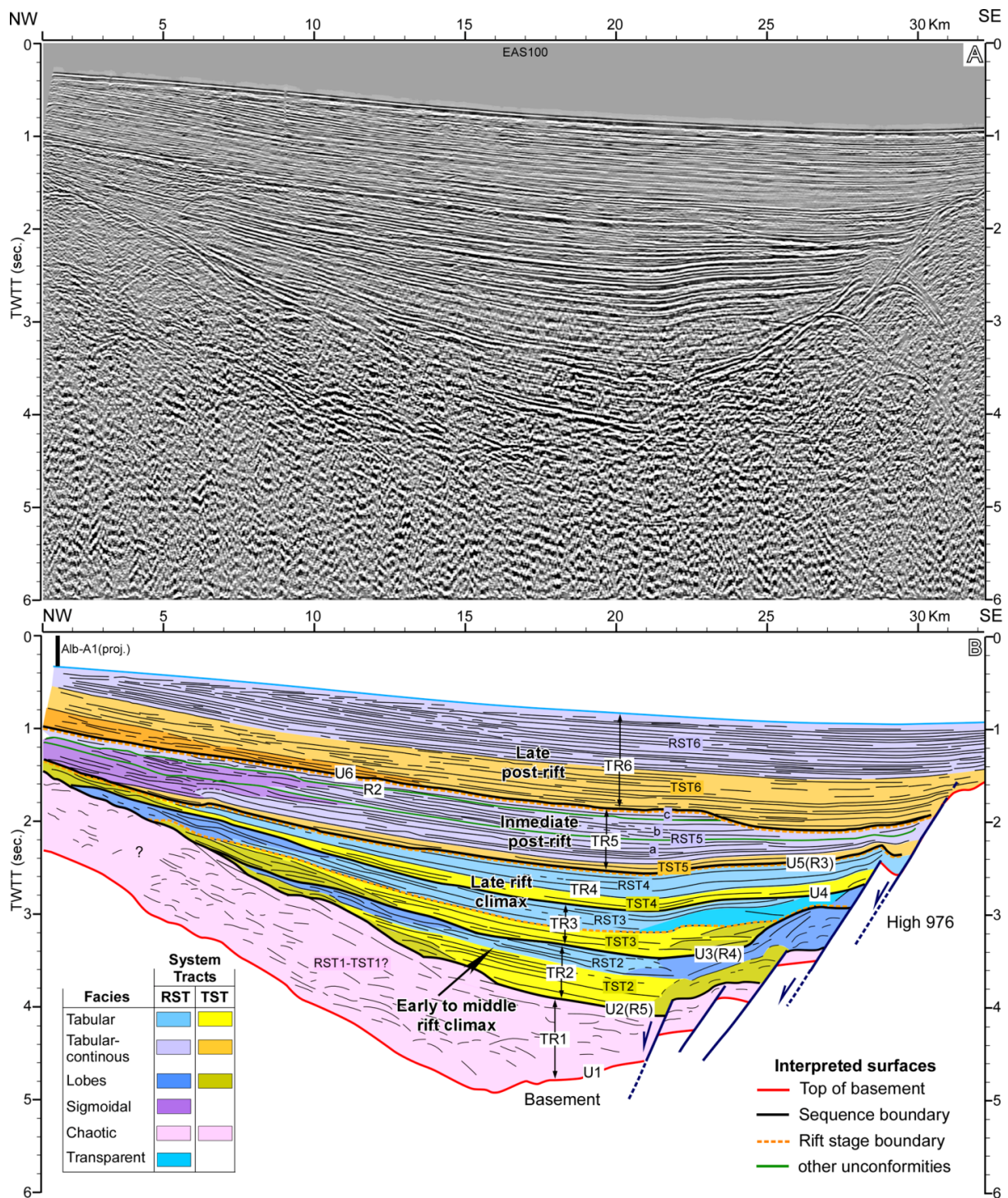


Figure 7: Un-interpreted (a) and sequence stratigraphic interpretation (b) of a seismic profile in the NE part of the Malaga Basin (line EAS100, location in Fig. 2) displaying an overall half-graben structure and the relationship between faulting and sedimentation. Figure conventions as in Fig. 6.

The TR sequences (TSTs and RSTs in Figs. 6, 7 and 8) are generally made up by tabular facies units located in a basin-ward position that onlap towards the basin margins over one or more lobes facies units (Figs. 6, 7 and 8). The transgressive or regressive system tracts do not contain divergent facies units, with the exception of TST2 (Fig. 6). In the upper part of the basin fill, the presence of lobe facies units decreases significantly and the continuous tabular sub-facies locally onlaps directly over the High 976 basin margin, while the north-western margin is characterized by tabular discontinuous sub-facies or sigmoidal facies units (Figs. 6 and 7). Similarly, the amount of lobe facies units decreases along the strike of the basin to the SW, where it is larger and more open when compared to the NE (compare Figs. 6 and 7 with Fig. 8). However, the antithetic normal fault located near the NW margin of the basin (near Km 5 in Fig. 8) truncates this general distribution and a larger amount of lobe facies units are observed in its vicinity (i.e. in TR3 sequences). The individual regressive or transgressive system tracts are composed by a combination between various facies units. Only the basal TST1-RST1 sequence contains the chaotic facies unit that shows a chaotic to hummocky reflectors pattern in the NE part of the basin (Figs. 6 and 7). This pattern prevented a further separation between transgressive and regressive system tracts in this sequence. To the SW, along the strike of the basin, the upper part of this TR1 sequence contains also lobes facies and partly tabular facies units that enabled the separation of two sub-cycles (TR1a and TR1b sub-sequences in Fig. 8).

The differentiation between the regressive and transgressive system tracts is mainly made up by the onlap and downlap patterns of the seismic facies units situated in a basin margin position. Regressive system tracts are observed by a basin-ward shift of the proximal facies units during progradation, while transgressive system tracts are characterized by a shoreline shift of these facies units during retrogradation. The lobe facies units are generally proximal in the studied seismic lines, which is diagnostic of footwall and/or hanging-wall erosion and short-range sediment transport over the basin slope. When erosion is reduced, and therefore lobe facies units are less developed, other relationships were used to discriminate between the regressive and transgressive system tracts. First, the inter-fingering between the tabular continuous and tabular discontinuous sub-facies units (Fig. 5) is likely to represent a contrast in lithology, such as from sand-rich deposition near the basin margins to mud-dominated sedimentation in the basin centre. The regressive or transgressive pattern of this inter-fingering is diagnostic for separating seismic system tracts (such as RST3 and TST4, Fig. 6). Another separation criterion was used in the upper part of the basin fill where the regressive pattern is observed by sigmoidal facies units that terminate with downlaps over the continuous-tabular facies (NW part of TR5 sequence in Figs. 6 and 7). Note that the rapid tectonic subsidence of the Malaga Basin combined with high sediment influx creates an apparent transgression over the basin margins (e.g. Figs 6 and 7) during the deposition of a regressive system tract.

The **transgressive system tract (TST)** is characterized by a variable retrogradational character, which depends on the variation of the rate of tectonic subsidence with time. This results in large and obvious retrogradation patterns in the lower part of the basin fill where the tectonic subsidence is high (e.g. TST2, Figs. 6 and 7), while towards its upper parts the retrogradational pattern decreases, being gradually replaced by aggradation (e.g., km 7 of TST3 in Fig. 6). The activation of the antithetic SE dipping fault observed on the westernmost profile (NW flank, Km 2 in Fig. 8) created a local increase in retrogradation during a relative late stage of rift evolution (RST3). The differential tectonic subsidence is also observed by the tilted geometry of coastal onlaps. These onlaps define unconformities at the base of each TST, especially in the lower part of the basin fill (e.g., at the base of TST3, from Km 10 to 13 in Fig. 6 and around Km 15 in Fig. 7), where the tilting of the hanging-wall gives an apparent downlap geometry (e.g., divergent facies of TST2, Km 11 to 17 in Fig. 6). Locally, true downlaps over the previous regressive system tracts are also observed (e.g., TST3 downlaps over the previous RST2, between Km 10 to 15 in Fig. 6). In the upper part of the basin fill, the number of TST onlaps diminishes, in particular along the north-western margin (e.g., NW corner of Fig. 6), being also associated with toplap terminations near the High 976 margin (e.g., TST5, km 40 in Fig. 8). Along the strike of the basin, the unconformities at the base of the TSTs are more pronounced in the NE narrow part of the basin (compare Figs. 6 and 7 with Fig. 8).

The **regressive system tract (RST)** is typically characterized by a progradation towards the basin centre. The prograding geometry over the NW basin margin is rather clear in all situations, while the lobe facies units aggrade or even retrograde over the High 976 margin (e.g., RST2, Fig. 6 and 7). This is due to the fact that although the sedimentation rate is high, tectonic subsidence is still active and enlarges the basin. This gradual subsidence buried the normal faults and enlarged the basin towards the SE (Figs. 6 and 7) being associated with gradual onlaps over the basin margin even during periods of facies regression (e.g., from km 5 to 10 in RST3 and RST4, Fig. 8). RSTs display less amount of tectonic tilting due to reduced differential tectonic subsidence across the basin. Toplaps and/or erosional truncations are common terminations in RSTs. They formed due to the rapid progradation towards the basin centre and, ultimately, exposure to erosion and formation of a sequence boundary. Such erosion is locally enhanced, as is the case of U3 in the NE part of the basin (NW of Km 16 in Fig. 6) or U5 in the basin centre (NW of Km 8 Fig. 8). This observation strongly points towards a forced regression character, suggesting base-level drop during tectonic uplift. The observation that this erosion is laterally less obvious in the basin centre (Fig. 8) may be related to localized uplift during deformation.

At higher resolution, the large amount of sediment deposited during some of the RSTs allows the separation of higher order cyclicity than the TR seismic sequences. This is observed locally, for instance in RST5 where two internal unconformities and

onlap terminations permit to separate three internal higher-order sequences (labelled a, b and c in Figs. 6, 7 and 8).

Lower-order system tracts

By analysing the large-scale sedimentary architecture of the Malaga Basin, the high-order transgressive-regressive system tracts and sequences can be grouped in a number of tectonic system tracts that define the main diagnostic rift sequence stratigraphy. Some of the observed tectonic system tracts may look similar with the ones defined by earlier models (e.g., Prosser, 1993; Martins-Neto & Catuneanu, 2010), but significant differences are detected, driven by the marked asymmetry of the extensional system.

Rift initiation system tract

The start of deposition in the Malaga Basin and the onset of the subsidence are associated with a rift initiation system tract. This is made up by the first sediments deposited over the basal unconformity (U1 in Figs. 6, 7 and 8), which are the chaotic facies units grouped in the TR1 sequence (RST1-TST1). The chaotic to hummocky reflectors of this facies is in agreement with the observation of a sedimentary olistostromic character in well Alb-A1 that suggests gravity-driven deposition (Fig. 2). There is a striking contrast along the entire Malaga Basin between the seismic character of the chaotic facies unit and the overlying facies units deposited subsequently (Fig. 4). Such contrast suggests that the chaotic facies was deposited in a different sedimentary environment than the rest of the overlying sequences. The change in the sedimentary environment must have been diachronous across the basin as shown by the high-order TR sequences correlations. In the NE part of the basin, the deposition of the first non-chaotic facies took place directly over the U2 unconformity during the TR2 sequence (Figs. 6 and 7). By contrast, in the SW part of the basin the change in the sedimentary environment took place earlier, during the deposition of the first TR sequence (TR1). This leads to the separation of this sequence into two sub-cycles (TR1a and TR1b, respectively, Fig. 8).

The rift initiation system tract ends with the formation of an unconformity at the top of TR1 sequence (U2, Figs. 6, 7 and 8). This unconformity has a pronounced paleo-relief character in the NE part of the basin (near Km 5 in Fig. 6). SW-wards, where the basin is larger and deeper, the amount of erosion decreases significantly (Fig. 8). Note that sedimentary depocenters during subsequent deposition are clearly shifted when compared with the rift initiation system tract, which shows mainly thickening towards the NW, away from the axis of the Malaga Basin.

Early to middle rift climax system tract

The period of enhanced tectonic subsidence is associated with the deposition of the early to middle rift climax system tract that is spatially correlated with the higher resolution TST2, RST2 and TST3 system tracts (i.e. TR2 and the transgressive part of the TR3 sequences). During this period, in the NE part of the basin the deposition of lobe facies units dominates the basin margins, which migrate basin-wards during periods of regression (e.g. during RST2 in Fig. 7). The larger amount of lobe-facies units is observed near the High 976, which indicates that the footwall was sub-aerial and acted as the source of the neighbouring lobes in the basin. Towards the central part of the basin, lobe facies are scarce and restricted to the area situated near the basin margins (Fig. 8). Therefore, this part of the basin was enlarged rapidly during the rift initiation and the onset of the rift climax. A regressive stage is recorded (RST2) that is more significant in the NE corner of the basin, where the unconformity U3 recorded significant erosion by removing parts of the tabular facies unit in the upper part of TR2 sequence (Fig. 6). This is consistent with a forced regression by tectonic uplift of the RST2 system tract.

As a whole, the pattern is that of a rapid tectonic subsidence, deepening and enlargement of the basin, which was interrupted by a short-lived period of decreased activity or even tectonic uplift. Note that the subsidence was probably higher during TST2 than during TST3, as inferred by the larger retrograding pattern of lobe facies units in the NW flank of the basin in TST2 (Figs. 6 and 7). Active faulting and hanging-wall tilting is evidenced by divergent facies units observed locally at the bottom of the tectonic system tract (TST2 in Fig. 6). This is also observed by its increase in thicknesses E-ward (around 500m). In contrast, in the SW deeper part of the basin, there is an increase of thickness towards the western flank (around 350m). This differential tectonic activity is marked by increased amounts of deposition of lobe facies units along the NW flank during the deposition of TST3 (Fig. 8). Hence, this is the result of the activation of a local normal fault, resulting in the deposition of a thick package of lobe facies units. The offset patterns and associated sedimentation suggest that this is a late-stage antithetic fault post-dating the main system of faults dipping NW-wards.

Late rift climax system tract

The tectonic activity in the Malaga Basin reduced gradually during the late rift climax tectonic system tract that marked the transition to a completely submerged basin. This tectonic system tract is composed by the RST3, TST4 and RST4 system tracts.

The main feature of this system tract is an abrupt drop in the amount of lobe facies units being deposited and the gradual expansion of the tabular facies units towards the basin margins. Clear and well-developed lobe facies units are observed only during the deposition of the RST3 and TST3 system tracts in the NE part of the basin (Fig. 7). In the SW deeper part of the basin, the lobe facies of RST3 system tract are a

late effect of the paleorelief created by the antithetic normal fault situated on the NW flank (Fig. 8). In addition, the divergent facies units thickening NW-wards near the High 976 (from Km 30 to 40 in Fig. 8) suggest that in this part of the basin the deposition of the TR3 sequence was controlled by this antithetic fault. The absence of lobe facies deposition near the High 976 margin indicates that this entire part of the basin was already in marine conditions (Figs. 6, 7 and 8). The presence of a transgressive stage (TST4), associated mainly with aggradation and low amounts of retrogradation (Km 7, Fig. 6), separating the overall late rift climax regression (RST3 and RST4), indicates yet another last pulse of tectonically-induced subsidence in the basin.

In the NE part of the basin, the onset of the late rift climax starts with strong onlapping reflectors over the High 976 margin at the base of the RST3 sequence (Km 18 to 30 in Fig. 6, Km 20 to 26 in Fig. 7). This geometry drapes an inherited basin topography that continues during the deposition of TST4 against the sequence boundary U4. By contrast, this onlap is significantly reduced in the north-western flank, which indicates that pre-existing differences in topography were already reduced in this sector by the time of late rift climax deposition and is in line with the overall marine conditions.

Post-rift system tract

The cessation of major deformation in the basin is marked by the onset of post-rift system tract, which is characterized by the gradual and regional burial of the entire basin.

The rapid progradation recorded during the last part of the late rift climax system tract is marked by an unconformity (U5) that locally has a pronounced erosional character near the basin margins. This erosion is observed by tolap terminations in the upper part of the RST4 system tract (Figs. 6 and 7) and locally in the upper part of TR3 sequence (NW margin of Fig. 8) which points to tectonic uplift. In addition, the U5 unconformity and clinofolds from RST4 sequence appear to be slightly folded near the High 976 margin (km 28 in Fig. 6 and Km 29 in Fig. 7).

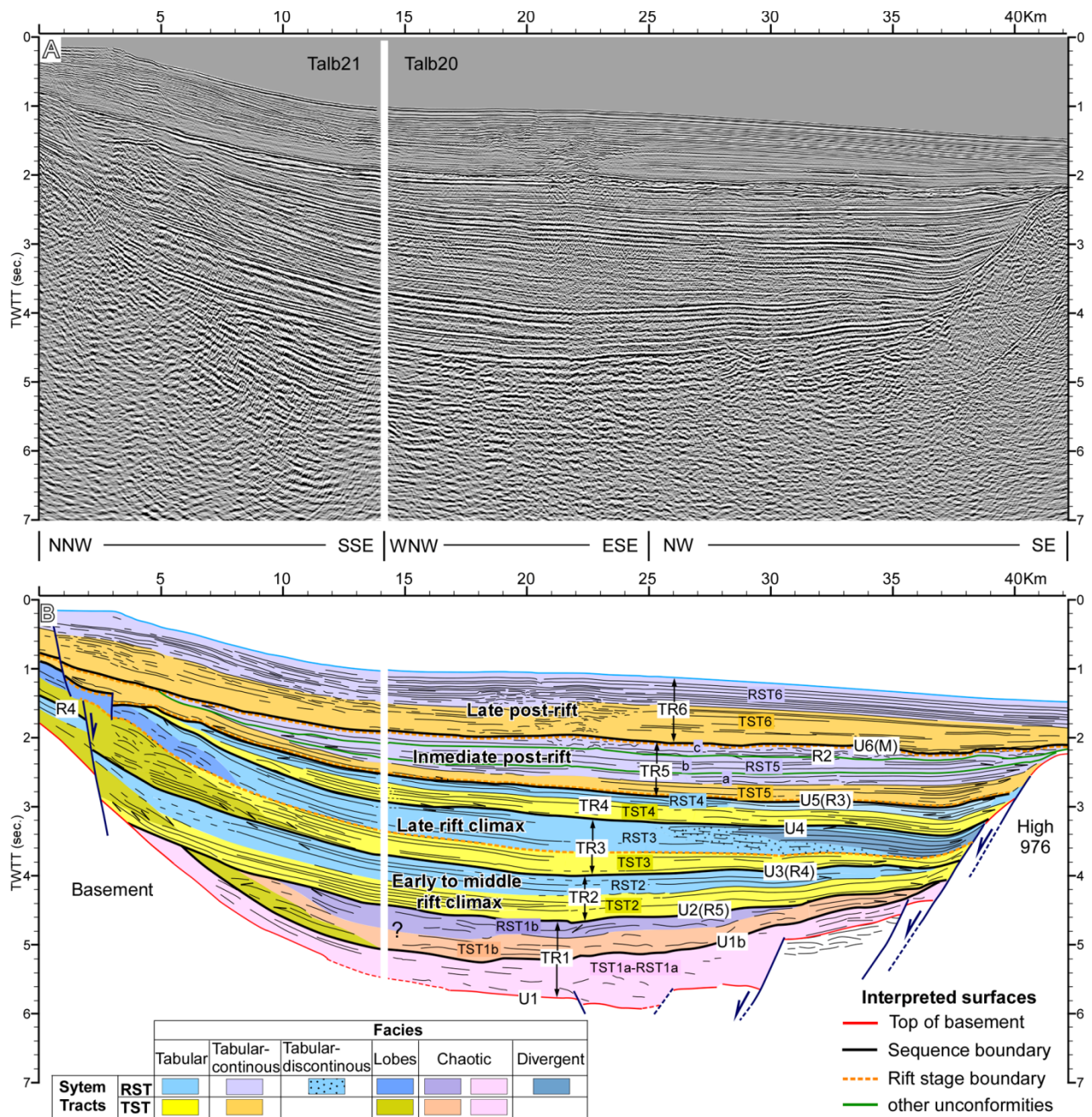


Figure 8: Un-interpreted (a) and sequence stratigraphic interpretation (b) of a seismic profile displaying the relationship between faulting and sedimentation in the central part of the Malaga Basin (lines Talb21 and Talb20, location in Fig. 2). Note the decrease in the asymmetry of the half-graben and the lower amount of lobe facies units when compared with other profiles located more to the NE (compare with Figs. 6 and 7). Figure conventions as in Fig. 6.

The start of the post-rift is characterized by a series of high amplitude reflectors that can be followed along the entire basin and onlap the eroded footwall scarp (TST5 system tract, Figs. 6, 7 and 8). During the immediate post-rift system tract, there is a significant increase of sigmoidal facies units in the NW flank that is particularly visible in the NE part of the basin (Figs. 6 and 7, NW of TR5 sequence). By contrast, in the SE flank their presence is scarce and only a couple of clinofolds are observed (Fig. 6). This

facies distribution suggests a gradual change in character of the source area as sigmoidal facies units are in fact progradational and/or retrogradational clinofolds that mark the transition of the tabular facies units to a passive margin- type of sedimentation.

The TST5 transgression indicates regional subsidence affecting both the centre and the flanks of the basin during the onset of immediate post-rift sedimentation. This system tract is generally thin and short lived because the gradually decreasing thermal sag subsidence is outpaced by the sediment supply and the onset of a regressive system tract (RST5, Figs. 6, 7 and 8). There is no evidence of moments of renewed tectonic activity during the overall decreasing thermal subsidence. Therefore, the higher resolution sub-cycles detected (a, b, and c in RST5, Figs. 6, 7 and 8) must reflect other genetic relationships, such as changes in the source area, climate or even Milankovitch cyclicity.

The upper part of the immediate post-rift system tract is truncated by the regional unconformity formed by the marine erosion after the Messinian Salinity Crisis (MSC, U6 and M in Figs. 6, 7 and 8) and discussed elsewhere (e.g., Clauzon et al., 1996; Krijgsman et al., 1999; Garcia-Castellanos et al., 2009; Estrada et al., 2011), including the geometry of this unconformity specifically in the Malaga Basin (Comas et al., 1992). Hence, it is remarkable the continuity of seismic facies below and above the unconformity and the apparent lack of massive progradation clinofolds that characterize most other Mediterranean regions (e.g., Clauzon et al., 1996; Gorini et al., 2005; Urgeles et al., 2011).

The Zanclean transgression over the U6/M unconformity marks onset of the late post-rift system tract that took place during the last phase of the basin infill (TR6 cycle, Figs. 6, 7 and 8). The pattern of the sigmoidal facies units (Figs. 6 and 7) is aggradational and slightly retrogradational. Locally, progradational clinofolds are also observed, most likely caused by a higher order cyclicity that cannot be separated due to the local resolution of the seismic lines. The Zanclean transgression was followed by a regressive pattern of basin fill that is gradually shifting the main sedimentation areas to deeper parts of the basin.

Interpretation

Our system tract analysis allows the study of processes that took place during and after the extensional episodes that affected the Malaga Basin through the relationship between fault activity and the sedimentary response along and across the basin. In addition, the tool we develop by studying the Malaga Basin can be used for the analysis of other half-grabens bounded by major low-angle detachments. In particular, the combination of previous well established sequence stratigraphic models with the higher resolution TR sequences permits to specify the subsidence pulses driven by episodes of high fault slip rate.

Time constraints on the evolution of tectonic system tracts

The timing of the TR sequences and the rift system tracts have been constrained through the correlation with the biostratigraphically controlled unconformities in the Alboran Sea (Fig. 3; e.g. Comas et al., 1999; Martínez del Olmo & Comas, 2008). The correlation demonstrates that the syn-rift deposition in the Malaga Basin took place over a 9-11Ma lasting period from early Burdigalian to early Tortonian. The transition between rift initiation and rift climax (limit between TR1 and TR2 sequences, Figs. 6, 7 and 8) took place at the end of Burdigalian times after the formation of the unconformity R5. The onset of late rift climax took place most probably during the early Serravallian (limit between TST3 and RST3 near R4 unconformity), while the final deposition of the late rift climax took place at around 9Ma (unconformity between TR4 and TR5 sequences, Fig. 3). In agreement with previous studies, the end of the syn-rift sequence took place with the R3 (U5) unconformity (Comas et al., 1999).

The lack of correlation between the observed system tracts and the 3rd or 4th order global/regional eustatic variations (i.e. correlation of rift episodes with the eustatic curves of, for instance, Haq et al., 1987, Fig. 3) points to tectonics as the controlling factor of the TR cyclicity. High-resolution climatic cycles are inferred in the neighbouring onshore during Upper Tortonian to Messinian times by the alternation of reefs and temperate carbonates related with subtropical/tropical cycles (Martín & Braga, 1994; Braga & Aguirre, 2001; Sánchez-Almazo et al., 2001). Given the time scales, this is a higher cyclicity event that affected the post-rift deposition in comparison to our TR sequences interpreted in the seismic lines crossing the Malaga Basin (see also Braga & Aguirre, 2001). The exception is the unconformity observed between TR5 and TR6, which is related to the Messinian Salinity Crisis event that took place before the Pliocene (see discussion in Garcia-Castellanos et al., 2009 and references therein).

In terms of sediment supply, studies of depositional rates in the Alboran Domain (Iribarren et al., 2009) inferred a decrease from 0.24 mm/yr to 0,17-0,19 mm/yr between rift initiation - rift climax system tracts (Burdigalian to early Tortonian) and immediate -

late post-rift system tracts (late Tortonian to Quaternary). This change is in agreement with our sequence stratigraphic interpretation, because it correlates with the disappearance of lobe facies after the rift climax, which could have facilitated the transgressive episode recorded during the immediate post-rift (TST5).

Given all available constraints, a tectonic genesis of TR2-4 sequences is inferred by the differentiation of three pulses of tectonic subsidence. They correspond to the transgressive system tracts included in the rift climax (TST2 to TST4). Our interpretation infers that these pulses have occurred at early Langhian (TST2), early Serravallian (TST3) and early Tortonian (TST4). These results can be compared with previous subsidence analysis from two wells situated in the northern margin of the Malaga Basin (Alb-A1 and And-G1; Fig. 3; Docherty & Banda, 1992; Watts et al., 1993; Rodríguez-Fernández et al., 1999). In Alb-A1, most of the tectonic subsidence occurred during Burdigalian times while in And-G1 a fast tectonic pulse during early Langhian was followed by a slower and constant subsidence until late Miocene (Fig. 3; Watts et al., 1993). The well ODP Site 976 records a short period of subsidence during early Tortonian, which could correspond with the TST4 system tract (Fig. 3, Rodríguez-Fernández et al., 1999). This overall apparent lack of correlation between wells and our inferred tectonic pulses is most likely a consequence of the fact that wells register the subsidence depending on their relative position with respect to the controlling fault system. The well Alb-A1 is situated in relative high position over the hanging-wall in which no sedimentation took place for most of the rift climax (Fig. 7), whereas And-G1 is situated south of a WNW-ESE oriented fault (Fig. 2) that clearly influenced deposition at a local scale. Finally, the High 976 (Fig. 2) was not affected by the subsidence of the rift climax, as it is situated in the footwall of the main normal fault system that controlled this subsidence. Hence, the High 976 should have been initially covered by marine Upper Serravallian deposits, as demonstrated by biostratigraphic dating of thin sedimentary elements at the contact with the metamorphic basement top (Comas et al., 1996). The subsequent exhumation in the footwall of the normal faults has probably caused the removal of the majority of these Serravallian sediments. Thus, the sedimentary record from Upper Serravallian onwards coincides with what we interpreted as late rift climax, when the site was already submerged (Fig. 3). This is in agreement with reconstructions of paleo-shorelines during upper Tortonian times (Braga et al., 2003) that infer an emerged area situated N and NE of the Malaga Basin, while the High 976 was submerged. The fact that a condensed section of this pulse is recorded on the footwall of the Malaga Basin indicates that subsidence and associated transgression (TST4) are not only related to fault slip in the Malaga Basin and can be explained by subsidence due to normal faulting that took place in more eastern position, such in the central or eastern half-grabens (Fig. 4).

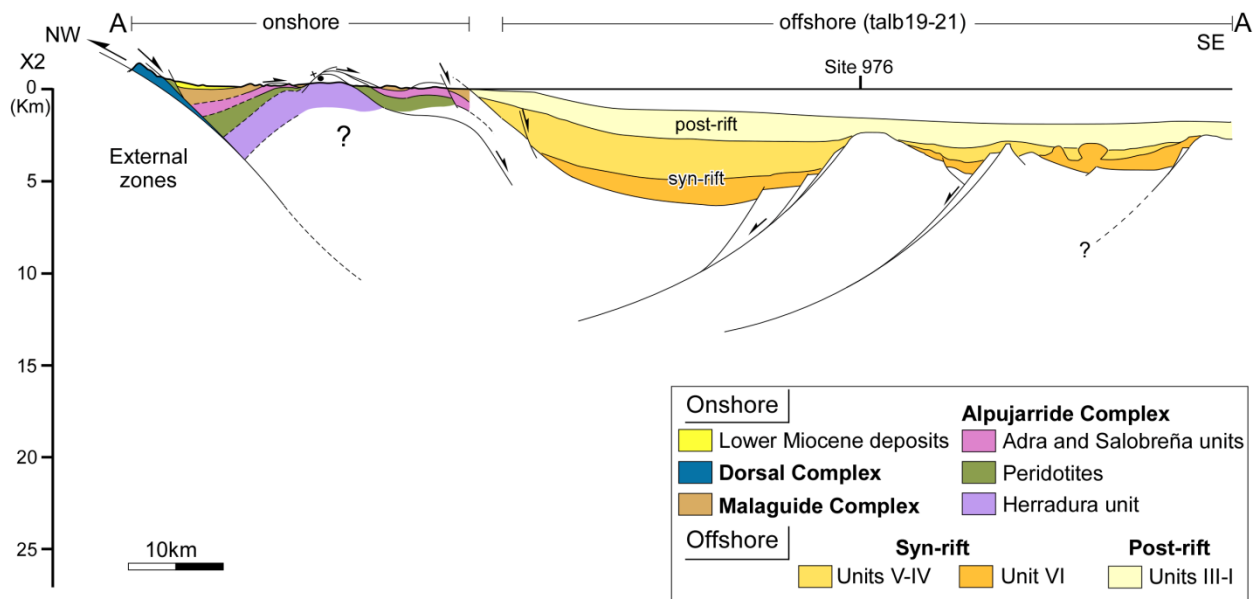


Figure 9: Regional schematic cross-section spanning the external western Betics to the centre of the Alboran Sea displaying the present-day structures of the coupled Alboran onshore and offshore (location in Figs. 1 and 2). Onshore part of the profile modified from García-Dueñas et al. 1992 and Crespo-Blanc & Campos 2001. Offshore part is drawn from Fig. 4 and converted in depth by using average interval velocities calculated by the oil exploration industry. For the extrapolation of offshore faults above the seismogenic crust (around 12km, Fernández-Ibáñez & Soto, 2008) we used a simple surface to depth projection when the hanging-wall is tilted against listric normal faults.

Extensional mechanism in the NW part of the Alboran Domain

The seismic stratigraphic analysis (Figs. 6, 7 and 8), together with the interpretation of a regional profile (Fig. 4), allows an improved and quantitative control of the mechanics of extension in the NW part of the Alboran Sea (Fig. 9).

In the studied seismic lines, the geometry of reflectors and facies distribution demonstrate that pulses of tectonic subsidence in the Malaga Basin were mostly controlled by offsets along the SE-ward located normal fault system bordering the NW flank of High 976. Our sequence stratigraphic interpretation infers that faults were activated gradually in a footwall direction; so that older faults are presently located near the graben centre, while younger ones are located near the High 976.

Locally, deformation was also associated with antithetic faults located on the opposite flank of the Malaga Basin (Fig. 8) but the overall transport direction was towards the NW. The resulting asymmetric geometry is clear near the north-eastern part of the basin (Figs. 6 and 7) while to the SW, along its strike (Fig. 8), the overall geometry is more symmetric. The NW-wards dipping faults have low angles and are likely genetically associated to extensional detachments at depth (Fig. 4). The listric character of these faults is demonstrated by the gradual tilting of the hanging-wall and the internal geometry of TR sequences (Figs. 6 and 7). They contributed to the exhumation of the High 976 (Fig. 2) and show similar geometry as the faults that bound

the metamorphic complexes of the Alboran Domain onshore (García-Dueñas et al., 1992).

West of the Malaga meridian, onshore extensional detachments in the Alboran Domain indicate transport towards the back-arc (Fig. 1), i.e. roughly in a SSE-ward direction (Fig. 9; e.g., García-Dueñas et al., 1992). This is derived by previous studies, which demonstrated the presence of a major Miocene detachment separating the limit between the Alboran Domain and the external zones of the Betics (Balanyá & García-Dueñas 1988; Crespo-Blanc & Campos, 2001; NW part of Fig. 9). Nevertheless, in the studied part of the Malaga Basin, the Langhian to early Tortonian rift climax deposition was controlled by the NW dipping faults from High 976, that dip in an opposite direction. Therefore, the SSE dipping detachment started its activity earlier than the NNE-dipping detachment bounding High 976 by thinning the crust and exhuming the Alpujarride units exposed onshore. Such an evolution is consistent with the crustal-scale geometry (Torné et al., 2000; Soto et al., 2008), which indicates that the Malaga Basin is overlying the transition zone between the 30-35 km continental crust of the onshore Betics and the thinned ~16km crust of the Alboran Domain beneath the Alboran Sea (Fig. 9).

The SE-wards extensional detachments onshore can be tentatively associated with the formation of supra-detachment basins, early Burdigalian in age, which contain clasts from Alpujarride units that indicate previous uplift and exhumation (Bourgeois et al., 1972; Balanyá & García-Dueñas 1988; Serrano et al., 2007). Furthermore, our study indicates that the extensional detachments of the Malaga Basin were active at least from the end of Burdigalian to early Tortonian (Fig. 3). Therefore, the overall evolution infers an earlier activity of the SE-ward dipping detachments onshore followed, or partly coeval, with the onset of the offshore NW-ward dipping detachments, which started around late Burdigalian times (Fig. 3). Accordingly, the Aquitanian to Burdigalian olistostromic lowermost unit is likely to be driven both by the SE-ward dipping detachments and, starting at the end of Burdigalian times, by the activity of the NW-ward dipping fault system. The onset of the NW-ward detachment system produced uplift in the half-grabens situated east of the Malaga Basin and probably eroded partially this olistostromic Unit VI (Fig. 4).

The asymmetric geometry with detachments dipping in an opposite direction (SSE-ward and NW-ward) formed at different moments in time (Fig. 9), allows a better explanation of the subsidence deduced by our system tracts analysis. The activity of the fault system controlling the Malaga Basin will induce relative uplift in the half-grabens located more to the SE (Internal Basin, Fig. 4). The sedimentation in these half-grabens would be rather restricted and affected by erosional unconformities during the rift climax system tract of the Malaga Basin (previous to R3 reflector in Fig. 4). Furthermore, the activity of the faults bounding the central and eastern half-grabens (Fig. 4) induced subsidence, not only in the Malaga Basin, but also in its footwall, in

agreement with the presence of Serravallian deposits on top of the High 976. In this context, the forced regression surface observed at the top of the RST2 system tract (Figs. 6 and 7) is not expected in a basin with continuous subsidence and can only be explained by tectonic uplift. This is likely the result of a short-lived extensional uplift in outside regions that placed the Malaga Basin in their footwall. Hence, such deformation cannot be identified precisely by our study.

Finally, from ~9Ma onwards the post-rift evolution was followed by limited tectonic inversion in the Malaga Basin because the overall geometry of the TR2-6 sequences indicates a simple progressive basin fill due to tectonic subsidence and thermal sag. The strike-slip components of deformation observed in others areas of the Alboran Domain (Woodside and Maldonado, 1992; Chalouan et al., 1997; Comas et al., 1999; Martínez-García et al., 2013), which could have influenced the architecture of the sedimentary infill, are not observed in our seismic sequence stratigraphic analysis. Local inverted normal faults have been documented in the western part of the Malaga Basin, south of Marbella High (Comas et al., 1992; Suades et al., 2013). At the same time, minor folds affecting the Miocene sequences near the High 976 margin might be associated with tectonic inversion of inherited normal faults (e.g., in the TST5 system tract, Figs. 6 and 7). Furthermore, the possibility of late Tortonian to Quaternary uplift of the easternmost basement high, adjacent to the Djibouti Bank, cannot be discarded (Figs. 1 and 4)

Sequence stratigraphic inferences for the evolution of asymmetric extensional back-arc systems

The characteristics of a rift initiation system tract in extensional structures buried beneath passive continental margins are the hummocky to chaotic reflector configuration and highly variable reflectivity associated with continental deposition (Prosser, 1993). These characteristics are partly present in the Malaga Basin, but the depositional environment of the rift initiation system tract was marine. This is proved by the Alb-A1 well (Fig. 3), where the lowermost sedimentary units contain planktonic foraminifera (e.g. Jurado & Comas, 1992; Martínez del Olmo & Comas, 2008). Furthermore, the first deposits that lie directly over the metamorphic basement onshore (Aquitanian to Lower Burdigalian in age) are open-marine (Serrano et al., 2007 and references therein). Hence, there is a clear difference in the mode of deposition between the chaotic facies units and younger sequences (Figs. 6, 7 and 8). Our interpretation is that the rift initiation developed in very dynamic settings with high relief that facilitated gravity-driven deposition. In such an evolution, the rift initiation system tract is independent of the transition from continental to marine environments. At high values of stretching, the tectonic subsidence may bring the basin below the marine level very early during the rift initiation (Fig. 10). In this scenario, the type of depositional

environment would be controlled by the amount of tectonic subsidence and the connection with the nearest marine basin.

The end of rift initiation is observed in the Malaga Basin by large-scale erosion recorded by the unconformity U2. This is the result of a base-level drop that affects the entire basin and brought the previous marine settings during the deposition of rift initiation system tract into sub-aerial conditions. It can only be the consequence of tectonic uplift and points to a change in the mode of extension in the basin. Note that towards the SW (Fig. 8) the amount of erosion decreases significantly, most likely because the basin had larger bathymetry already during rift initiation and therefore the subsequent tectonic uplift did not brought the entire sedimentary fill in sub-aerial conditions. This is also observed by a less abrupt transition to the rift climax, as recorded by the gradual change from chaotic to hummocky configuration in the upper parts of the rift initiation (Fig. 10).

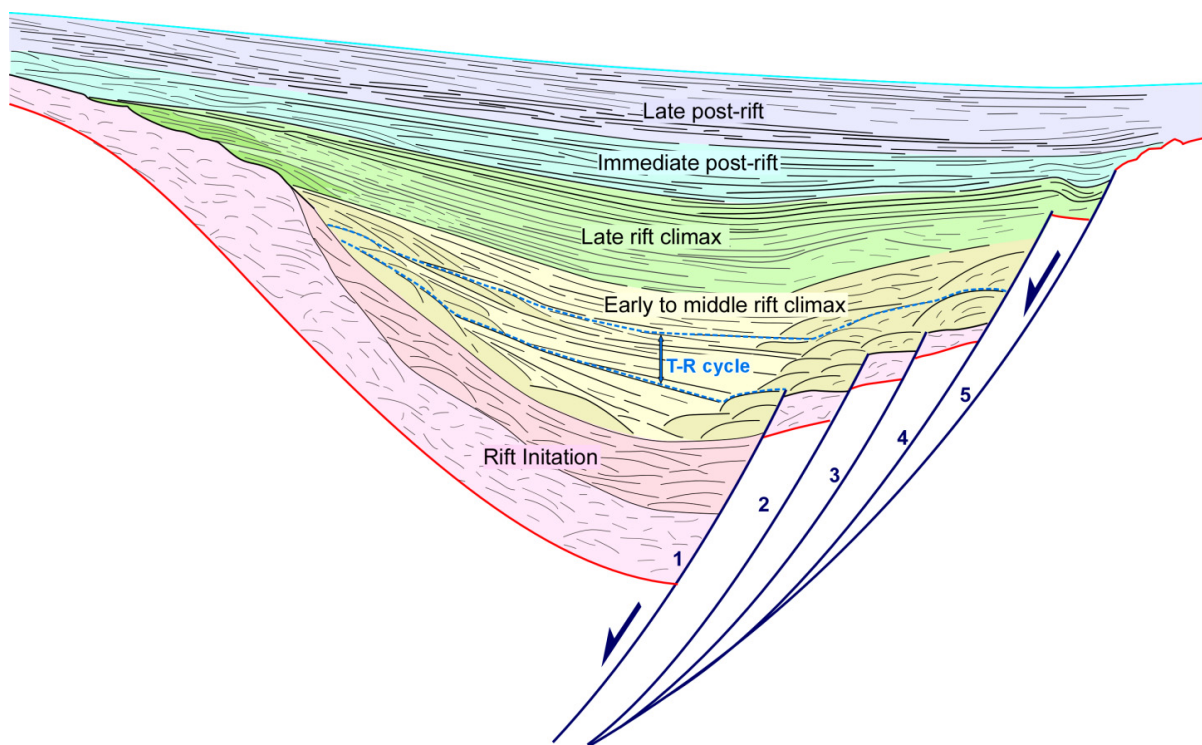


Figure 10: Idealized seismic sequence-stratigraphic model for half-graben rift basins bounded by major detachments. Blue dashed lines: sequence boundaries of a TR system tract. Footwall faults are numbered in their formation sequence. Rift initiation – lower part: discontinuous reflectors with a wide range of amplitudes characterized by a single seismic facies with chaotic reflectors; upper part: hummocky, tabular and lobe facies units better organized. Early to middle rift climax - continuous to discontinuous reflectors and abundance of lobe facies units; wedge shaped pattern is not always observed; aggradation to retrogradation of footwall-derived deposits and alternation of prograding to retrograding reflectors over the hanging-wall. Late rift climax – sub-parallel reflectors of high amplitude and good continuity on top of this sequence; overall drop in the amount of lobe facies; predominance of progradation over the hanging-wall; strong onlap at the base of the sequence against the footwall. Immediate post-rift - sigmoid to hummocky reflectors of high amplitude that show progradation onto the hanging-wall; no deposits are expected to come from the footwall; significant onlap over the previous sequence and against the eroded footwall scarp. Late post-rift – sub-parallel, high amplitude, continuous to discontinuous reflectors.

The main subsidence takes place during the rift climax system tract. Rapid subsidence occurred in the Malaga Basin during the initial stages of rift climax system tract as inferred by the deep marine deposits reported from well And-G1 in the centre of the basin (Fig. 2; Martínez del Olmo & Comas, 2008). In its NE part, the rift climax system tract is characterized by large-scale deposition of lobe facies units that rapidly prograde or retrograde over the footwall and the proximal parts of the hanging-wall. The higher order TSTs are associated with episodes of increased tectonic subsidence due to higher slip rates along the controlling faults (Fig. 10). At the start of the early to middle rift climax, the tectonic subsidence and associated transgression was rapid and created characteristic divergent facies units that covered the earlier rift initiation system tract (Fig. 10). It diminished progressively during the late rift climax system tract, when transgressive patterns are weak and short lived (such as TST4, Figs. 6, 7 and 8). At this stage the overall regression is dominant. Nevertheless, the drop in the amount of lobe facies and the increase of longitudinal tabular facies primarily defines the separation between the early to middle and the late rift climax system tracts (Fig. 10). Interestingly, the drop in the amount of lobe facies units with time is especially large near the footwall margin (Figs. 6 and 7).

Similarly with earlier studies (Prosser, 1993), we also infer that the lobe facies units are derived from the erosion of the exposed parts of the footwall and hanging-wall. Thus, we associate their deposition with significant exhumation. The source of large amounts of footwall-derived lobes during early to middle rift climax is the High 976 (Figs. 6, 7 and 8) and a marked erosional surface can be observed at its top (Fig. 10). Furthermore, the steeper morphology in the narrower NE part of the basin increased the amount of lobe facies units, while this amount decreases in the SW-ward, larger and open part of the basin (compare Figs. 6 and 7 with Fig. 8). By contrast, the mechanism of sourcing the hanging-wall lobes is not straightforward. We consider that the progressive hanging-wall tilting driven by offsets along listric normal faults kept its proximal margins at higher, sub-aerial elevations than the subsiding marine basin centre, thus providing a source area. This is coherent with the observed gradual tilting of the transgressive and regressive system tracts and the absence of equivalent rift climax deposits NE of the Malaga Basin (Bourgois, 1978). Our interpretation implies a subsequent gradual transition into marine conditions of the hanging-wall parts that were likely exposed to sub-aerial erosion during the early to middle rift climax period. This is in agreement with the coeval deposition of fan delta deposits combining proximal and distal sedimentary sources (Martínez del Olmo & Comas, 2008). During the late rift climax, the fault slip rates diminished, which resulted in a rate of sediment supply higher than the rate of creating accommodation space. Consequently, the morphological differences in the basin decreased, so did the erosion. This has resulted in a significant drop on the distribution of lobe facies units (Fig. 10).

An interesting feature is that the facies units gradually cover the footwall of the basin. We interpret this geometry as a response to a gradual migration of faulting and associated sedimentation towards the footwall (Fig. 10). It is likely that relative footwall uplift and passive rotation creates unstable geometries for normal faulting. Therefore, the position of the active normal fault migrates in a footwall direction and truncates the footwall basement as incisement splays (Fig. 10). This migration of the uplifting footwall has eroded the footwall flank of the basin that is not just faulted, but it contains also erosional surfaces for a large part of its length. In fact, this is an interesting characteristic of such asymmetric extensional system: it might look as a half-graben, but the footwall is not bounded just by a fault, being replaced partly by an erosional surface (Fig. 10). This combined geometry creates an overall look of a lower angle dipping slope that in many other situations may be difficult to differentiate from the low-angle dip of the hanging-wall, which is tilted by the listric character of the normal faults.

A clear onlap over a basin-wide unconformity marks the onset of the post-rift stage (Fig. 10). The rapid burial of the footwall could be the combined response of thermal subsidence and an effect of the migration of normal faulting to other extensional half-grabens, such as the ones situated SE of the Malaga Basin (Internal Basin, Fig. 4). The migration could bring the whole Malaga Basin, including its footwall, in a hanging-wall position with respect to the newly formed normal faults and will induce subsidence. This could have enhanced the subsidence during initial phases of immediate post-rift and, therefore, induced the short-lived period of transgression (TST5 in Figs. 6, 7 and 8). The transgression that took place during the late post-rift system tract in the Malaga Basin (TST6) is driven by the eustatic sea-level change that occurred during the Zanclean flooding, which follows the MSC, and therefore specific to the Mediterranean Sea. The late post-rift evolution of basins located elsewhere (Fig. 10) is likely to be dominated by glacio-eustatic/climatic events that create other high order TR sequences.

Conclusions

The sequence stratigraphy methodology is available for generic rift systems, but the understanding of asymmetric basins formed in the hanging-wall of extensional detachment requires the analysis of the basin fill at multiple levels of sequence stratigraphic cyclicity. Higher-order cycles characterize individual or differential fault movements, while the lower-order ones characterize the overall rift evolution. This approach, which includes the role of footwall exhumation and the rapid migration of normal faulting in space and time, has been applied to the northern branch of the Alboran Basin (the Malaga Basin), situated in the western Mediterranean Sea.

In such settings, we show that the rift initiation system tract is not necessarily characterized by continental deposition, as sediments during this stage can be already marine. The continental-marine transition is controlled by the amount of tectonic subsidence and the possibility of connection with the nearest marine domain, but does not necessarily correspond to the start of the rift climax. Early to middle rift-climax system tract corresponds to periods with abundance of lobes facies units that are shed from the hanging-wall due to tilting, and from the footwall crest due to exhumation. The late rift climax is characterized by an abrupt decrease in the amount of axial deposits, while during the post-rift system tracts a rapid burial of the entire extensional structure is observed.

Our analysis infers that asymmetric extensional systems may show an overall symmetric geometry of the basin, as the fault migration has eroded the footwall flank of the basin. Accordingly, this footwall flank is not only faulted, but also contains erosional surfaces for a large part of its length. The resulting low-angle dipping slope may be difficult to differentiate from the low-angle dip of the hanging-wall flank. However, in these situations the internal architecture of system tracts and sequences is rather clear and defines the position of uplifting footwall and tilted hanging-wall, in other words the real asymmetry of the basin.

Forced regression surfaces or deposition over the basin footwall indicate that some subsidence pulses recorded by higher-order system tracts can be related to faulting in a more external position than the fault zones that bound the basin. In the Malaga Basin, subsidence during the late rift climax was produced by faults located SE-ward which revealed a migration of the extension in the same direction.

The structural and seismic sequence stratigraphic analysis provides new constrains on the evolution of the Malaga Basin. Extension was produced by a NW-ward dipping fault system that probably converges along a deep crustal shear zone with a SE-ward extensional system characterized onshore in the western Betics. This latter started before Langhian times and is associated with the rift initiation. It was followed by, or partially coeval with, the NW-ward dipping system that corresponds with the rift climax and the large-scale formation of the Malaga Basin. Most of the fault activity took place from Langhian to Early Serravallian (early to middle rift climax) and diminished from Early Serravallian to Early Tortonian (late rift climax). The late stage inversion, from Late Tortonian onwards (post rift), has surprisingly limited effects in the Malaga Basin, in contrast with the large offset structures interpreted elsewhere in the Alboran Basin.

**6 Tectonic and sedimentary
evolution of the northern WAB
(offshore studies)**

6.1) The basement of the Malaga Basin

The acoustic basement of the Malaga Basin corresponds to the pre-rift metamorphic basement that, onshore, is represented by the Alboran Domain complexes (i.e. Nevado-filabride, Alpujarride, Malaguide complexes, and Dorsal Units). The top of this basement is most of the times characterized by a thick, discontinuous reflector with very high amplitudes (e.g. Fig. 6.02). Due to its strong character, this reflector has been identified in all the available seismic profiles and resulted in the contour map of figures 6.01 and 6.03 which shows the depth of the basement in two way travel time with a spacing between lines of 100msec. It must be stressed that the loss in the seismic signal at depth prevented the identification of the top basement surface below the 4-5 seconds. Therefore, this surface is not represented in the deepest parts of the basin (Figs. 6.01 and 6.03). This map shows the geometry of the Malaga Basin without sedimentary cover and provides information regarding the structures affecting this surface, which corresponds with the top of the pre-rift sequence (i.e. the acoustic basement).

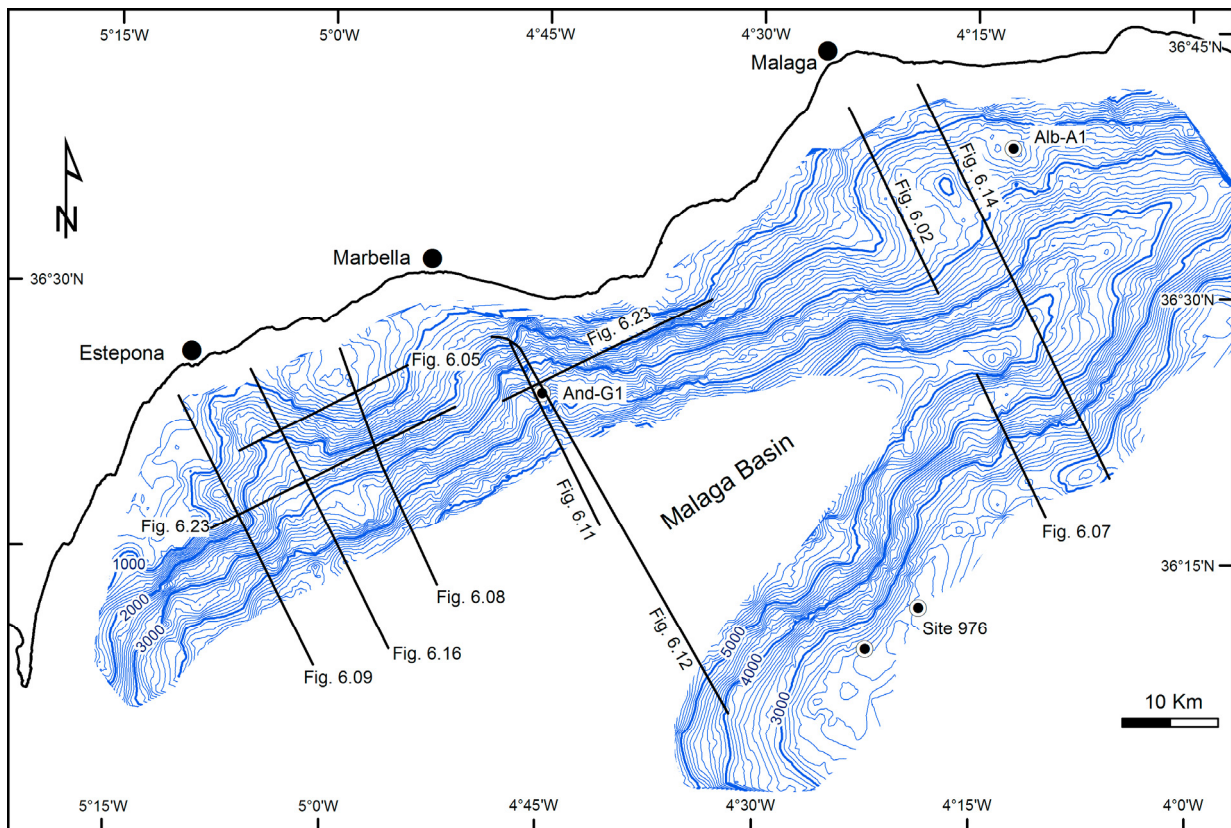


Figure 6.01: Location of seismic lines used in this chapter accompanied by a basement contour map of the basement surface of the Malaga Basin. Contour lines every 100msec. (twtt).

Morphological features

Figure 6.03 reveals that the Malaga Basin is a deep and narrow half-graben, flanked to the north by the actual shelf, and by a structural high to the south, named High 976 (Fig. 6.03). The graben is NE-SW oriented. In the southern flank, towards the SW, it swings progressively to a N-S direction, following the trend of the Gibraltar Arc. In contrast, at the northern flank, the direction changes abruptly to N-S at the westernmost part of the basin (East of the Gibraltar Strait). These direction variations coincide with the transition towards the southern branch of the Western Alboran Basin (Moroccan margin). The graben is about 30km wide in the north-eastern part, and becomes wider towards the west where it reaches 50km wide. In its southernmost part, from Gibraltar strait to the High 976, the Basin is 70km wide.

The axis of the graben is tilted towards the SW and has been only drawn in the northeastern sector where the basin basement is at shallow depth. In this area, it can be observed that the NE-SW axis is, in fact, represented by three segments, 20-25km long, with directions that are around N30 and N75 (Fig. 6.03).

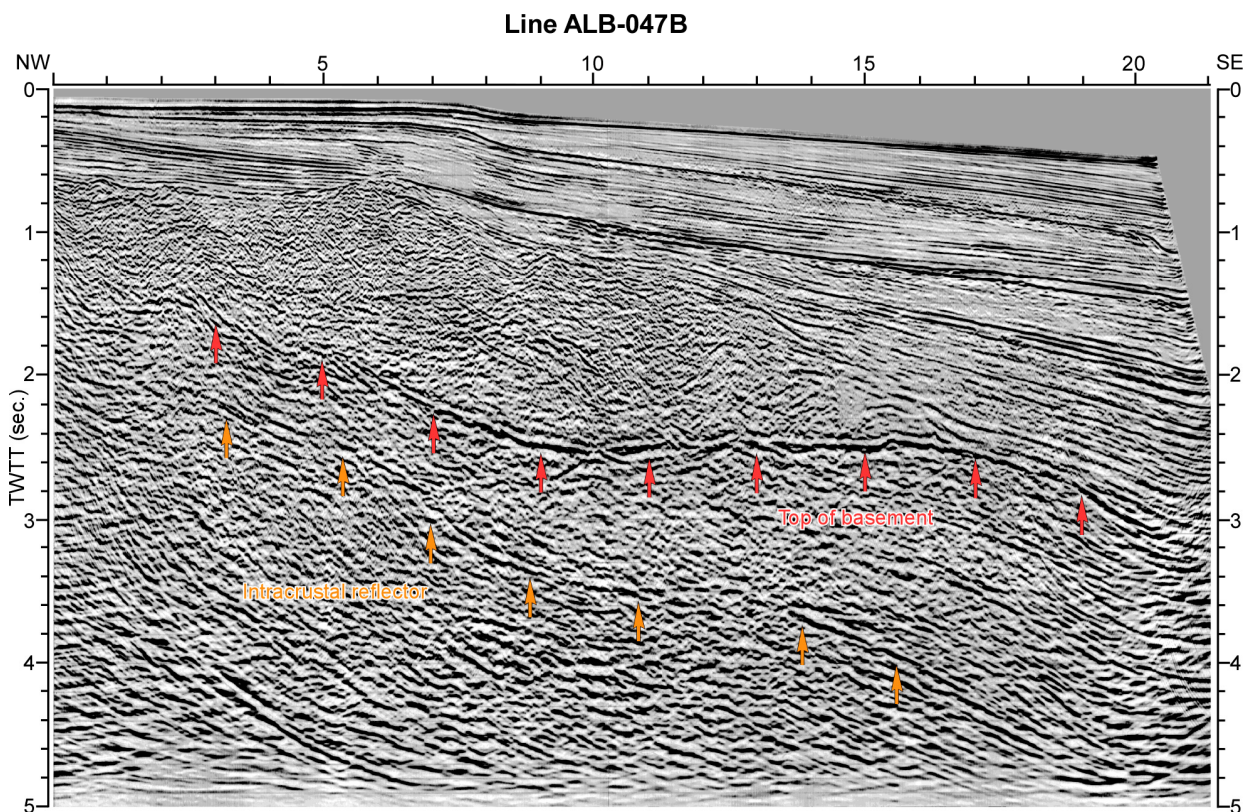


Figure 6.02: Seismic line illustrating the seismic characteristics of the top of the basement surface (red arrows). A well imagined intracrustal reflector is also outlined (orange arrows). Location on Figure 6.01.

At large scale the northern flank is ENE-WSW directed, meanwhile the southern one is NE-SW directed. Nevertheless, at a smaller scale it can be observed that both flanks show escarpments with several predominant directions which are different for each one of the flanks (Fig. 6.04). Alternating with the ENE-WSW main direction, the northern flank shows a secondary WNW-ESE alignment of the escarpments while, in the southern flank, a NNW-SSE direction is observed. It is noticeable the fact that, in the northeastern part of the basin, the two directions observed in the southern flank (NE-SW and NNW-ESE) mimics the ones drawn by the basin axis (compare Fig. 6.03 with 6.04).

In the map of figure 6.04 the contour lines have been overlapped with the dips of the basement using a color scale. Since the vertical scale of the seismic profiles is expressed in two way travel time (twtt) the dips are not represented in absolute values but are illustrative of the relative ones. There are several remarkable features that can be seen by comparing the different dip values observed along and across the basin. It is noticeable the asymmetry between both flank of the basin. While the southern flank shows relatively homogeneous high dips, the northern flank is more heterogeneous ranging from areas with very high dips (e.g. northeast of And-G1 well) to nearly flat ones. For easiness in future descriptions the flat areas have been named as Marbella High by De la Linde *et al.* (1996) and what I defined as Mijas plateau (Fig. 6.03). The Marbella High is situated south of Marbella city and it is a structural high with low slopes at its top where the basement nearly reaches the sea floor. On the other hand, the Mijas plateau receives this name because it is situated east of “Sierra de Mijas” and corresponds to an area of low slopes in a relative high position at the margin of the northern flank of the graben.

The northern flank can be differentiated into four main segments from NE to SW:

- 1) The segment situated east of Sierra de Mijas (from approximately the 4° 30' meridian towards the east) is characterized by low to moderate dips and includes the Mijas plateau.
- 2) Between the meridians 4° 30' and 4° 45', the northern flank shows the highest dips of the basement top, even higher than in the southern flank. The western end of this segment coincides with the end of the WNW-ESE escarpment situated north of And-G1 well.
- 3) Delimited to the east by the 4° 45' meridian and to the west by the escarpment (WNW-ESE directed) that bounds the Marbella High, this segment of the northern flank is characterized by the flat area which corresponds the Marbella High and an escarpment with a moderate and homogeneous dip to the SE.
- 4) West of Marbella High, the topography of the northern flank is complex. First, it is characterized by a top of basement recess towards Estepona. To

the southwest, a NE-SW directed escarpment with very high dips stands out. The top of this escarpment is a nearly flat area where the basement surface even shows slopes dipping slightly towards the actual coastline.

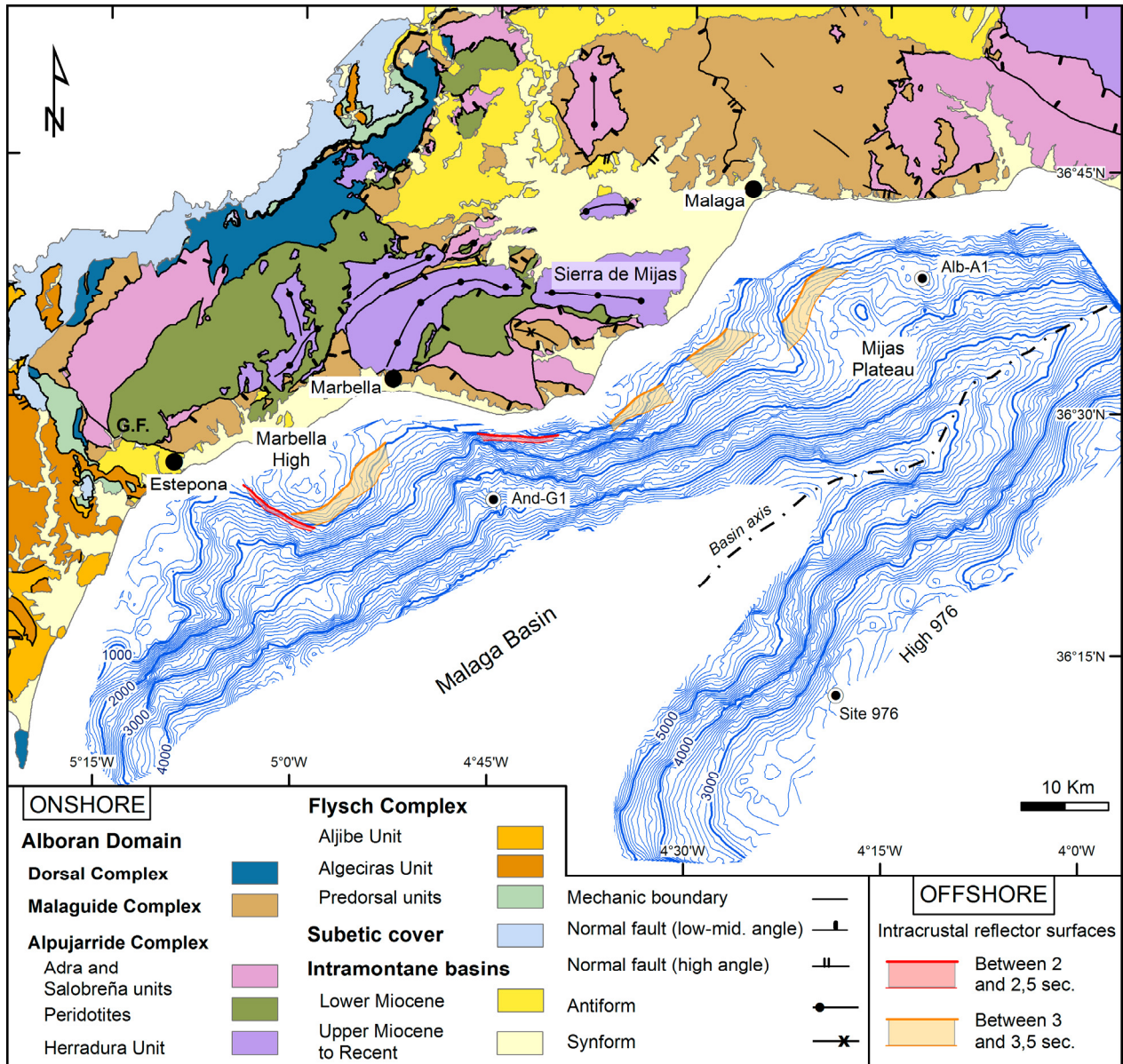


Figure 6.03: Basement contour map of the Malaga Basin. Contour lines every 100msec (twtt). The identified intracrustal reflectors surface is partially represented.

The morphological complexity of the top of the basement surface, along and across the basin, points to significant variations related with the geometry and structure of the basement. The several escarpments directions observed indicate that the structure of the Malaga Basin is not only that of a simple half graben bounded by a unique fault system. Most likely, more than one simple tectonic process was involved during its evolution. This is especially true for the western part of the northern flank were

remarkable escarpments have an oblique direction (WNW-ESE) with respect the overall NE-SW direction of the basin margins.

Intracrustal reflectors

The basement of the Malaga Basin is most of the times an acoustic basement. Therefore, below its surface is not possible to identify clear seismic patterns that permit to interpret its internal structure. However, in some cases is possible to observe prominent and continuous reflectors inside the basement that stand out with respect to the typical chaotic reflections of an acoustic basement (Figs. 6.02, 6.05; see also Fig. 6.08).

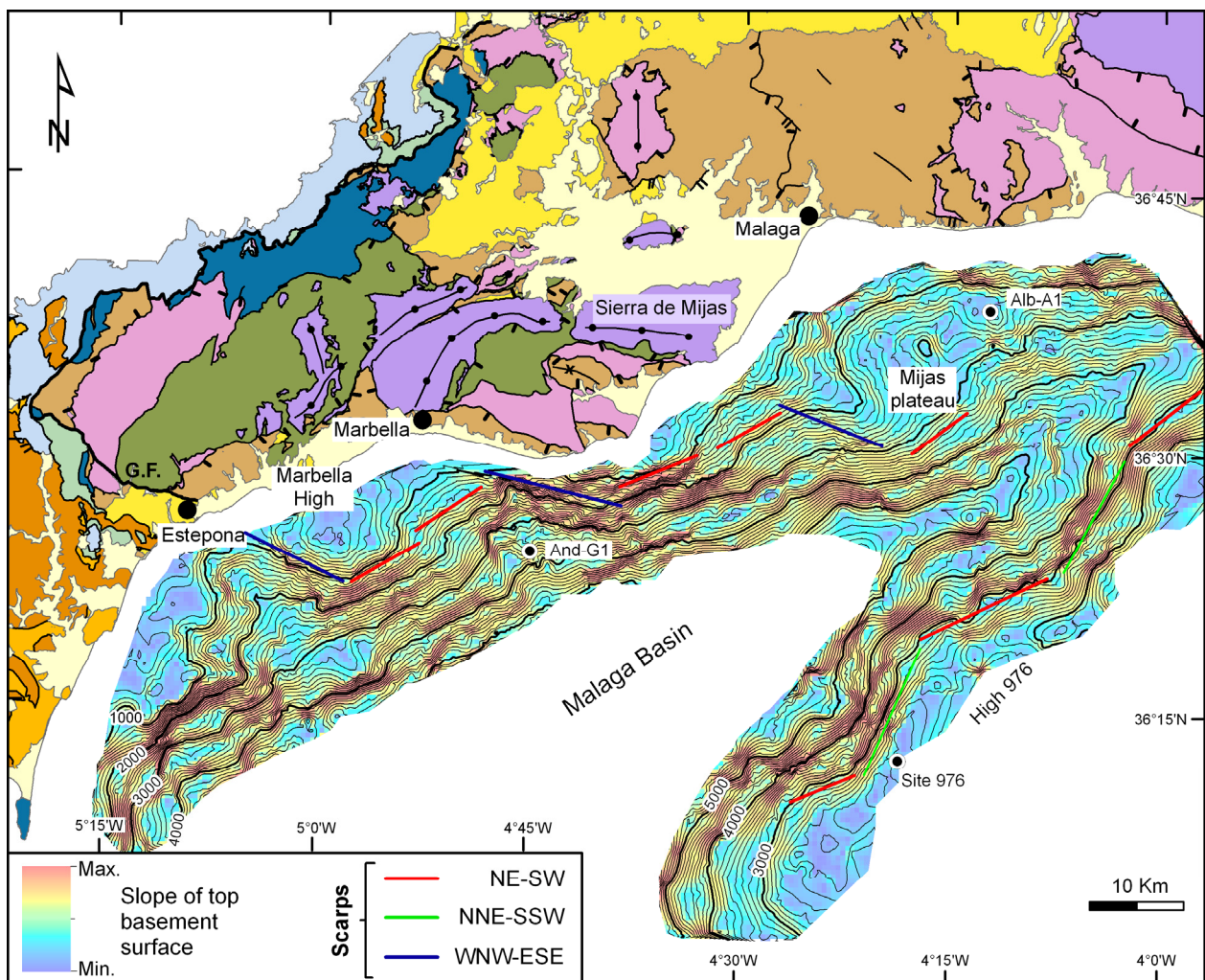


Figure 6.04: Contour map superposed with relative slope values of the top of the basement surface. The direction of the main identified scarps is also shown. Contour lines every 100msec (twtt). Same onshore legend as figure 6.03.

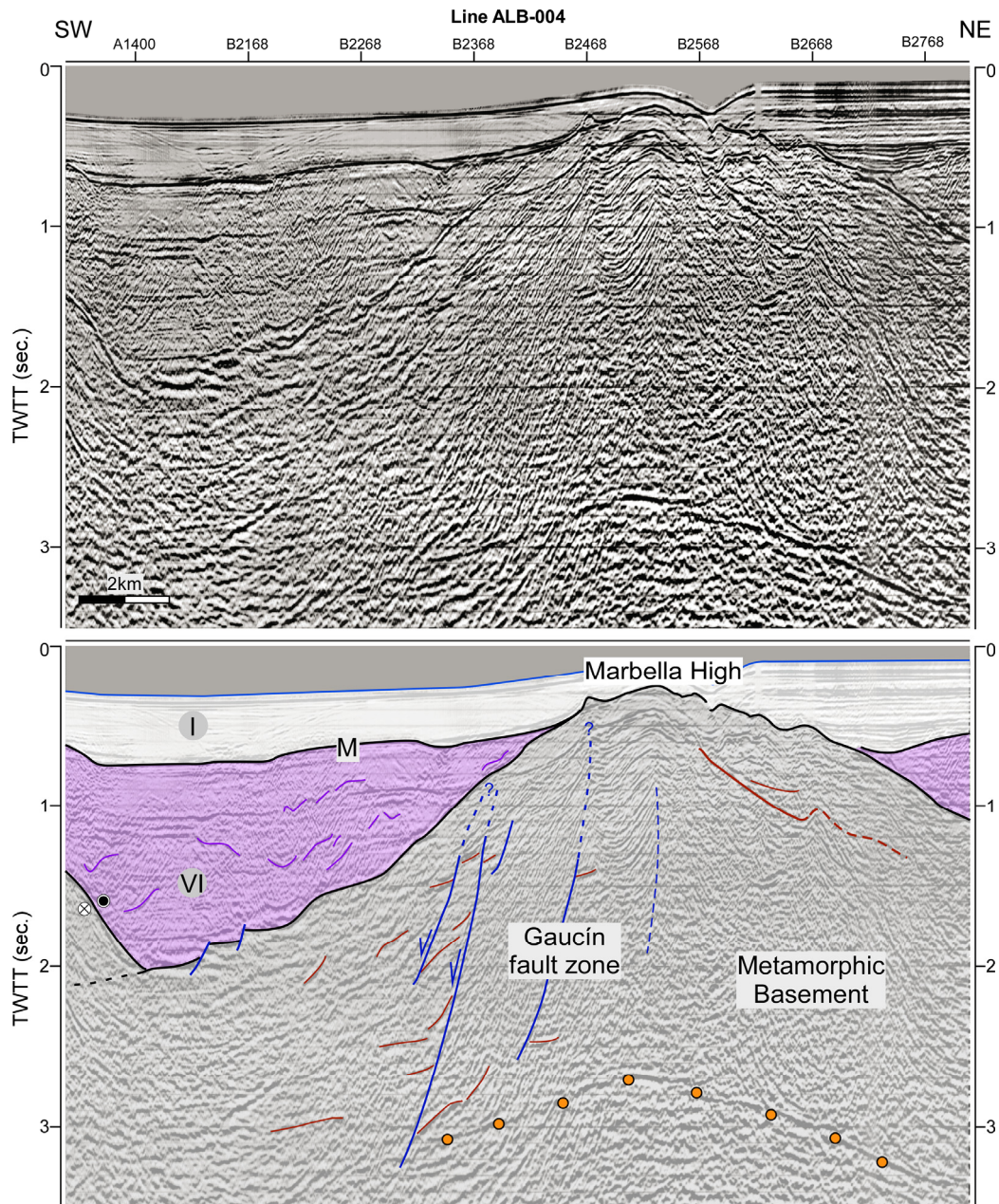


Figure 6.05: Seismic profile that crosses the Marbella High and its corresponding interpretation (Alb-004; location in Fig. 6.01). Note the disrupted reflectors that define a high-angle fault zone (Gaucín fault zone) dipping zone. An intracrustal reflector situated at high depths is marked in orange dots. Same legend as figure 6.07. Location on Figure 6.01.

All the intracrustal reflectors are found in the northern flank of the basin. This could be a consequence of the higher depths of the basement in the southern flank (the top basement surface at southern flank is mostly below the 2 seconds twtt; Fig. 6.03). The loss of resolution at depth may have prevented that reflectors can be properly observed in the profiles. It is also possible that the high number of faults which crosscut the basement of High 976 (Comas and Soto 1999; See also chapter 5) breaks the continuity of the intracrustal reflectors and prevents to see them in the seismic lines.

The four intracrustal reflectors drawn between 3 and 3,5 seconds dip towards the SE, coinciding with the dipping direction of the top basement surface (Fig. 6.03). The profile of figure 6.02 shows an example of such reflectors. Its slope is very low and sub-parallel with respect to the top basement surface.

By contrast with the first group of reflectors, those drawn between 2 and 2,5 seconds show higher slopes and have a different dip direction. The dip of these two reflectors has been estimated by assuming an average P-wave velocity of 5.7km s⁻¹ which corresponds with the metamorphic basement (velocity according to Calvert *et al.*, 2000). Since the lower velocities of the sedimentary cover have not been taken in to account the estimated dips are maximum values: the first one dips about 70-75° towards the SW and is situated at the southwestern scarp of Marbella High; the second one dips approximately 65° towards the South and is located North of And-G1 well (Fig. 6.03). Both reflectors coincide in direction and position with WNW-ESE directed escarpments drawn by the top of the basement, although the reflector situated north of And-G1 shows a little deviation with respect to the escarpment (E-W direction).

This second group of reflectors is usually not observed as a prominent reflector due to its high dip. Instead, they are revealed by a heavy contrast in the reflectivity pattern of the basement, as well as by an alignment of reflector terminations along a plane. This is illustrated in figure 6.05 where the reflector situated south of Marbella High has been interpreted. It contrasts with the low angle dipping reflector situated at 3 seconds twtt which mimics the top of the basement surface. Note that in this case, even it is interpreted as a single plane in the map (Fig. 6.03), several discontinuity surfaces can be drawn in a 2-4 km wide zone (Fig. 6.05). These discontinuities have been interpreted as basement faults which all together form a fault zone, here named as Gaucín fault zone. A full interpretation regarding the Gaucín fault zone can be found in epigraph 6.3.

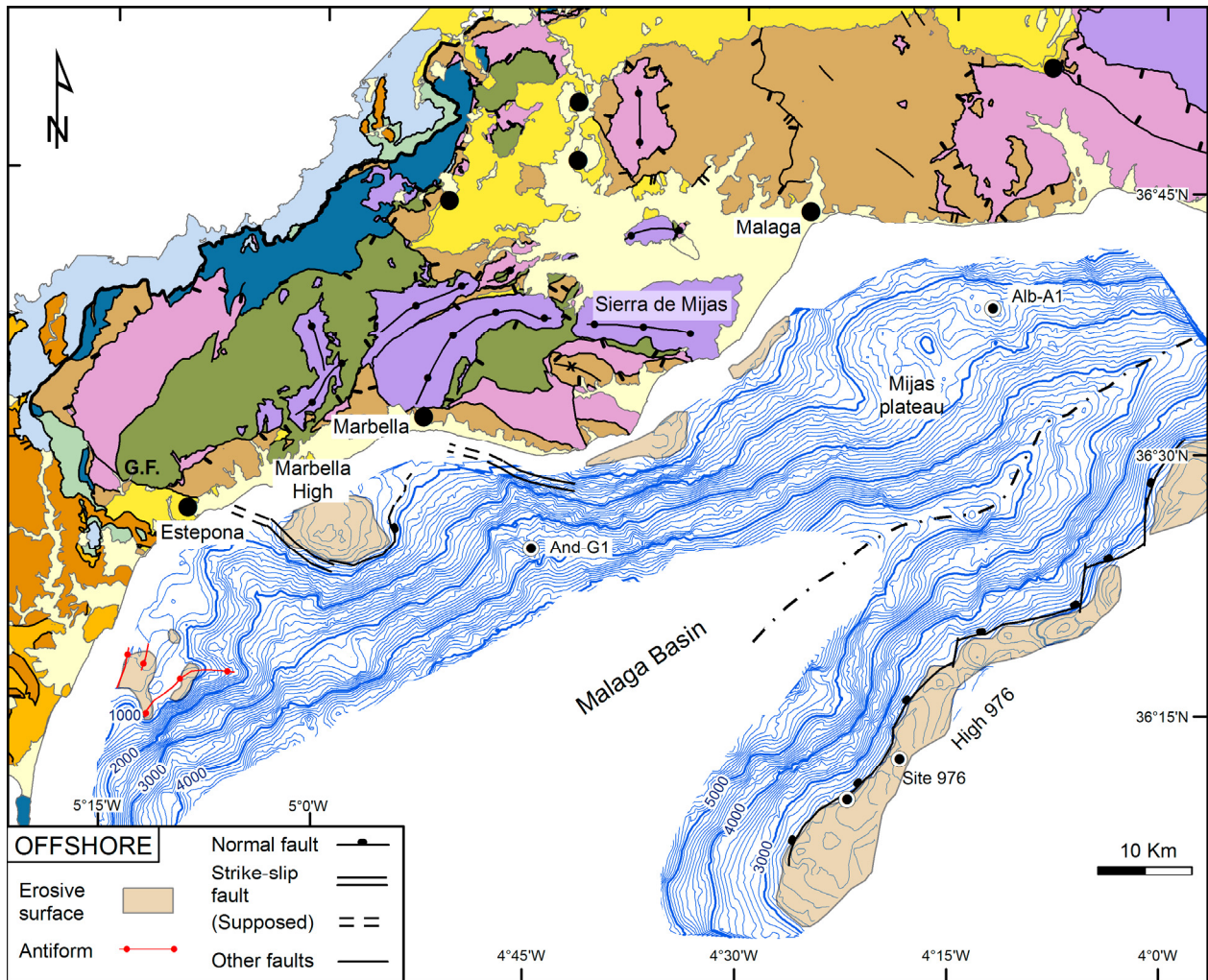


Figure 6.06: Basement contour map with interpretation of sedimentary and structural features on top of it. Contour lines every 100msec (twtt). Same onshore legend as figure 6.03.

Interpretation of the top basement surface

The complex geometry of the top of the basement surface described in the previous paragraphs is the result of different processes, not only faulting but also erosion, as it can be seen from the geometrical relationships with the sedimentary cover. Three main types of top basement surface are present:

- 1) Erosional surface
- 2) Low to medium angle normal fault (LANF) at the bottom of the sedimentary cover and situated on top of the basement surface.
- 3) High angle normal faults with normal and/or strike-slip component. This type includes faults that cut the boundary between the basement and the sedimentary cover.

Locally, some of these surfaces are folded.

The distribution of these different types of the top basement surface is illustrated in the map of figure 6.06. It must be stressed that in many cases there are not enough criteria to truly differentiate the nature of the basement. Therefore, in figure 6.06 the structures are only interpreted in the areas where there are enough criteria to make a clear differentiation. In order to illustrate these interpretations four representative seismic profiles have been selected (Figs. 6.05, 6.07, 6.08 and 6.09).

Erosional Surface

In the Malaga Basin erosional surfaces are mainly observed on top of structural highs as Marbella High or High 976. This surface is also observed at the westernmost corner of the basin, where the basement is nearly flat, and also south and southeast of Sierra de Mijas in the uppermost part of the northern flank (Fig. 6.06).

In the seismic profiles the erosional nature of the basement top is revealed by an irregular, wrinkled surface, characterized by very discontinuous reflectors that show a wide range of amplitudes. These features can be clearly observed in the profile of figure 6.07, on top of High 976 (around shotpoint 500). It contrasts with the clean and continuous reflector corresponding with the top of the basement surface at both sides of the same high.

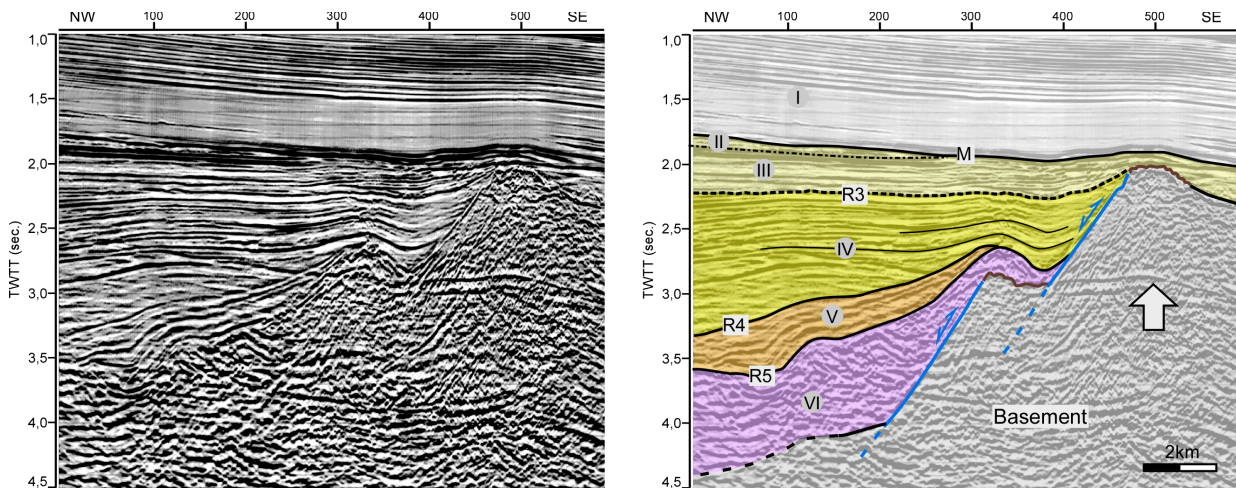


Figure 6.07: Seismic profile and its corresponding interpretation (Alb-047; location in Fig. 6.01). Major unconformities (R5 to M reflectors) are according to Jurado and Comas (1992). The main seismic units and the basement are differentiated in colors. Basement: grey; Unit VI: pink; Unit V: orange; Unit IV: yellow; units II and III: light yellow; Unit I: white. Marker reflectors: brown: erosional surfaces; blue: faults. The white arrow indicates uplift during the post-rift stage. Note the slightly folded reflectors that indicate minor uplift and reactivation in compression of previous normal faults. Location on Figure 6.01.

When comparing the erosional surfaces of different profiles it is observed that several erosional episodes affected the top of the basement surface. The last event correspond with the erosion occurred at the end of Messinian (reflector M) that affects the entire Miocene cover, including the basement. This is the case for the erosional surface observed on top of Marbella High (Fig. 6.06). For example, in the profiles of figures 6.05 and 6.08 it can be observed that the M reflector cuts the basement top (e.g. between shotpoints 700-800 in Fig. 6.08) which indicates that the erosional episode represented by this reflector affected the basement.

Previous erosional surfaces below the M reflector are also present. In the Malaga Basin they are observed only around High 976. Two of them are observed in figure 6.07: the one located below unit III deposits (around shotpoint 500) already described, and another one situated below the lowest unit VI (between shotpoints 300 and 400) which indicates erosion of the top basement surface previous to Langhian times. Both erosional surfaces are local as they cannot be related with any basin-wide reflector that shows up as an erosional surface (in contrast with M reflector case). They are most likely related with the extensional episode that formed the Malaga Basin as, during this period, High 976 was part of the footwall block of the extensional system and affected by erosion (see also chapter 5). Therefore, the erosional surface at High 976 drawn in the map (Fig. 6.06) corresponds partially to a superposition of various erosional episodes: the late Messinian and the extensional-related one. This is observed in the north-eastern part of the basin, where High 976 is in a higher position and reaches 2 seconds twtt (Fig. 6.06). There, the M reflector intersects with the basement top which indicates that Messinian erosion reworked the previous erosional surface developed during the extensional episode (see Fig. 6.14 in epigraph 6.2).

Low to medium angle normal faults (LMANF)

In the northern flank of the Malaga Basin, the interpretation of the top-basement surface as a low angle normal fault bounding the basement and the sedimentary cover was initially proposed by Comas *et al.* (1992). The presence of low-angle intracrustal reflectors dipping in the same direction as the top of the basement surface supports this interpretation as they can be related to extensional duplexes (e.g. Fig. 6.08 between shotpoints A800 and B1075). However, to clearly demonstrate if these surfaces acted as LMANFs during a determined time interval, it is necessary to determine syn-kinematic criteria in the sedimentary cover that indicate movement along this surface. Additionally, it would also permit to know the time span in which those faults were active. In the next paragraphs we will present some arguments which favor the LMANF hypothesis although the relationships between the sedimentary cover and the basement will be explained in detail as they are described in the next epigraph (6.2 Sedimentary infill and associated tectonic structures).

6 Tectonic and sedimentary evolution of the northern WAB

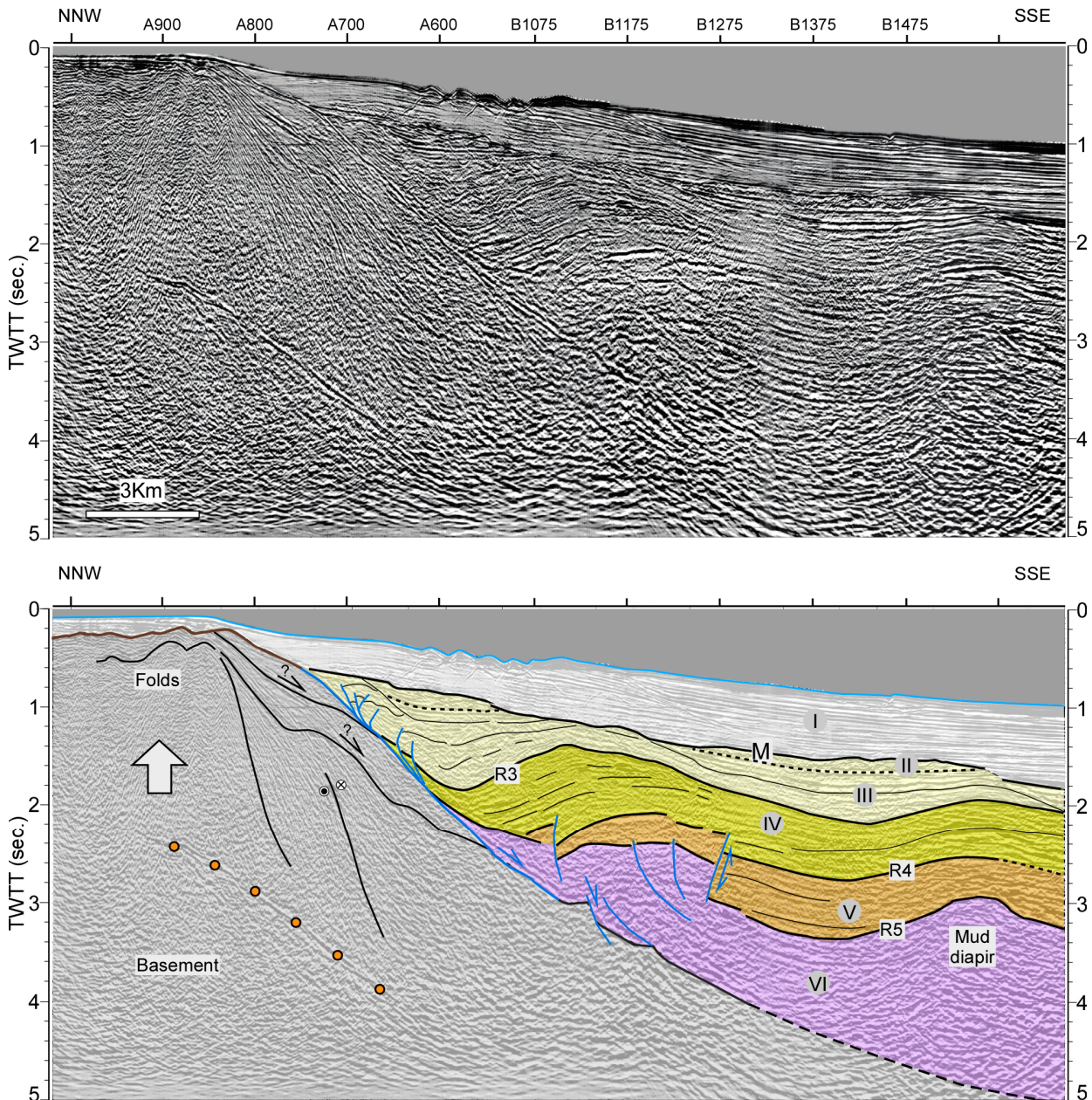


Figure 6.08: Seismic profile crossing the Marbella High and its corresponding interpretation (Alb-019; location in Fig. 6.01). An intracrustal reflector with low dip is marked by orange dots (represented in Fig. 6.03). Higher dip intracrustal reflectors are drawn in black lines. Note the folds affecting the top of Marbella High. Same legend as figure 6.07. Location on Figure 6.01.

First, it must be stressed that in many cases unit VI deposits lie on top of the basement surface. The chaotic internal geometry of this unit does not permit to characterize feasible kinematic criteria, despite that some internal structures can be inferred from the reflector patterns (e.g. Fig. 6.09 and 6.14). In addition, it must be taken in to account that these structures inside unit VI can be due to the shale tectonics and not to extensional processes. In other cases, such the area west of Mijas Plateau (see Fig. 8 in chapter 5), an on-lap of the sedimentary cover against the basement point that the surface was passive during the deposition of most of the sedimentary sequence.

Therefore, in the map of figure 6.06 there are only drawn as top-basement faults the areas in which enough criteria from units V to III was observed, which means they were active during their deposition. This does not exclude that in the remaining areas, the top-basement surface could have been active as a LMANF previous to their deposition.

Figure 6.06 shows the fault traces from LMANFs that correspond with the top of the basement surface. The fault traces has been drawn at the top of the fault planes when they reach an erosional surface (e.g. Fig. 6.08 between shotpoints A800 and A700; Fig. 6.07 between shotpoints 400 and 500; see also Fig. 3.04). The top basement surface as a LMANF has been clearly identified only in two areas. The first one corresponds with the escarpment that bounds High 976 in the Malaga Basin southern flank (Fig. 6.07). Along this escarpment syn-kinematic criteria are observed such as a thickening of the sedimentary sequence or, in a few cases, divergent reflector patterns drawing growth strata against escarpment which accordingly is interpreted as a LMANF (see Fig. 6 in chapter 5). It is remarkable that the top of the basement along High 976 is not always a regular dip but can also be stepped downdip (e.g. Fig. 6.07). This feature points that the southern flank contains not a single fault, but a sequence of faults dipping towards the basin center. However, only the uppermost fault has been traced in the map and corresponds with the top of the escarpment (around shotpoint 480 in Fig. 6.07). By contrast, in the northern flank of the Malaga Basin, only the basement scarp situated immediately at southeast of Marbella High shows the characteristics of a LANF (Fig. 6.06 and 6.08). Even the overall structure has been affected by tectonic inversion, the roll-over of the sedimentary sequence against the basement scarp can be clearly observed (between shotpoints A600 and B1275 of figure 6.08). Additionally, the sedimentary sequences below and above R3 unconformity (units IV and III) are thickened towards the basement surface indicating the presence of a growth fault. Finally, note how several faults are rooted along the top of the basement which represent a detachment level.

High angle normal faults

The basement top is barely observed as a high angle normal fault as these structures have affected most of the times the sedimentary cover and show an asymptotic geometry with the basement surface (e.g. Fig. 6.08). When these structures are observed crosscutting the basement, the fault offset is always small (e.g. less than 200msec at the fault found between shotpoints B1075 and B1175 in Fig. 6.08).

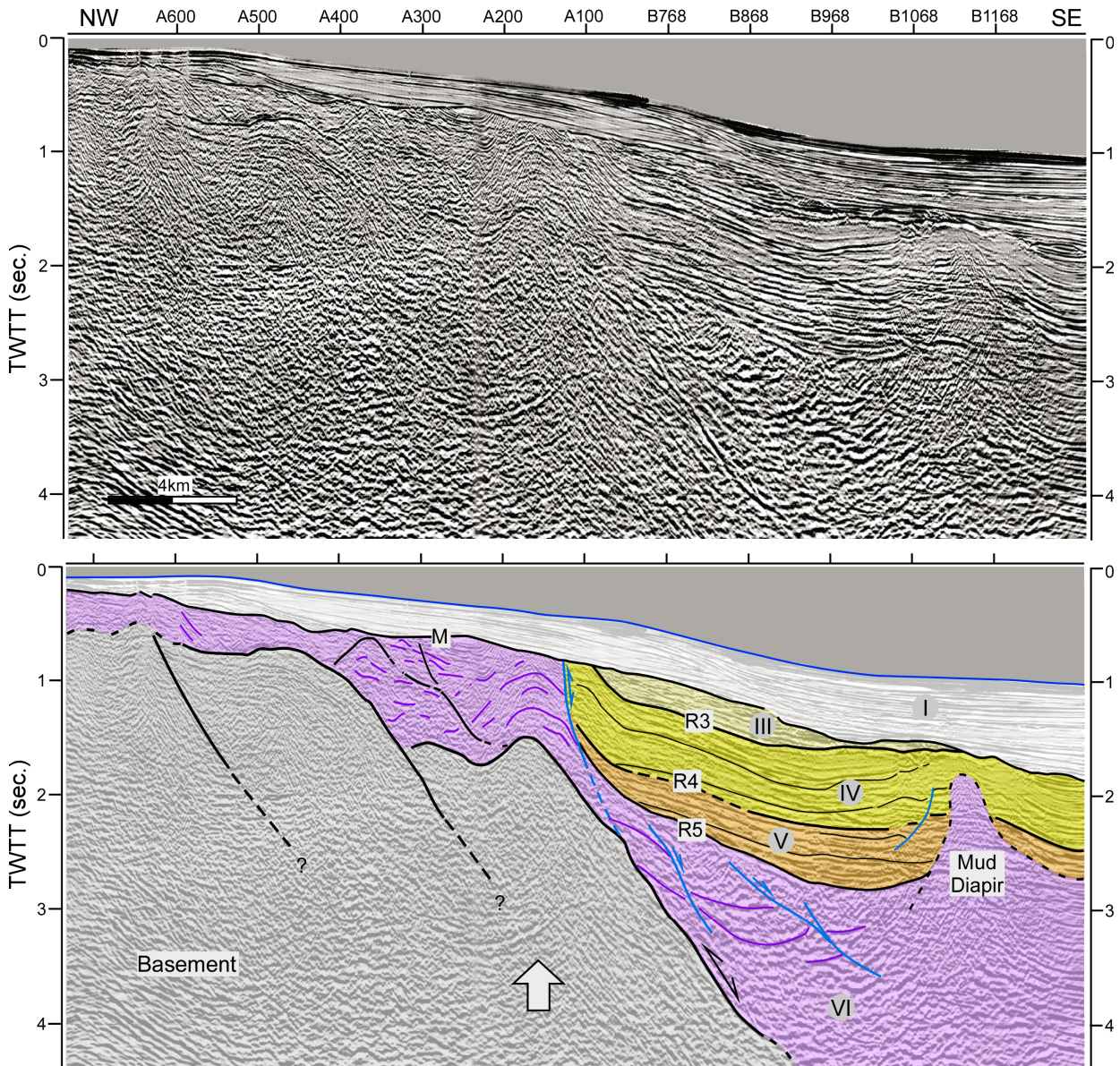


Figure 6.09: Seismic profile of the Malaga Basin westernmost margin and its corresponding interpretation (Alb-011; location in Fig. 6.01). The folds drawn by the basement surface and Unit VI reflectors (shotpoint A200) indicate compression previous to the main extensional event. Same legend as figure 6.07. Location on Figure 6.01.

Basement folds

South of Estepona, near of the coast where the basin is mostly flat, several basement folds have been observed (Fig. 6.06). They have broadly a NNE-SSW direction despite that the axis of the most significant one (situated in a more distal position with respect to the actual coastline) swings to a W-E direction at its eastern termination. The easternmost part of this antiform is interpreted in the profile of figure 6.09 (between shotpoints A100 and A200). In accordance with the basement, the Unit VI reflectors also draw an antiform, which indicates that folding started most likely during or after Burdigalian. Unfortunately, the upper limit of the folding process cannot

be well constrained because the Messinian unconformity (M) eroded the rest of the Miocene sequence (Fig. 6.09). Only Unit I rest over the unconformity which constrains the upper limit of the folding at Plio-Quaternary.

Where these folds are observed, intrabasement discontinuities drawn from reflectors terminations are present. They show roughly a SE dipping direction, sub-parallel with the top basement surface (roughly between shotpoints A600 and A200 in Fig. 6.09). The genesis of these folds will be discussed later (chapter 6.3).

6.2) Sedimentary infill and associated tectonic structures

This epigraph describes the characteristics of the sedimentary cover that rest over the metamorphic basement of the Malaga Basin together with the tectonic structures that affected them. We focus on the sedimentary cover which belongs to the Burdigalian to Messinian time interval, both inclusive, when the main tectonic events in the Gibraltar Arc occurred. The sediments from Pliocene to Recent have not been studied in detail, mainly because Pérez Belzuz (1999) studied them specifically in his Ph.D. thesis. He used monochannel seismic profiles which have a better resolution for shallow deposits than the multichannel seismic ones used in this work and are therefore more appropriate for the study of these sediments.

In the sedimentary infill of the Malaga basin six main unconformities have been identified, including the top of the basement surface (R1 to R6; according to Jurado and Comas, 1992). These unconformities have been correlated all along the seismic profile grid and also with the wells Alb-A1, And-G1 and Site 976, (Fig. 6.10). Our correlations with the wells are mostly in accordance with previously published studies (see Comas *et al.*, 1992; Diaz-Merino *et al.*, 2003; Martínez del Olmo and Comas 2008). Nevertheless, a significant modification with respect to previous correlations must be highlighted. Indeed, the lower part of well And-G1, which was previously considered part of unit V, has been correlated in this work with Unit VI (Fig. 6.10). This new correlation has been possible due to the seismic interpretation of seismic profiles carried out in 2003 by ConocoPhillips (i.e. Cab lines; see Fig. 3.01) which have a deeper penetration and a much better resolution than the old lines (EAS, ALB, AM, etc.).

A comparison of the correlation proposed here and the traditional one established by Comas *et al.* (1992) is shown in figure 6.11. The good imaging of Cab01-1121 regarding the mud diapirs permits to better constrain the R5 unconformity and shows that it intersects the well And-G1 at 2,6 seconds (Fig. 6.11, Km. 5). Accordingly to our Time-Depth chart of And-G1 (see annex), the R5 unconformity would coincide with the top of the formally known as subunit Vb (see Jurado and Comas 1992; Comas *et al.*, 1992) which is situated at 3104m (Fig. 6.10). Therefore, in

the oldest seismic lines, the lower part of the unit interpreted as subunit Vb is, in fact, part of unit VI.

This new interpretation is also more coherent with the log data (gamma ray logs in Fig. 6.10; see also Jurado and Comas, 1992), which revealed undercompacted sediments below 3100m at well And-G1, and below 1450m at well Alb-A1. Unit VI sequence is finer grained in And-G1 when compared with Alb-A1 well but both series show strong lithological similarities. In And-G1 a sequence of clays with silty intervals is described while in Alb-A1 the clays are interbedded with sandy levels. In addition, the And-G1 sequence was also considered from well reports as probably olistostromic in nature due to the presence of Eocene and Cretaceous fauna.

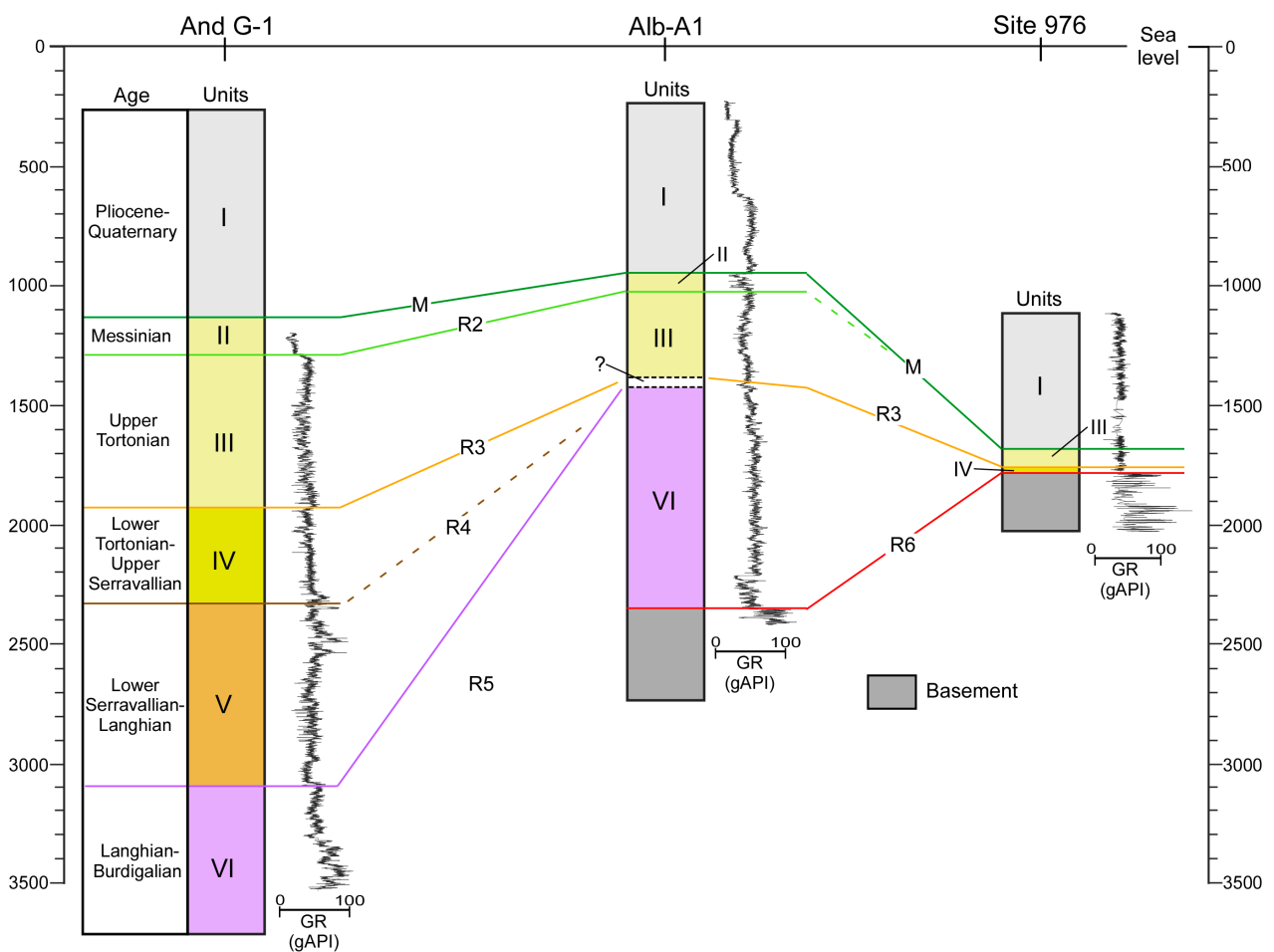


Figure 6.10: Correlation between wells of the major unconformities and seismic units in the Malaga Basin (location of wells in Fig. 6.01). The correlation is based on seismic profile analysis, stratigraphic well reports, and well logs. In the left margin, the correlation in well And-G1 from Jurado and Comas (1992) is shown. The major difference with the previous interpretation is the presence of unit VI in well And-G1.

This new correlation has two important consequences: 1) unit VI is the only unit that shows undercompaction and the source rock of the mud diapirism which, in turn, agrees with the seismic interpretation where unit V is pierced by mud diapirs (e.g. Fig. 6.12); 2) unit VI is partially Langhian in age. As a matter of fact, a younger age for the upper part of the olistostromic unit VI has also been proposed previously in the sequential stratigraphic model of Díaz-Merino *et al.* (2003).

The correlation of the main unconformities permits to constrain the distribution and thickness of each one of the seismic-stratigraphic units (VI to I) in the entire Malaga Basin. This is represented by four isopach maps that correspond to the thickness of units VI, V, IV, and a last one which is the sum of units III and II (Figs. 6.13, 6.15, 6.17 and 6.18). Additionally, each isopach map is accompanied by a contour map of the unconformity at the bottom of the represented unit (e.g. reflector R5 in the case of unit V map; Fig. 6.15). Finally the structures that were active at the same time as the deposition of each one of the units are also represented in each map, with the exception of unit VI map. Those maps provide a precise picture of the tectonic evolution of the Malaga Basin from Burdigalian (Unit VI) to late Tortonian-Messinian (Unit II and III).

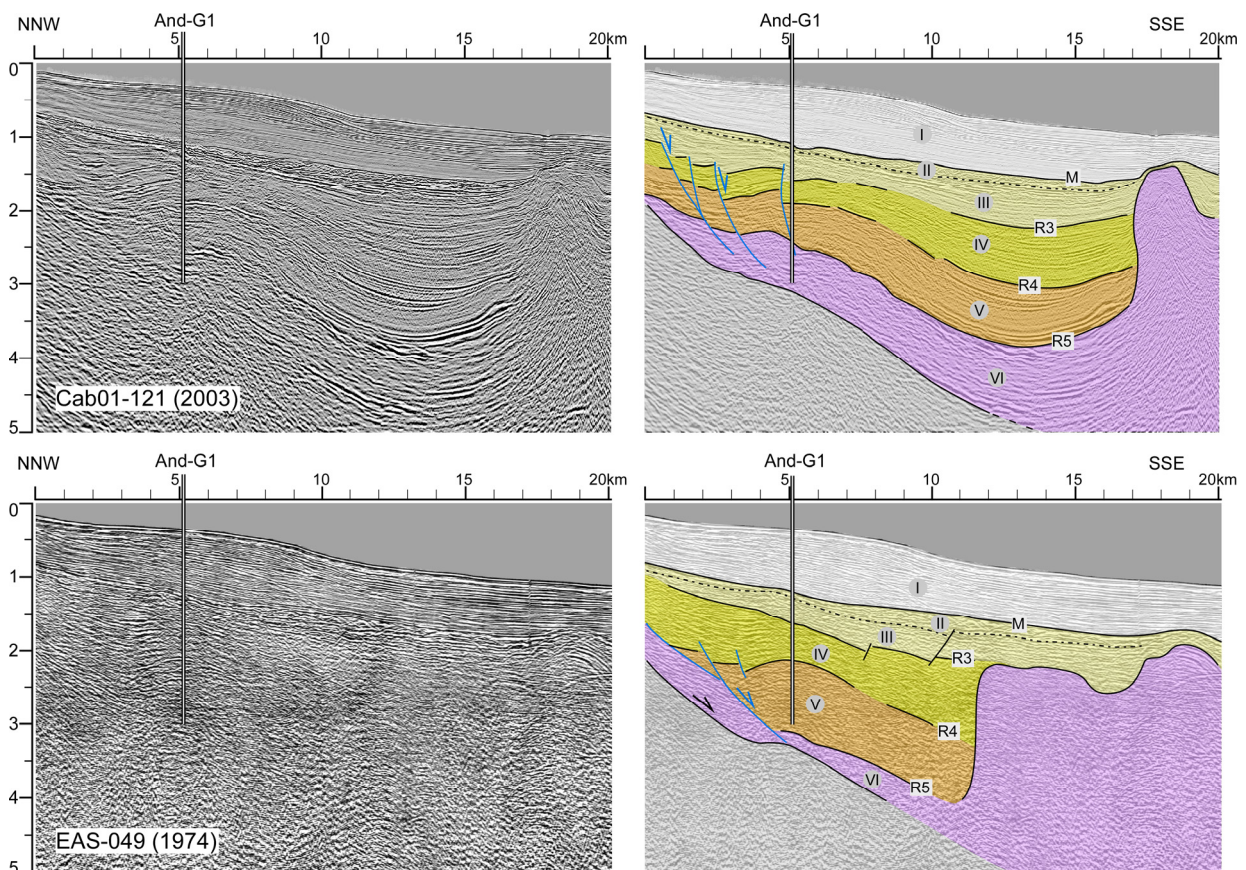
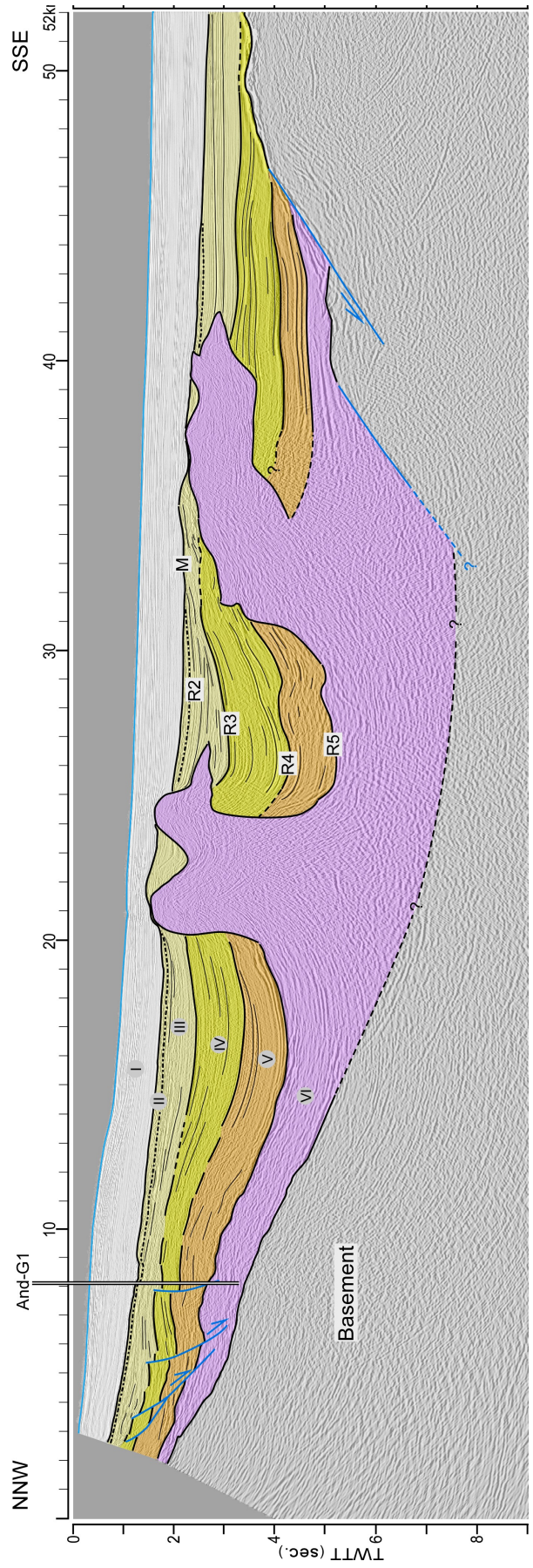
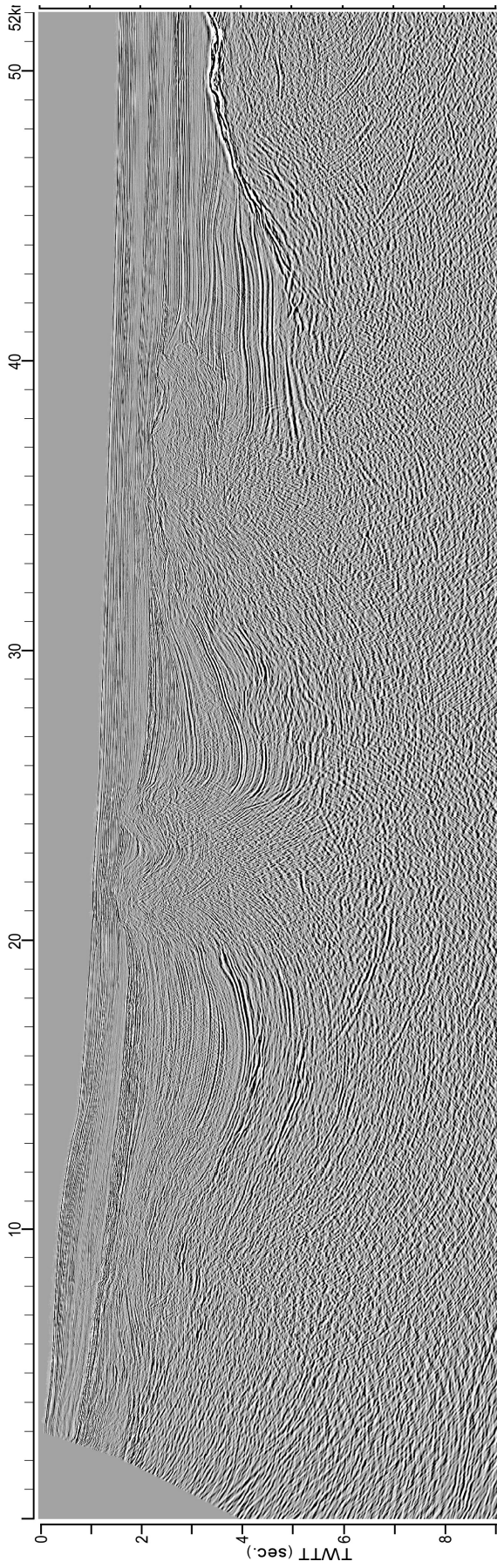


Figure 6.11: Comparison between an old (EAS-049) and a modern (Cab01-121) seismic profile that intersect the well And-G1 (location in Fig. 6.01). The increased seismic resolution of the modern profile permits to reinterpret the major unconformities (according to Comas *et al.*, 1992) and redefine the seismic units in well And-G1 (see Fig. 6.10). Same legend as figure 6.07. Location on Figure 6.01.



Unit VI: Burdigalian to Langhian

Unit VI represents the first Miocene sediments in the Malaga Basin and lies directly over the metamorphic basement. This unit is characterized by reflections with a seismic signature that varies significantly from one profile to another. The most common geometry is that of chaotic reflectors. In the deepest and central area of the basin, the upper part of this unit can be also characterized by less chaotic reflector geometries, being dominated mostly by hummocky and also by scarce tabular reflections (Fig. 6.12; Fig. 8 in chapter 5). Overall the reflectors show a wide range of amplitudes which is observed laterally along the profiles. These variations are usually sharp, and abrupt transitions from clear reflectors to mostly transparent seismic facies can be observed. In all these cases, the reflectors are highly discontinuous and most of times do not show coherent internal geometry.

The top of unit VI corresponds to the R5 unconformity. This surface is usually seen as a very high amplitude reflector, most likely due to the strong competence contrast between unit VI, overpressured, and the overlying deposits. The R5 unconformity is most of the times observed as an irregular surface, especially in the basin margins (e.g. Fig. 6.14; see also Fig. 6 in chapter 5), and only appears as a clean surface in the deepest parts of the basin, coinciding with the areas where the internal reflectors are less chaotic (e.g. Fig. 6.12 around km. 17 and km. 40; Fig. 8 in Chapter 5). This features points that R5 is an erosional surface in most parts of the basin and, only in the deepest parts of the basin may correspond to a paraconformity (Fig. 8 in chapter 5). Additionally, the R5 is often affected by shale tectonics which disrupts and deforms its original geometry (Fig. 6.12; between the 3 and 10km in Fig. 6.14).

The isopach map of unit VI (Fig. 6.13) shows the thickness of this unit in the Malaga Basin. It must be stressed that in the central part of the basin, the top of the basement is deeper than 5-6 seconds twtt (e.g. basement contour map of Figure 6.03) which is beyond the resolution of the seismic lines. Since the top of the basement corresponds to the lower limit of unit VI its total thickness cannot be known in this part of the basin. Despite this limitation, an approximation has been done in order to complete the isopach map: the surface has been extrapolated along each one of the seismic profiles keeping the same slope for the basement top, up to a maximum of 6 seconds depth, and then virtually considered flat (note the lack of top of the basement contour lines in the centre of the basin (Fig. 6.13). The boundary of the area where the

Figure 6.12: (previous page) Seismic profile crossing the Malaga Basin and its corresponding interpretation (Cab01-121; location in Fig. 6.01). The basement surface in the center of the basin is not well imaged and has been extrapolated. Note the major faults affecting the basement in the eastern margin in comparison with the small offset faults affecting only the sedimentary cover in the western margin. Same legend as figure 6.07. Location on Figure 6.01.

top of the basement has been extrapolated is underlined. In this area at the centre of the Malaga Basin, unit VI thicknesses are minimum values as the real thicknesses are probably greater than those represented in the map. Indeed, the real basement top clearly goes beyond the 6 seconds depth in the centre of the basin as it can be observed in some of the modern seismic profiles (Fig. 6.12). Also note that the apparent thinning of this unit towards the eastern end of the mud diapirs (between 4° 45' and 4° 30' meridians) is, in fact, a consequence of the top of the basement extrapolation and may not be a real thinning of unit VI.

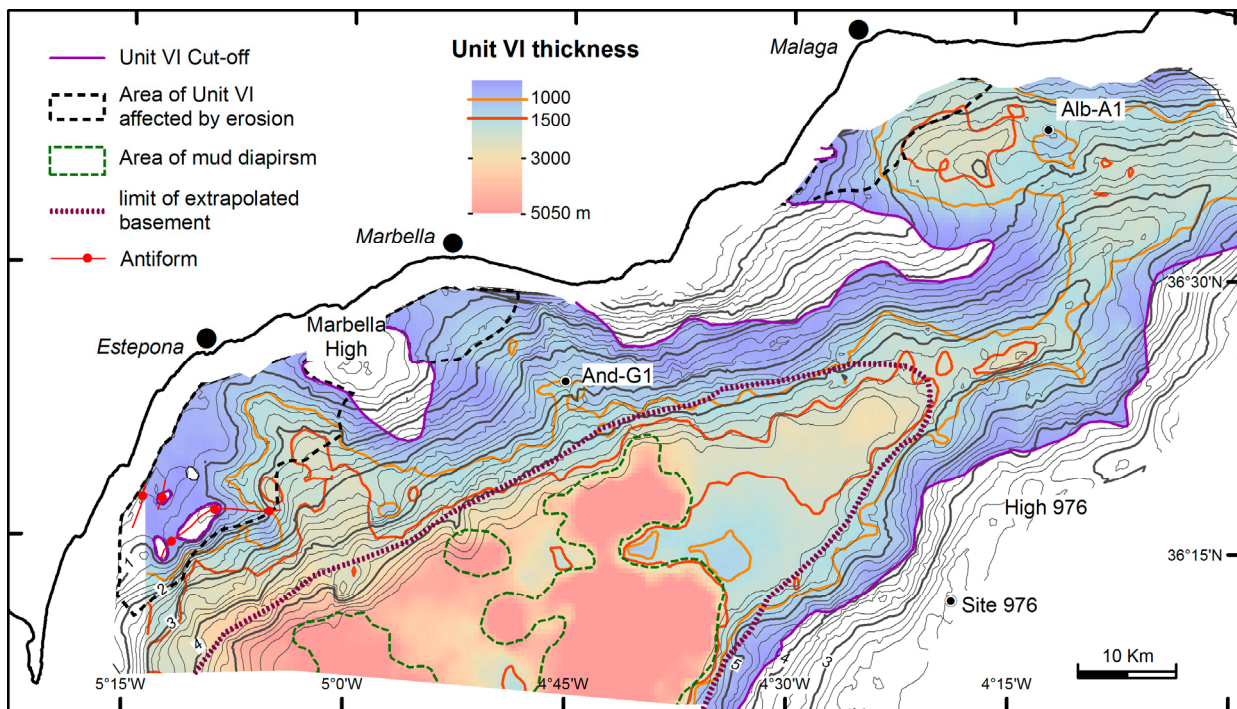


Figure 6.13: Isopach map of Unit VI superposed with a contour map of the basement top (contour lines every 200msec.). The thickness of unit VI in the center of the basin has been extrapolated considering a flat basement of 6 sec. (twtt) and shows minimum values. Thicknesses in areas affected by erosion are also unreliable. Note the overall increase in thickness towards the SW and the local depocenters situated over flat areas drawn by basement top (e.g. Mijas plateau, West of Alb-A1).

Even though, the major accumulations of this unit are still observed, by far, in the centre of the basin roughly coinciding with the mud diapirism area (Fig. 6.13). There, the limits of mud diapirs correspond to the inflection point of R5, where steepening and piercing of the overburden units are observed. If such diapirs are considered part of unit VI, the thickness predicted by the isopach map in the core of those structures is more than 5000m. If the mud diapirs are excluded, the map also reveals a thickening of this unit towards the westernmost part of the basin, where accumulations of more than 3000m are observed (e.g. Fig. 6.09). It must be stressed that this large amount of unit VI sediments could be also consequence of shale migration during the growing of the diapirs which are situated nearby.

In the north-eastern part of the basin, outside the mud diapirs influence and where the two flanks of the basin are observed, the major accumulations of unit VI are observed in two different positions (Fig. 6.13). The first one is observed in the centre of the basin coinciding with the basin axis drawn by the top of the basement surface. The second depocenter is situated over the north-western flank, coinciding with the flat top-basement area of Mijas plateau. This second depocenter shows thicknesses between 1000 and 1700m and continues to the northwest, towards the Malaga Basin which appears onshore. Near of the coastline, thicknesses of more than 800m are still observed at the north-western end of the seismic lines. By contrast, in the same flank, southwest of Mijas plateau, where the slope of the top of the basement is higher, the cut-off of unit VI is in a relative low position and the thicknesses are lower. A similar observation can be done southwest of Marbella High, where the basement recess area with low slope shows a significant unit VI accumulation (up to 1600m). By contrast, towards the east, the Marbella High sedimentary cover does not contain any unit VI deposits, and thicknesses of only 1000m are observed south-east of this High. Note that in this case, the top of the basement slopes are low, but not as low as in the case of Mijas plateau or the recess southwest of Marbella High. Furthermore, along the north-western flank, unit VI was partially eroded during the Messinian salinity crisis (M reflector in Figs. 6.14 and 6.16). Therefore it is expected that the original thicknesses observed in the eroded parts were greater. In summary, towards the northwest and in an onshore direction, this unit probably has had similar thicknesses. By contrast, unit VI cut-off is observed along the whole south-eastern flank, below High 976 (Fig. 6.13).

Unlike the other units, most of the structures active during the deposition of Unit VI (Burdigalian to Langhian) are not represented in its isopach map, mainly because it is not possible to characterize with confidence how this unit is structured. The lack of a coherent internal geometry in the seismic reflectors of unit VI does not permit to define reliable sedimentary patterns that could indicate a syn-kinematic deposition relative to the faults observed in the seismic profiles.

The only structure that can be mapped is a fold drawn by internal reflectors of unit VI which is situated near the Gibraltar Strait (Fig. 6.09, between shotpoints A200 and A100). The age of this fold can be constrained to Burdigalian-Langhian times as it is cut by a normal fault syn-kinematic with unit V deposition (Langhian).

In addition, it has been possible to infer some structures within unit VI by looking carefully the directions of the reflectors and analysing their patterns, although it was not been possible to follow them in adjacent profiles. This is the case of figure 6.16 profile where reflectors inside unit VI draw smooth folds cut by SE dipping structures interpreted as faults. Their mechanics cannot be known with precision but the relative low angle dip and the associated folds point that they could be: a) Faults related with thrusting (with the associated propagation folds), or b) roll-over folds related to extensional faults, in turn either due to extension or to shale migration.

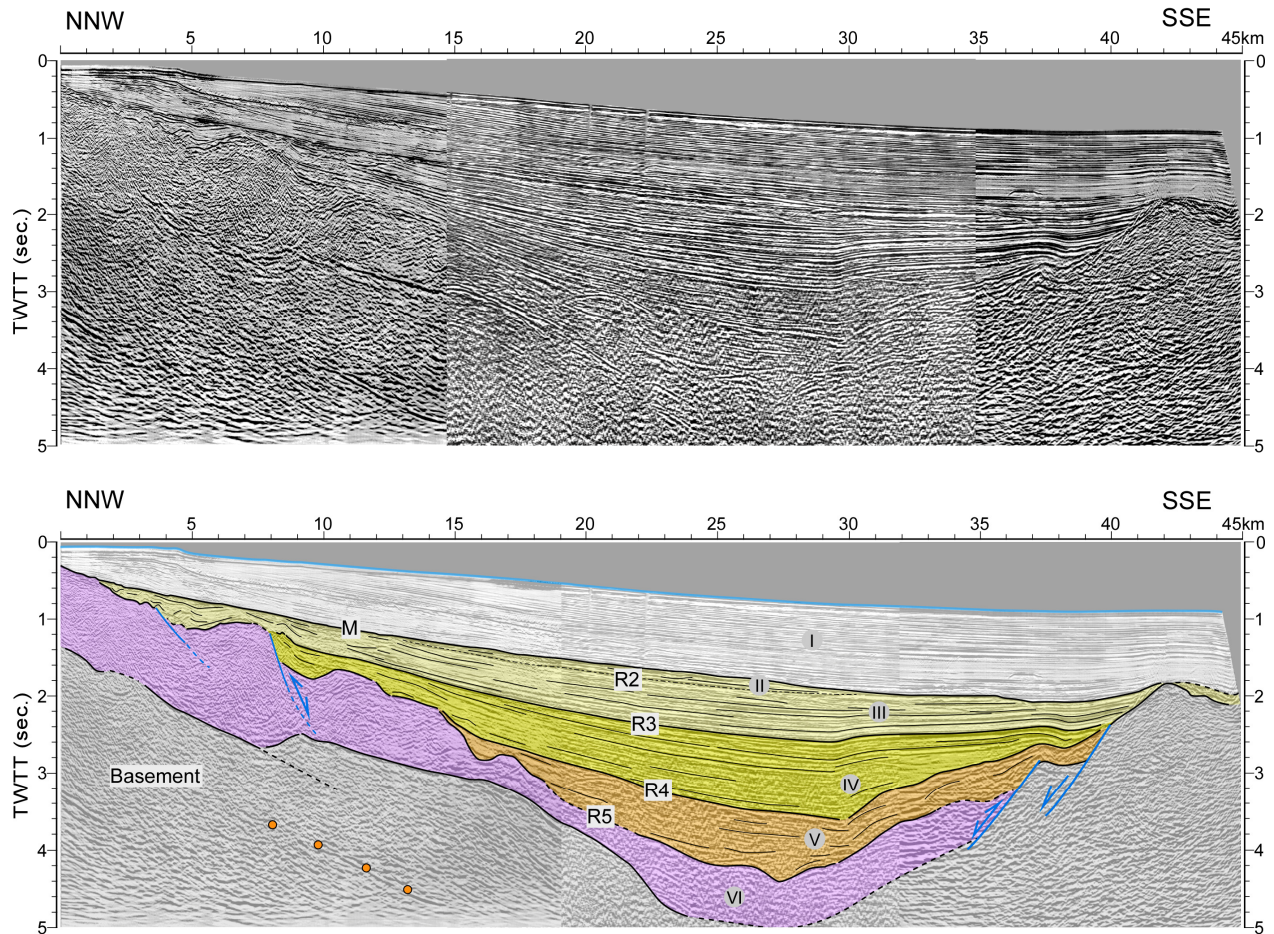


Figure 6.14: Seismic profile in the northeastern part of the Malaga Basin and its corresponding interpretation (merge of profiles EAS-096, Alb-051, Alb-051B; location in Fig. 6.01). Units V to III are thicker in the centre of the basin while there is an increase of unit VI thickness towards the western margin. Note the slight folds drawn by the sedimentary cover indicating minor reactivation in compression of normal faults that previously affected Unit VI (western margin; km. 5-10) or the basement (eastern margin; km. 35-40). An intracrustal reflector is marked by orange dots (represented in Fig. 6.03). Same legend as figure 6.07. Location on Figure 6.01.

Unit V: Langhian to Lower Serravallian

Unit V, Langhian to lower Serravallian in age, is mostly characterized by high amplitude and continuous reflectors in its lower part. They become more discontinuous and less reflective in its upper part. This unit is the only one that shows clear syn-kinematic wedges, although they are scarce and observed only in the south-eastern part of the basin in the vicinity of High 976. Unit V onlaps the unconformity R5 and, in general, fills the paleorelief marked by this surface being only a paraconformity with Unit VI in the central and deepest parts of the basin (e.g. in km. 16-19 and km. 38-41 in Fig. 6.12). The uppermost reflectors of this unit terminate as a toplap in the margins of the basin and the top of unit V corresponds with the high-amplitude reflector R4.

The isopach map of figure 6.15 shows that unit V is observed in the deepest parts of the basin. It does not show continuity with the Neogene deposits on-land as its cut-off is observed along the entire Malaga Basin, with the exception of a small area

situated north of well And-G1. In addition there is no erosion observed on top of it. Two main depocenters of Unit V can be differentiated: a) a widespread one at the centre of the basin, roughly following its axis and with thicknesses around 1000 to 1300m; and b) a narrower one located south of well And-G1. Surprisingly, the highest thicknesses of unit V are observed in this second depocenter (1600m) and not in the basin axis. Furthermore, Unit V depocenter is interrupted by the mud diapirism and shows a significant thinning towards the westernmost part of the basin (west of mud diapirs) which contrasts with the thickening observed for unit VI in the same margin (compare Figs. 6.13 and 6.15).

The tectonic structures involved during the deposition of Unit V vary significantly along and across the basin. The south-eastern flank is controlled by a single major fault, or a system of two or more faults, which can be traced along High 976. The offset produced by these faults can be high as it is observed in seismic profiles (Figs. 6.07 and 6.14). Even though the total amount of displacement cannot be quantified, a minimum of 1,4 seconds (twtt) of vertical displacement can be estimated. The syn-kinematics of this fault with respect to unit V is established by the presence some sedimentary wedges drawn by this unit and by the sequence-stratigraphic analysis (See Chapter 5).

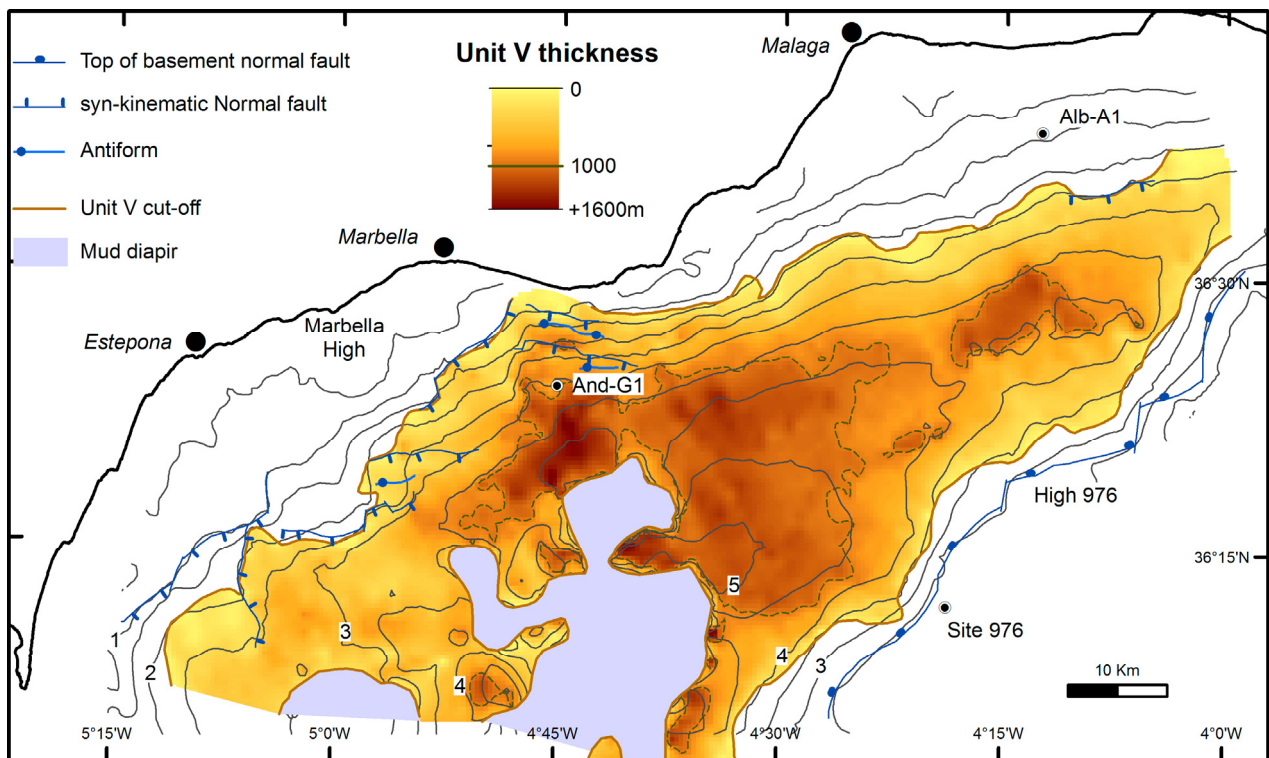


Figure 6.15: Isopach map of Unit V superposed with a contour map of the basement top (contour lines every 500msec.). Major tectonic structures that were active during Unit V deposition are also shown. Note the lack of erosion affecting this unit and the major depocenter situated south of And-G1 well.

6 Tectonic and sedimentary evolution of the northern WAB

The tectonic structures observed in the north-eastern flank are more complex. From this point of view, the basin can be differentiated between an eastern and a western part, with the limit between both situated around the 4° 30' meridian (Fig. 6.15). In the eastern part, the lack of tectonic structures affecting Unit V stands out and only one fault, with a small offset, is observed south of Alb-A1 well. In the western part of the basin (West of 4° 30' meridian), the northern flank contains a significant number of normal faults, syn-kinematic with respect to the deposition of unit V. North of And-G1 well a set of faults dipping S or SSW can be observed (Fig. 6.12; 2-8 km.) and are associated with roll-over antiforms. West of well And-G1 unit V is affected by faults dipping with an eastwards component even their directions vary significantly ranging from E-W to N-S (Fig. 6.15). Those faults show moderate offsets and can either delimitate significant variations on Unit V thickness or correspond with unit V cut-off. This argues for their syn-kinematic activity (e.g. Fig. 6.16, around shotpoint C1073).

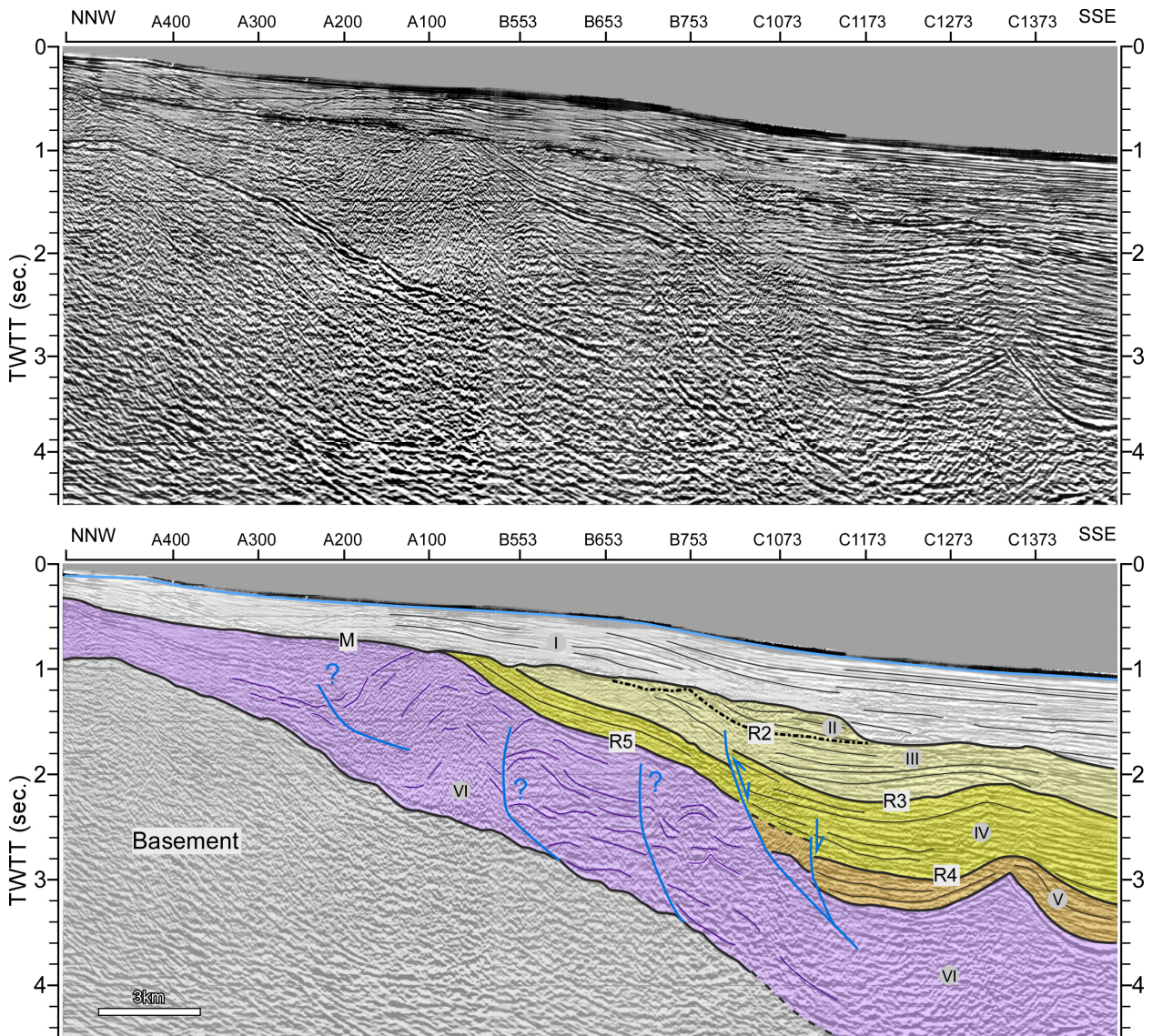


Figure 6.16: Seismic profile and its corresponding interpretation (Alb-015; location in Fig. 6.01). Note the inverted normal fault affecting reflector R3 (shotpoints B753-C1073). Possible faults of undetermined kinematics previous to Malaga Basin rift episode are also observed inside unit VI. Same legend as figure 6.07. Location on Figure 6.01.

Unit IV: Upper Serravallian to Lower Tortonian

Unit IV represents the last syn-rift deposits in the Malaga Basin (see also chapter 5). It is characterized by an alternation of discontinuous and low amplitude reflectors with high amplitude and continuous reflectors being these latter more common in the upper parts of the sequence. Unit IV lies mostly conformably over the R4 unconformity. Onlap terminations can be observed only in the basin margins. The onlap is weak on the north-western flank (and not always observed) while it is well marked on High 976 flank (e.g. Fig. 6.14, at Km39). The top of unit IV corresponds with the R3 unconformity, which is usually characterized by a relative high-amplitude and continuous reflector, especially in the eastern part of the basin (e.g. Fig. 6.14). Toplap

terminations of Unit IV reflectors can be observed, especially in the northern flank (Fig. 6.12 at Km12; Fig. 6.14 at Km15).

Concerning the thicknesses, Unit IV represents the second sedimentary accumulations in the Malaga Basin after Unit VI. The isopach map (Fig. 6.17) shows that it has a widespread depocenter that follows the main axis of the basin. From east to west there is an important thickening of this unit in the proximities of the mud diapirs, where thicknesses of up to 2100m are observed. By contrast, and similar with what is observed in Unit V, the thicknesses are much lower west of the mud diapirs (west of 4° 45' meridian) as they barely surpass 1100m of thickness. On the other hand, there is no important depocenter south of And-G1 which contrasts with Unit V isopach map (Fig. 6.15). Note that Unit IV, unlike Unit V, reaches the margins of the basin and is therefore moderately affected by Messinian erosion in the northern flank of the basin (e.g. Fig. 6.16, shotpoint B553).

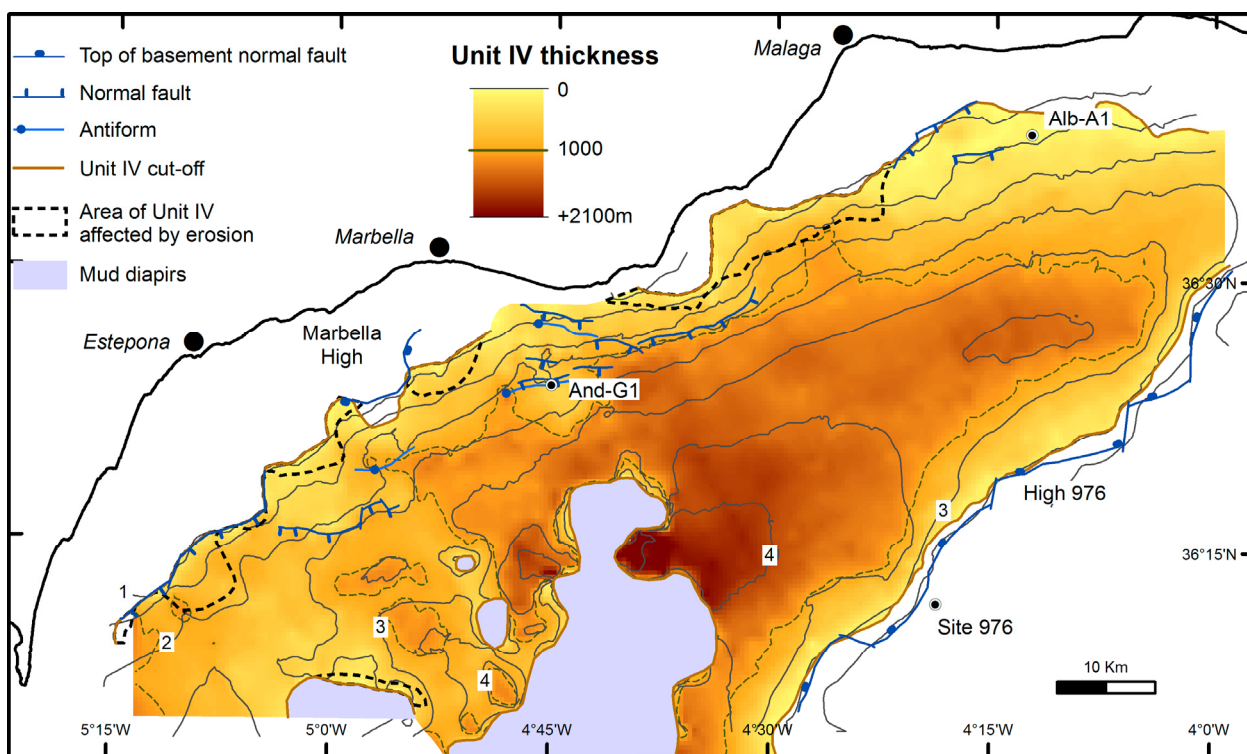


Figure 6.17: Isopach map of Unit IV superposed with a contour map of the basement top (contour lines every 500msec.). Major tectonic structures that were active during Unit IV deposition are also shown. Note that this unit has been partially eroded in the northwestern flank.

The distribution of faults active during unit IV deposition is similar with Unit V (compare Figs. 6.15 and 6.17). To the east, the southern flank is controlled by the High 976 basement faults; meanwhile scarce faults are present in the northern flank. To the west (west of 4° 30' meridian), the S to SSW dipping faults near And-G1 are still active (see Fig. 6.22, Km 8-11), including a new fault (situated northeast of And-G1) which dips towards the SE (see Fig. 8 from Chapter 5). Interestingly, west of And-G1, the

amount of active faults decreased with respect unit V and their directions are more homogeneous, clearly dominated by SE dipping faults (Fig. 6.17).

Units III and II: Upper Tortonian to Messinian

Unit III and II, Upper Tortonian to Messinian in age, are part of the post-rift sequence deposited during the tectonic inversion that occurred in the Alboran Domain. Meanwhile Unit II is a thin sequence, even absent in some areas, and characterized by high amplitude discontinuous reflectors which usually show a chaotic geometry, Unit III is thicker, more widespread, and shows variable seismic characteristics. Continuous and high amplitude reflectors with tabular geometry are mainly observed in the centre of the basin. Towards the basin margin less reflective and discontinuous reflectors are present.

Unit III is mainly congruent with R3 unconformity, although high angle onlaps can be observed in the northern flank of the basin (e.g. shotpoint C1073 in Fig. 6.16). Both unit II and III are truncated by the erosional surface that corresponds with the end of the Messinian. Only towards the South-eastern margin, approaching the High 976, this surface appears as a paraconformity (e.g. km. 50 in Fig. 6.12).

The isopach map (Fig. 6.18) shows how this post-rift sequence is distributed across and along the basin. In the eastern part of the basin there is a widespread NE-SW directed depocenter following the axis of the basin. The thicknesses in this area do not reach more than 1200m. By contrast, the major sedimentary accumulations are observed close to some mud diapirs where several depocenters can be observed with maximum thicknesses of 1300 to 1600m. North of the mud diapirs, another NE-SW directed depocenter can be observed. It starts 5km SSE of And-G1 well and extends towards the ESE. Finally, south of Marbella High it stands out the presence of a narrow depocenter where up to 1200m of sediments are observed.

The deposition of unit II and III is characterized by the cease on the activity of most of the extensional faults. In addition some of these previous extensional faults show tectonic inversion which is also accompanied by folding of the sedimentary infill. Even though, the isopach map reveals that these compressive features are observed only locally as most of the sedimentary cover remains unaffected and most of the normal faults are not reactivated (compare Figs. 6.17 with 6.18).

The set of faults that bounds the southern flank of the graben along High 976 shows minor inversion. The fault offset produced by this inversion is not observed but locally, the sedimentary cover is slightly folded (Fig. 6.07). Note that folding is mostly observed in unit IV beds while it is minor in unit III and plio-cuaternary deposits (Fig. 6.07, shotpoints 300 to 500).

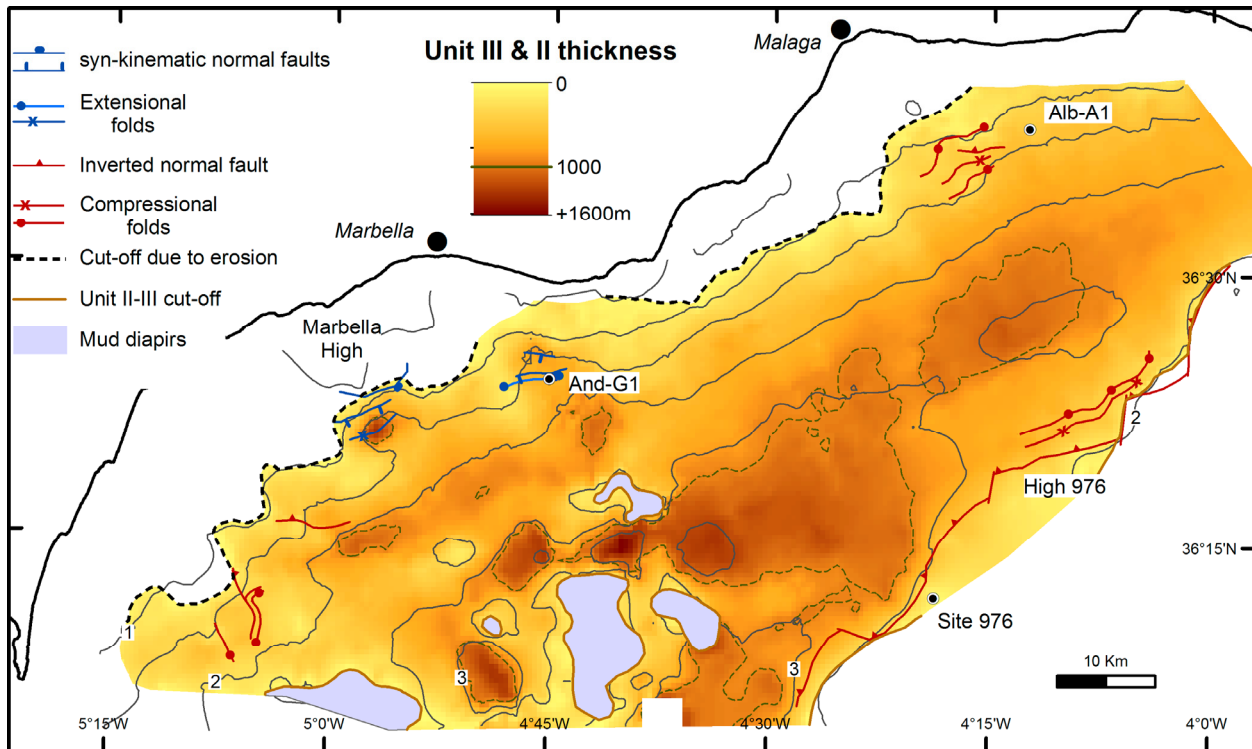


Figure 6.18: Isopach map of Unit III and II superposed with a contour map of the basement top (contour lines every 500msec.). Note that the distribution of these units is more widespread in comparison with units V and IV (Figs. 6.15 and 6.17). Major tectonic structures active during Unit III and II deposition are also shown. Most of these structures were reactivated in compression. Also note the significant erosion that occurred in the northwestern flank.

In the northern flank, folding of unit VI and III is observed west of Alb-A1 (Fig. 6.18 and profile of Fig. 6.14, Km. 3-9). The folds occur on top of inverted normal faults that affected unit VI and where active during unit V deposition (Fig. 6.15). Towards the west, SSE of Marbella High, two inverted normal faults are observed, with perpendicular directions, N-S and E-W. Their offset is very small as shown in the seismic profile of figure 6.16 (around 100msec. between shotpoints B753 and C1073). Note that, in this case, unit II deposits are not affected by the inverted fault as R2 unconformity seals it.

Despite the inverted structures, in the western part of the northern flank of the basin, a few extensional faults are still active during unit III deposition (Fig. 6.18). They are situated in two specific areas: a) next to And-G1 well, E-W directed faults with small offsets are observed (less than 100msec. Fig. 6.12, Km 3-7). b) south of Marbella High, the basement fault was still active as shown by the divergent geometry drawn by unit III beds (Fig. 6.08, around shotpoint A600). It also results in a thickening of unit III towards the fault, as observed in the isopach map (Fig. 6.18). This is indicative of an important offset during deposition, even it cannot be quantified.

6.3) Tectonic evolution of the Malaga Basin

The characterization of both the Miocene sedimentary sequence and the top of the basement surface provides new insights on the tectonic evolution of the Malaga Basin, which is characterized broadly by a rifting event that last approximately from 20Ma to 9Ma, and by a contractive reorganization from 9Ma onwards (Comas *et al.*, 1999).

The tectonic events that took place in Malaga Basin are summarized in the tectonic chart of figure 6.19. Note that given the differences observed between the sedimentation of Units IV and V and of Unit VI, the rifting event has been subdivided into two different episodes: a oldest one named “Main extensional event”, and the younger one considered as the “Malaga Basin rift episode”. Meanwhile the first one correspond to the Alboran Domain main exhumation, the second one corresponds with the opening of the Malaga Basin as a half-graben.

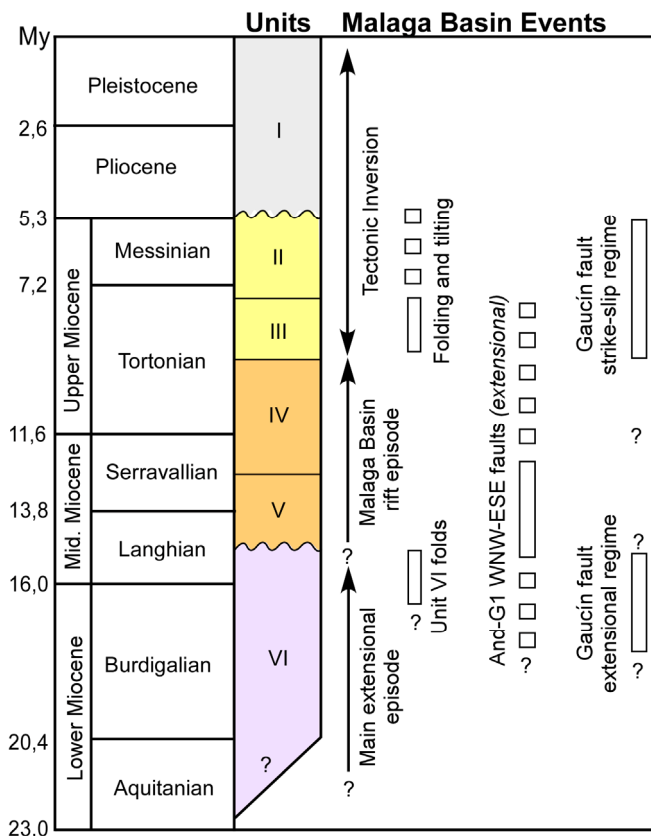


Figure 6.19: Tectonic chart of the Malaga Basin and seismic units. Black arrows indicate the time span of the main tectonic episodes. White rectangles indicate the time span of specific structures present in the basin.

Main extensional episode: Burdigalian to Langhian (Unit VI)

This stage corresponds to unit VI deposition and predates unit V. It is not well constrained due to the chaotic geometry of its reflectors. Nevertheless, the seismic interpretation and the isopach analysis reveal that unit VI was deposited in a very different setting, in terms of sedimentary environment, than the rest of the Miocene sequence.

Indeed, its reflectors geometry is characteristic of an energetic environment. This is in agreement with the reports of the wells which define Unit VI as an olistostrome characterized by blocks of several lithologies embedded in a muddy matrix (Jurado and Comas, 1992). In addition, the log correlation proposed in this work implies that this stage would extend up to Langhian times (fig. 6.19). It also shows that the latter stages of unit VI were dominated by finer grained deposits (Unit Vb description of Jurado and Comas, 1992) which suggest a progressive transition towards less energetic deposition during Langhian times. It must be stressed that Unit VI extends further to the NE outside the Malaga Basin *sensu stricto*, towards the onshore Malaga Basin (Fig. 6.14) and towards Estepona (Fig. 6.16). As consequence, Unit VI was deposited in a much wider basin than the observed nowadays, which extended towards the NE.

The SE wards dipping intracrustal reflectors observed near Marbella High and Mijas plateau (Fig. 6.03) could be associated with low-angle normal faults described onshore, where a transport direction towards the SE or SSE has been described by García-Dueñas *et al.* (1992). In the same way, the top of the basement surface could also correspond to one of these low-angle detachments as claimed by Comas *et al.* (1992; 1999) or Martínez del Olmo and Comas (2008). Nevertheless, the lack of a coherent internal structure of Unit VI reflectors does not permit to confirm (or refute) this interpretation.

Along the northern flank, the relatively flat areas drawn by the top of the basement coincide with the position of significant depocenters of unit VI (Mijas plateau, SE of Marbella, and SE of Estepona; Fig. 6.13). These flat areas are delimited by WNW-ESE directed escarpments (with the exception of Mijas plateau whose margin is outside the seismic grid; Fig. 6.04). In the contour map of R5 unconformity (Fig. 6.15) the flat areas disappear, as well as the WNW-ESE escarpments, with the exception of that situated north of And-G1 well. This is indicative that the processes that controlled the presence of these flat areas probably also controlled the deposition of unit VI during the early rift stage. It must be stressed that the SSW dipping intracrustal reflectors with high-angle dip (Fig. 6.03; estimated dip between 60° and 75°) are sub-parallel with the escarpments marked by the top of the basement which bound these areas (compare Figs. 6.03 and 6.04). It suggests that the two WNW-ESE directed intracrustal reflectors correspond to normal faults that produced extension towards the SSW during this stage (And-G1 and Gaucín faults in Fig. 6.19). If that is the case, these faults have to be

younger than the NE-SW intracrustal reflectors producing extension towards the SE-SSE since those high angle reflectors crosscut the low angle ones (e.g. Fig. 6.05, at 3 seconds depth near shotpoint B2368).

Special attention has to be paid to the westernmost one of these two faults. Given its direction and position, the described fault can be correlated onshore towards the Gaucín fault: a previously described NW-SE directed major fault (Fig. 6.23; Balanyá, 1991; Balanyá *et al.*, 2007; Balanyá *et al.*, 2014). The Gaucín fault is a sinistral fault that has transpressive kinematics in its westernmost parts, while becomes transtensional towards the east with its hanging-wall situated in the SW (Balanyá *et al.*, 2014). In the easternmost part, near Estepona village, a displacement of 3 km and a vertical offset of 1,6km have been estimated (*op cit.*). The normal movement produced that Lower Miocene deposits (LaJOC deposits) are in contact with lower Alpujarride units (Balanyá *et al.*, 2014). All these features indicate that the WNW-ESE directed fault is the prolongation of the Gaucín fault offshore. Even though the sinistral component is not observed during this stage, the extensional component is in agreement with the kinematics observed offshore. Indeed, a significant vertical slip is inferred as the difference of the top-basement depth at both flanks of the fault exceeds 1.5 sec twtt (Fig. 6.05).

During the latter stages of the early rift episode, in the westernmost margin of the basin folds drawn by unit VI and the basement surface suggest compression (folds situated South of Estepona in Fig. 6.13; unit VI folds in Fig. 6.19). This compression was restricted to this margin of the basin as extension was taking place coetaneous in most of the areas of the Malaga Basin. In the profiles where these folds have been observed (e.g. Fig. 6.09) it stands out the presence of intrabasement surfaces dipping towards the centre of the basin. They could be thrusts which would explain the presence of these folds and also would be in agreement with the SE dipping structures observed inside unit VI in figure 6.16, which could be compressive in nature.

The restricted nature of these compressive structures, only observed in the westernmost end of the basin, suggests that they could be related with the folding and thrusting observed in the Flysch Trough complex which outcrops onshore. As a matter of fact, scattered NNE-SSW oriented thrust, dipping towards the east, are observed along the coast from Gibraltar to Estepona (García de Domingo, A *et al.* 1994; Balanyá *et al.*, 2007) coinciding with the direction of the folds observed offshore. In addition, thrusting of the Flysch Trough complex occurred after Burdigalian times (Luján *et al.*, 2006) which is in accordance with the age of unit VI (Burdigalian to Langhian).

Malaga Basin rift episode: Langhian to early Tortonian (Units V and IV)

For the Malaga Basin, the main rift stage occurred during the sedimentation of units V and IV, which is from Langhian to early Tortonian (Fig. 6.19). It is characterized by a change in the depositional environment as well as the extensional processes that controlled the formation of the Malaga Basin. This is deduced from the differences between the depocenter geometry of unit VI and units IV-V (compare Fig. 6.13 with Figs. 6.15 and 6.17) and also from the sharp contrast in terms of seismic reflectors geometry.

Regarding this rifting episode, extension in the Malaga Basin was considered by Comas *et al.*, (1999) to be produced also by SE dipping low-angle detachments situated at the northern flank, which would correspond with both the intracrustal reflectors and the top of the basement surface. Nevertheless, the sequence stratigraphic analysis done in the eastern part of the basin (chapter 5) already revealed that the opening of the Malaga Basin during this period results in a half-graben geometry controlled by the High 976 fault system dipping towards the NW. Indeed, the distribution of units IV and V thicknesses in the north-eastern part of the basin show a sedimentary wedge produced in response of the activity of High 976 fault system (Fig. 6.14).

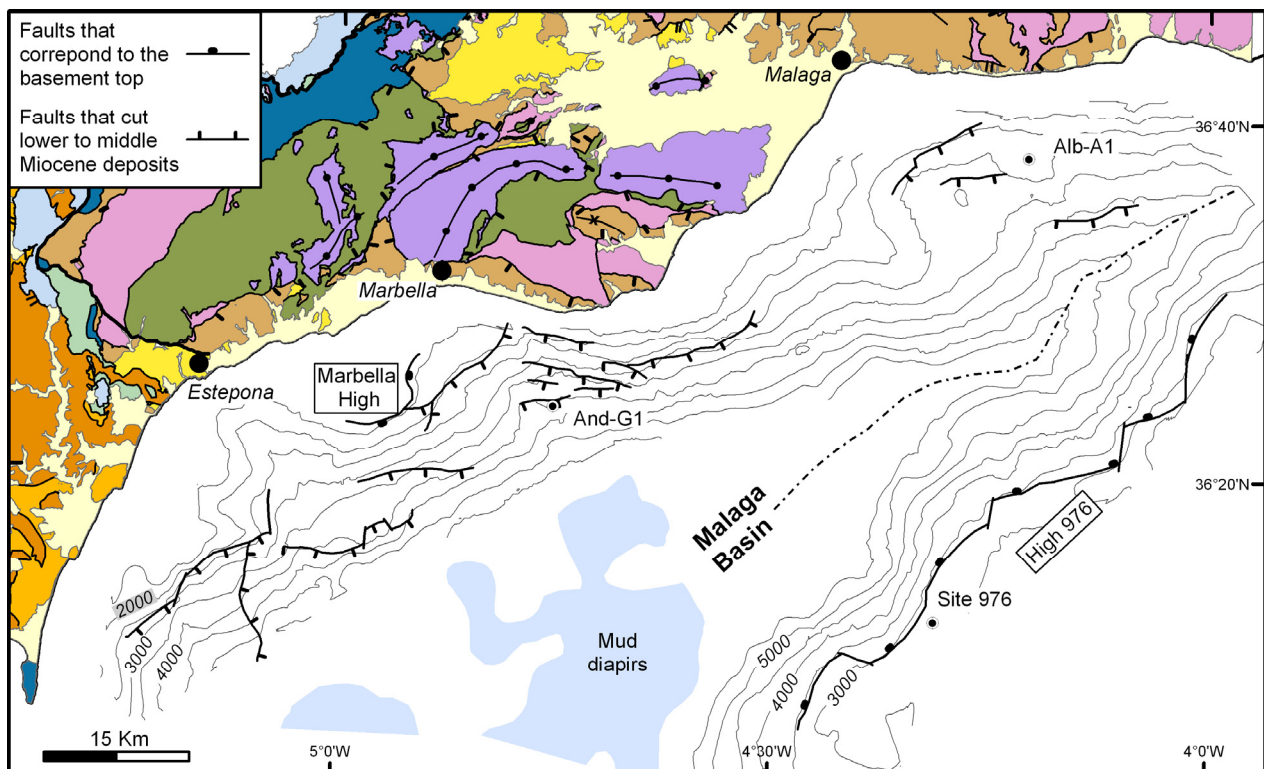


Figure 6.20: Structural map of the Malaga Basin during the Malaga Basin rift episode with a contour map of the basement top (contour lines every 500msec.). An onshore map of the Malaga area is also shown (same legend as figure 6.03). The major fault that corresponds with the basement top is situated at the southern flank of the basin.

In the western part of the basin the interpretation is less straight forward as the basin is wider, deeper, and no profiles are available that permit to interpret the whole basin from one flank to the other. Nevertheless, note that north of mud diapirs (south east of And-G1 well) there is a depocenter associated to the WNW-ESE directed faults but, towards the west, the thicknesses of units IV and V are always lower in comparison to the south-eastern part of the basin (Figs. 6.15 and 6.17) which points towards a thickening of the sedimentary sequence towards the High 976. It is true that, in the northern flank, the sedimentary cover was affected by normal faults (Fig. 6.20) but, it is interesting to note that most of them have small offsets (less than 200msec; see Figs. 6.12, 6.14 and 6.22). Additionally, these faults are mostly rooted in Unit VI or on top of the basement surface. In consequence, they do not contribute to the extension of the basement and the opening of the Malaga Basin but only to the movement of the sedimentary cover towards the centre of the basin. In particular they are most likely produced by the migration of the shale from unit VI down-dip towards the basin centre during the growing of the mud diapirs. Nevertheless, it cannot be discarded that some faults crosscutting the basement could exist below the seismic resolution.

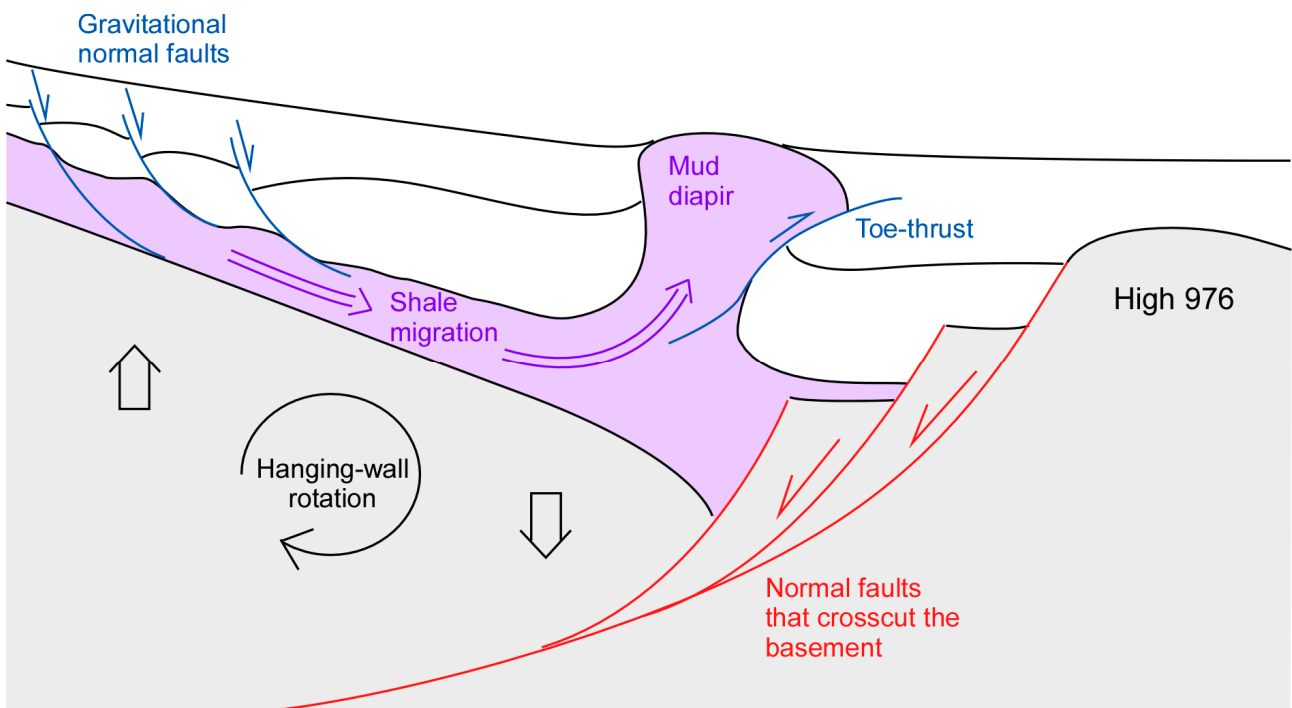


Figure 6.21: Scheme illustrating the relationship between rift-related extension, block rotation, shale migrating, and diapirism in the Malaga Basin. Red faults affect the basement and contribute to the opening of the basin. Blue faults that affect the sedimentary cover are detached in Unit VI and are produced by shale migration. The continuous rotation of the hanging-wall block increases the slope of the margin which produces the shale to migrate by gravity towards the centre of the basin where diapirs are formed.

This process is similar to that observed in passive margins where normal faulting is related with the gravitational migration of shale or salt and the associated diapirism (Morley and Guerin, 1996; Rowan *et al.*, 2004; Krézsek and Bally, 2006; Cartwright *et al.*, 2012). In our case study, Unit VI corresponds with the décollement level and is illustrated in the scheme of figure 6.21. Extension produced by the normal faults which affected the sedimentary cover in the basin margin is thought to be accommodated through mud diapirs toe-thrusts, in the basin centre. These toe-thrust in the mud diapirs has been described by Soto *et al.* (2010) which already pointed out the relationship between basement dip and downdip shale migration. The geometry of the fault system described in the southern flank (Chapter 5), and illustrated in figure 6.21, implies a progressive rotation and tilting of the basement surface in the northern flank. This continuous increase in dip could have triggered the migration of shale towards the basin centre. This interpretation is coherent with the presence of important depocenters of unit VI over the flat areas situated East and west of Marbella high (Fig. 6.13) as lower dips would have prevented the migration of shale and retained unit VI sediments over the margin of the basin. This interpretation implies that the opening of the Malaga Basin most likely did not occur through faulting in the northern flank which is congruent with what is observed in the eastern part of the basin.

Some particularities need to be taken in consideration regarding the faults near And-G1 with a WNW-ESE to E-W direction and that show a similar direction as both, the basement escarpments, and the intracrustal reflectors with high dip (Figs 6.03 and 6.20). The seismic profile of figure 6.22 crosscuts these faults in a slightly oblique direction. Despite that the major faults, syn-kinematic with unit V and IV deposition, do not seem to penetrate within the basement, the irregular shape of the top of the basement points to the presence of some faults crosscutting it with a WNW-ESE direction (Fig. 6.22). This set of faults must have been active, at least, during the Malaga Basin rift episode and have produced extension towards the SSW (Fig. 6.19). The increase of unit V thickness observed south of these faults (Fig. 6.15; south of And-G1 well) reveals that extension was relevant during Langhian to serravallian times. By contrast, Unit IV does not show any increase in thickness in this area (Fig. 6.17) pointing that the extension produced by this set of faults diminished during the late stages of the rift.

On the other hand, in the contour map of unit V (Fig. 6.15), the top of unit V (R4) do not mimic the depression drawn by the basement top near Gaucín fault. This would indicate that R4 surface has not been later affected by the SW directed extension, and that the Gaucín fault was not active during the Malaga Basin rift episode (Fig. 6.19).

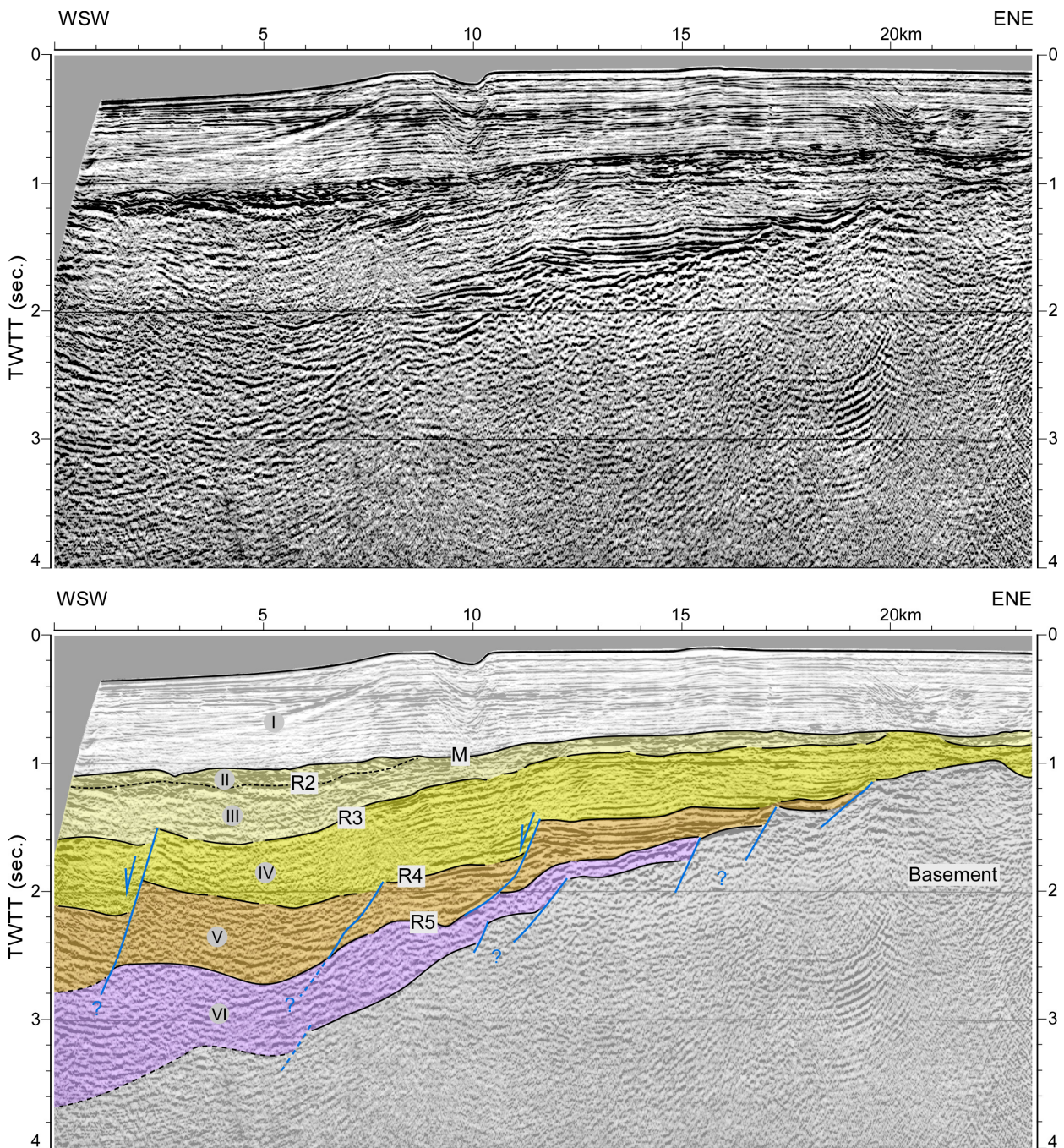


Figure 6.22: Seismic profile crossing a WNW-ESE directed scarp near well And-G1 (Fig. 6.04) and its corresponding interpretation (AM-303; location in Fig. 6.01). Note that the scarp is affected by faults that crosscut the top of the basement surface. Also note that faults are oblique with respect to the seismic profile. Same legend as figure 6.07. Location on Figure 6.01.

Post-rift stage: Late Tortonian to recent

From late Tortonian onwards the tectonics of the Malaga Basin is encompassed by the end of the Alboran Domain back-arc extension and the start of the tectonic inversion due to the continuous NW-SE convergence between Africa and Eurasia from 9Ma onwards (Mazzoli & Helman, 1994; Pedrera *et al.*, 2011). Despite the tectonic

inversion is notorious in others parts of the Alboran Basin (see Comas *et al.*, 1999; Ballesteros *et al.*, 2008; Martínez-García *et al.*, 2011; 2013), in the Malaga Basin the reflector geometries are that of a passive margin infill and most of the sedimentary cover is unaffected by this inversion (e.g. reflectors of unit III to I in Figs. 6.12 and 6.14; see also chapter 5). It is only towards the margin of the basin where some inversion of the previous architecture can be observed. This is the case of High 976 fault system (Fig. 6.18) where folding of the sedimentary cover (Fig. 6.07 between shotpoints 300 and 400; Fig. 6.14 at Km 38) reveals the inversion of the previous normal faults, although weak. This inversion also accommodated the reactivation of the mud diapirism as previously described (Talukder *et al.*, 2004; Comas *et al.*, 2012). This latter process is also observed locally outside the mud diapir province, west of Alb-A1, where reflectors of unit III are slightly folded due to the reactivation of previous normal faults rooted in unit VI or on top of the basement surface (Figs. 6.14). It is noticeable that during this period of tectonic inversion, the WNW-ESE directed normal faults near the And-G1 affect the R3 reflector (Fig. 6.22) which indicates that they are still related to extension (Fig. 6.19).

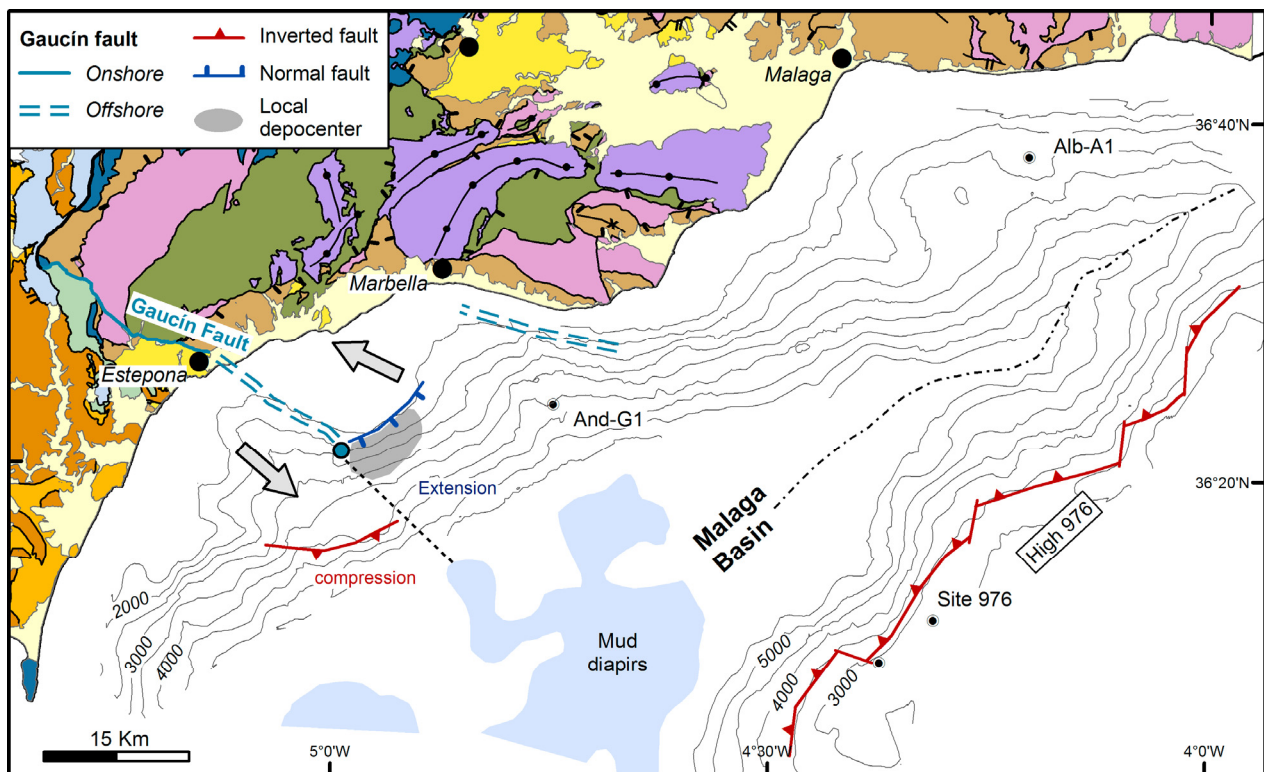


Figure 6.23: Structural scheme of the Malaga Basin during the post rift stage accompanied with a contour map of the basement top (contour lines every 500msec.). An onshore map of the malaga area is also shown (same legend as figure 6.03). The Gaucin Fault is correlated offshore. Beyond the fault tip (blue dot), extensional and compressional structures are developed due to the sinistral motion of the fault.

It must be stressed that the coexistence of both extensional and compressive structures in the basin is coherent with the stress field resulted from overall NW-SE convergence

between Africa and Eurasia. Indeed, an inversion of NE-SW directed faults is expected while the WNW-ESE structures acted as normal faults.

In addition, there are some tectonic structures observed south and southwest of Marbella High that are a response of a local phenomenon and must be analysed separately. Indeed, in this part of the basin, the NE-SW normal faults that produce the formation of a local depocenter (Fig. 6.18, south-east of Marbella High) is not congruent with the regional stress field. Additionally, just southeast of this feature, inversion of normal faults affecting the sedimentary cover is observed. (E-W and N-S directed faults; Fig. 6.18). The presence of these structures (normal and reverse faults) in this margin of the basin can be explained as a response of a sinistral motion of Gaucín fault. First, the termination of the WSW-ESE escarpment is considered as the fault tip of the Gaucín fault (blue point in Fig. 6.23). Consequently, two half-planes can be defined according to the movement of two blocks separated by the fault (Fig. 6.23): one under compressional stress (SW), and one under extensional stress (NE).

Indeed, the strike-slip displacement produced in the south-western half-plane is accommodated by folding and reactivation in compression of previous normal faults (Figs. 6.16 and 6.23). On the other side, in the north-eastern half-plane, the movement is accommodated by normal faults situated at the top of Marbella High (Figs. 6.08 and 6.23). Note that the displacement associated to this strike-slip motion is small as the vertical offset of reverse fault in the compressive quadrant does not exceed the 200msec. (Fig. 6.16), while the extensional faults only produce a local thickening of unit III up to 700m (Figs. 6.18 and 6.24). These features indicate that, even though the Gaucín fault started as a normal fault during the early rift episode, it became mainly directional during the post-rift stage, probably due to the tectonic inversion of the Alboran Basin. The seismic profiles show that the Gaucín fault strike-slip motion took place during Upper tortonian and maybe messinian times (Fig. 6.19) but ceased after Miocene as unit I is unaffected (Figs. 6.05, 6.08 and 6.16). This is fairly in agreement with onshore studies which suggest that the Gaucín fault could have been active until upper Miocene or Pliocene times (Balanyá *et al.*, 2014).

The kinematics deduced for the prolongation offshore of Gaucín fault permit a better understanding of the post-rift tectonic evolution of the Malaga Basin. Overall, the basin was characterized by a deformation partitioning with little amount of tectonically inverted structures which was accompanied by transtensional structures with a WNW-ESE and NW-SE direction.

6 Tectonic and sedimentary evolution of the northern WAB

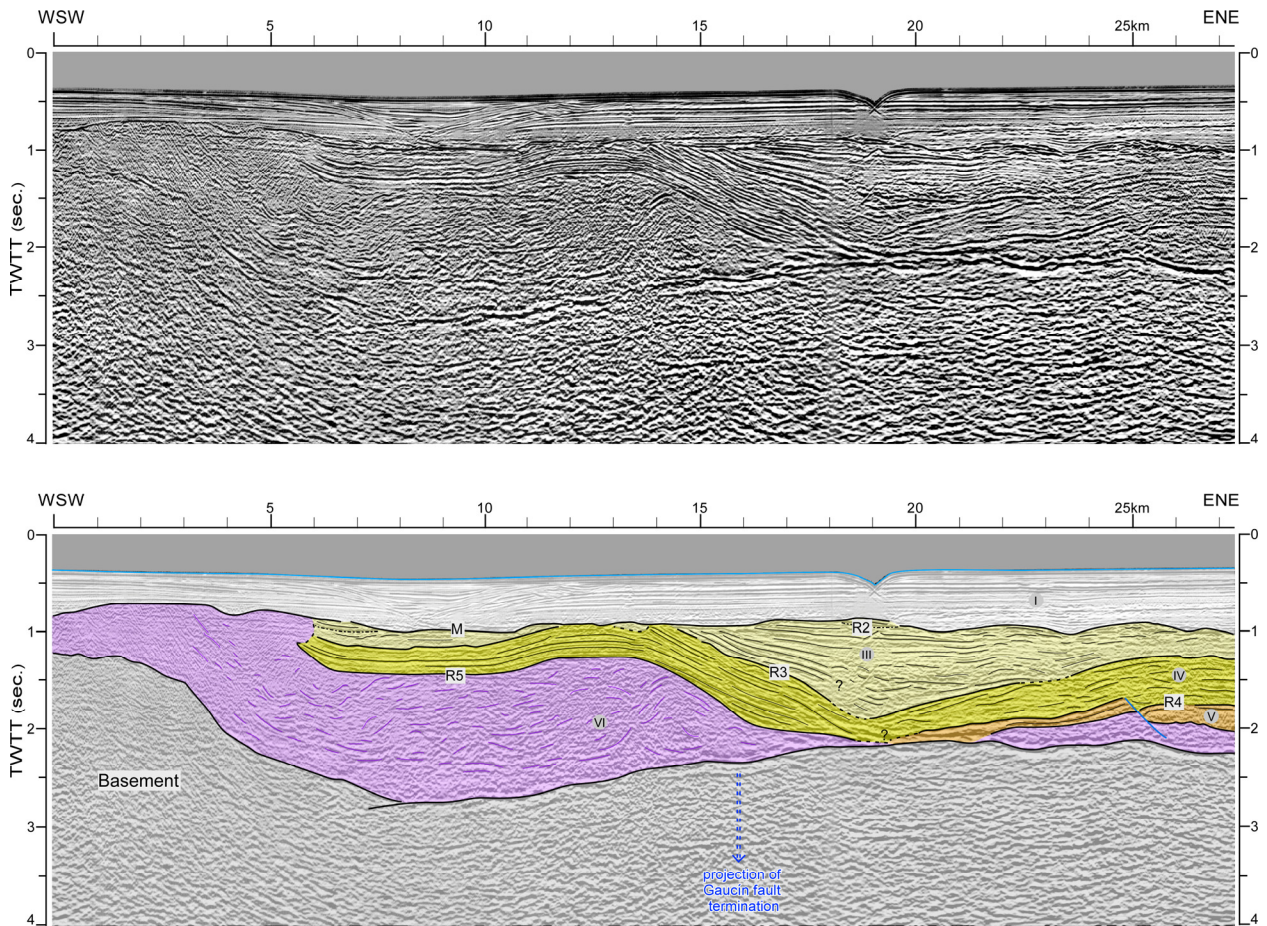


Figure 6.24: Seismic profile oriented along the northwestern flank of the basin and its corresponding interpretation (Alb-006; location in Fig. 6.01). The position of the Gaucin Fault is projected. It can be noticed the local depocenter formed East of the fault in contrast with folding of the sedimentary cover West of the fault. Same legend as figure 6.07. Location on Figure 6.01.

7 Discussion

7.1) Introduction

This chapter integrates all the studies previously presented in this volume (Chapters 4, 5 and 6) and focuses on the onshore-offshore correlations. In the first part of the chapter (epigraph 7.2) we will discuss the tectonic evolution of the Alboran Domain in the studied area, that is: in the western part of the Alboran Domain of the northern branch of the Gibraltar Arc. The second part of the chapter (epigraph 7.3) tries to compare the most important observations of this study with what is observed in other areas of the Alboran Domain and their fitting with the available geodynamic models of the Gibraltar arc.

It must be stressed that the publications presented in chapter 4 were done previously to the offshore studies that correspond to chapters 5 and 6. Since, the offshore studies have provided new insights on the tectonic evolution of the area, and especially on the relationship between Miocene sediments and tectonic activity, some of the open questions in chapter 4 are now addressed.

7.2) Offshore-onshore correlations and tectonic evolution

The tectonic evolution of the area studied in this PhD. thesis corresponds with the Alboran Domain extensional evolution, and the subsequent tectonic inversion that occurred from Miocene times onwards in the northern branch of the western Gibraltar Arc (west of 4°30'W meridian). This area has specific structural features in comparison with the rest of the northern branch situated further to the east (Balanyá *et al.*, 2007; Balanyá *et al.*, 2012). In order to better understand its tectonic evolution it is important to integrate the study done in this thesis, which focuses on the Miocene sediments present offshore and onshore, and the previous knowledge on the tectonics that affected the metamorphic complexes of the Alboran Domain. In addition, it is also necessary to take in to consideration some aspects of the tectonic evolution of the external zones as the development of the fold-and-thrust belt in this area was partially coetaneous with the crustal extension of the Alboran Domain. Accordingly, the main objective of this chapter is to correlate events observed onshore and offshore to get a wider picture of the geodynamic evolution of the studied area.

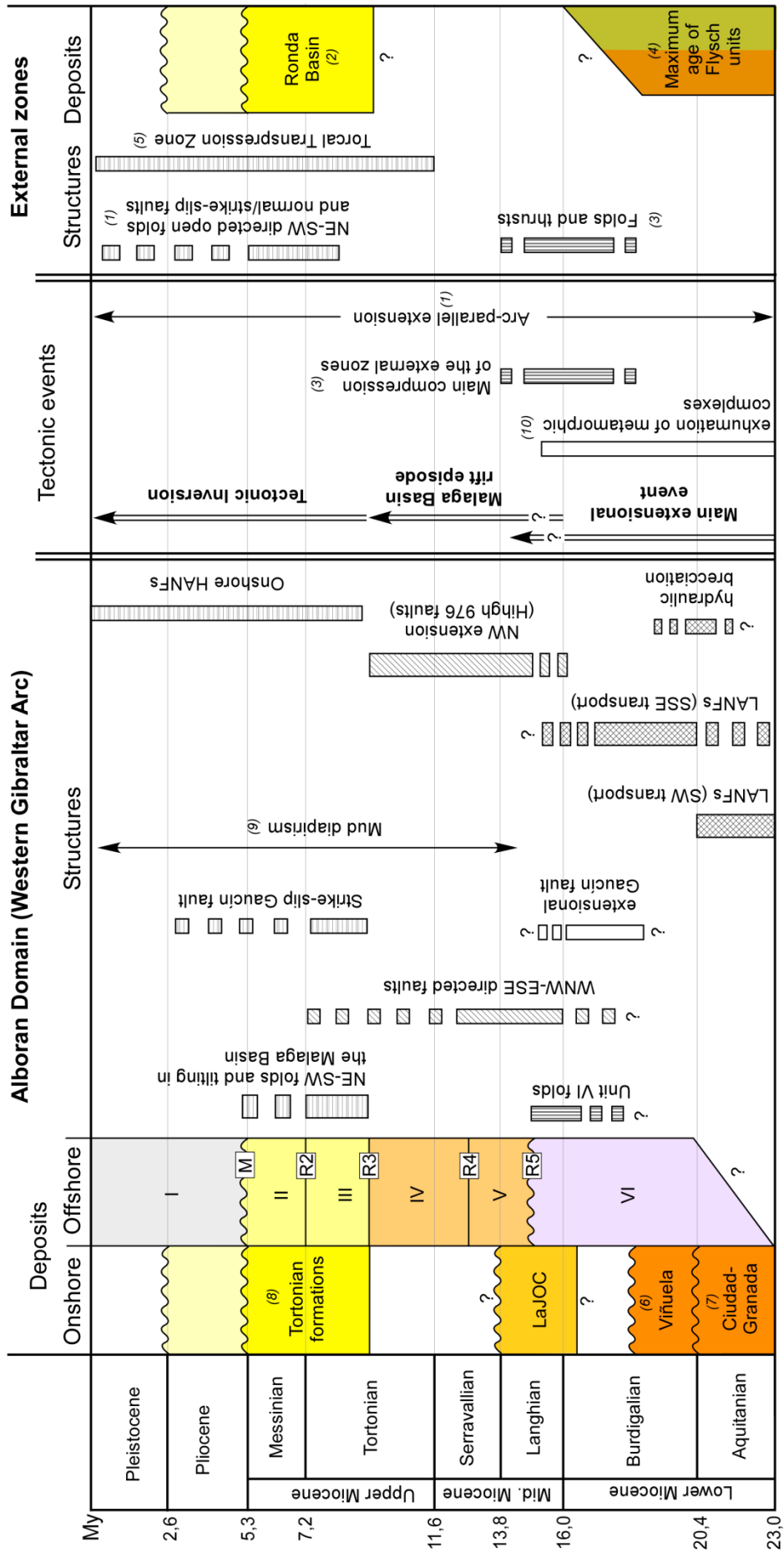
The onshore-offshore correlations have been carried out through the chronology of the sedimentary record together with the tectonic structures and processes that took place in the studied area. This is summarized in the chronostratigraphic chart of figure 7.01. Some of the events and structures represented are results of this PhD. thesis and others of publication of previous authors. The control of all these factors permitted to characterize three main episodes in the studied area (Fig. 7.01). Within the Miocene extensional event two extensional episodes have been differentiated. The first one

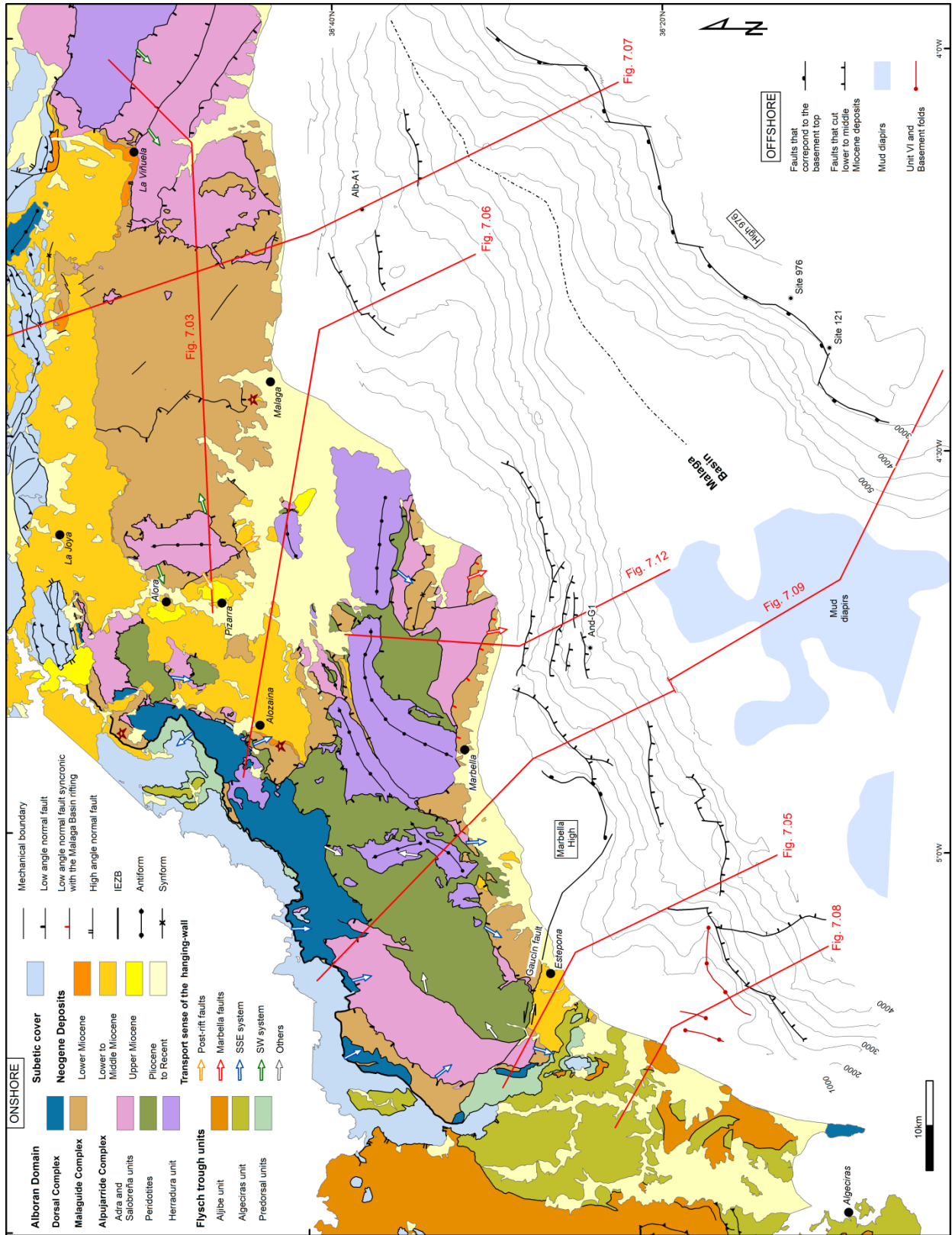
(Aquitanian to Langhian) corresponds with the thinning and main exhumation of the Alboran Domain hinterland through extensional detachment systems. The second episode (Langhian to lower Tortonian) corresponds with the formation of the Malaga Basin. These two extensional episodes were followed by a third event (upper Tortonian to recent times) that corresponds with the tectonic inversion described in the whole Alboran Domain. These three milestones of the western Gibraltar Arc history and the processes that took place within them are described in detail in the next epigraphs.

Regarding the onshore-offshore correlations, it must be stressed that a direct correlation of the offshore seismic units (Units VI to I) with the onshore sediments present several problems. First, neither seismic profiles nor wells were made onshore. This would be the most reliable way for an onshore-offshore correlation with the seismic profiles from the Malaga Basin. Second, the sedimentary cover is highly eroded and most of the outcropping area corresponds with the metamorphic complexes of the Alboran Domain which in turn corresponds with the acoustic basement in the seismic profiles. Despite these limitations, some reliable correlations can be done by comparing the age and the stratigraphical similarities of the offshore seismic units with the deposits that outcrop onshore. As it is shown, the offshore register in the Alboran Domain is fairly continuous while the onshore counterpart (partially described in chapter 4) contains significant hiatus and erosional unconformities. The most noticeable difference is the absence of Serravallian to lower Tortonian sediments in the onshore area.

In order to strengthen the correlations between deposits, a series of onshore-offshore cross-section has been done. Their location is shown in the map of figure 7.02. These cross-sections also permit to correlate some of the tectonic structures, even though these correlations are not always well constrained. The onshore-offshore cross-sections have been done by combining the interpretation of seismic profiles and onshore cross-sections. The seismic profiles have been roughly converted at depth assuming an average p-wave velocity of 2500m/s. The onshore cross-sections have been interpreted from the available Geological Maps (IGME) and also by taking in consideration previous publications done in the area. Note that each cross-section shows an interpolated area between the end of the seismic profile offshore and the coastline (semi-opaque area in the cross-sections; e.g. Fig. 7.05).

Figure 7.01: (next page) Tectono-stratigraphic chart showing the onshore/offshore deposits, the tectonic structures, and the main events that took place during Miocene to recent times in the studied area (Western Alboran Domain) and in the External zones. Onshore deposits are filled with the same colour as the map of Fig. 7.02. Data taken from: 1) Balanyá et al. (2012) and reference therein, 2) Serrano (1979), Rodríguez-Fernández et al. (1999) 3) Crespo-Blanc and Frizon de la motte (2006) and reference therein, 4) Lujan et al. (2006) and reference therein; De Capoa et al. (2007), 5) Barcos et al. (2011), 6-7) Serrano et al. (2007) and reference therein; 8) López-Garrido and Sanz de Galdeano (1991), Serrano (1979); 9) Talukder et al. (2003); Soto et al. (2010), 10) Zeck et al. (1992), Monié et al. (1994); Platt et al. (2003).





7.2.1) Main extensional event (Aquitanian-Lower(?) Langhian)

The main extensional episode in the Alboran Domain, which outcrops in the studied area, started before Miocene times and lasted up to Langhian times (Fig. 7.01). Coetaneously in the external zones, and until Burdigalian times, the youngest sediments which belong to the Flysch units were deposited while, from upper Burdigalian to Serravallian times, the main shortening of the external zones took place forming the western Subbetic fold and thrust belt (Fig. 7.01; Vera, 2000; Crespo-Blanc and Campos, 2001; Crespo-Blanc and Frizon de Lamotte, 2006; Luján *et al.*, 2006).

Over the Alboran Domain, sedimentation took place at the same time and is represented by the deposits of Ciudad-Granada Group, Viñuela Group, the LaJOC, and the offshore Unit VI. The extensional structures of this period were mostly the LANF's (low angle normal faults) that are observed onshore and bound the metamorphic complexes (Fig. 7.02). They lead to the exhumation of medium to high pressure metamorphic rocks of the middle Alpujarride units (García-Dueñas *et al.*, 1992; Balanyá *et al.*, 1997; Booth-Rea *et al.*, 2003). Different sets of LANF's were described in the Alboran Domain which outcrop in the study area and they show an interference pattern produced by several directions of extension (Fig. 7.02; Balanyá, 1991; Soto and Gervilla, 1991; García-Dueñas *et al.*, 1992; Alonso-Chaves and Orozco, 1998; Booth-Rea *et al.*, 2003). These sets of faults have different ages but two clear sets were active during this period: one that shows transport direction towards the SW, observed north of Malaga City (Fig. 7.02), and a second one with transport towards the SSE, observed west of Malaga city (e.g. the main detachment that limits the internal and the external zones; Fig. 7.02). The geometry of the LANF's can be observed in figure 7.03 where it can be observe their very low angle in comparison with most modern faults (blue fault in figure 7.03).

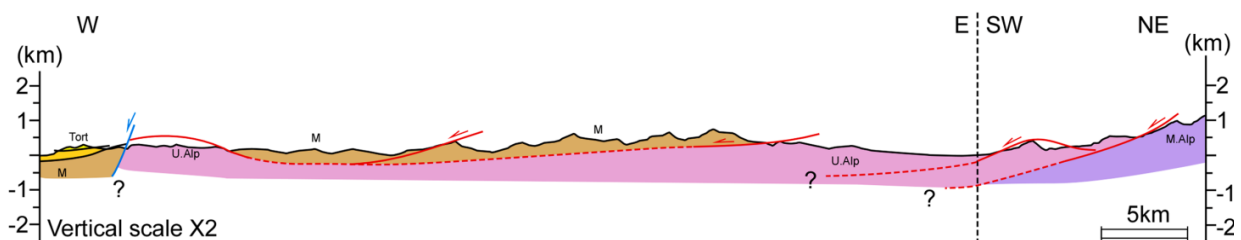


Figure 7.03: Cross-section (location in Fig. 7.02) showing the geometry of the SW directed LANF system (red lines). A post-extensional fault marked in blue. The interpretation has been done according to previous data from Booth-Rea *et al.* (2003), Alonso-Chavez *et al.* (1993), and various Spanish geological maps (MAGNA's). Legend: U.Alp: Upper Alpujarrides; M.Alp: Middle Alpujarrides; M: Malaguides; Tort: Tortonian formations. Colours are according to legend of Fig. 7.02.

Figure 7.02: (previous page) Onshore: geological map of the Malaga area. Kinematic indicators of normal faults according to Soto and Gervilla (1991), García-Dueñas *et al.* (1992), Alonso-Chaves and Orozco (1998), Booth-Rea *et al.* (2003). Offshore: structural scheme of the Malaga Basin during the second extensional episode accompanied with a contour map of the basement top (contour lines every 500msec.). Red lines show the location of Onshore-offshore profiles. The red stars locate the outcrops of Ciudad-Granada group deposits (Aquitanian).

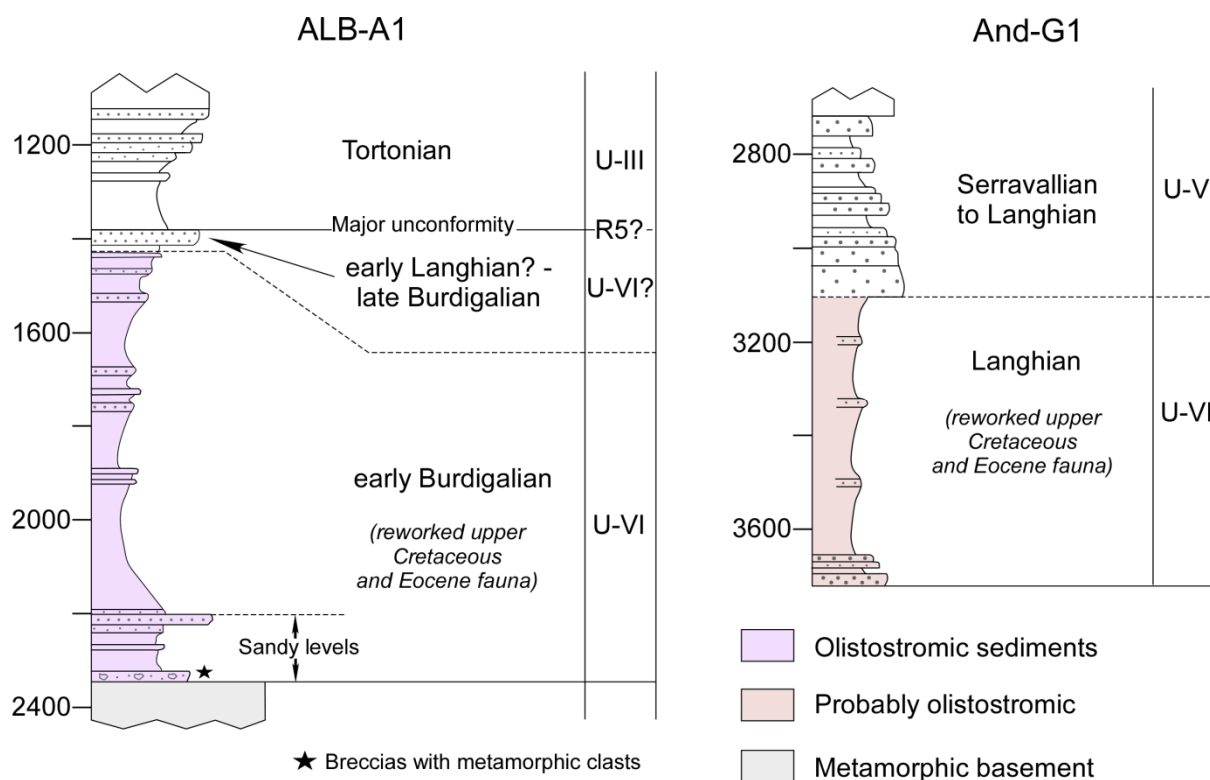


Figure 7.04: Simplified chrono-stratigraphic reports from wells (Alb-A1 and And-G1) and correlations with seismic units proposed in this PhD thesis. Stratigraphic columns according to Díaz Merino et al. (2003).

It must be stressed that the age of these LANF's was considered to extend up to Serravallian times by previous authors (García-Dueñas *et al.*, 1992) based on an extrapolation from observations further to the east. Indeed, in the central Betics there is a better time constraint as syn-kinematic deposits are well exposed (García-Dueñas *et al.*, 1992; Crespo-Blanc, 1995; Martínez-Martínez and Azañón, 1997). Nevertheless, in the studied area, the LANF's are sealed by the Langhian deposits of the LaJOC onshore (see chapter 4) and the seismic unit VI offshore (Burdigalian to Langhian) as it will be shown below. This age is also supported by several isotopic chronometers (K-Ar, Ar/Ar, U-Pb, Rb-Sr, among others) in the Alpujarride Complex that indicate uplift and exhumation between 22 to 15Ma (Zeck *et al.*, 1992; Monié *et al.*, 1994; Platt *et al.*, 2003).

Several periods can be differentiated within this main Alboran Domain exhumation event: Aquitanian, Lower (?) Burdigalian and Upper Burdigalian – lower (?) Langhian.

Aquitanian (deposits of Ciudad-Granada Group)

During Aquitanian times the main tectonic process that took place in the studied area was the crustal thinning of the Alboran Domain and the deposition of the first transgressive cover over the metamorphic complexes. The extensional processes were accompanied by very limited deposition as outcrops of Aquitanian deposits. They are represented by the sediments of Ciudad-Granada Group (Fig. 7.01; see Serrano *et al.*, 2007) and are very scarce in the Malaga area. As a matter of fact, all the lower Miocene deposits represented in the map of figure 7.02 correspond with the Burdigalian deposits of La Viñuela Group, as the outcrops of Ciudad-Granada are too small to be represented in the map and their location is shown with stars (Fig. 7.02). In addition, the offshore unit VI is mainly Burdigalian-Langhian in age and only one specimen of Aquitanian age has been found in well Alb-A1 (Jurado and Comas, 1992).

During this period, the LANFs systems with transport sense towards the SW and SSE (Fig. 7.01) were most likely active. The limited outcrops of Ciudad-Granada Group do not seal the faults but appear on top of thinned Malaguide units. In addition, the lowermost member of Ciudad-Granada Group is characterized by breccias that contain clasts eroded only from the Malaguide Complex (Bourgeois *et al.*, 1972; Bourgeois, 1978; Martín-Algarra, 1987; Serrano *et al.*, 2007) which is indicative that the exhumation of the Alpujarride complex was still taking place.

Lower(?) Burdigalian (deposits of Viñuela Group and lower part of unit VI)

During this period deposition was more important in comparison with Aquitanian times. Onshore, the Viñuela Group deposits were dated as early Burdigalian in the studied area (Serrano *et al.*, 2007 and reference therein). Even though these deposits are restricted to scattered outcrops, their extension is sufficient to be represented on the map (e.g. near La Viñuela and Alozaina Villages; Fig. 7.02).

The Viñuela Group is characterized by breccias made of clasts from Malaguide and Alpujarride complexes, fining upwards into marls alternated by sandy and conglomeratic levels. This lithostratigraphy is very similar with the one described offshore in Unit VI at the base of Alb-1 well, which corresponds with the last 110m of Miocene deposits before the well reached the metamorphic basement (Fig. 7.04). These last deposits are differentiated in the Alb-A1 well report (Bailey *et al.*, 1986) by the appearance of sandy levels with metamorphic fragments and even basal breccias in the last 10m. Moreover, Diaz-Merino *et al.* (2003) and Martinez del Olmo and Comas (2008), using a sequence-stratigraphic approach, already differentiated these deposits as a separate sequence from the rest of the olistostromic sequence (sequences A1 and A2 from Diaz-Merino *et al.*, 2003). Considering that unit VI is also partially Burdigalian in age, it is likely that this lower sequence of sandy levels and breccias was

contemporaneous with the one of the Viñuela Group. Unfortunately the rather restricted outcrops of the Viñuela Group and the limited thickness of the bottom sequence observed in well Alb-A1 (see Fig. 7.07A) do not permit to correlate them with an onshore-offshore cross-section. Nevertheless this is indicative that sedimentation was already taken place in the nowadays offshore area.

During this period of time extension continued. The hydraulic brecciation observed in the uppermost Malaguide Complex, associated with LANFs activity (see chapter 4), shows that the LANFs could have nourished the Burdigalian deposits of la Viñuela Group which is indicative of its syn-tectonic nature. Even though, the Viñuela deposits post-date the LANF's with SW transport sense near La Viñuela village (Fig. 7.02; see also Alonso-Chavez and Orozco 1998) which suggests that the SW directed LANF system ceased its activity during lower Burdigalian times. Probably, during this period of time only the system with transport towards the SSE was still active (Fig. 7.01).

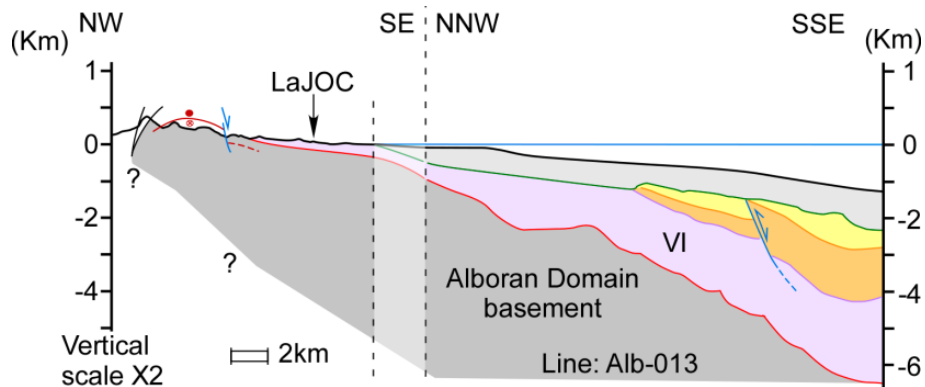


Figure 7.05: Onshore-offshore profile (location in Fig. 7.02) showing the correlation between LaJOC and Unit VI. Onshore LANF's bounding the Alboran Domain metamorphic complexes are coloured in red while latter faults are coloured in blue. Colours of Miocene units are according to Fig. 7.01. Seismic line used: Alb-013.

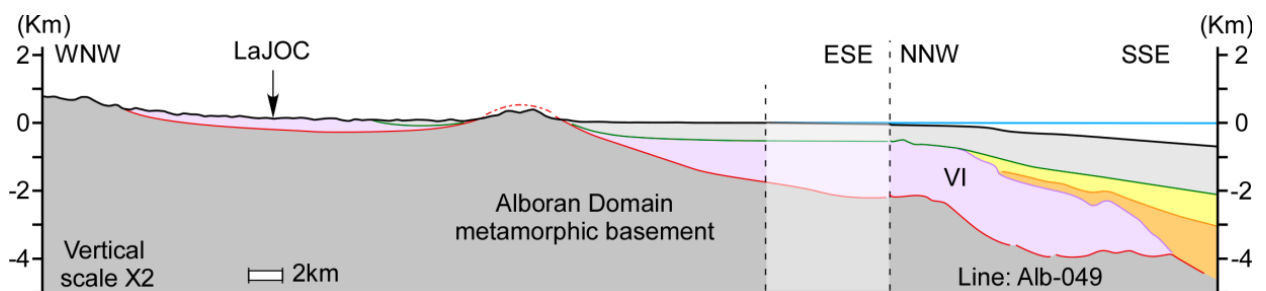


Figure 7.06 Onshore-offshore profile (location in Fig. 7.02) showing the correlation between LaJOC and Unit VI. Same figure conventions as in Fig. 7.05. Seismic line used: Alb-049.

Upper Burdigalian – lower (?) Langhian (deposits of LaJOC and upper part of Unit VI)

This period was characterized by a change in the mode of extension and the deposition of olistostromic type deposits onshore and offshore. The olistostromic deposits are represented by the LaJOC onshore and Unit VI offshore. In that respect a detailed discussion is needed regarding the correlation between both deposits. Indeed, since the early 90's, several authors pointed out a possible correlation between unit VI and the lower Miocene deposits named here as LaJOC (e.g. Comas *et al.*, 1992; García-Dueñas *et al.*, 1992; Martínez del Olmo and Comas, 2008).

Concerning their age, in this Ph.D. Thesis it has been shown that the age interval of LaJOC is comprised between upper Burdigalian and lower Tortonian (see chapter 4). Indeed, even though no Langhian fauna has been found in the paleontological studies, the lower Burdigalian fauna has been considered as resedimented by several authors (Bourgeois, 1978; Feinberg and Olivier, 1983; González-Donoso *et al.*, 1987; among others).

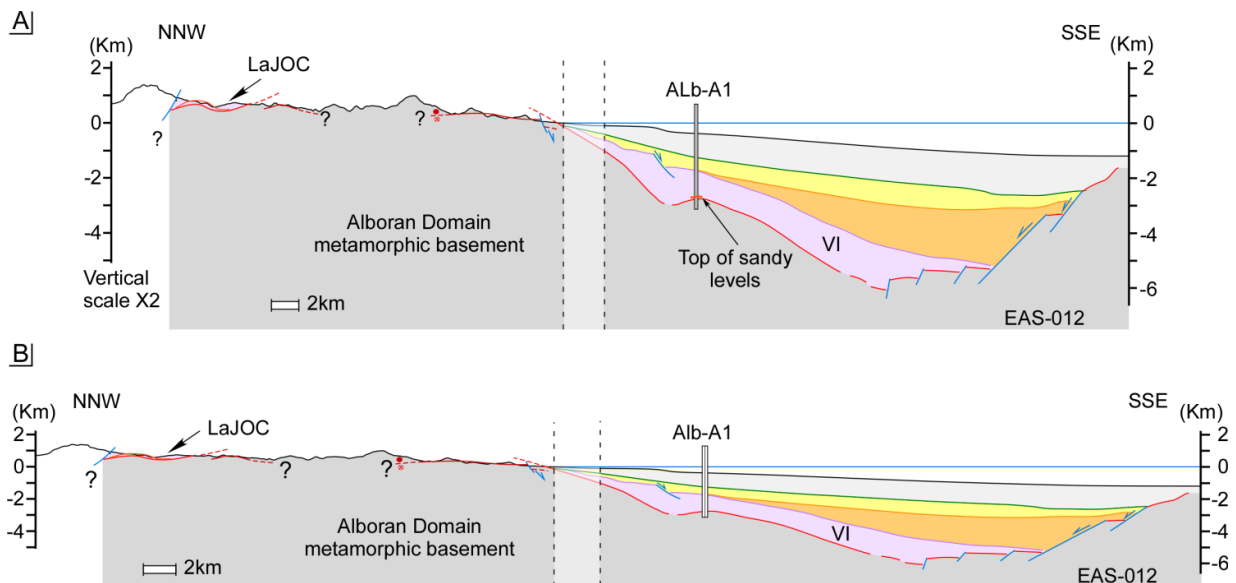


Figure 7.06 – A) Onshore-offshore profile (location in Fig. 7.02) connecting the Malaga Basin and the northern branch of LaJOC. The wedge shaped deposits indicate that the Malaga Basin opening was towards the NW. B) Same profile without vertical exaggeration. It reveals the true geometry of the Malaga Basin and the low angle of tectonic structures involved. Same figure conventions as in Fig. 7.05. Seismic line used: EAS-102.

Offshore, and after the revised seismic correlation (see chapter 6), unit VI is most likely younger than previously thought. Indeed, the younger deposits of unit VI are lower (?) Langhian in age according to the seismic correlation done in And-G1 well (Fig. 7.04; see also Fig.6.10 from Chapter 6). This would be in agreement with our age estimation for the LaJOC which include olistoliths with lower Miocene structures. In

well Alb-A1, the fauna found in most of Unit VI is older (early Burdigalian), but could be re-sedimented, as the late Cretaceous and Eocene fauna that the well report considered as reworked (Bailey *et al.*, 1986). In the same well, at top of unit VI, early Langhian to late Burdigalian fauna is reported in a short section (about 40m thick), just before a major unconformity (Bailey *et al.*, 1986; Fig. 7.04).

In this Ph.D. Thesis we were not able to correlate this late Burdigalian to early Langhian episode with any seismic unit as the resolution of our seismic lines is not high enough (Fig. 6.10). This Langhian section could correspond either to Unit VI deposits or younger ones (Unit V?) depending if the top of this section corresponds with the R5 unconformity or another one (fig. 6.10). If we analyze the section in detail (fig. 7.04), it stands out that the major unconformity described in the well report is found on top of the section and not at its bottom (before the 1300m in Fig. 7.04; Bailey *et al.*, 1986). It is more likely that this major unconformity corresponds with R5 reflector which is observed as a major unconformity in the whole Malaga Basin. This would imply that this section is included in Unit VI and that Langhian fauna is also present in well Alb-A1. If it is the case, the presence of Langhian fauna in both wells, Alb-A1 and And-G1, strengthen a correlation in terms of age between unit VI and LaJOC, at least partially. Finally, the difference in the age of the fauna between both wells could be explained by the fact that the basin is wider and deeper in well And-G1. This could be eventually related with a less energetic environment of deposition which would have decreased the olistostromic sedimentation and reduced the presence of reworked fauna.

In terms of lithology, LaJOC and most of unit VI sequence reported from wells show significant similarities. First, Unit VI deposits are reported as olistostromic (Alb-A1) or probably olistostromic (And-G1) in nature and contain blocks embedded in a fine grained matrix (see fig. 7.04). This is in agreement with the block-in-matrix and the olistostromic nature of the LaJOC (chapter 4). The matrix of unit VI is also described in wells as being composed mostly by clays, sometimes alternating with fine-grained sandstone (see Jurado and Comas, 1992; Martínez del Olmo and Comas, 2008). This is congruent with the clays and marls observed in LaJOC and the thin intercalations of fine-grained sandstones observed in its turbiditic units (e.g. see Fig. 5 from epigraph 4.2). Finally, the reworked upper Cretaceous and Eocene fauna in unit VI reported in both wells (Fig. 7.04) can be most likely associated with the upper cretaceous blocks and olistoliths of LaJOC (see Fig. 2 from epigraph 4.2).

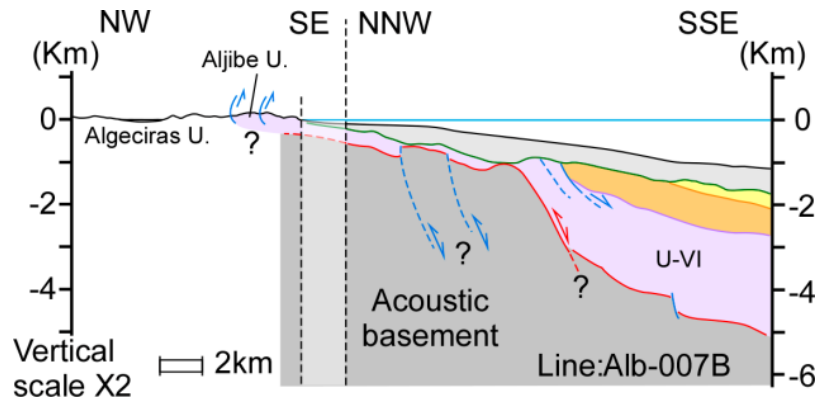


Figure 7.08 Onshore-offshore profile (location in Fig. 7.02) showing the relationship of Unit VI with the Flysch Trough units. Offshore, note the presence of probable thrust latter reactivated as extensional faults. Same figure conventions as in Fig. 7.05. Colors of Miocene units are according to Fig. 7.01. Thrusts and normal faults are colored in blue. Seismic line used: Alb-007B.

The correlation between LaJOC and Unit VI is strengthened by two onshore-offshore cross-sections (Figs. 7.05 and 7.06) that reveal a lateral continuity between these deposits. The first one (Fig. 7.05) is situated near Estepona city and crosses and isolated outcrop of LaJOC, close to the coast line (Fig. 7.02). The cross-section reveals continuity onshore of Units I and VI (e.g. Fig. 6.16). Indeed, the cut-off of Unit VI has not been observed in this area (see Fig. 6.13). Given that seismic profiles are less than 3km away from the coast, the lateral correlation of Unit VI and LaJOC is very likely (Fig. 7.05). The second cross-section (Fig. 7.06) includes a seismic profile that crosses the northern flank of the Malaga Basin and continues onshore, in an ESE-WNW direction, following the depression where Neogene deposits outcrop (Fig. 7.02). In this area, it can be seen again how Unit VI and I can be followed outside the seismic profiles in an onshore direction (e.g. Fig. 6.14). Also note that the thickness of unit VI is more than 1000m at the NW termination of the seismic profiles (see Fig. 6.13; Fig. 7.06). Therefore, it is likely that unit VI extends until the nearest LaJOC deposits even though they are found 30km away from the seismic profiles. In this interpretation, the limit between LaJOC and the Pliocene deposits would be the onshore counterpart of the Messinian unconformity. In fact, the seismic reflector can be extended onshore if assumed that it dips gently towards the west and is slightly deformed by the open fold drawn by the metamorphic basement. Therefore, the Pliocene deposits outcrop along the profile until the recent erosion exposes the Lower Miocene ones (Fig. 7.06).

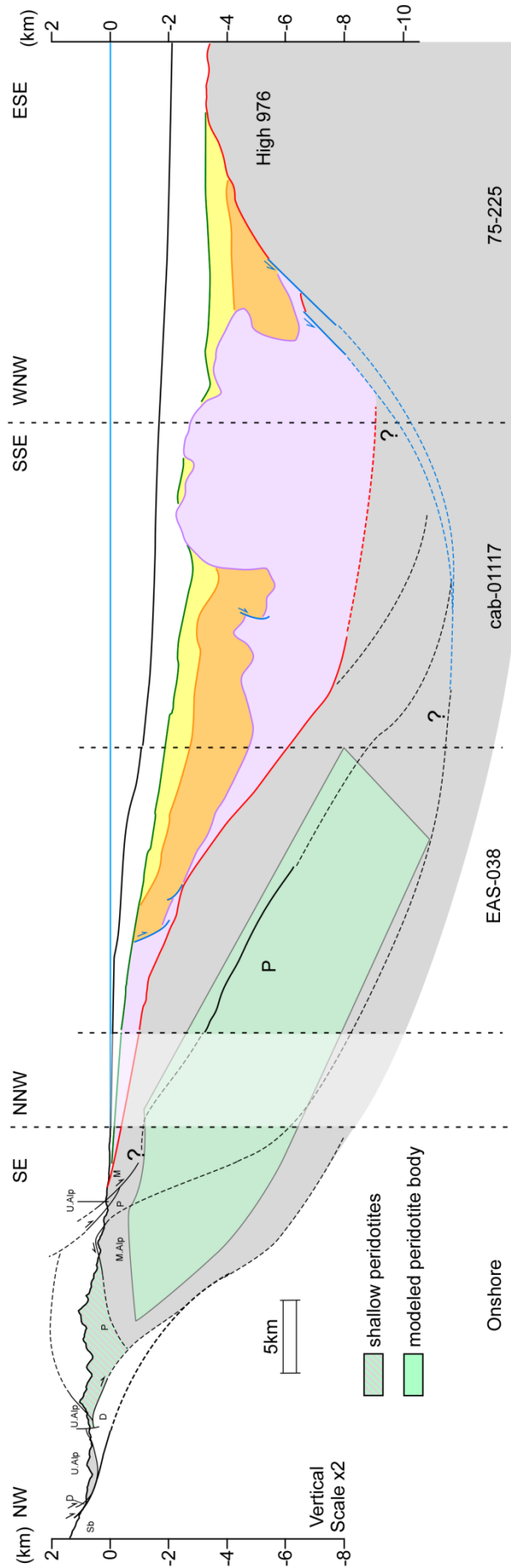
The similarities in age and lithologies, together with the onshore-offshore cross-sections show that Unit VI and LaJOC can be correlated, even though Unit VI includes older deposits, Burdigalian in age, represented in its lowermost parts. Furthermore, the offshore-onshore correlation permits to better constrain the age of the LaJOC estimated in the onshore study (see chapter 4). Indeed, Unit V (Langhian) on-laps the deposits of Unit VI, and therefore the LaJOC ones, which reveals that its deposition cannot extend beyond Langhian times (fig. 7.01). Finally, it also shows that the olistostromic-type

sedimentation took place extensively in this part of the Alboran Domain during Langhian times.

Regarding the extensional structures that were active during this period, the onshore study (chapter 4) shows that LaJOC deposits post-date the SW-ward LANF system in the easternmost part of the study area, and the LANF system with transport towards the SSE near Alora and Alozaina (Fig. 7.01 and 7.02).

Offshore, the sedimentary cover is not affected by the LANFs (including Unit VI) but some intracrustal reflectors observed in the acoustic basement at the northern flank of the Malaga Basin have been associated to these LANFs (see chapter 6; Fig. 6.03). In order to shed light on the relationship between the onshore LANF systems and the Malaga Basin basement a large onshore-offshore cross-section has been done (Fig. 7.09). It crosses the entire Malaga Basin in its deepest parts and continues onshore in a NW-SE direction up to the internal-external zone boundary and is localized in figure 7.02. The offshore part corresponds with the interpretation of the seismic profiles while the onshore part has been done according to previous interpretations (García-Dueñas *et al.*, 1992; Crespo-Blanc and Campos, 2001). The cross-section shows that the distribution of unit VI deposits thickens towards the SE and does not appear to be controlled by the onshore LANFs. It is probable that the NW extension associated with the faults which bound High 976 already started its activity during this episode (Fig. 7.01; see also chapter 5). The onshore LANF's go through the metamorphic basement and the intracrustal reflector in EAS-038 is interpreted as one of these LANF's (Fig. 7.09; see also Fig. 7.12). In addition, even the deep structure is highly speculative, it is expected that the onshore LANF's with transport towards the SSE converge at depth with the NW dipping ones of High 976 (see also Fig. 9 of chapter 5).

Figure 7.09: (next page) Large Onshore-offshore cross-section. The offshore corresponds with the interpretation of three seismic profiles. Onshore part is interpreted from geological maps and according to previous interpretations in the same area (García-Dueñas *et al.*, 1992; Crespo-Blanc and Campos, 2001). The modelled peridotite body is a modified from Torné *et al.* (1992), see figure 7.11. Extensional detachments active during the second extensional episode are coloured in blue and converge at deep with the onshore ones. Legend: U.Alp: Upper Alpujarrides; M.Alp: Middle Alpujarrides; P: Peridotites; M: Malaguides; D: Dorsal; Sb: Subbetic.



This interpretation is also coherent with the gravimetric studies of Torné and Banda (1992). The authors analyzed four NNW-SSE oriented gravimetric profiles situated in the studied area (near Marbella city) where an important gravimetric anomaly is found (7.10A). In these profiles the authors modeled a peridotite slab dipping towards the SE. The modeled peridotite bodies of two of these profiles (Profiles II and III in Fig. 7.10B) were overlapped to the cross-section (figs. 7.11 A and B). After that, an approximate interpolation between the two peridotite bodies was done in order to create a new one, considering the fact that the cross-section is situated between the two profiles (Fig. 7.11C). Even, the position and size of the interpolated peridotite body is estimated, its top matches the position of the intracrustal reflector (Fig. 7.10C). This correspondence supports the hypothesis that the intracrustal reflector corresponds with a LANF, specifically, the top of the peridotite body as its higher density makes it a good candidate to generate a strong reflector at its top. This correlation helps to better constrain the structural interpretation at depth in figure 7.09 where the position of the estimated peridotite body is shown. It must be stress that the westernmost part of the modeled peridotite body does not fit with the onshore interpretation as it would imply that peridotites are found below the lower Alpujarride units (fig. 7.09). One explanation is that the deep peridotite body does not extend that far towards the NW and that the gravimetric anomaly in this area is likely produced by the peridotites outcropping in the surface (dashed green lines in Fig. 7.09). This interpretation contrasts with previous studies that considered the top of the basement surface as one of the onshore LANF's (Comas *et al.*, 1992). Nevertheless, such normal fault would have affected the deposition of unit VI during Burdigalian to Langhian times. Unfortunately the syn-depositional nature of unit VI with this fault system is not observed.

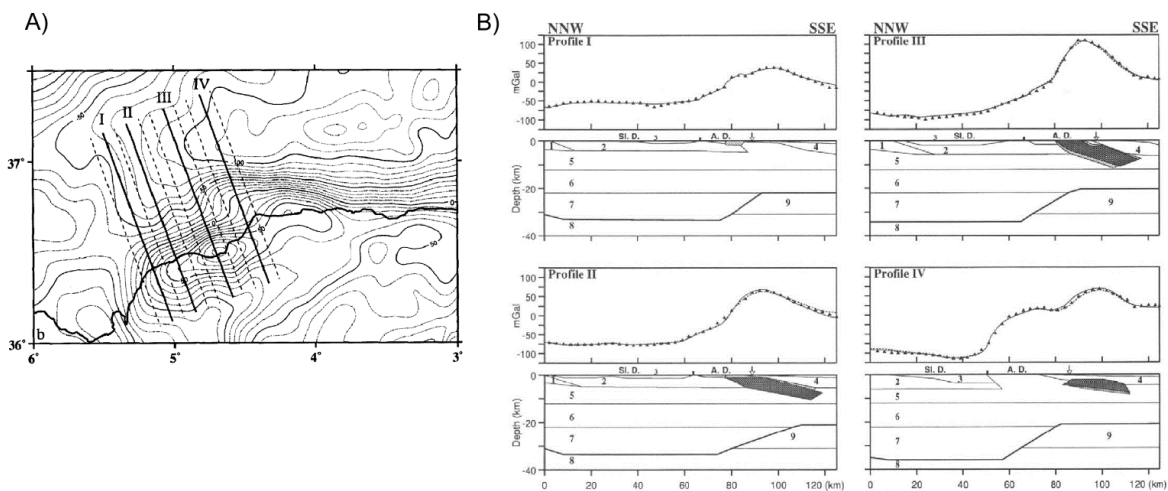
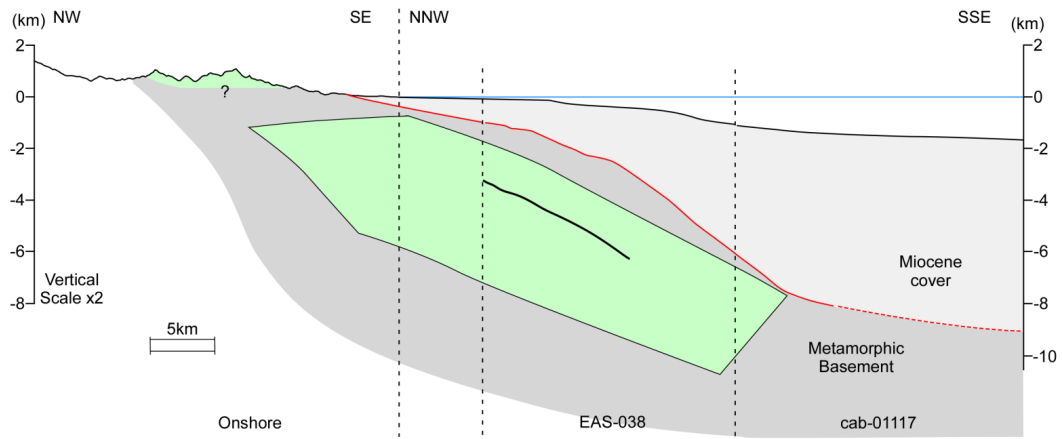


Figure 7.10: Figures are taken from Torne *et al.* (1992). A) Bouguer anomaly map and location of the gravimetric profiles. B) Gravimetric profiles and their crustal model with the peridotite bodies marked in black.

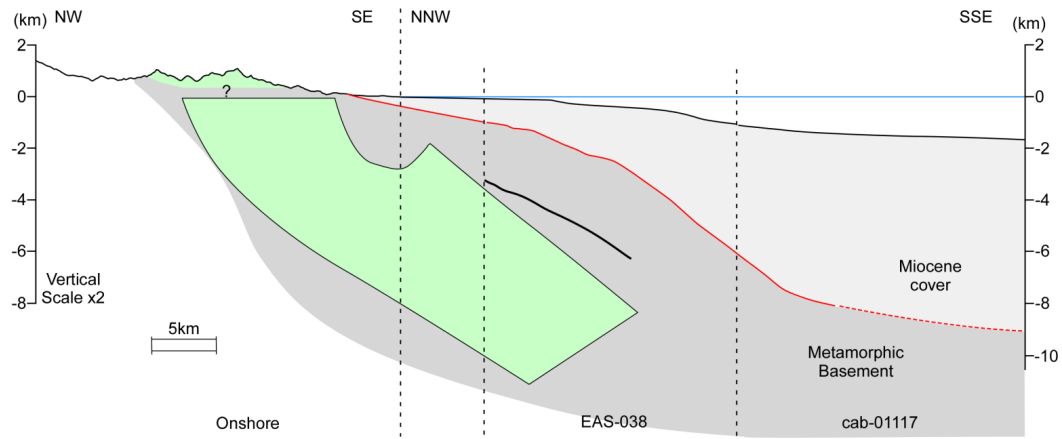
During this period of time (upper Burdigalian to lower (?) Langhian), the tectonic evolution of the Alboran Domain in the western Betics was accompanied with the formation of the fold and thrust belt of the Subbetic cover and Flysch Trough (Fig. 7.01). Indeed, some NNE-SSW oriented thrusts, dipping towards the east, are observed along the coast between Gibraltar and Estepona (García de Domingo *et al.*, 1994; Balanyá *et al.*, 2007). The direction of these thrusts coincides with the offshore N-S to NE-SW directed folds observed in the basement and Unit VI (Fig. 6.13; Fig. 7.08). An onshore-offshore cross-section (Fig. 7.08) shows that these offshore folds could be related with the onshore thrust, indicating that thrusting of the external zones also took place in the westernmost part of the nowadays Malaga Basin (from Gibraltar to Estepona). In addition, it is likely that the Gaucín fault, was active during this period with mainly a normal component (Fig. 7.01; see also Fig. 6.05 from chapter 6). The Gaucín fault activity during this period contrast with the LANFs which were active previously to this period. As a matter of fact, the associated SSW extension is perpendicular with respect to the ENE-WSW shortening of the external zones (i.e. parallel to the arc). Probably, the Gaucín fault activity during this period was related with the characteristic arc-parallel extension observed broadly in the external zones of this part of the Gibraltar Arc (Fig. 7.01; Luján *et al.*, 2000; Balanyá *et al.*, 2007, Balanyá *et al.*, 2012).

The overall picture given by the onshore-offshore data is that, during Langhian times, dismantling of the already structured mountain front occurred, which would have favored the mass transport deposition of LaJOC and Unit VI deposits (Fig. 7.01; see also chapter 4; Suades and Crespo Blanc, 2013). This deposition was not triggered by the LANFs with transport towards the SSE that bound the metamorphic complexes of the Alboran Domain. Instead, this part of the Alboran Domain was probably transported as a supra-detachment basin associated with the migration of the extensional locus towards the external zones, when the IEZB (internal-external zones boundary) started to act as an extensional detachment (Crespo-Blanc and Campos, 2001). The age of this tectonic inversion, even it is not well constrained, has to be post early-Burdigalian (*op. cit.*). This extension in the IEZB would have favored the gravitational processes that lead to the deposition of blocks and large olistoliths coming from the external zones into the Alboran Domain (chapter 4; Suades and Crespo Blanc, 2013). Most likely, this migration of the extension also affected the previously compressive structures in the westernmost Malaga Basin, postdating the folds that affected unit VI and the basement (Figs. 7.01 and 7.08).

A) Peridotite body from Profile II (Torné et al., 1992)



B) Peridotite body from Profile III (Torné et al., 1992)



C) Estimated Peridotite body

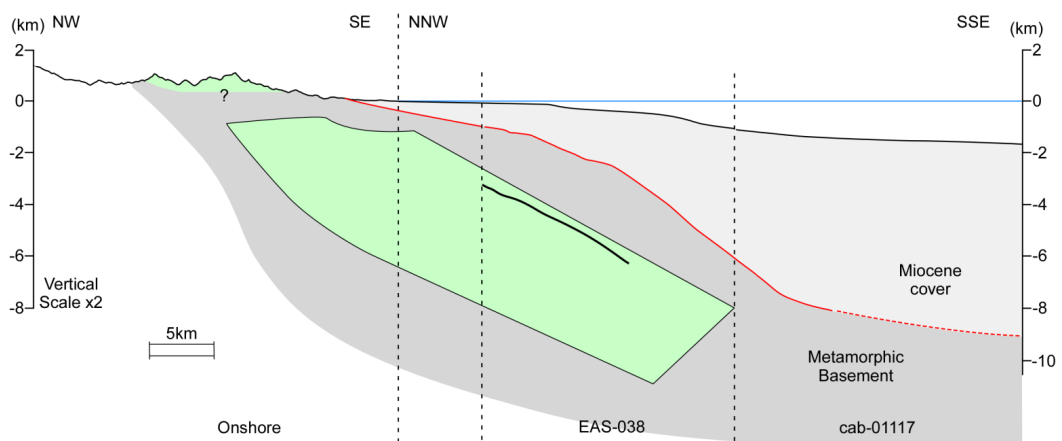


Figure 7.11: Peridotites bodies (green) superimposed with a simplified version of Fig. 7.09 onshore-offshore cross-section (location in Fig. 7.02). A and B) Geometry of the Peridotites bodies from Torné et al. (1992). C) Estimated geometry of the peridotite body for the position of the cross-section (see text for explanation). Note how the top of the estimated peridotite body adjusts to the intracrustal reflector from seismic line EAS-038 (black line).

7.2.2) Malaga Basin rift episode (upper(?) Langhian-lower Tortonian)

This episode is characterized by the opening of the Malaga Basin *s.s.* and the end of the extension produced by the onshore LANF's. It is also contemporaneous with the external zones folding and thrusting (Fig. 7.01).

During this episode most of the extension was accommodated by the offshore NW dipping extensional detachments, with a transport sense also towards the NW, that are related with the formation of the Malaga Basin (Fig. 7.01). The NW dipping faults are represented by the High 976 fault system (Fig. 7.02; see also chapter 6) but, in a broad sense, the High 976 faults are most likely the westernmost expression of wider extensional detachment system. This system formed a series of half-grabens (The Malaga Basin, the central half-graben, and the eastern half-graben; see Figs. 4 and 9 from chapter 5) wherein the largest amount of extension took place in the Malaga Basin.

The Malaga Basin rift episode started with the deposition of the offshore Unit V which shows divergent geometries towards the southeastern flank of the basin in response to High 976 fault activity (see Fig. 7.07). The extension continued during Unit IV deposition and lasted until the formation of R3 unconformity, before the deposition of Unit III (Upper Tortonian in age). Accordingly, the episode is constrained between Langhian and early Tortonian times (Fig. 7.01).

There is no equivalent onshore for Units V (upper (?) Langhian to Serravallian) and IV (Serravallian to Tortonian). Indeed, no deposits dated as Serravallian or lower Tortonian are found in the studied area (Fig. 7.01). These units are restricted to the Malaga Basin as they always onlap the flanks of the Basin (Figs. 6.15 and 6.17). The total absence of onshore deposits clearly indicates that there was no deposition in the nowadays onshore area (NE and N of the Malaga Basin; Fig. 7.01) as it was, in fact, the emerged part of the Malaga Basin's hanging-wall.

The lack of onshore deposits restricts the amount of onshore-offshore correlations that can be done and the possibility to know the tectonic processes that could have taken place during this period of time. The only place where it has been possible is the area east of Marbella city where the set of offshore faults with WNW-ESE direction (Fig. 6.21) can be tentatively correlated with onshore faults that show the same direction. These are the so-called Marbella normal faults that bound the Alpujarride and Malaguide complexes east of Marbella city (Figs. 7.02; 7.12). Those faults have a higher dip and post-date the other LANF's faults in the area (García-Dueñas *et al.*, 1992; see also Fig. 7.12). Both, the onshore and offshore faults have the same WNW-ESE direction which strongly suggests that they are part of the same fault set. In terms of the direction of the extension, there is a slight discrepancy. Indeed, the onshore faults kinematics indicate normal and sinistral movement with transport towards the SSE (García-Dueñas *et al.*, 1992) while, for the offshore faults, the recess drawn by the top of the basement suggests a dextral component (Fig. 7.02). Nevertheless, the dextral

component is probably apparent, produced by the normal component of those faults being much higher than the directional one and the top of the basement being a surface that dips towards the SE. This is similar to the Gaucín fault as its sinistral movement does not correspond with what is observed from the basement top (Fig. 6.22). These faults were active for the whole second extensional episode but they were especially active during Langhian-Serravallian as shown by the thickened unit V depocenter south of the faults (Fig. 6.15). The extension produced by the Marbella faults (East of Marbella city; Fig. 7.02) is parallel to the arc, similar with other faults described in the external zones. These faults could be related with the strain partitioning pattern observed in this part of the Betics (Balanyá *et al.*, 2007; Balanyá *et al.*, 2012).

The sequence-stratigraphic analysis done in the northeastern part of Malaga Basin (Chapter 5), together with the isopach maps of the major seismic units (Chapter 6) and the comparison with onshore data, permit to differentiate two main stages during the Malaga Basin rift episode.

Early to middle rift climax

The *early to middle rift climax* took place from upper (?) Langhian to lower Serravallian and corresponds with the deposition of Unit V and the lowermost part of Unit IV (Fig. 7.01). This episode is characterized by two pulses of greater tectonic subsidence that correspond with two TR cycles (see chapter 5). It is characterized by the highest amount of tectonic subsidence which produced that sedimentation was restricted to the deepest parts of the basin (see unit V cut-off in Fig. 6.15). Extension was associated with important uplift of the footwall block which kept High 976 emerged during this period. The erosion of High 976 provided a source of proximal sedimentation and large amounts of axial deposits were deposited close to the SE flank, especially in the northeastern half of the basin (see Figs. 6 and 7 from chapter 5). The emerged area situated northwest of the basin also provided a source of axial deposits into the basin, even though the amount of these deposits was minor in comparison with those provided by the High 976.

Simultaneously, the geometry of the High 976 extensional detachments produced the rotation of the hanging-wall. The resultant steepening of the NE flank of the Malaga Basin triggered the migration of the undercompacted unit VI towards the center of the basin and the formation of gravitational normal faults affecting the overlying units V and IV (see Fig. 6.15). Indeed, other seismic-stratigraphic studies that focused on mud diapirs (Talukder *et al.*, 2003; Soto *et al.*, 2010) shown that diapirism started during this stage, at middle Miocene, before the formation of R4 unconformity.

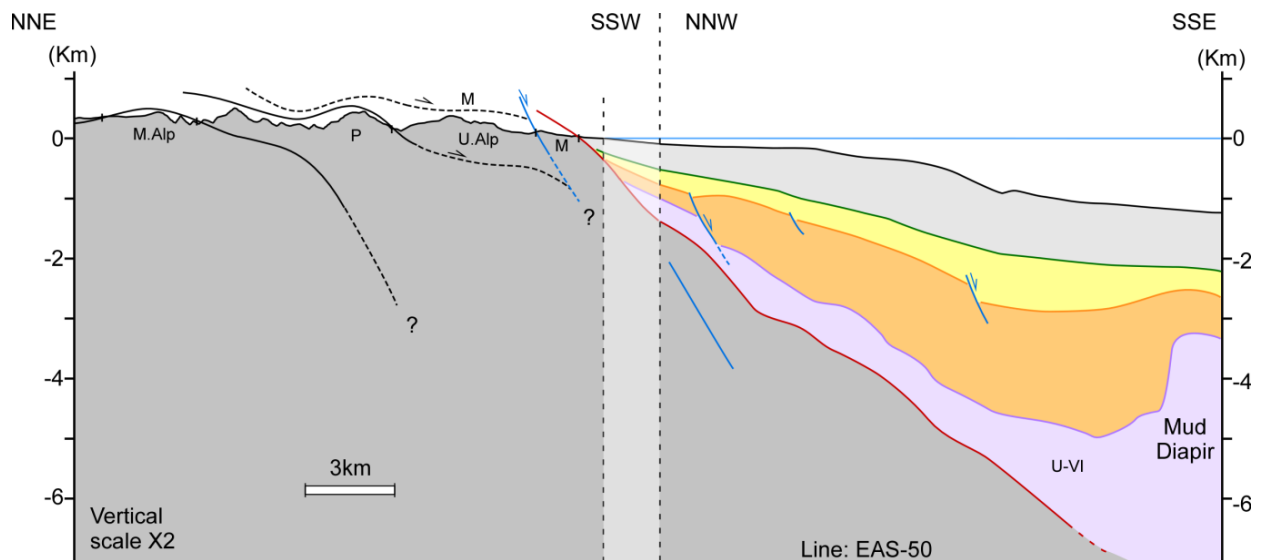


Figure 7.10: onshore offshore cross-sections showing the correlation of the onshore Marbella faults with the intracrustal reflectors offshore. The geometry of the detachments active during the Malaga Basin extensional episode (blue lines) contrasts with those from the Main extensional episode (black lines). Legend: U.Alp: Upper Alpujarrides; M.Alp: Middle Alpujarrides; P: Peridotites; M: Malaguides.

Late rift climax

The *late rift climax* took place during upper (?) Serravallian to lower Tortonian and is represented by the Upper part of Unit IV. It is characterized by a single pulse of tectonic subsidence and an overall decrease in the tectonic activity during basin widening (compare units IV and V cut-offs; Figs. 6.15 and 6.17). The decrease of tectonic subsidence produced a significant drop of proximal deposition (lobes) into the basin which is especially true for the SE flank. This is also a consequence of the footwall block being submerged during this period as shown by the presence of Unit IV deposits over the High 976. Deposition over High 976 indicates that tectonic subsidence during this period was not only triggered by High 976 fault system but also by extensional detachments of basins situated SE of the Malaga Basin, that is, in a more internal position of the Alboran Domain (Fig. 4; chapter 5). This could be indicative of a progressive migration towards the SE of the extensional locus during the later stage of rifting.

7.2.3) Tectonic inversion (upper Tortonian to Recent)

The post extensional evolution in the studied area took place from upper Tortonian, onwards. Offshore, this period is represented by Units III to I (upper Tortonian to recent). Onshore it is represented by the upper Tortonian formations (Serrano, 1979; Rodríguez-Fernández *et al.*, 1991; Fig. 7.01) that outcrop scattered

along Guadalhorce River (e.g. near Alora and Pizarra villages; see Fig. 7.02) and the Pliocene to recent sediments.

A continuity of Unit I with the onshore Pliocene to recent sediments is observed from onshore-offshore cross-sections (Figs. 7.06 and 7.12). On the other hand, the cross-sections do not show a clear continuity of units II and III onshore. Even though, it is expected that these units were deposited also onshore as they do not on-lap the northern flank of the basin. Their cut-off is caused by the erosion marked by the Messinian unconformity (e.g. Figs. 6.14 and 6.18). Indeed, unit III has the same age as the onshore Tortonian formations (Fig. 7.01). Messinian deposits (unit II) are mostly not present onshore even very few outcrops of upper Messinian deposits have been described north of Malaga city (Guerra-Merchán *et al.*, 2010). Regarding the lithology of the onshore upper Tortonian deposits, they are mostly characterized by a fining upwards sequence of conglomerates, calcarenites and sandstones (López-Garrido and Sanz de Galdeano, 1999). Offshore, unit III shows clays intercalated with sandstones levels (Alb-A1 well) which could be consequence of a more distal sedimentary environment. This is indicative that during Late Tortonian and maybe Messinian the onshore area was partially submerged along a corridor, called the Guadalhorce pathway, which was one of the pathways that connected the Mediterranean Sea with the Atlantic Ocean (Serrano, 1979; López-Garrido and Sanz de Galdeano, 1999; Martin *et al.*, 2001; Schoorl and Veldkamp, 2003). In addition, High 976 was submerged and progressively covered by deposits from units I to III as it can be observed in the seismic profiles (e.g. Figs. 6.07; 6.12; 6.14). After the Messinian the Guadalhorce pathways closed and most of the Tortonian sediments have been eroded progressively leaving only the scattered deposits observed nowadays (Fig. 7.02).

The contractional history was governed by the regional SE-NW direction of convergence between Africa and Iberia plates (Mazzoli and Helman, 1994). During this period compressive and extensional structures developed coetaneously in the studied area (Crespo-Blanc and Campos, 2001; Balanyá *et al.*, 2012). The pattern of deformation is that of a strain partitioning producing coeval arc-parallel extension and arc-perpendicular shortening (Balanyá *et al.*, 2012).

In the studied area there are two main types of extensional structures: a) a set of faults with WNW-ESE direction and sinistral movement, described onshore and offshore. These are the Gaucín fault and so-called Marbella faults (Fig. 7.02). b) NW-SE oriented normal faults that are observed onshore, mostly north and northwest of Malaga city (e.g. east of Pizarra village in Fig. 7.02).

Regarding the contractional structures, onshore they are mostly formed by scarce very open folds NE-SW and E-W oriented (Sánchez-Gómez *et al.*, 1996; Crespo-Blanc *et al.*, 2001; Booth-Rea *et al.*, 2003; Insua-Arévalo *et al.*, 2012; see also chapter 4). It must be stressed that some open folds observed are not related to this episode. Instead,

they were produced in response to extensional detachments during extensional episode (e.g. N-S oriented fold situated east of Pizarra Village; see Booth-Rea *et al.*, 2003).

In addition, the TTZ (Torcal Transpression Zone), an E-W shear zone that produced dextral transpression, is also considered to be active during this period (Barcos *et al.*, 2011; Balanyá *et al.*, 2012; Díaz-Azpiroz, *et al.*, 2014). Offshore, in the Malaga Basin, only minor and local tectonic inversion of the structural highs is observed (e.g. High 976; see chapter 5), due to inversion of previous extensional detachments (e.g. Fig. 6.07), and also minor tilting of the Miocene cover in the northwestern flank. It must be stressed that tilting and folding of the offshore sedimentary cover is mostly observed in the upper Tortonian deposits of unit III but is minor in the post-Miocene deposits of unit I (Fig. 7.01; see chapter 6). This indicates that tectonic inversion in the Malaga Basin occurred mostly during Upper Miocene times (fig. 7.01). Moreover, compression could also have produced the reactivation of the mud diapirism as previously described (Talukder *et al.*, 2004; Comas *et al.*, 2012). Despite of that, no contractional structures have been observed in the central part of the basin and, overall, the amount of tectonic inversion in the Malaga Basin is very low.

In conclusion, both onshore and offshore area were characterized by little amount of tectonically inverted structures and were accompanied by few extensional and transtensional structures (sinistral) with a WNW-ESE and NW-SE direction respectively.

7.3) Some regional implications in the context of the Gibraltar Arc System

The present study sheds light into the tectonic evolution of an area situated in the western part of the northern branch of the Gibraltar Arc. Nevertheless, it must be stressed that the Miocene tectonic processes that took place in the Gibraltar Arc orogenic system show important variations along and across the Arc, and the strain partitioning is very important, as expected in any strongly arcuate orogen. This has already put forward in terms of timing, either in the external (Vera, 2000; Crespo-Blanc and Frizon de Lamotte, 2006; Crespo-Blanc *et al.*, 2007), or the internal zones (e.g. Rodríguez-Fernández and Sanz de Galdeano, 1992; García-Dueñas *et al.*, 1992; Crespo-Blanc, 1995; Comas *et al.*, 1999; Booth-Rea *et al.*, 2002; Serrano *et al.*, 2007). As a consequence, an exhaustive tectonic model of the Gibraltar Arc during Miocene times would require a complete description of each one of the processes that took place in any area of the orogenic system for a determined time interval, which is out the scope of this PhD Thesis volume. Accordingly, only a few comments concerning the age and kinematics of the concerning the LANF systems that affected the Alboran Domain and the formation of the Malaga basin will be made.

As it has been shown, brittle extension in the Western Alboran Domain took place through several LANS systems: a SW directed one previous to Burdigalian times, and a second one SSE directed that was active most likely during late Burdigalian to Langhian times (Fig. 7.01; 7.02). By contrast, in the central Betics, two main systems have been differentiated (Crespo-Blanc, 1995): a first one with a roughly N-S direction of extension during Burdigalian to Langhian times, and a second one with SW transport direction during the Aquitanian to lower Tortonian.

This data implies that the N-S LANS system in the central Betics was coetaneous with the SSE directed one in the western Betics. At the same time, it implies that the SW directed system in the central Betics is much younger than that observed in the western Betics. Moreover the High 976 LANS system, responsible of the Malaga Basin extension with transport towards the NW, would have been synchronous with the SW directed one from the central Betics. The coexistence of two major, near-orthogonal, LANS systems (SW and NW directed) separated only by a distance of approximately 100km presents a complex kinematic pattern that needs to be addressed.

A recent study (Crespo-Blanc *et al.*, 2013; Crespo-Blanc *et al.* submitted) propose a paleotectonic reconstruction of the GAS that simplifies substantially this apparent kinematic complexity. The authors propose important vertical-axis rotation of the western and the central Betics as rigid blocks from 9Ma onwards. This is based on revisited previous paleomagnetic studies (e.g. Villalaín *et al.*, 1996; Osete *et al.*, 2004), enlightened by recent structural data which evidence the superposition of structures. Consequently, the age of the folds used for fold-test is questioned. Therefore, the authors propose a clockwise rotation of 53° for the western Betics block and a 12° clockwise rotation for the central Betics block which gives a relative clockwise rotation of 41° for the western Betics blocks with respect to the central Betics. This implies that if these rotations are restored at 9Ma, during the extensional evolution of the Alboran Domain, the SSE directed LANS system had the same direction of extension than the SW directed one from the Central Betics but, even more important, it implies that the High 976 LANS system that produced the opening of the Malaga Basin also had the same direction and, in this case, the same transport sense (roughly towards the WSW).

The scenario that brings this paleotectonic reconstruction at 9Ma simplifies the implications of the results presented in this PhD. Thesis as the extensional evolution during Serravallian times can be explained by a major LANS system with transport sense towards the WSW. Within this scenario, the Malaga Basin, and by extension the Western Alboran Basin (Fig. 2.01), was situated on top of this system, at a higher structural level. Furthermore, during Burdigalian to Langhian times, the onshore LANS system with transport nowadays towards the SSE would have produced extension in the opposite direction which would explain the presence of Unit VI and LaJOC deposits in this part of the GAS and not further to the east. Finally, it strengthens the proposal of

two opposite major LANE systems that converges along a deep crustal shear zone (See Fig. 9 from chapter 5).

In a complex, strongly arcuate orogenic system as the Gibraltar Arc, it is very difficult to propose a geodynamic model that explains the deep sitting processes that governed its formation. Because of that, a large number of models have been proposed in the last decades (Dercourt *et al.*, 1986; Platt and Vissers, 1989; Seber *et al.*, 1996; Lonergan and White 1997; Michard *et al.*, 2002; Duggen *et al.*, 2004; Faccenna *et al.*, 2004; Vergés and Fernández, 2012; among others). A discussion of these geodynamic models is out of scope of this study as the analysis presented in this volume deal with the external processes that take place in the GAS and not with the crustal or lithospheric ones. Nevertheless, the presence of a dominant transport to the west trough extensional detachments favors the models that propose an original position of the Alboran Domain situated to the east of the nowadays position and imply a westward movement (in the order of several hundred of kilometer) of this domain during Miocene times (e.g. Dercourt *et al.*, 1986; Lonergan and White, 1997; Michard *et al.*, 2002; Faccenna *et al.*, 2004). These models also propose that the extensional process in the GAS were driven by the retreat of a roughly westward dipping subducting slab (either continental or oceanic) which is also congruent with a main E-W directed extension of the Alboran Domain complexes.

8 Conclusions

- 1) The Miocene deposits which lie on the westernmost Alboran Domain have been analyzed. I characterized the **La Joya Olistostromic Complex (LaJOC)**, a complex which lies unconformably over the internal-external zone boundary and post-dates the low-angle normal faults that affect the Alboran Domain metamorphic complexes. It is composed by turbiditic deposits alternating with *mélange* units that contain blocks and olistoliths of mainly extrabasinal in origins as they proceed from the gravitational dismantling of the Miocene mountain front of the western Gibraltar Arc. The blocks and olistoliths include rocks which come from the Malaguide complex, Dorsal Complex, Predorsal units, Flysch Trough Complex and Subbetic units
- 2) Kilometre-scale olistoliths from the Flysch Trough Complex preserve the internal structure prior to their emplacement within the *mélange*. This permits to constrain the age of this sedimentary complex to the **Late Burdigalian and Langhian** age interval.
- 3) **Hydraulic and cataclastic brecciation** has been observed in the uppermost Malaguide complex. Brecciation was likely triggered by normal faulting and the resulting blocks and fragments have nourished the Aquitanian to lower BurdigalianL sedimentary deposits of La Viñuela group, in turn situated below the sedimentary deposits of the LAJOC.
- 4) Extension of the Malaga Basin has been analysed in terms of seismic sequence stratigraphy. A **new sequence stratigraphy method** has been developed that combines the rift related system-tracts (Prosser, 1993) with the transgressive-regressive cycles of Embry (1993). In the case-study, this method revealed two types of cyclicity that distinguish the rift episode: high-order cycles (T-R cycles) characterize individual or differential fault movements, while the low-order ones characterize the overall rift evolution.
- 5) The **low-order cycle in the Malaga Basin** comprise: 1) the rift initiation system tract, dominated by olistostromic deposition when the Malaga basin was not developed yet as a semi-graben; 2) early to middle rift-climax system tract (Langhian to Early Serravallian), which corresponds to the period of greater tectonic activity and is characterized by abundant lobes facies, especially from the footwall crest due to exhumation; 3) the late rift climax system tract (Late Serravallian to Early Tortonian) which

is characterized by an abrupt decrease in the amount of axial deposits and the fault-related tectonic activity; and 4) the post-rift system tract (Late Tortonian to Recent times) which records a rapid burial of the entire extensional structure.

- 6) Several **onshore-offshore correlations** have been established: 1) the onshore low-angle normal faults with transport towards the SSE correspond with the SE-dipping intracrustal reflectors of the Malaga Basin; 2) unit VI and LaJOC can be correlated not only in terms of age, lithology and nature but also by cross-sections which cross the coast-line; 3) the NW-SE-directed Gaucín fault, which bound the Alboran Domain to the west can be followed offshore. It acted as a high dipping normal fault during Early Miocene followed by strike-slip tectonics during Late Miocene; 4) the WNW-ESE directed faults around Marbella city, transtensional and active until Late Miocene, are observed both onshore and offshore.
- 7) In the Western Betics, the **low-angle normal faults systems** observed onshore **are previous to Langhian times** (LaJOC deposition). They produced the exhumation of the metamorphic complexes and are characterized by extension towards the SSE and SW, crustal thinning, and limited deposition followed by mass-transport deposition. By contrast, extension in the Malaga Basin was produced by a **NW-ward dipping fault system** that generated a geometry of semi-graben from Langhian(?) to early Tortonian. It is suggested that this fault system converges with the same crustal shear zone in which are rooted the extensional systems observed onshore.
- 8) During the Malaga Basin rift episode, erosion of the onshore area and development of transtensional counter faults took place. Tilting of the NE flank of the Malaga Basin caused the migration of unit VI shales towards the centre of the basin and the formation of gravitational listric faults of the overburden cover and development of diapirism.
- 9) Tectonic inversion in the studied area has been minor when compared with other areas of the Gibraltar Arc system. It is characterized by restricted and minor folding of the sedimentary cover in the basins margins, uplift of the structural Highs and tilting. Most of these structures developed during Late Miocene.

[Escriba texto]

8 Conclusiones

- 1) Se han analizado los depósitos del Mioceno que se encuentran en la zona oeste del Dominio de Alborán, y en concreto el complejo olistostrómico de la Joya (LaJOC). Este complejo reposa de forma discordante sobre el límite de las zonas internas-externas y es posterior a las fallas de bajo ángulo que afectan los complejos Metamórficos del Dominio de Alborán. Está compuesto por una alternancia de depósitos turbidíticos con unidades tipo mélange que contienen bloques y olistolitos provenientes del desmantelamiento gravitacional del frente montañoso del Arco de Gibraltar durante el Mioceno. Los bloques y olistolitos incluyen rocas provenientes del Complejo Maláguide, Dorsal, unidades de la Predorsal, Complejo del surco de los Flysch y unidades Subbéticas.
- 2) Los Olistolitos de escala kilométrica mantienen su estructura interna previa a su emplazamiento en la mélange. Este hecho ha permitido restringir la edad de deposición de LaJOC entre el Burdigaliense tardío y el Langhiense.
- 3) En la parte superior del Complejo Maláguide se ha observado una brechificación de tipo cataclástica e hidráulica. La brechificación probablemente fue causada por el movimiento de las fallas normales que facilitaron la fractura en bloques y fragmentos que, a su vez, nutrieron los depósitos del Aquitaniense-Burdigaliense inferior, pertenecientes al grupo La Viñuela. Dichos depósitos se encuentran a su vez situados por debajo de LaJOC.
- 4) La extensión de la Cuenca de Málaga ha sido analizada desde el punto de vista de la estratigrafía secuencial. Se ha desarrollado un nuevo método que combina los “rift system tracts” de Prosser (1993) con las secuencias transgresivas-regresivas de Embry (1993). En la Cuenca de Málaga este método ha revelado la existencia de dos tipos de ciclicidad dentro de la etapa del rift: ciclos de alta frecuencia que indican episodios de más o menos actividad de las fallas que controlan la cuenca, y ciclos de baja frecuencia que caracterizan la evolución general del rift.
- 5) Los ciclos de baja frecuencia en la Cuenca de Málaga constan de: 1) el “Rift initiation system tract”, dominado por una deposición de tipo olistostrómica durante un periodo en que la cuenca de Málaga aún no se había desarrollado como semi-fosa tectónica; 2) el “early to middle rift climax system tract” (Langhiense – Serravaliense temprano), que se corresponde con el periodo de mayor actividad tectónica en la cuenca y se caracteriza por una presencia abundante de facies lobulares provenientes de la exhumación del bloque de

muro.; 3) el “late rift climax system tract” (Serravaliense tardío – Tortoniense temprano), caracterizado por un descenso abrupto de la presencia de depósitos axiales y de la actividad tectónica de las fallas normales; y 4) el “post-rift system tract” (Tortoniense tardío hasta la actualidad) que registra la subsidencia generalizada de la cuenca extensional.

- 6) Se han podido establecer varias correlaciones tierra-mar: 1) las fallas normales con transporte hacia el SSE en tierra se corresponden con los reflectores del basamento de la Cuenca de Málaga con buzamiento hacia el SE; 2) la unidad VI y LaJOC se pueden correlacionar en términos de edad, litología y naturaleza así como mediante cortes geológicos que crucen la línea de costa; 3) La falla del Gaucín, de dirección NW-SE y que delimita el Dominio de Alboran por el Oeste, puede ser seguida hacia mar. Dicha falla actuó como falla normal durante el Mioceno temprano y como falla de dirección durante el Mioceno tardío; 4) las fallas transtensionales de dirección WNW-ESE cerca de Marbella son observadas tanto en tierra como en mar. Dichas fallas fueron activas hasta el Mioceno tardío.
- 7) En las Béticas occidentales los sistemas de fallas de bajo ángulo que se observan en tierra solo fueron activos antes del Langhiense, previamente a la deposición de LaJOC. Estos sistemas causaron la exhumación de los complejos metamórficos y el adelgazamiento de la corteza. Se caracterizan por unas direcciones de extensión hacia el SSE y SW que dieron lugar a una sedimentación escasa, seguida de una deposición masiva de tipo gravitacional. Por el contrario, en la cuenca de Málaga la extensión se produjo por un sistema de fallas normales con transporte hacia el NW que generó la geometría de semi-fosa entre el Langhiense (?) y el Tortoniense inferior. Se sugiere que este sistema extensional converge en profundidad en una misma zona de cizalla donde también se enraízan los sistemas extensionales observados en tierra.
- 8) Durante el episodio de rift de la Cuenca de Málaga la zona de tierra fue sujeta a erosión y se desarrollaron fallas transtensionales de dirección WNW-ESE. La inclinación progresiva del flanco NE de la Cuenca de Málaga causó la migración de las arcillas de la unidad VI hacia el centro de la cuenca propiciando la generación del diapirismo de barro. A su vez, esto provocó la formación de fallas lítricas de tipo gravitacional en los niveles superiores de la cobertera sedimentaria.
- 9) La inversión tectónica es poco relevante en el área estudiada cuando se compara con otras áreas del Arco de Gibraltar. Se caracteriza por la

[Escriba texto]

presencia de pliegues menores afectando la cobertera sedimentaria en los márgenes de la cuenca, así como por el levantamiento de los altos estructurales. La mayor parte de estas estructuras compresivas se desarrollaron durante el Mioceno tardío.

9 References

- Aguado, R., Feinberg, H., Durand-Delga, M., Martín-Algarra, A., Esteras, M. and Didon, J., (1990). New data on the age of transgressive Miocene Formation of the Betic Internal Zones: the San Pedro de Alcántara Formation. *Revista de la Sociedad Geológica de España*, **3**, 79-85.
- Alcalá-García, F.J., López-Galindo, A. and Martín-Martín, M., (2002). El Paleoceno de la Alta Cadena (Subbético interno, cordillera Bética). Implicaciones en la evolución geodinámica del paleomargen sud-Ibérico. *Estudios Geológicos*, **58**, 75-85.
- Alonso-Chaves, F.M. and Orozco, M., (1998). El sistema de fallas extensionales de La Axarquía (Sierras de Tejeda y La Almirajara, Cordilleras Béticas). *Geogaceta*, **24**, 15-18.
- Alonso-Chaves, F.M. and Rodriguez-Vidal, J., (1998). Tectonic subsidence and synrift sedimentation associated with the rifting of the lower Miocene in the Alboran Domain (Betic Chain, Spain). *Comptes Rendus de l'Academie de Sciences - Serie Ila: Sciences de la Terre et des Planetes*, **326**(1), 51-56.
- Alonso, J.L., Marcos, A. and Suárez, A., (2006). Structure and organization of the Porma Mélange: progressive denudation of a submarine nappe toe by gravitational collapse. *American Journal of Science*, **306**, 32-65.
- Andrieux, J., Fontbote, J.M. and Mattauer, M., (1971). Sur un modele explicatif de l'arc de Gibraltar. *Earth and Planetary Science Letters*, **12**, 191-198.
- Aragón-Arreola, M. and Martín-Barajas, A., (2007). Westward migration of extension in the northern Gulf of California, Mexico. *Geology*, **35**(6), 571-574.
- Azañón, J.M., (1994). Metamorfismo de alta presión/baja temperatura, baja presión/alta temperatura y tectónica del Complejo Alpujárride (Cordilleras Bético-Rifeñas). PhD. Thesis. University of Granada, 331pp.
- Azañón, J.M., García-Dueñas, V. and Goffé, B., (1998). Exhumation of high-pressure metapelites and coeval crustal extension in the Alpujárride complex (Betic Cordillera). *Tectonophysics*, **285**, 231-252.
- Azañón, J.M. and Crespo-Blanc, A., (2000). Exhumation during a continental collision inferred from the tectonometamorphic evolution of the Alpujárride Complex in the central Betics (Alboran Domain, SE Spain). *Tectonics*, **19**(3): 549-565.
- Bailey, H.W., Bon, J. and Drummond, M.E., (1986). Well Alboran-A1, Stratigraphical/Paleontological final report. Chevron Petroleum Company of Spain. Project nº1730.
- Balanyá, J.C. and García-Dueñas, V., (1986). Grandes fallas de contracción y de extensión implicadas en el contacto entre los dominios de Alborán y Sudibérico en el arco de Gibraltar. *Geogaceta*, **1**, 19-21.
- Balanyá, J.C. and García-Dueñas, V., (1988). El Cabalgamiento Cortical de Gibraltar y la Tectónica de Béticas y Rif. *Sociedad Geológica de España, Actas, Granada, Spain*, 35-44.
- Balanyá, J.C., (1991). Estructura del Dominio de Alborán en la parte norte del arco de Gibraltar. PhD. Thesis. University of Granada, 210pp.
- Balanyá, J.C., García-Dueñas, V., Azañón, J.M. and Sánchez-Gómez, M., (1997). Alternating contractional and extensional events in the Alpujárride nappes of the Alboran Domain (Betics, Gibraltar Arc). *Tectonics*, **16**(2): 226-238.
- Balanyá, J.C., García-Dueñas, V., Azañón, J.M. and Sánchez-Gómez, M., (1998). Reply. *Tectonics*, **17**(6), 977-981

- Balanyá, J.C., Crespo-Blanc, A., Díaz Azpiroz, M., Expósito, I. and Luján, M., (2007). Structural trend line pattern and strain partitioning around the Gibraltar Arc accretionary wedge: Insights as to the mode of orogenic arc building. *Tectonics*, **26**(2), TC2005
- Balanyá, J.C., Crespo-Blanc, A., Díaz-Azpiroz, M., Expósito, I., Torcal, F., Pérez-Peña, V. and Booth-Rea, G., (2012). Arc-parallel vs. back-arc extension in the Western Gibraltar Arc: Is the Gibraltar forearc still active? *Geologica Acta*, **10**(3), 249-263.
- Balanyá, J.C., Barcos, L., Jiménez-Bonilla, A., Matito, E., Expósito, I. and Díaz Azpiroz, M., (2014). La zona de falla de Gaucín (Cadenas Béticas Occidentales) cinemática y rasgos morfoestructurales asociados. *Geogaceta*, **55**, 3-6.
- Ballesteros, M., Rivera, J., Muñoz, A., Muñoz-Martín, A., Acosta, J., Carbó, A. and Uchupi, E., (2009). Alboran Basin, southern Spain-Part II: Neogene tectonic implications for the orogenic float model. *Marine and Petroleum Geology*, **25**(1), 75-101.
- Barba-Martín, A., Martín-Serrano García, A. and Piles Mateo, E., (1979). Mapa Geológico de España. Scale 1:50.000, 2nd series, nº 1039, Colmenar. Madrid, Instituto Geológico y Minero de España, 88pp.
- Barcos, L., Díaz-Azpiroz, M., Balanyá, J.C. and Expósito, I., (2011). Dominios estructurales y reparto de la deformación en zonas transpresivas de corteza superior (Torcal de Antequera, Cadena Bética). *Geogaceta*, **50**, 31-34.
- Barcos, L., Balanyá, J.C., Díaz-Azpiroz, M., Expósito, I. and Jiménez-Bonilla, A., (2014). Kinematics of the Torcal Shear Zone: Transpressional tectonics in a salient-recess transition at the northern Gibraltar Arc. *Tectonophysics*, in press.
- Battistini, G., Toscani, L., Iacarino, S. and Villa, I.M., (1987). K/Ar ages and the geological setting of calc-alkaline volcanic rocks from Sierra de Gata, SE Spain. *Neues Jahrbuch für Mineralogie, Monatshefte*, 369-383.
- Beaumont, C., (1981). Foreland basins. *Geophysical Journal, Royal Astronomical Society*, **65**(2): 291-329.
- Bettelli, G. and Vannucchi, P., (2003). Structural style of the offscraped Ligurian oceanic sequences of the Northern Apennines: new hypothesis concerning the development of mélange block-in-matrix fabric. *Journal of Structural Geology*, **25**, 371-388.
- Booth-Rea, G., García-Dueñas, V. and Azañón, J.M., (2002). Extensional attenuation of the Malaguide and Alpujarride thrust sheets in a segment of the Alboran basin folded during the Tortonian (Lorca area, Eastern Betics). *Comptes Rendus Geoscience*, **334**, 557-563
- Booth-Rea, G., Azañón, J.M., García-Dueñas, V., Augier, R. and Sánchez-Gómez, M., (2003). A 'core-complex-like structure' formed by superimposed extension, folding and high-angle normal faulting. The Santi Petri dome (western Betics, Spain). *Comptes Rendus Geoscience*, **335**, 265-274.
- Booth-Rea, G., Azañón, J.M. and García-Dueñas, V., (2004). Extensional tectonics in the northeastern Betics (SE Spain): case study of extension in a multilayered upper crust with contrasting rheologies. *Journal of Structural Geology*, **26**(11), 2039-2058.
- Booth-Rea, G., Ranero, C.R., Martínez-Martínez, J.M. and Grevenmeyer, I., (2007). Crustal types and Tertiary tectonic evolution of the Alborán sea, western Mediterranean. *Geochemistry Geophysics Geosystems*, **8**(10), Q10005.
- Boulin, J., (1970). Les Zones Internes des Cordillères Bétiques de Málaga à Motril (Espagne méridionale). *Annales Hébert et Haug, Laboratoire de Géologie Historique, Faculté des Sciences de l'Université de Paris*, Paris, 237pp.

- Bourgeois, J., Chauve, P., Magne, J., Monnot, J., Y., P., Rigo, E. and Rivière, M., (1972). la Formation de las Millanas. Série Burdigalienne Transgressive, sur les Zones Internes des Cordillères Bétiques Occidentales (Région d'Alozaina-Tolox, Province de Malaga, Espagne). *Comptes Rendus Académie des Sciences (Paris) Série D*, **275**, 169-172.
- Bourgeois, J., Chauve, P., Lorenz, C., Monnot, J., Peyre, Y., Rigo, E. and Rivière, M., (1972). La formation d'Alozaina. Série d'âge Oligocène et Aquitanien transgressive sur le Bétique de Málaga (région d'Alozaina-Tolox, province de Málaga, Espagne). *Comptes Rendus de l'Académie des Sciences, Série B*, **275**, 531-534.
- Bourgeois, J., (1978). La transversale de Ronda. Cordillères Bétiques, Espagne. Données géologiques pour un modèle d'évolution de l'Arc de Gibraltar. *Annales Scientifiques de l'Université de Besançon*, **30**, 445.
- Braga, J.C. and Aguirre, J., (2001). Coralline algal assemblages in upper Neogene reef and temperate carbonates in Southern Spain. *Palaeogeography, Palaeoclimatology, Palaeoecology*, **175**(1-4), 27-41.
- Braga, J.C., Martín, J.M. and Quesada, C., (2003). Patterns and average rates of late Neogene–Recent uplift of the Betic Cordillera, SE Spain. *Geomorphology*, **50**(1–3), 3-26.
- Brown, L.F. and Fisher, W.L., (1977). Seismic-stratigraphic interpretation of depositional systems: Examples from Brazilian rift and pull-apart basins, C.E. Payton, ed. *Seismic Stratigraphy—applications to hydrocarbon exploration*. AAPG Memoir, **26**, 213-248.
- Brun, J.-P. and Faccenna, C., 2008. Exhumation of high-pressure rocks driven by slab rollback. *Earth and Planetary Science Letters*, **272**(1–2), 1-7.
- Calvert, A., Sandvol, E., Seber, D., Barazangi, M., Roecker, S., Mourabit, T., Vidal, F., Alguacil, G. and Jabour, N., (2000). Geodynamic evolution of the lithosphere and upper mantle beneath the Alboran region of the western Mediterranean: Constraints from travel time tomography. *Journal of Geophysical Research: Solid Earth*, **105**(B5), 10871-10898.
- Camerlenghi, A. and Pini, G.A., (2009). Mud volcanoes, olistostromes and Argille scagliose in the Mediterranean region. *Sedimentology*, **56**(1), 319-365.
- Campillo, A.C., Maldonado, A. and Mauffret, A., (1992). Stratigraphic and tectonic evolution of the western Alboran Sea: Late miocene to recent. *Geo-Marine Letters*, **12**(2-3), 165-172.
- Cano Medina, F., Ruiz Reig, P., (1982). Mapa Geológico de España. Scale 1:50.000, 2nd series, nº 1038, Ardales. Madrid, Instituto Geológico y Minero de España, 56pp.
- Cartwright, J., Jackson, M., Dooley, T. and Higgins, S., (2012). Strain partitioning in gravity-driven shortening of a thick, multilayered evaporite sequence, *Geological Society Special Publication*, pp. 449-470.
- Catuneanu, O., (2002). Sequence stratigraphy of clastic systems: Concepts, merits, and pitfalls. *Journal of African Earth Sciences*, **35**(1), 1-43.
- Catuneanu, O., Khalifa, M.A. and Wanas, H.A., (2006). Sequence stratigraphy of the Lower Cenomanian Bahariya Formation, Bahariya Oasis, Western Desert, Egypt. *Sedimentary Geology*, **190**(1–4), 121-137.
- Catuneanu, O., Abreu, V., Bhattacharya, J.P., Blum, M.D., Dalrymple, R.W., Eriksson, P.G., Fielding, C.R., Fisher, W.L., Galloway, W.E., Gibling, M.R., Giles, K.A., Holbrook, J.M., Jordan, R., Kendall, C.G.S.C., Macurda, B., Martinsen, O.J., Miall, A.D., Neal, J.E., Nummedal, D., Pomar, L., Posamentier, H.W., Pratt, B.R., Sarg, J.F., Shanley, K.W., Steel, R.J., Strasser, A., Tucker,

- M.E. and Winker, C., (2009). Towards the standardization of sequence stratigraphy. *Earth-Science Reviews*, **92**(1–2), 1-33.
- Catuneanu, O., Galloway, W.E., Kendall, C.G.S.C., Miall, A.D., Posamentier, H.W., Strasser, A. and Tucker, M.E., (2011). Sequence Stratigraphy: Methodology and nomenclature. *Newsletters on Stratigraphy*, **44**(3), 173-245.
- Cavazza, W. and Barone, M., (2011). Large-scale sedimentary recycling of tectonic mélange in a forearc setting: The Ionian basin (Oligocene-Quaternary, southern Italy). *Geological Society of America Bulletin*, **122**, 1932-949.
- Chalouan, A. and Michard, A., (1990). The Ghomarides nappes, Rif costal range, Morocco: A variscan chip in the Alpine belt. *Tectonics*, **9**, 1565-1583.
- Chalouan, A., Ouazani-Touhami, A., Mouhir, L., Saji, R. and Benmakhlouf, M., (1995). Les failles normales a faible pendage du Rif interne (Maroc) et leur effet sur l'amincissement crustal du domaine d'Alborán. *Geogaceta*, **17**, 107-109.
- Chalouan, A., Saji, R., Michard, A. and Bally, A.W., (1997). Neogene tectonic evolution of the southwestern Alboran basin as inferred from seismic data off Morocco. *AAPG Bulletin*, **81**(7), 1161-1184.
- Chalouan, A., Michard, A., El Kadiri, K., Negro, F., Frizon de Lamotte, D., Soto, J.I. and Saddiqi, O., (2008). The Rift Belt. In: *The Rif belt continental evolution: the geology of Morocco. Structure, stratigraphy, and tectonics of the Africa-Atlantic-Mediterranean triple junction. Lecture in Earth Sciences* (Ed. by A. Michard, O. Saddiqi, A. Chalouan and D. Frizon de Lamotte), **116**, 203-302.
- Chamón Cobos, C., Quinquer Agut, R., Crespo, V., Aguilar, M. and Reyes, J.L., (1976). Mapa Geológico de España. Scale 1:50.000, 2nd series, nº 1052, Alora. Madrid, Instituto Geológico y Minero de España, 71pp.
- Chamón Cobos, C., Estévez González, C. and Piles Mateo, E., (1977). Mapa Geológico de España. Scale 1:50.000, 2nd series, nº 1072, Estepona. Madrid, Instituto Geológico y Minero de España, 33pp.
- Christie-Blick, N. and Driscoll, N.W., (1995). Sequence stratigraphy. *Annual Review of Earth & Planetary Sciences*, **23**, 451-478.
- Clauzon, G., Suc, J.-P., Gautier, F., Berger, A. and Loutre, M.-F., (1996). Alternate interpretation of the Messinian salinity crisis: Controversy resolved? *Geology*, **24**(4), 363-366.
- Comas, M.C., García-Dueñas, V. and Navarra Vila, F., (1978). Mapa Geológico de España. Scale 1:50.000, 2nd series, nº 992, Moreda. Madrid, Instituto Geológico y Minero de España, 51pp.
- Comas, M.C., García-Dueñas, V. and Jurado, M.J., (1992). Neogene tectonic evolution of the Alboran Sea from MCS data. *Geo-Marine Letters*, **12**(2-3), 157-164.
- Comas, M.C., Zahn, R., Klaus, A., Aubourg, C., Belanger, P.E., Bernasconi, S.M., Cornell, W., De Kaenel, E.P., De Larouzière, F.D., Doglioni, C., Doose, H., Fukusawa, H., Hobart, M., Iaccarino, S.M., Ippach, P., Marsaglia, K., Meyers, P., Murtan, A., O'Sullivan, G.M., Platt, J.P., Prasad, M., Siesser, W.G., Skilbeck, C.G., Soto, J.I., Tandon, K., Torii, M., Tribble, J.S. and Wilkens, R.H., (1996). Proceedings ODP, Initial Reports. Ocean Drilling Program, College Station, TX, 161.
- Comas, M.C., Platt, J.P., Soto, J.I. and Watts, A.B., (1999). The origin and tectonic history of the Alboran Basin: Insights from Leg 161 results. *Proceedings of the Ocean Drilling Program: Scientific Results*, **161**, 555-580.
- Comas, M.C. and Soto, J.I., (1999). Brittle deformation in the metamorphic basement at Site 976: Implications for middle Miocene extensional tectonics in the Western Alboran Basin. *Proceedings of the Ocean Drilling Program: Scientific Results*, **161**, 331-344.

- Comas, M.C., Suades, E. and Crespo-Blanc, A., (2012). From Mud Diapirs to Mud Volcanoes: Shale Tectonics within the Structural Evolution of the Alboran Sea Basin, VIII Congreso Geológico de España. Geotemas, Oviedo.
- Cowan, D.S. and Pini, G.A., (2001). Disrupted and chaotic rock units in the Apennines. In: Vai, G.B., Martini, I.P. (eds.). *Anatomy of a Mountain Belt: The Apennines and Adjacent Mediterranean basins*. Dordrecht, Kluwer Academic Publishers, 165-176.
- Crespo-Blanc, A., (1995). Interference pattern of extensional fault systems: a case study of the Miocene rifting of the Alboran basement (North of Sierra Nevada, Betic Chain). *Journal of Structural Geology*, **17**(11), 1559-1569.
- Crespo-Blanc, A. and Campos, J., (2001). Structure and kinematics of the South Iberian paleomargin and its relationship with the Flysch Trough units: extensional tectonics within the Gibraltar Arc fold-and-thrust belt (western Betics). *Journal of Structural Geology*, **23**(10), 1615-1630.
- Crespo-Blanc, A. and de Lamotte, D.F., (2006). Structural evolution of the external zones derived from the Flysch trough and the South Iberian and Maghrebian paleomargins around the Gibraltar arc: A comparative study. *Bulletin de la Societe Geologique de France*, **177**(5), 267-282.
- Crespo-Blanc, A., Balanyá, J.C., Expósito, I. and Luján, M., (2010). Fault-bounded imbricate stacks vs. chaotic structure in the westernmost Flysch Trough units (northern Gibraltar Arc): a revised geological map. *Geogaceta*, **48**, 187-190.
- Crespo-Blanc, A., Comas, M.C. and Balanyá, J.C., (2012). Updating of Tectonic Maps from the Betics: A Tool to Establish First Order Milestones of the Geodynamic Evolution of the Gibraltar Arc System, VIII Congreso Geológico de España. Geotemas, Oviedo.
- Crespo-Blanc, A., Balanyá, J.C., Expósito, I., Luján, M. and Suades, E., (2012). Crescent-like large-scale structures in the external zones of the western Gibraltar Arc (Betic-Rif orogenic wedge). London, *Journal of the Geological Society*, **169**(6), 667-679.
- Crespo-Blanc, A., Comas, M. and Balanyá, J.C., (2013). Miocene Paleotectonic restorations of the Gibraltar Arc System: structural domains, transfer fault zones, main detachments and vertical-axis rotations. *The Circum-Mediterranean basins and analogues*, ILP Marseille.
- Crespo-Blanc, A., Comas, M. and Balanyá, J.C., (Submitted). Clues for a Tortonian reconstruction of the Gibraltar Arc: structural pattern, deformation diachronism and block rotations. *Tectonophysics*.
- Cruz-Sanjulián, J. and Ruiz Reig, P., (1980). Mapa Geológico de España. Scale 1:50.000, 2nd series, nº 1037, Teba. Madrid, Instituto Geológico y Minero de España, 89pp.
- Cuevas, J., Navarro-Vilá, F. and Tubía, J.M., (2001). Evolución estructural poliorogénica del Complejo Maláguide (cordilleras Béticas). *Boletín Geológico y Minero*, **112**(3), 47-58.
- De Capoa, P., Di Staso, A., Perrone, V. and Najib-Zaghloul, M., (2007). The age of the foredeep sedimentation in the Betic-Rifian Mauretanic units. A major constraint of the reconstruction of the tectonic evolution of the Gibraltar Arc. *Comptes Rendus Geoscience*, **339**, 161-170.
- De la Linde, J., Comas, M.C. and Soto, J.I., (1996). Morfología del Basamento en el Noroeste del Mar de Alborán. *Geogaceta*, **20**, 355-358.
- De Larouziere, F.D., Pezard, P.A., Comas, M.C., Celerier, B. and Vergniault, C. (1999). Structure and tectonic stresses in metamorphic basement, Site 976, Alboran Sea. *Proceedings of the Ocean Drilling Program: Scientific Results*, **161**, 319-329.
- De Lis Mancilla, F., Stich, D., Berrocoso, M., Martín, R., Morales, J., Fernandez-Ros, A., Páez, R. and Pérez-Peña, A., (2013). Delamination in the Betic Range: Deep structure, seismicity, and GPS motion. *Geology*, **41**(3), 307-310.

- Del Olmo Sanz, A., Moreno Serrano, F., Campos Fernández, J., Estevez, A., García-Dueñas, V., García-Rossell, L., Martín Algarra, A., Orozco, M. and Sanz de Galdeano, C., (1981). Mapa Geológico de España. Scale 1:50.000, 2nd series, nº 1051, Ronda. Madrid, Instituto Geológico y Minero de España, 56pp.
- Dercourt, J., Zonenshain, L.P., Ricou, L.E., Kazmin, V.G., Le Pichon, X., Knipper, A.L., Grandjacquet, C., Sbertshikov, I.M., Geysant, J., Lepvrier, C., Pechersky, D.H., Boulin, J., Sibuet, J.C., Savostin, L.A., Sorokhtin, O., Westphal, M., Bazhenov, M.L., Lauer, J.P. and Biju-Duval, B., (1986). Geological evolution of the tethys belt from the atlantic to the pamirs since the LIAS. *Tectonophysics*, **123**(1-4), 241-315.
- Dewey, J.F., (1980). Episodicity, sequence, and style at convergent plate boundaries. The continental crust and its mineral deposits. Proc. symposium held for J.Tuzo Wilson, Toronto, May 1979, 553-573.
- Díaz-Azpiroz, M., Barcos, L., Balanyá, J.C., Fernández, C., Expósito, I. and Czeck, D.M., (2014). Applying a general triclinic transpression model to highly partitioned brittle-ductile shear zones: A case study from the Torcal de Antequera massif, external Betics, southern Spain. *Journal of Structural Geology*, **68**, 316-336.
- Díaz Merino, C., Comas, C.M. and Martínez del Olmo, W., (2003). Secuencias de depósito neógenas del margen noroeste del Mar de Alborán, Cuenca de Málaga. *Geotemas*, **5**, 61-65.
- Dickey, J.S., Obata, M. and Suen, C.J., (1979). Chemical differentiation of the lower lithosphere as represented by the Ronda ultramafic massif, southern Spain. *Physics and Chemistry of the Earth*, **11**(C), 587-595.
- Didon, J., (1969). Etude géologique du Campo de Gibraltar (Espagne méridionale). Doctoral Thesis. Université Paris, 539pp.
- Do Couto, D., Gumiaux, C., Augier, R., Le Bret, N., Folcher, N., Jouannic, G., Jolivet, L., Suc, J.P. and Gorini, C., (2014). Tectonic inversion of an asymmetric graben: Insights from a combined field and gravity survey in the sorbas basin. *Tectonics*, **33**(7), 1360-1385.
- Docherty, J. and Banda, E., (1992). A note on the subsidence history of the northern margin of the Alboran Basin. *Geo-Marine Letters*, **12**(2-3), 82-87.
- Doglioni, C., Carminati, E., Cuffaro, M. and Scrocca, D., (2007). Subduction kinematics and dynamic constraints. *Earth-Science Reviews*, **83**(3-4), 125-175.
- Doglioni, C., Harabaglia, P., Merlini, S., Mongelli, F., Peccerillo, A. and Piromallo, C., (1998). Orogens and slabs vs. their direction of subduction. *Earth Science Reviews*, **45**(3-4), 167-208.
- Duggen, S., Hoernle, K., van den Bogaard, P. and Harris, C., (2004). Magmatic evolution of the Alboran region: The role of subduction in forming the western Mediterranean and causing the Messinian Salinity Crisis. *Earth and Planetary Science Letters*, **218**(1-2), 91-108.
- Duggen, S., Hoernle, K., Klügel, A., Geldmacher, J., Thirlwall, M., Hauff, F., Lowry, D. and Oates, N. (2008). Geochemical zonation of the Miocene Alborán Basin volcanism (westernmost Mediterranean): geodynamic implications. *Contributions to Mineralogy and Petrology*. *Contributions to Mineralogy and Petrology*, **156**(5), 577-593.
- Dunbar, C.O., Rodgers, J., (1957). Principles of Stratigraphy. New York, Wiley & Sons, 356pp.
- Durand-Delga, M. and Foucault, A., (1967). La dorsale Bétique, nouvel élément paléogéographique et structural des cordillères Bétiques au bord sud de la Sierra Arana (Province de Grenade, Espagne). *Bulletin de la Société Géologique de France*, **9**, 723-728.
- Durand-Delga, M., (1972). La courbure de Gibraltar, extrémité occidentale des chaînes Alpines, unit l'Europe et l'Afrique. *Eclogae Geologicae Helveticae*, **65**(2), 267-278.

- Durand-Delga, M. and Fonboté, J.M., (1980). Le cadre structural de la Méditerranée occidentale. 26^o Congrès Géol. Intern. Paris, Colloque n^o 5 (Les chaines alpines issues de la Téthys), Mem. B.R.G.M.
- Durand-Delga, M., Feinberg, H., Magné, J., Olivier, P. and Anglada, R., (1993). The Oligo-Miocene deposits resting in discordance upon the Maláguides and Alpujarrides and their implications in the geodynamic evolution of the Betic Cordillera and the Alborán Mediterranean. *Comptes Rendus de l'Académie des Sciences, Serie IIA, Sciences de la Terre et des Planètes*, **317**, 679-687.
- Durand-Delga, M., Rossi, P., Olivier, P. and Puglisi, D., (2000). Situation structurale et nature ophiolitique de roches basiques jurassiques associées aux flysch maghrébins du Rif (Maroc) et de Sicile (Italie). *Comptes Rendus Acad. Sci. Paris*, **331**, 29-38.
- El Kadiri, K., Chalouan, A., El Mrihi, A., Hlila, R., López-Garrido, A.C., Sanz de Galdeano, C., Serrano, F. and Kerzazi, K., (2001). Les formations sédimentaires olistolitiques de l'Oligocène supérieur-Miocène inférieur dans l'unité ghomaride des Béni Hozmar (secteur de Talembote, Rif septentrional, Maroc). *Eclogae Geologicae Helveticae*, **94**, 313-320.
- Elorza, J.J., García Dueñas, V., and González Donoso, J.M., (1978). Mapa Geológico de España. Scale 1:50.000, 2nd series, n^o 1040, Zafarraya. Madrid, Instituto Geológico y Minero de España, 54pp.
- Elorza, J.J. and García Dueñas, V., (1980). Mapa Geológico de España. Scale 1:50.000, 2nd series, n^o 1054, Velez-Málaga. Madrid, Instituto Geológico y Minero de España.
- Embry, A.F. and Johannessen, E., (1992). T-R Sequence Stratigraphy, Facies Analysis and Reservoir Distribution in the Uppermost Triassic-Lower Jurassic Succession, Western Sverdrup Basin, Arctic Canada. In: T. Vorren (Editor), *Arctic Geology and Petroleum Potential Norwegian Petroleum Society Special Publication*.
- Embry, A.F., (1993). Transgressive-regressive (T-R) sequence analysis of the Jurassic succession of the Sverdrup Basin, Canadian Arctic Archipelago. *Canadian Journal of Earth Sciences*, **30**(2), 301-320.
- Embry, A.F., (2009). Practical Sequence Stratigraphy. Online at www.cspg.org, 79 p.
- Estévez González, C. and Chamón Cobos, C., (1978). Mapa Geológico de España. Scale 1:50.000, 2nd series, n^o 1053/1067, Málaga/Torremolinos. Madrid, Instituto Geológico y Minero de España, 33pp.
- Esteras, M., Feinberg, H. and Durand-Delga M., (1995). Nouveaux éléments sur l'âge des grès numidiens de la nappe de l'Aljibe (Sud-Ouest de l'Andalousie. Espagne), IV Coloquio Internacional sobre el enlace fijo del Estrecho de Gibraltar, Soc. Esp. De Estud. para la Comun. fija a Través del Estrecho de Gibraltar, Seville, Spain.
- Estrada, F., Ercilla, G., Gorini, C., Alonso, B., Vázquez, J.T., García-Castellanos, D., Juan, C., Maldonado, A., Ammar, A. and Elabbassi, M., (2011). Impact of pulsed Atlantic water inflow into the Alboran Basin at the time of the Zanclean flooding. *Geo-Marine Letters*, **31**(5-6), 361-376.
- Faccenna, C., Piromallo, C., Crespo-Blanc, A., Jolivet, L. and Rossetti, F., (2004). Lateral slab deformation and the origin of the western Mediterranean arcs. *Tectonics*, **23**(1), TC1012.
- Feinberg, H. and Olivier, P., (1983). Dating of Aquitanian and Burdigalian levels in the Betic-Rifian 'Zone Predorsalienne' and consequences. *Comptes Rendus des Seances - Academie des Sciences, Serie II*, **296**(6), 473-476.
- Fernández-Ibáñez, F., Soto, J.I., Zoback, M.D. and Morales, J., (2007). Present-day stress field in the Gibraltar Arc (western Mediterranean). *Journal of Geophysical Research: Solid Earth*, **112**(B8), B08404.

- Fernández-Ibáñez, F. and Soto, J.I., (2008). Crustal rheology and seismicity in the Gibraltar Arc (western Mediterranean). *Tectonics*, **27**(2), TC2007.
- Festa, A., Pini, G.A., Yildirim, D. and Giulia, C., (2010). Mélanges and mélange-forming processes: a historical overview and new concepts. *International Geology Review*, **52**(10), 1040-1105.
- Flores, G., (1959). Evidence of slump phenomena (olistostromes) in areas of hydrocarbon exploration in Sicily. *Proceedings, Fifth World Petroleum Congress*, 259-275.
- Frasca, G., Gueydan, F. and Brun, J.P., (2015). Structural record of Lower Miocene westward motion of the Alboran Domain in the Western Betics, Spain. *Tectonophysics*, (2015), doi: 10.1016/j.tecto.2015.05.017.
- Frazier, D.E., (1974). Depositional episodes: their relationship to the Quaternary stratigraphic framework in the northwestern portion of the Gulf Basin. *Bureau of Economic Geology, Geological Circular*, **4**, 1-28.
- Galloway, W.E., (1989). Genetic stratigraphic sequences in basin analysis, I: Architecture and genesis of flooding surface bounded depositional units. *The American Association of Petroleum Geologists Bulletin*, **73**(2), 125-142.
- Galindo-Zaldívar, J., Jabaloy, A., González-Lodeiro, F. and Aldaya, F., (1997). Crustal structure of the central sector of the Betic Cordillera (SE Spain). *Tectonics*, **16**(1), 18-37.
- García-Castellanos, D., Estrada, F., Jiménez-Munt, I., Gorini, C., Fernández, M., Vergés, J. and De Vicente, R., (2009). Catastrophic flood of the Mediterranean after the Messinian salinity crisis. *Nature*, **462**(7274), 778-781.
- García de Domingo, A., Hernaíz Huerta, P.P., Balanyá, J.C., García-Dueñas, V. and Ruiz Reig, P., (1994). Mapa Geológico de España. Scale 1:200.000, 1st series, nº 87, Algeciras. Madrid, Instituto Geológico y Minero de España, 89pp.
- García-Dueñas, V., Balanyá, J.C. and Martínez-Martínez, J.M., (1992). Miocene extensional detachments in the outcropping basement of the northern Alboran Basin (Betics) and their tectonic implications. *Geo-Marine Letters*, **12**(2-3), 88-95.
- González Donoso, J.M., Linares, D., Martín-Algarra, A. and Serrano, F., (1987). El complejo tectosedimentario del Campo de Gibraltar. Datos sobre su edad y significado geológico. *Boletín de la Real Sociedad Española de Historia Natural (Geol.)*, **82**(1-4), 233-251.
- Gorini, C., Lofi, J., Duvail, C., Dos Reis, A.T., Guennoc, P., Lestrat, P. and Mauffret, A., (2005). The Late Messinian salinity crisis and Late Miocene tectonism: Interaction and consequences on the physiography and post-rift evolution of the Gulf of Lions margin. *Marine and Petroleum Geology*, **22**(6-7), 695-712.
- Guerra-Merchán A, Serrano, F., Garcés, M., Gofas, S., Esu, D., Gliozzi, E. and Grossi, F., (2010). Messinian Lago-Mare deposits near the Strait of Gibraltar (Malaga Basin, S Spain). *Palaeogeography, Palaeoclimatology, Palaeoecology*, **285**, 264-276.
- Gutscher, M.A., (2012). Subduction beneath Gibraltar? Recent studies provide answers. *Eos*, **93**(13), 133-134.
- Haq, B.U., Hardenbol, J. and Vail, P.R., (1987). Chronology of fluctuating sea levels since the Triassic. *Science*, **235**(4793), 1156-1167.
- Helland-Hansen, W. and Martinsen, O.J., (1996). Shoreline trajectories and sequences: description of variable depositional-dip scenarios. *Journal of Sedimentary Research* **66** (4), 670-688.

- Hinsken, S., Ustaszewski, K. and Wetzel, A., (2007). Graben Width Controlling Syn-Rift Sedimentation: The Palaeogene Southern Upper Rhine Graben as an Example. *International Journal of Earth Sciences*, **96**, 979-1002.
- Hlila, R., Chalouan, A., El Kadiri, K., Sanz de Galdeano, C., Martín-Pérez, J.A., Serrano, F., López-Garrido, A.C., Maaté, A. and Guerra-Merchán, A., (2008). New stratigraphic data of the oligo-miocene transgressive cover of the Ghomaride units (Northern internal Rif, Morocco): Implications on tectonosedimentary evolution. *Revista de la Sociedad Geológica de España*, **21**(1-2), 59-71.
- Hunt, D. and Tucker, M.E., (1992). Stranded parasequences and the forced regressive wedge systems tract: deposition during base-level fall. *Sedimentary Geology*, **81**, 1-9.
- Horváth, F., Bada, G., Szafián, P., Tari, G., Ádám, A. and Cloetingh, S., (2006). Formation and deformation of the Pannonian Basin: Constraints from observational data. In: D.G. Gee and R.A. Stephenson (Editors), pp. 191-206.
- Insua-Arévalo, J.M., Martínez-Díaz, J.J., García-Mayordomo, J. and Martín-González, F., (2012). Active tectonics in the Malaga Basin: evidences from mophotectonic markers (Western Betic Cordillera, Spain). *Journal of Iberian geology*, **38**(1), 185-199.
- Iribarren, L., Vergés, J. and Fernández, M., (2009). Sediment supply from the Betic-Rif orogen to basins through Neogene. *Tectonophysics*, **475**(1), 68-84.
- Jeanbourquin, P., (1994). Early deformation of ultrahelvetetic mélanges in the helvetic nappes (Western Swiss Alps). *Journal of Structural Geology*, **16**(10), 1367-1383.
- Johnson, J.G. and Murphy, M.A., (1984). Time-rock model for Siluro- Devonian continental shelf, western United States. *Geological Society of America Bulletin*, **95**(11), 1349-1359.
- Jolivet, L. and Faccenna, C., (2000). Mediterranean extension and the Africa-Eurasia collision. *Tectonics*, **19**(6), 1095-1106.
- Juhász, G., Pogácsás, G., Magyar, I. and Vakarcs, G., (2007). Tectonic versus climatic control on the evolution of fluvio-deltaic systems in a lake basin, Eastern Pannonian Basin. *Sedimentary Geology*, **202**(1-2), 72-95.
- Jurado, M.J. and Comas, M.C., (1992). Well log interpretation and seismic character of the cenozoic sequence in the northern Alboran Sea. *Geo-Marine Letters*, **12**(2-3), 129-136.
- Kaenel, E., Siesser, W.G. and Murat, A., (1999). Pleistocene calcareous nannofossil biostratigraphy and the western mediterranean sapropels, sites 974 to 977 and 979. *Proceedings of the Ocean Drilling Program: Scientific Results*, **161**, 159-183.
- Krézsek, C. and Bally, A.W., (2006). The Transylvanian Basin (Romania) and its relation to the Carpathian fold and thrust belt: Insights in gravitational salt tectonics. *Marine and Petroleum Geology*, **23**(4), 405-442.
- Krijgsman, W., Hilgen, F.J., Raffi, I., Sierro, F.J. and Wilson, D.S., (1999). Chronology, causes and progression of the Messinian salinity crisis. *Nature*, **400**(6745), 652-655.
- Lenoir, X., Garrido, C.J., Bodinier, J.L., Dautria, J.M. and Gervilla, F., (2001). The recrystallization front of the Ronda periodite: Evidence for melting and thermal erosion of subcontinental lithospheric mantle beneath the Alboran basin. *Journal of Petrology*, **42**(1), 141-158.
- Lister, G.S. and Davis, G.A., (1989). The origin of metamorphic core complexes and detachment faults formed during Tertiary continental extension in the northern Colorado River region, U.S.A. *Journal of Structural Geology*, **11**(1-2), 65-94.
- Lonergan, L. and White, N., (1997). Origin of the Betic-Rif mountain belt. *Tectonics*, **16**(3), 504-522.

- López-Garrido, A.C. and Sanz de Galdeano, C., (1999). Neogene sedimentation and tectonic-eustatic control of the Málaga Basin, South Spain. *Journal of Petroleum Geology*, **22**(1), 81-96.
- López-Garrido, A.C. and Sanz de Galdeano, C., (1991). La comunicación en el Tortonense entre el Atlántico y el Mediterráneo por la cuenca del Guadalhorce (Málaga). *Primer Congreso Español del Terciario*, Vic, Barcelona, 190-193.
- López Olmedo, F., Díaz de Neira, A., Enrile Alvir, A. and Hernaiz Huerta, P., (1988). Mapa Geológico de España. Scale 1:50.000, 2nd series, nº 991, Iznalloz. Madrid, Instituto Geológico y Minero de España, 84pp.
- Lucente, C.C. and Pini, G.A., (2008). Basin-wide mass-wasting complexes as markers of the Oligo-Miocene foredeepaccretionary wedge evolution in the Northern Apennines, Italy. *Basin Research*, **20**, 49-71.
- Luján, M., Balanyá, J.C. and Crespo-Blanc, A., (2000). Contractional and extensional tectonics in Flysch and Penibetic units (Gibraltar Arc, SW Spain): New constraints on emplacement mechanisms. *Comptes Rendus de l'Académie des Sciences*, **330**, 631-638.
- Luján, M., Storti, F., Balanyá, J.C., Crespo-Blanc, A. and Rossetti, F., (2003). Role of decollement material with different rheological properties in the structure of the Aljibe thrust imbricates (Flysch Trough, Gibraltar Arc): An analogue modelling approach. *Journal of structural Geology*, **25**, 867-881.
- Luján, M., Crespo-Blanc, A. and Balanyá, J.C., (2006). The Flysch Trough thrust imbricate (Betic Cordillera): A key element of the Gibraltar Arc orogenic wedge. *Tectonics*, **25**(6), TC6001.
- Lupiani Moreno, E. and Soria Mingorance J.M., (1985). Mapa Geológico de España. Scale 1:50.000, 2nd series, nº 1025, Loja. Madrid, Instituto Geológico y Minero de España, 53pp.
- Maldonado, A., Campillo, A.C., Mauffret, A., Alonso, B., Woodside, J. and Campos, J., (1992). Alboran Sea Late Cenozoic tectonic and Stratigraphic evolution. *Geo-Marine Letters*, **12**, 179-186.
- Marín-Lechado, C., Galino-Zaldívar, J., Rodríguez-Fernández, L.R. and Pedrera, A., (2007). Mountain front development by folding and crustal thickening in the internal zone of the Betic Cordillera-Alboran Sea Boundary. *Pure and applied Geophysics*, **167**, 1-21
- Marsaglia, K.M., Latter, K.K. and Cline, V., (1999). Sand provenance in the Alboran and Tyrrhenian basin. In: *Proc. ODP, Sci. Results* (Ed. by R. Zahn, M. C. Comas and A. Klaus), Ocean Drilling Program, College Station, TX, **161**, 37-56.
- Martín-Algarra, A., (1987). Evolución Geológica Alpina del Contacto entre las Zonas Internas y las Zonas Externas de la Cordillera Bética (Sector Central y Occidental). PhD. Thesis, Universidad de Granada, 1171 pp.
- Martín-Algarra, A., Gervilla, F., Garrido, C.J., Estévez, A., García-Casco, A., Sánchez-Gómez, M., Balanyá, J.C., García-Dueñas, V. and Torres-Roldán, R.L., (2004). Peridotitas de Ronda. In: Vera, J.A. (ed.). *Geología de España*. Madrid, Sociedad Geológica de España, Instituto Geológico y Minero de España (SGE-IGME), 414-416.
- Martín-Algarra, A., Mazzoli, S., Perrone, V. and Rodríguez-Cañero, R., (2009). Variscan tectonics in the malaguide complex (Betic Cordillera, Southern Spain): Stratigraphie and structural alpine versus pre-alpine constraints from the ardales area (Province of Malaga). II. structure. *Journal of Geology*, **117**(3), 263-284.
- Martín-Barajas, A., Vázquez-Hernández, S., Carreño, A.L., Helenes, J., Suárez-Vidal, F. and Alvarez-Rosales, J., (2001). Late Neogene stratigraphy and tectonic control on facies evolution in the Laguna Salada Basin, northern Baja California, Mexico. *Sedimentary Geology*, **144**(1-2), 5-35.

- Martin-Martin, M., El Mamoune, B., Martin-Algarra, A. and Martin-Perez, J.A., (1996). Internal-external zone boundary in the eastern Betic Cordillera, SE Spain: discussion. *Journal of Structural Geology*, **18**(4), 523-524.
- Martín, J. and Braga, J.C., (1994). Messinian events in the Sorbas Basin in southeastern Spain and their implications in the recent history of the Mediterranean. *Sedimentary Geology*, **90**(3-4), 257-268.
- Martín, J., Braga, J.C. and Betzler, C., (2001). The messinian Guadalquivir corridor: The last Northern, Atlantic-Mediterranean gateway. *Terra Nova*, **13**(6), 418-424.
- Martín-Serrano García A., (1982). Mapa Geológico de España. Scale 1:50.000, 2nd series, nº 1023, Antequera. Madrid, Instituto Geológico y Minero de España, 48pp.
- Martínez-García, P., Soto, J. and Comas, M., (2011). Recent structures in the Alboran Ridge and Yusuf fault zones based on swath bathymetry and sub-bottom profiling: evidence of active tectonics. *Geo-Marine Letters*, **(1)**, 19-36.
- Martínez-García, P., (2012). Recent tectonic evolution of the Alboran Ridge and Yusuf regions. PhD. Thesis, Universidad de Granada, 269 pp.
- Martínez-García, P., Comas, M., Soto, J.I., Lonergan, L. and Watts, A.B., (2013). Strike-slip tectonics and basin inversion in the Western Mediterranean: The Post-Messinian evolution of the Alboran Sea. *Basin Research*, **25**(4), 361-387.
- Martínez-Martínez, J.M. and Azañón, J.M., (1997). Mode of extensional tectonics in the southeastern Betics (SE Spain): Implications for the tectonic evolution of the peri-Alborán orogenic system. *Tectonics*, **16**(2), 205-225.
- Martínez-Martínez, J.M., Soto, J.I. and Balanyá, J.C., (2002). Orthogonal folding of extensional detachments: Structure and origin of the Sierra Nevada elongated dome (Betics, SE Spain). *Tectonics*, **21**(3), 3-13-20.
- Martínez del Olmo, W. and Comas, M.C., (2008). Arquitectura Sísmica, Olistostromas y Fallas Extensionales en el Norte de la Cuenca Oeste del Mar de Alborán. *Revista de la Sociedad Geológica de España*, **21**, 151-167.
- Martins-Neto, M.A. and Catuneanu, O., (2010). Rift sequence stratigraphy. *Marine and Petroleum Geology*, **27**(1), 247-253.
- Martinsen, O.J., Sømme, T.O., Thurmond, J.B., Helland-Hansen, W. and Lunt, I., (2010). Source-to-sink systems on passive margins: Theory and practice with an example from the Norwegian continental margin, pp. 913-920.
- Matenco, L. and Andriessen, P., (2013). Quantifying the mass transfer from mountain ranges to deposition in sedimentary basins: Source to sink studies in the Danube Basin-Black Sea system. *Global and Planetary Change*, **103**, 1-18.
- Matenco, L. and Radivojević, D., (2012). On the formation and evolution of the Pannonian Basin: Constraints derived from the structure of the junction area between the Carpathians and Dinarides. *Tectonics*, **31**(6), TC6007.
- Mathisen, M.E. and Vondra, C.F., (1983). The fluvial and pyroclastic deposits of the Cagayan basin, Northern Luzon, Philippines - an example of non-marine volcanoclastic sedimentation in an interarc basin. *Sedimentology*, **30**(3), 369-392.
- Mauffret, A., Ammar, A., Gorini, C. and Jabour, H., (2007). The Alboran Sea (Western Mediterranean) revisited with a view from the Moroccan Margin. *Terra Nova*, **19**(3), 195-203.
- Mazzoli, S. and Helman, M., (1994). Neogene patterns of relative plate motion for Africa-Europe: some implications for recent central Mediterranean tectonics. *Geologische Rundschau*, **83**(2), 464-468.

- Medialdea, T., Vegas, R., Somoza, L., Vázquez, J.T., Maldonado, A., Díaz-del-Río, V., Maestro, A., Córdoba, D. and Fernández-Puga, M.C., (2004). Structure and evolution of the “Olistostrome” complex of the Gibraltar Arc in the Gulf of Cádiz (eastern Central Atlantic): evidence from two long seismic cross-sections. *Marine Geology*, **209**, 173-198.
- Miall, A.D., (1995). Whither stratigraphy? *Sedimentary Geology*, **100**, 5-20.
- Miall, A.D. and Miall, C.E., (2001). Sequence stratigraphy as a scientific enterprise: The evolution and persistence of conflicting paradigms. *Earth-Science Reviews*, **54**(4), 321-348.
- Michard, A. and Martinotti, G., (2002). The Eocene unconformity of the Briançonnais domain in the French-Italian Alps, revisited (Marguareis massif, Cuneo); a hint for a Late Cretaceous-Middle Eocene frontal bulge setting. *Geodinamica Acta*, **15**(5-6), 289-301.
- Michard A., Chalouan A., Feinberg H., Goffé B. and Montigny R., (2002). How does the Alpine belt end between Spain and Morocco? *Bulletin de la Societe Geologique de France*, **173**, 3-15.
- Mitchum R.M., (1977). Seismic stratigraphy and global changes of sea level, part 11: glossary of terms used in seismic stratigraphy. In: Payton, C.E. (Ed.), *Seismic Stratigraphy— Applications to Hydrocarbon Exploration*. AAPG Memoir, **26**, 205–212.
- Monié, P., Torres-Roldán, R.L. and García-Casco, A., (1994). Cooling and exhumation of the Western Betic Cordilleras, $^{40}\text{Ar}/^{39}\text{Ar}$ thermochronological constraints on a collapsed terrane. *Tectonophysics*, **238**(1-4), 353-379.
- Morley, C.K. and Guerin, G., (1996). Comparison of gravity-driven deformation styles and behavior associated with mobile shales and salt. *Tectonics*, **15**(6), 1154-1170.
- Muñoz, A., Ballesteros, M., Montoya, I., Rivera, J., Acosta, J. and Uchupi, E., (2008). Alborán Basin, southern Spain-Part I: Geomorphology. *Marine and Petroleum Geology*, **25**(1), 59-73.
- Nemcok, M. and Nemcok, J., (1994). Late Cretaceous deformation of the Pieniny Klippen Belt, West Carpathians. *Tectonophysics*, **239**, 81-109.
- Nottvedt, A., Gabrielsen, R.H. and Steel, R.J., (1995). Tectonostratigraphy and sedimentary architecture of rift basins, with reference to the northern North Sea. *Marine and Petroleum Geology*, **12**(8), 881-901.
- Nystuen, J.P., (1995). History and development of sequence stratigraphy. *Sequence stratigraphy - concepts and applications*: 31-116.
- Okay, A.I., Ozcan, E., Cavazza, W., Okay, N. and Less, G., (2010). Basement types, Lower Eocene series, Upper Eocene olistostromes and the initiation of the southern Thrace Basin, NW Turkey. *Turkish Journal of Earth Sciences*, **19**, 1-25.
- Olivier, P., (1984). Evolution de la limite entre Zones Internes et Zones Externes dans l’arc de Gibraltar (Maroc-Espagne). Doctoral Thesis. Toulouse, Université Paul Sabatier, 229pp.
- Osete, M.L., Villalaín, J.J., Palencia, A., Osete, C., Sandoval, J. and García-Dueñas, V., (2004). New palaeomagnetic data from the Betic Cordillera: Constraints on the timing and the geographical distribution of Tectonic rotations in Southern Spain. *Pure and Applied Geophysics*, **161**, 701-722.
- Payton, C.E., (1977). *Seismic Stratigraphy – Applications to hydrocarbon exploration*. AAPG, Memoir, **26**, 516p.
- Pedreira, A., Ruiz-Constán, A., Galindo-Zaldívar, J., Chalouan, A., Sanz de Galdeano, C., Marín-Lechado, C., Ruano, P., Benmakhlouf, M., Akil, M., López-Garrido, A.C., Chabli, A., Ahmamou, M. and González-Castillo, L., (2011). Is there an active subduction beneath the Gibraltar orogenic arc? Constraints from Pliocene to present-day stress field. *Journal of Geodynamics*, **52**(2), 83-96.

- Pereira, R. and Alves, T.M., (2012). Tectono-stratigraphic signature of multiphased rifting on divergent margins (deep-offshore southwest Iberia, North Atlantic). *Tectonics*, **31**(4), TC4001.
- Pérez-Belzuz, F., (1999). Geología del margen y cuenca del Mar de Alborán durante el Plio-Cuaternario: sedimentación y tectónica. PhD. Thesis, Universitat de Barcelona, Barcelona, 538 pp.
- Peyre, Y., (1974). Géologie d'Antequera et de sa région (Cordillères Bétiques, Espagne). Doctoral Thesis. Université Paris, Institut National Agronomique Paris, 528pp.
- Piles Mateo, E., Chamón Cobos, C., Estévez González, C., Crespo, V., Aguilar, M. and Reyes, J.L., (1978). Mapa Geológico de España. Scale 1:50.000, 2nd series, nº 1065, Marbella. Madrid, Instituto Geológico y Minero de España, 65pp.
- Piles Mateo, E., Estévez González, C., Barba Martín, A., Crespo, V., Aguilar, M. and Reyes, J.L., (1977). Mapa Geológico de España. Scale 1:50.000, 2nd series, nº 1066, Coín. Madrid, Instituto Geológico y Minero de España, 71pp.
- Pineda Velasco, A. and Ruiz Reig, P., (1983). Mapa Geológico de España. Scale 1:50.000, 2nd series, nº 1024, Archidona. Madrid, Instituto Geológico y Minero de España, 67pp.
- Platt, J.P. and Vissers, R.L.M., (1989). Extensional collapse of thickened continental lithosphere: A working hypothesis for the Alboran Sea and Gibraltar arc. *Geology*, **17**(6), 540-543.
- Platt, J.P., Soto, J.I., Whitehouse, M.J., Hurford, A.J. and Kelley, S.P., (1998). Thermal evolution, rate of exhumation, and tectonic significance of metamorphic rocks from the floor of the Alboran extensional basin, western Mediterranean. *Tectonics*, **17**(5), 671-689.
- Platt, J.P., Allerton, S., Kirker, A., Mandeville, C., Mayfield, A., Platzman, E.S. and Rimi, A. (2003). The ultimate arc: Differential displacement, oroclinal bending, and vertical axis rotation in the External Betic-Rif arc. *Tectonics*, **22**, 1017-1046.
- Posamentier, H.W., Jervey, M.T. and Vail, P.R., (1988). Eustatic controls on clastic deposition (I) conceptual framework. Sea-level changes: an integrated approach: 109-124.
- Posamentier, H.W. and Allen, G.P., (1993). Variability of the sequence stratigraphic model: effects of local basin factors. *Sedimentary Geology*, **86**(1-2), 91-109.
- Prosser, S., (1993). Rift-related linked depositional systems and their seismic expression. Geological Society, London, Special Publications, **71**(1), 35-66.
- Puga, E., Nieto, J.M. and Díaz de Federico, A., (2000). Contrasting P-T paths in eclogites of the Betic ophiolitic association, Mulhacén Complex, Southeastern Spain. *Canadian Mineralogist*, **38**, 1137-1161.
- Răbăgia, T., Matenco, L. and Cloetingh, S., (2011). The interplay between eustacy, tectonics and surface processes during the growth of a fault-related structure as derived from sequence stratigraphy: The Govora-Ocnele Mari antiform, South Carpathians. *Tectonophysics*, **502**(1-2), 196-220.
- Ravnås, R. and Steel, R.J., (1998). Architecture of marine rift-basin successions. *AAPG Bulletin*, **82**(1), 110-146.
- Rodríguez-Fernández, J. and Sanz de Galdeano, C., (1992). Onshore neogene stratigraphy in the north of the Alboran Sea (Betic internal zones): Paleogeographic implications. *Geo-Marine Letters*, **12**, 123-128.
- Rodríguez-Fernández, J., Comas, M.C., Soria, J., Martín-Pérez, J.A. and Soto, J.I., (1999). The sedimentary record of the Alboran Basin: An attempt at sedimentary sequence correlation and subsidence analysis. *Proceedings of the Ocean Drilling Program: Scientific Results*, **161**, 69-76.

- Rowan, M. G., Peel F. J., and Vendeville B. C., (2004). Gravity-driven fold belts on passive margins, in McClay, K. R., ed., Thrust tectonics and hydrocarbon systems: AAPG Memoir, **82**, 157– 182.
- Royden, L.H., (1993). Evolution of retreating subduction boundaries formed during continental collision. *Tectonics*, **12**(3), 629-638.
- Sánchez-Almazo, I.M., Spiro, B., Braga, J.C. and Martín, J.M., (2001). Constraints of stable isotope signatures on the depositional palaeoenvironments of upper Miocene reef and temperate carbonates in the Sorbas Basin, SE Spain. *Palaeogeography, Palaeoclimatology, Palaeoecology*, **175**(1-4), 153-172.
- Sánchez-Gómez, M., García-Dueñas, V. and Muñoz, M., (1996). Relations structurales entre les Péridotites de Sierra Bermeja et les unités Alpujárrides sous-jacentes (Benahavis, Ronda, Espagne). *Comptes Rendus de l'Académie des Sciences, Serie Iia, Sciences de la Terre et des Planètes*, **321**, 885-892.
- Sautkin, A., Talukder, A.R., Comas, M.C., Soto, J.I. and Alekseev, A., (2003). Mud volcanoes in the Alboran Sea: evidence from micropaleontological and geophysical data. *Marine Geology*, **195**(1–4), 237-261.
- Schoorl, J.M. and Verdkamp, A., (2003). Late cenozoic landscape development and its tectonic implications for the Guadalhorce Valley near Álora (Southern Spain). *Geomorphology*, **50**, 43-57.
- Schlager, W., (1993). Accommodation and supply—a dual control on stratigraphic sequences. *Sedimentary Geology*, **86**(1–2), 111-136.
- Seber, D., Barazangi, M., Ibenbrahim, A. and Demnati, A., (1996). Geophysical evidence for lithospheric delamination beneath the Alboran Sea and the Rif-Betic mountains. *Nature*, **379**, 785-790.
- Serrano, F., (1979). Los foraminíferos planctónicos del Mioceno superior de la cuenca de Ronda y su comparación con los de otras áreas de las Cordilleras Béticas. PhD. Thesis, University of Granada.
- Serrano, F., Guerra-Merchán, A., El Kadiri, K., de Galdeano, C.S., López-Garrido, Á.C., Martín-Martín, M. and Hlila, R., (2007). Tectono-sedimentary setting of the Oligocene-early Miocene deposits on the Betic-Rifian Internal Zone (Spain and Morocco). *Geobios*, **40**(2), 191-205.
- Sloss, L.L., Krumbein, W.C. and Dapples, E.C., (1949). Integrated facies analysis. In: Longwell, C.R. (Ed.), *Sedimentary Facies in Geologic History*. Geological Society of America Memoir, **39**, 91–124.
- Soto, J.I. and Gervilla, F., (1991). Los macizos ultramáficos de Sierra de las Aguas y Sierra de la Robla como una ventana extensional (Béticas occidentales). *Geogaceta*, **9**, 21-23.
- Soto, J.I., Comas, M.C. and De la Linde, J., (1996). Espesor de Sedimentos en la Cuenca de Alborán Mediante una Conversión Sísmica Corregida. *Geogaceta*, **20**, 382-385.
- Soto, J.I. and Platt, J.P., (1999). Petrological and Structural Evolution of High-Grade Metamorphic Rocks from the Floor of the Alboran Sea Basin, Western Mediterranean. *Journal of Petrology*, **40**(1), 21-60.
- Soto, J.I., Fernández-Ibáñez, F., Fernández, M. and García-Casco, A., (2008). Thermal structure of the crust in the Gibraltar Arc: Influence on active tectonics in the western Mediterranean. *Geochemistry, Geophysics, Geosystems*, **9**(10), Q10011.
- Soto, J.I., Fernández-Ibáñez, F., Talukder, A.R. and Martínez-García, P., (2010). Miocene shale tectonics in the northern Alboran Sea (Western Mediterranean). *AAPG Memoir*, **93**, 119-144.

- Spakman, W. and Wortel, R., (2004). A Tomographic View on Western Mediterranean Geodynamics. In: F.R. W. Cavazza, W. Spakman, G. M. Stampfli & P. A. Ziegler (Editor), *The Transmet Atlas: The Mediterranean Region from Crust to Mantle* Springer-Verlag, pp. 31-52.
- Stromberg, S. and Bluck, B. (1998). Turbidite facies, fluid-escape structures and mechanisms of emplacement of the Oligo-Miocene Aljibe Flysch, Gibraltar Arc, Betics, southern Spain, *Sedimentary Geology*, **115**(1-4), 267-288.
- Suades, E. and Crespo-Blanc, A., (2010). Hydraulic brecciation on top of the Alborán Domain and its relationship with Lower Miocene deposits (Western Betics). *Geogaceta*, **49**, 71-74.
- Suades, E., Comas, M.C. and Crespo-Blanc, A., (2012). Learning from the Top of the Basement in the Malaga Basin (Alboran Sea): Extensional Versus Compressional Structures and Onshore-Offshore Correlations, VIII Congreso Geológico de España. *Geotemas*, Oviedo, pp. 1607-1610.
- Suades, E., Comas, M.C. and Crespo-Blanc, A., (2013). Tectonic Evolution of the Malaga Basin (Alboran Sea): Insights from Its Sedimentary Infill. *Geogaceta*, **54**, 87-90.
- Suades, E. and Crespo-Blanc, A., (2013). Gravitational dismantling of the Miocene mountain front of the Gibraltar Arc system deduced from the analysis of an olistostromic complex (western Betics). *Geologica Acta*, **11**(2), 215-229.
- Talukder, A.R., Comas, M.C. and Soto, J.I., (2003). Pliocene to Recent Mud Diapirism and Related Mud Volcanoes in the Alboran Sea (Western Mediterranean). Geological Society, London, Special Publications, **216**, 443-459.
- Talukder, A.R., Comas, M.C. and Soto, J.I., (2004). Estructura y evolución durante el Mioceno del diapirismo de lodo en el sector septentrional de la Cuenca Oeste de Alborán (Mediterráneo occidental), *Boletín Geológico y Minero*, **115**(3), 439-452.
- Tari, G., Horváth, F. and Rumpfer, J., (1992). Styles of extension in the Pannonian Basin. *Tectonophysics*, **208**(1-3), 203-219.
- ter Borgh, M., Stoica, M., Donselaar, M.E., Matenco, L. and Krijgsman, W., (2014). Miocene connectivity between the Central and Eastern Paratethys: Constraints from the western Dacian Basin. *Palaeogeography, Palaeoclimatology, Palaeoecology*, **412**, 45-67.
- Torné, M. and Banda, E., (1992). Crustal thinning from the Betic Cordillera to the Alboran Sea. *Geo-Marine Letters*, **12**(2-3), 76-81.
- Torne, M., Fernández, M., Comas, M.C. and Soto, J.I., (2000). Lithospheric structure beneath the Alboran Basin: Results from 3D gravity modeling and tectonic relevance. *Journal of Geophysical Research B: Solid Earth*, **105**(B2), 3209-3228.
- Urgeles, R., Camerlenghi, A., Garcia-Castellanos, D., De Mol, B., Garcés, M., Vergés, J., Haslam, I. and Hardman, M., (2011). New constraints on the Messinian sealevel drawdown from 3D seismic data of the Ebro Margin, western Mediterranean. *Basin Research*, **23**(2), 123-145.
- Uyeda, S. and Kanamori, H., (1979). Back-arc opening and the mode of subduction. *Journal of Geophysical Research: Solid Earth*, **84**(B3), 1049-1061.
- Vail, P.R., Mitchum, R.M., Campion, K.M. and Rahmanian, V.D., (1977). Seismic Stratigraphy and Global Changes of Sea Level, Part 3: Relative Changes of Sea Level from Coastal Onlap. In: C.E. Payton (Editor), *Seismic Stratigraphy-Application to Hydrocarbon Exploration* AAPG Memoir, pp. 83-97.
- Van Wagoner, J.C., Mitchum, R.M., Campion, K.M. and Rahmanian, V.D., (1990). Siliciclastic sequence stratigraphy in well logs, core, and outcrops. *Siliciclastic sequence stratigraphy in well logs, core, and outcrops*.

- Vannucchi, P., Maltman, A., Bettelli, G. and Clennell, B., (2003). On the nature of scaly fabric and scaly clay. *Journal of Structural Geology*, **25**(5), 673-688.
- Vera, J.A., (2000). El terciario de la cordillera Bética: Estado actual de conocimientos. *Revista de la Sociedad Geológica de España*, **13**(2), 345-373.
- Vera, J.A., (2001). Evolution of the South Iberian continental margin. In: PeriThethys Memoir: Peri Thethyan Rif/wrench basins and passive margins (Ed. by P. A. Ziegler, W. Cavazza and A. F. H. Robertson). *Mémoires du Muséum national d'histoire naturelle*, Paris, 109-143.
- Vera, J.A., Arias, C., García-Hernández, M., López-Garrido, A.C., Martín-Algarra, A., Marín-Chivelet, J., Molina, J.M., Rivas, P., Ruiz-Ortiz, P.A., Sanz de Galdeano, C. and Vilas, L., (2004). Las zonas Externas Béticas y el Paleomargen Sudibérico. In: Vera, J.A. (ed.). *Geología de España*. Madrid, Sociedad Geológica de España, Instituto Geológico y Minero de España (SGE-IGME), 354-389.
- Vergés, J. and Fernández, M., (2012). Tethys-Atlantic interaction along the Iberia-Africa plate boundary: The Betic-Rif orogenic system. *Tectonophysics*, **579**, 144-172.
- Vernant, P., Fadil, A., Mourabit, T., Ouazar, D., Koulali, A., Davila, J.M., Garate, J., McClusky, S. and Reilinger, R., (2010). Geodetic constraints on active tectonics of the Western Mediterranean: Implications for the kinematics and dynamics of the Nubia-Eurasia plate boundary zone. *Journal of Geodynamics*, **49**, 123-129.
- Villalaín, J.J., Osete, M.L., Vegas, R., García-Dueñas, V. and Heller, F., (1996). The Neogene remagnetization in the western Betics: a brief comment on the reliability of paleomagnetic directions. In: Morris A., Tarling, D.H. (Eds.). *Paleomagnetism and Tectonics of the Mediterranean region*. Geological Society Special Publication, **105**, 33-41.
- Watts, A.B., Platt, J.P. and Buhl, P., (1993). Tectonic Evolution of the Alboran Sea Basin. *Basin Research*, **5**, 153-177.
- Wernicke, B., (1985). Uniform-sense normal simple shear of the continental lithosphere. *Canadian Journal of Earth Sciences*, **22**(1), 108-125.
- Wernicke, B. and Axen, G.J., (1988). On the role of isostasy in the evolution of normal fault systems. *Geology*, **16**(9), 848-851.
- Woodside, J.M. and Maldonado, A., (1992). Styles of compressional neotectonics in the eastern Alboran Sea. *Geo-Marine Letters*, **12**(2-3), 111-116.
- Zahn, R., Comas, M.C. and Klaus, A., (1999). Proceedings, scientific results, Ocean Drilling Program, Leg 161, Mediterranean Sea II, the western Mediterranean. *Proceedings of the Ocean Drilling Program: Scientific Results*, **161**, 1-607.
- Zeck, H.P., Albat, F., Hansen, B.T., Torres-Roldán, R.L., García-Casco, A. and Martín-Algarra, A., (1989). A 21 ± 2 Ma age for the termination of the ductile alpine deformation in the internal zone of the betic cordilleras, South Spain. *Tectonophysics*, **169**(1-3), 215-220.
- Ziegler, P.A. and Cloetingh, S., (2004). Dynamic processes controlling evolution of rifted basins. *Earth-Science Reviews*, **64**(1-2), 1-50.

10 Annex

Estimation of Units velocity

And-G1

Units	Total thickness/Unit	Average Vel.
II	86,4	5066,526792
III	643,35	2836,039989
IV	393,75	2775,905136
V	770,85	2929,207035
VI	444,9	2461,622828

Alb-A1

Units	Total thickness/Unit	Average Vel.
I	339,6	2206,5223
II	67,8	3082,520669
III	363,45	2682,592286
IV (V?)	46,65	2747,567825
VI	477	2139,945481

Site-976

Units	Total thickness/Unit	Average Vel.
I	568,95	1776,596722
II	83,88	2253,657776

Unit II	Thickness	Average Vel.	Vel. Final
II (And-G1)	86,4	5066,526792	3510,49912
II (Alb-A1)	67,8	3082,520669	
II (976)	83,88	2253,657776	
Total	238,08		

Unit III	Thickness	Average Vel.	Vel. Final
III (And-G1)	643,35	2836,039989	2780,6461
III (Alb- A1)	363,45	2682,592286	
Total	1006,8		

Units	thickness	Average Vel.	Units II+III Vel.
II	86,4	3510	2866,4296
III	643,35	2780	
II+III	729,75		

Unit IV	Thickness	Average Vel.	Vel. Final
IV (And-G1)	393,75	2775,905136	2775,90514

Unit V	Thickness	Average Vel.	Vel. Final
V (And-G1)	770,85	2929,207035	2929,20703

Unit VI	Thickness	Average Vel.	Vel. Final
VI (And-G1)	444,9	2461,622828	2295,18385
VI (Alb-A1)	477	2139,945481	
Total	921,9		

Isopach maps	Velocities
II+III	2865
IV	2775
V	2930
VI	2295